Wetlands for dry land

Role of bio-physical interactions in tidal marshes for nature-based shoreline protection

Ken Schoutens

Universiteit Antwerpen
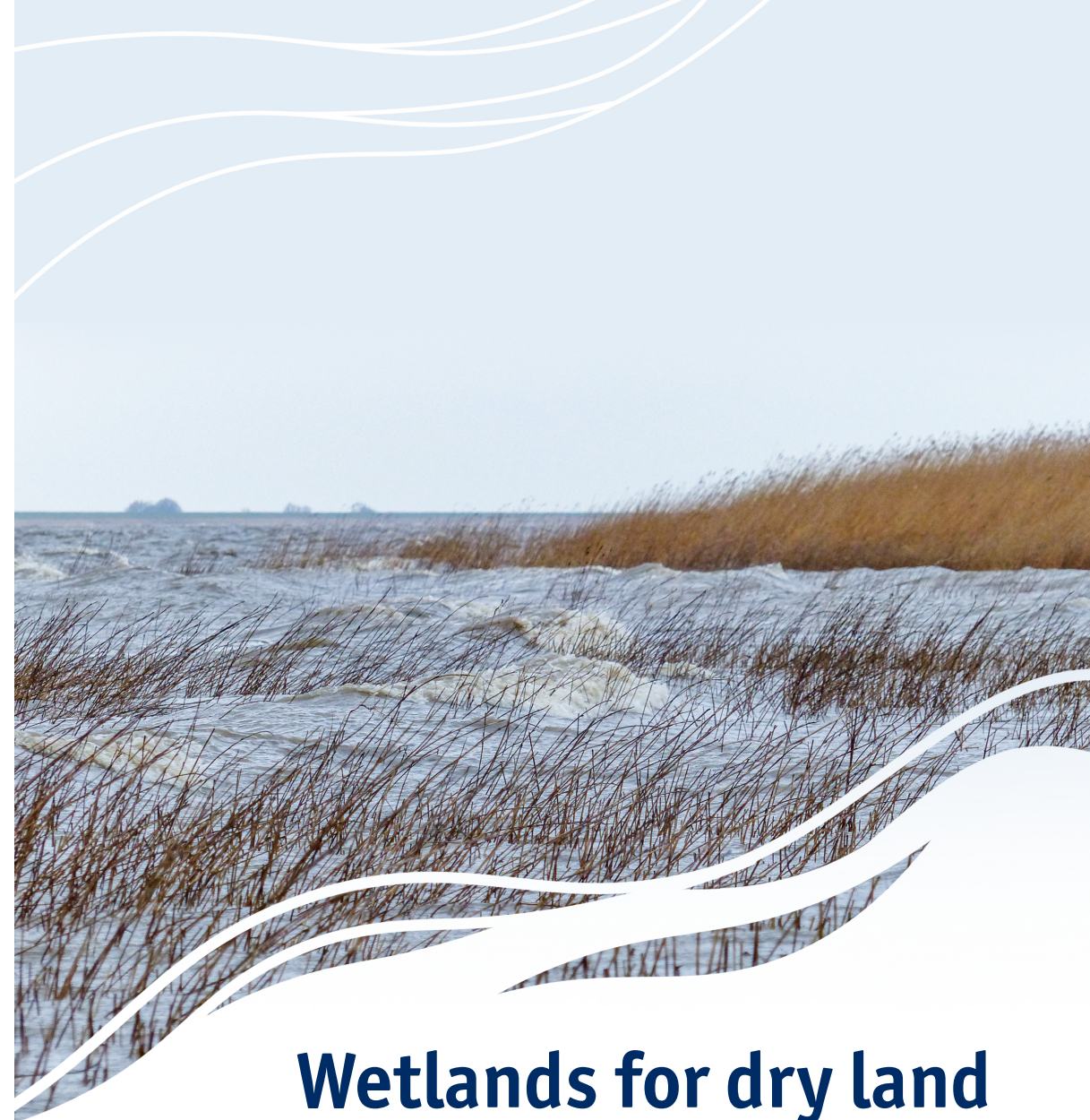
Wetlands for dry land
Role of bio-physical interactions in tidal marshes for nature-based shoreline protection

Droge voeten door natte natuur
Rol van biofysische interacties in schorren voor natuur-gebaseerde kustverdediging

Dissertation for the degree of doctor in Science: Biology at the University of Antwerp to be defended by

Ken Schoutens

Promotor
Prof. dr. Stijn Temmerman

Faculty of Science
Department of Biology
Antwerp 2022

Jury members

Internal
Ivan Janssens
Ivan Nijs
Jonas Schoelynck

External
Iris Möller (University of Dublin, Ireland)
Bas Borsje (University of Twente, The Netherlands)

Table of contents

Summary

Global climate changes impose multiple challenges, including the increasing risk of coastal flood hazards due to sea level rise and increasing impact of storm activity. Social and economic cost of flood hazards are huge since low elevated coastal zones often house densely populated and industrialized communities. Hence, there is a strong urge to implement sustainable climate adaptation strategies which strengthen the existing protection infrastructure, e.g. dikes or sea walls. Nature-based shoreline protection approaches are increasingly studied and proposed and in this context, conservation or (re)creation of tidal marsh ecosystems provide multiple opportunities. First of all, tidal marshes have a shoreline protection function by reducing wave energy and forming a temporary water storage during storm surges, while secondly they provide ecological benefits such as water purification, biodiversity, carbon storage etc.

Nevertheless, effective implementation of tidal marsh ecosystems as a complementary shoreline protection is hampered by the uncertainties about their effectiveness and reliability. This thesis elaborates on the role of species-specific plant traits, how they vary spatially and over time, how they interact with hydrodynamics and sediment dynamics and, how these feedbacks contribute to the shoreline protection capacity of tidal marshes. Field monitoring and field experiments were done along the brackish part of the Elbe estuary, Germany and flume experiments took place in the Large Wave Flume, Hannover, Germany and the Mesodrome tidal flume facility, Antwerp, Belgium.

Research has shown that the capacity of tidal marsh vegetation to attenuate hydrodynamic forces from waves and currents depends on plant traits. These plant traits vary between species and can even vary within a species. In addition to this knowledge, our research shows that plant traits of brackish marsh species in temperate climate zones vary throughout the season, i.e. the presence of aboveground biomass is significantly reduced in winter. In NW Europe, winter is typically the storm season and hydrodynamic forces are strongest, thus shoreline protection is most needed. Unfortunately, the reduced amount of aboveground biomass also diminishes the wave and current attenuation capacity of the vegetation. Although hydrodynamics can penetrate further landwards, towards the embankment, we found that the belowground biomass does seem to stabilize the sediment bed by limiting erosion, hence protecting the more landward situated higher marshes adjacent to the embankments.

Apart from the direct effect of plant traits on the protection capacity of tidal marshes, this thesis elaborates on the role of species-specific growth and survival in response to hydrodynamics. We show that for successful species establishment (i.e. seedling survival) and species growth, the exposure to mechanical stress from hydrodynamic forces coming from waves and currents can form an extra stress in addition to existing stress from e.g. tidal inundation. This species-specific and plant trait dependent growth

and survival was linked to spatial differences in environmental stress and hence might result in spatial distribution of species. Moreover, we illustrate that plant traits allowing growth and survival under hydrodynamic forces are the same plant traits that reduce the hydrodynamic attenuation capacity, i.e. flexible shoots with a low biomass reducing the experienced drag forces on the plant, also reduce the capacity of the plants to attenuate waves and currents. This trade-off has consequences for the shoreline protection capacity of the tidal marsh, i.e. the conditions in hydrodynamic exposed shorelines only allow species with the suitable set of, stress avoiding, plant traits to grow and survive. Although the hydrodynamic attenuation capacity of such species is low, it might be enough to create slightly more sheltered conditions more landwards to allow other species, with a lower capacity to grow under hydrodynamic exposure, but higher wave and current attenuation capacity, to grow. Such interspecific growth facilitation is possible when there is enough space for tidal marshes to expand. When tidal marshes have space to develop a gradient from low lying, shoreward pioneer zones towards higher, more landward mature marshes, the overall resilience and reliability of the shoreline protection capacity of tidal marshes might increase. Within that context, this thesis provides first experimental evidence confirming that the high sediment stability of higher, mature tidal marshes under extreme flow velocities can function as an extra natural 'dike' in case of a dike breach, hence reducing the flow discharge towards the breach and limiting the dimensions of the breach.

This thesis provides new insights in the role of species-specific plant traits within the mutual interactions between hydrodynamic forces, sediment dynamics and vegetation that are crucial in understanding the spatial-temporal shoreline protection efficiency of tidal marshes. We show that hydrodynamic forces from waves and currents form a not to be neglected additional stressor for plant growth and survival and we illustrate how these forces constrain suitable conditions for successful tidal marsh conservation, restoration and creation. Moreover, we argue how providing enough space to allow marsh expansion will increase the resilience and reliability of the nature-based shoreline protection function of tidal marsh in a changing climate.

Samenvatting

Klimaatsverandering zorgt voor vele uitdagingen waaronder een grotere kans op overstromingen langsheen kustgebieden veroorzaakt door de combinatie van zeespiegelstijging en een hogere impact van stormen. De sociaaleconomische kosten die gepaard gaan met dit type overstroming zijn zeer hoog. De laaggelegen kustgebieden zijn immers vaak dichtbevolkt en sterk geïndustrialiseerd. Er is dus nood aan duurzame klimaatadaptatiestrategieën die de huidige kustbescherming, zoals dijken, versterken. In deze context worden op natuur gebaseerde manieren van kustbescherming steeds vaker bestudeerd en naar voor gebracht. Hierin biedt behoud of (her)inrichting van schorren verschillende opportuniteiten zoals (1) een kustbeschermingsfunctie dankzij de reductie van golfenergie en de vorming van een tijdelijke waterbuffer bij stormtij, en (2) het leveren van ecologische waarden waaronder de verbetering van waterkwaliteit, biodiversiteit, koolstofopslag, etc.

Ondanks deze opportuniteiten wordt de implementatie van schorren als ondersteunende kustbescherming gehinderd door de onzekerheid rond hun effectiviteit en betrouwbaarheid. In deze thesis wordt er dieper ingegaan op de rol van soortspecifieke planteigenschappen, hoe ze variëren in ruimte en tijd, hun wederzijdse interactie met hydrodynamische krachten en sedimentdynamiek en hoe deze feedbacks bijdragen aan de kustbeschermingsfunctie van schorren. Veldmonitoring en veldexperimenten vonden plaats in het brakwatergedeelte van het Elbe-estuarium (Duitsland) en stroomgootexperimenten vonden plaats in de Large Wave Flume te Hannover (Duitsland) en in de Mesodrome-getijdenstroomgoot in Antwerpen (België).

Onderzoek heeft aangetoond dat de capaciteit van schorrenvegetatie om hydrodynamische krachten van golven en stroming af te zwakken, afhankelijk is van planteigenschappen. De eigenschappen variëren tussen plantsoorten en zelfs binnen eenzelfde soort. Ons onderzoek voegt hieraan toe dat planteigenschappen van brakwatervegetatie in een gematigd klimaat ook variëren over de seizoenen heen, i.e. de bovengrondse biomassa vermindert sterk tijdens de winter. In NW-Europa is het winterseizoen ook typisch het stormseizoen waarbij de hydrodynamische krachten het grootst zijn en dus wanneer de nood aan kustbescherming het grootst is. Helaas zorgt de verminderde aanwezigheid van bovengrondse biomassa in de winter ook voor een daling in de capaciteit van de vegetatie om golven en stromingen af te zwakken. Hierdoor kunnen hydrodynamische krachten verder landinwaarts, richting de dijken propageren. Dit onderzoek toont echter aan dat de ondergrondse biomassa een stabiliserende functie heeft op het sediment, wat het risico op sedimenterosie vermindert en waardoor de hoger gelegen landinwaartse schorren naast de dijk ook beschermd worden.

Naast het directe effect van planteigenschappen op de beschermingscapaciteit van schorren gaat deze thesis dieper in op de rol van soortspecifieke groei en overleving

onder stress van hydrodynamische krachten. Hier tonen we aan dat voor een succesvolle vestiging (bv. overleving van zaailingen) en groei van een soort, de blootstelling aan mechanische stress van golven en stroming een extra stress kan vormen bovenop de bestaande stress van bv. overstroming door getij. Deze soortspecifieke en planteigenschapafhankelijke groei en overleving is gekoppeld aan de ruimtelijke variatie in omgevingsstressoren, wat uiteindelijk tot een ruimtelijke verdeling van soorten kan leiden. Verder illustreren onze resultaten dat de planteigenschappen die groei en overleving onder hydrodynamische stress bevorderen, dezelfde zijn als de planteigenschappen die de capaciteit om hydrodynamische krachten af te zwakken, verminderen. Dit wil zeggen dat flexibele stengels met een lage biomassa minder wrijving met het water voelen, maar ook een lagere capaciteit hebben om golven en stroming af te zwakken. Een trade-off zoals deze heeft gevolgen voor de kustbeschermingscapaciteit van schorren, i.e. wanneer oevers sterk blootgesteld worden aan hydrodynamische krachten, zullen enkel een beperkt aantal soorten, met de juiste, stressontwijkende eigenschappen kunnen groeien en overleven. Ondanks dat die soorten een lage capaciteit hebben om hydrodynamische krachten af te zwakken, kan het toch voldoende zijn om landinwaarts een iets meer beschutte omgeving te creëren waar andere soorten wel kunnen groeien. Deze andere, landinwaarts groeiende soorten hebben dan wel een lagere capaciteit om onder blootstelling van hydrodynamische krachten te groeien, maar ze hebben daardoor ook een hogere capaciteit om die hydrodynamische krachten af te zwakken. De beschreven intraspecifieke facilitering van groei is enkel mogelijk wanneer er voldoende ruimte is voor het schor om uit te breiden. Wanneer schorren de ruimte hebben om te ontwikkelen tot een gradiënt gaande van laaggelegen pioniersschorren, dichtbij het water, naar hoger gelegen, meer landinwaartse volgroeide schorren, dan kan de veerkracht en betrouwbaarheid van de kustbeschermende capaciteit van schorren toenemen. In die context biedt deze thesis voor het eerst experimenteel bewijs voor de hoge sedimentstabiliteit van hoger gelegen, volgroeide schorren die blootgesteld zijn aan zeer hoge stroomsnelheden. Hierdoor functioneren schorren als een extra 'dijk' in het geval van een dijkbreuk, i.e. ze verminderen het debiet naar de dijkbres en beperken de dimensies van de bres.

Deze thesis levert nieuwe inzichten in de rol van soortspecifieke planteigenschappen in de wederzijdse interacties tussen hydrodynamische krachten, sedimentdynamiek en schorvegetatie. Om de spatio-temporele efficiëntie van de kustbeschermende capaciteit van schorren beter te begrijpen, zijn deze interacties cruciaal. Hydrodynamische krachten van golven en stromingen vormen een niet te onderschatten stress voor de groei en overleving van schorvegetatie en zijn bepalend in een succesvolle schorbehoud of (her)inrichting. De thesis onderbouwt dat voldoende ruimtevoorziening voor schorontwikkeling, een toename van de veerkrachtigheid en betrouwbaarheid van de op natuur gebaseerde kustbeschermingsfunctie van schorren in een veranderend klimaat zal vergroten.

Acknowledgements

Over a period of almost seven PhD years, I met many people who deserve a big thank you! But let me start a bit earlier…

Studying agriculture and biotechnical sciences in secondary school, who would have thought that I would end up doing a doctoral research in biology? I did not, but some people who inspired me by showing the wonderful world of biology already planted a seed. Thank you Marijke Faes and Steven Druyts for your enthusiasm and all the efforts you put in the biology and ecology classes. Especially, the excursions to the Schelde and Schiermonnikoog left quite an impression and definitely had a very important impact on my further studies.

The choice of my master thesis topic was evident, I took the opportunity to do 'something with vegetation' in a tidal environment, which eventually formed the base for my doctoral research later on. I was very lucky to meet Alexandra Silinski as my direct supervisor. Not only did she provide a great amount of skills and knowledge, in addition she managed to teach (or unknowingly forced?) me to speak and write in English! Now, I am already looking forward to the moment when we will walk around in Saeftinghe together with Valery!

Special thanks goes to my promotor, Stijn Temmerman, who gave me the chance to start a PhD on the wonderful topic of nature-based shoreline protection. I still remember very well how overwhelmed I was when you proposed the topic during the 'Wemeldinge party'. You believed in my capacities and encouraged me to strengthen them. Thanks to your enthusiasm and all your constructive feedback, I got the opportunity to develop my scientific skills in a very motivational and pleasant environment.

My research started in 2015 within the TIBASS project, led by Maike Heuner (Bundesanstalt für Gewässerkunde (Germany)), who deserves special thanks. Maike, you gave many useful feedbacks and suggestions for the data analysis and the data interpretation towards a more applied audience. Moreover, you always had my back when I was in need of logistical support or when I needed a German translator. I would also like to thank Vanessa Minden and Elmar Fuchs for all the input and nice meetings we had during the project. Tilla Schulte-Ostermann deserves a big thank you for the good cooperation we had, it was always nice to find out that I was not the only one suffering in (or enjoying?) the Elbe marshes when it was cold, rainy or spring tide! During the transplantation experiments, I was lucky to have the help of Pieter Luys, who did his master thesis on this topic. Thank you Pieter for all your good work and the many enjoyable trips to the Elbe! As many of you know, I spent a lot of time along the Elbe (i.e. more than 40 field campaigns) and therefore, I am especially grateful to all the people who helped me during fieldwork.

Now, at the end of my doctoral study, I thank the jury members: Iris Möller, Bas Borsje, Jonas Schoelynck, Ivan Nijs and Ivan Janssens for their positive feedback and insightful advice, which helped improve the thesis, especially in this last stage of the process.

Om af te sluiten, wil ik ook graag mijn familie en vrienden bedanken. Ondanks dat jullie misschien niet altijd begrepen waarover mijn onderzoek ging, bleven jullie interesse tonen en zijn jullie mij blijven steunen. Bedankt aan mijn ouders voor de warme thuis waar ik steeds welkom ben en om altijd klaar te staan wanneer ik jullie hulp vroeg. Merci aussi a BM's pour l'accueil chaleureux que tu as offert a Corinne et moi pendant une grande partie de mes études doctorales. Corinne, ook jij bedankt voor de vele fijne momenten die we gedurende al die jaren hebben beleefd. Ondanks dat ik vaak in het buitenland zat of pas laat thuis kwam, was jouw luisterend oor, steun en zorg een constante. Merci!

After almost seven years, this chapter is now finished. Time to start a new chapter!

1

Introduction

1.1 Coastal shorelines and their flood risk

Coastal and estuarine shorelines have traditionally attracted humans to form settlements and small communities. To date, communities, industry and hence the whole agglomeration in low-elevated coastal zones are still developing and expanding, forming densely populated areas with high economical value (Small and Nicholls 2003; Neumann et al. 2015). The strong urbanization of coastal areas is often illustrated by comparing the population size within low elevated coastal zones (LECZ, < 10 m above mean sea level) compared to the land surface cover of these areas, i.e. the LECZ occupies 2 % of the global land area and is populated with 10-15 % of the global human population (McGranahan et al. 2007; MacManus et al. 2021). Together with the growing population and economic activity, human interference with the coastal and estuarine habitats has increased and hence, modified the landscape implying changes in geomorphology, sediment dynamics, hydrodynamic exposure and tidal dynamics. For example, land reclamation by building dikes and draining coastal wetlands created land for agriculture and industry, and deepening of estuarine channels for shipping delivered better access to port cities.

Although multiple of the world's biggest cities are located along coastal and estuarine shorelines (e.g. Tokyo, Shanghai, New York, Mumbai, London and Antwerp), living along shorelines carries risks (Hanson et al. 2011). The embanked areas for instance, need dikes and seawalls to prevent daily flooding by the tides. These human-induced land use changes combined with climate change induced sea level rise and increased storminess in certain regions place our shorelines under increasing flood risk (Feser et al. 2015; Vitousek et al. 2017; Kirezci et al. 2020). Storm surges are the result of low atmospheric pressure generated winds pushing sea water towards the shore, creating abnormal high water levels. The drastic change in atmospheric pressure creates instable weather which often generates heavy precipitation, increasing the river discharge and increasing the water levels in estuaries. When the storm occurs around spring tide, the water level set-up results in a storm tide with extreme high water levels. Moreover, the storm winds blowing over the water surface generate waves which amplify in function of higher wind speed and longer wind fetch length. Such high energy storm waves impose a significant stress on the shoreline protection infrastructure by increasing the erosion risk and potential wave overtopping which can eventually lead to structural failures such as breaching dikes. Additionally, mean sea level rise, which is mainly caused by climate warming that expands the water and melts land ice, is predicted to be 0.43 m (RCP2.6) up to 0.84 m (RCP8.5) by 2100 relative to 1986-2005 (Oppenheimer et al. 2019). When the mean water level rises, the peak water levels around spring- and storm-tide will also move upwards to even higher peak water levels, e.g. the present-day critical water level will be exceeded daily before the end of this century along 90 % of the USA coast (Taherkhani et al. 2020). Apart from the rising sea levels, climate change will also impact wave conditions for which especially the

extreme wave conditions are predicted to become even more extreme (Young and Ribal 2019). The combination of higher water levels and more wave exposure increase the risk of wave overtopping and sediment erosion and thereby increase the impact on the shoreline protection infrastructure, i.e. exposure will rise in duration, frequency and intensity. Moreover, lateral erosion rates of tidal marshes increase linearly with increasing wave exposure and therefore extreme storm conditions only contribute less than 1 % to the observed dynamics (Leonardi et al. 2015).

Consequences for coastal communities such as infrastructural damage and even victims will be inevitable (Hinkel et al. 2014; Boettle et al. 2016; Prahl et al. 2018). Following the RCP8.5 scenario, 52 % of the global population will be at risk of flooding by 2100 (Kirezci et al. 2020) and expected annual damage for Europe will rise from present day €1.25 billion to €93-961 billion by 2100 (Vousdoukas et al. 2018). The devastating impact of single storm events for the community has become clear over the past decades in which Typhoon Hagibis and Hurricane Harvey are just two of many examples, i.e. Typhoon Hagibis (2019, Asia) > 100 casualties and $ 15 billion damage and Hurricane Harvey, (2017, USA) > 100 casualties and $ 125 billion damage. Without adaptations to the existing protection infrastructure, costs of storm surge damage and coastal flooding are estimated to increase only further in the coming decades (Vousdoukas et al. 2018). Adapting and maintaining the traditional engineered shoreline protection measures such as dikes, breakwaters and storm surge barriers is costly (Lenk et al. 2016; Jonkman et al. 2021). In search for more sustainable adaptation strategies, novel approaches of nature-based shoreline protection are increasingly proposed (Arkema et al. 2013; Cheong et al. 2013; Temmerman et al. 2013; Morris et al. 2020; van Zelst et al. 2021) as ecological complements to the existing infrastructure (Sutton-Grier et al. 2015; van Loon-Steensma and Schelfhout 2017; Schoonees et al. 2019; Marijnissen et al. 2020).

1.2 Nature-based shoreline protection by tidal marshes

1.2.1 Tidal marshes: brief description of ecosystem functioning and services
Tidal marsh ecosystems can be found in mid-latitude, temperate climate zones, where they form the natural transition between land and sea. These intertidal areas can be found along coasts and within estuaries where they form a highly dynamic and challenging environment for organisms (Townend et al. 2011). Species living in these ecosystems have to cope with regular flooding predominantly depending on the marsh elevation relative to mean sea level and on the daily (ebb – flood) and monthly (spring-neap) tidal cycles (Allen 2000; Mcluskey and Elliott 2004). Forming the transition between land and sea, tidal marshes are influenced by both salty seawater and fresh water from the river and terrestrial runoff. Although tidal marshes typically develop in areas that are shallow and slightly sheltered from the open sea, tidal currents and wind

(or ship) waves create hydrodynamic stressful conditions, especially close to the seaward marsh edge. These hydrodynamics and tidal dynamics also generate sediment dynamics with periods of sediment accretion and periods of sediment erosion. In tidal marshes, the vegetation forms a crucial element, but often consists of a limited species diversity as a consequence of the stressful and dynamic growth conditions. This vegetation is dominated by specialized herbaceous species with a high productivity, often forming monospecific clonal stands.

Coastal ecosystems such as tidal marshes are regarded among the world's most valuable ecosystems (Costanza et al. 1997, 2014; Barbier et al. 2011). From an ecological perspective, tidal marsh food webs provide important functions for both fauna and flora such as nursing ground for fish (Joyeux et al. 2017), feeding ground for birds (Hughes 2004) and a high primary production (Cloern et al. 2014). They deliver a purification function by improving the water quality and by trapping sediments (Mudd et al. 2010), removing nutrients and pollutants (de Groot et al. 2012). Additionally, high biomass production and anaerobic conditions result in a perfect environment for carbon sequestration (Burden et al. 2013; Macreadie et al. 2017). Resulting from their high ecological value, tidal marshes are often protected by international directives (e.g. EU habitat and bird directives, RAMSAR convention).

1.2.2 Tidal marshes: contribution to flood defense and shoreline erosion protection

In the past decade, nature-based shoreline protection got an increased attention by scientists, policy makers and coastal managers. In this context, tidal marshes were proposed as a durable complement to traditional protective measures such as dikes. The presence of marsh vegetation reduces the energy from waves and tidal currents which reduces the hydrodynamic forces acting on the shoreward situated shoreline protection infrastructure (Ysebaert et al. 2011; Carus et al. 2016; Garzon et al. 2019a; Schulze et al. 2019; Zhang et al. 2020). Combined with the reduction of hydrodynamic forces, the sediment stabilizing function of a belowground root network reduces the sediment erosion risk (Brooks et al. 2021). Tidal marshes can attenuate storm surge propagation by providing friction and temporal floodwater storage (Paquier et al., 2016; Smolders et al., 2015; Stark et al., 2015). Moreover, in case of a dike breach landward of a tidal marsh, the presence of the marsh reduces the flood discharge towards the embanked area (Zhu et al. 2020). In addition, tidal marshes have the capacity to trap sediments, i.e. the reduction of hydrodynamic forces enhances sediment settling, which allows them to build-up elevation at similar rates as the climate induced sea level rise (Barber et al. 2016; Kirwan et al. 2016; Schuerch et al. 2018; Cahoon et al. 2020).

As such, tidal marshes amongst other coastal habitats could provide an efficient and sustainable addition to conventional shoreline engineering (Temmerman and Kirwan

2015). Even with a limited amount of space available in heavily embanked estuaries, the presence of fringing tidal marshes (i.e., ~20-100 m wide marshes shoreward of the embankment) could significantly reduce construction costs and maintenance costs of shoreline protection infrastructure (Narayan et al. 2016; Reguero et al. 2018; Vuik et al. 2019; van Zelst et al. 2021).

Despite the numerous services provided by tidal marshes and coastal habitats in general, they are still under pressure (Duarte 2009; Mcowen et al. 2017) by direct human interference such as land reclamation and by climate-change induced challenges such as drowning due to sea level rise (Lotze et al. 2006; Nicholls and Cazenave 2010; Van Asselen et al. 2013). Tidal marsh loss and tidal marsh degradation diminish the ecological and protective functions of tidal marshes which increases the vulnerability of shorelines to flood hazards (Van Niekerk et al. 2013; Prosser et al. 2019). To counteract the growing loss of services that tidal marshes provide, implementations of ecosystem conservation, restoration and creation are crucial (Adams et al. 2021). To support these management measures, a better understanding of the processes that drive the shoreline protection capacity of tidal marshes is needed (Möller 2019).

1.3 Interactions between plants, water and sediments

1.3.1 Vegetation effect

Tidal marsh vegetation plays a crucial role in the shoreline protection function of tidal marshes (Shepard et al. 2011). At the shoreward edge of the marsh, vegetation is most exposed to tidal currents and incoming waves. When the marsh is inundated during high water, the physical presence of tidal marsh vegetation forms an obstruction for the water. The friction with the plants takes out energy from the water motion which results in reduced wave heights and reduced flow velocities (Dalrymple and Dean 1991; Mendez and Losada 2004). This process of wave and flow attenuation is well studied over the past years in the field (Möller 2006; Koch et al. 2009; Ysebaert et al. 2011; Yang et al. 2012; Schulze et al. 2019; Xue et al. 2021), in lab flume experiments (Augustin et al. 2009; Anderson and Smith 2014; Hu et al. 2014; Möller et al. 2014; Rupprecht et al. 2017) and has been described in model simulations (van Rooijen et al. 2015; Vuik et al. 2016; Wu et al. 2016; Garzon et al. 2019b; Mury et al. 2020; Willemsen et al. 2020). Studies have shown that wave and flow attenuation is a function of plant traits such as tall canopy height, high aboveground biomass and stiffness of the stems (Bouma et al. 2010; Ysebaert et al. 2011; Tempest et al. 2015; Carus et al. 2016; Silinski et al. 2018). Nevertheless, little knowledge exists on the effect of local variation in plant traits between species and throughout seasons on the shoreline protection capacity of tidal marshes.

Resulting from the reduction of hydrodynamic forces by the aboveground biomass of tidal marsh vegetation, the shear stress on the sediment bed and hence the risk for erosion is reduced (Brooks et al. 2021). At the same time, sedimentation is promoted by tidally supplied suspended sediments that can settle more easily in water with low hydrodynamic forces (Mudd et al. 2010) resulting in large scale accretion of the marsh platform in response to e.g. sea level rise (French 2006; Kirwan and Megonigal 2013). Apart from the aboveground plant material, belowground biomass such as roots and rhizomes can provide a stabilizing function of the sediment bed (Chen et al. 2012; Francalanci et al. 2013). Combined with reduced hydrodynamic forces, fine sediments and organic particles will settle more easily, forming sediment aggregates that are kept together through structural support from the root network (Gyssels et al. 2005; Chirol et al. 2021). Although sediment type is a key determinant for the erosion risk (Christiansen et al. 2000; Feagin et al. 2009) it is also highly important for the growth of marsh plants, e.g. well aerated sediments provide better growth conditions compared to poorly drained sediments (Silvestri et al. 2005; Xin et al. 2010). When the conditions are suitable, tidal marshes have a very high biomass production that is often locally stored as organic litter (Van De Broek et al. 2016) which can be an important part of the sediment composition (Lefeuvre et al. 2000). Small organic compounds will add to the cohesiveness of the sediment bed (De Baets et al. 2006), which increases the shear strength of the sediment bed (Ford et al. 2016).

Interestingly, these local plant-scale interactions can stimulate larger-scale dynamics (Wang et al. 2017) such as the formation of vegetation patches. Through density-depended feedbacks that generate scale-dependent feedbacks, sedimentation is promoted on the local scale within growing patches due to the attenuation of hydrodynamic forces. On the larger scale, erosion risk is increased along the patch as a result of flow acceleration (Bouma et al. 2009b; Schoelynck et al. 2012) which eventually results in the formation of tidal channels (Temmerman et al. 2007). Small-scale landscape features such as cliffs, ponds, runnels or hummocks change the topography of the sediment surface within the marsh and will impact the hydrodynamic attenuation capacity of the marsh (Möller and Spencer 2002; Yang et al. 2012). Moreover, these features might act as an important sediment source, e.g. runnels and ridges (Schuerch et al. 2019). The transition from bare mudflat towards vegetated marsh takes often place on very short distance, i.e. even abrupt transitions on less than one meter are common. Due to this transition, sediment accretion within the marsh is faster than on the mudflat which steepens the slope of the transition from the bare tidal flat towards the vegetated tidal marsh. Eventually, the steep slope might initiate the formation of a cliff which ultimately results in lateral retreat of the marsh edge (Van de Koppel et al. 2005; Bouma et al. 2016). It is clear that apart from the vegetation structure, also variation in the marsh surface topography and how it interacts with the vegetation should be taken into account when considering the shoreline protection function of the marsh (Reed et al. 2018).

1.3.2 Hydrodynamic forces

Although wave and flow attenuation are crucial to understand the shoreline protection capacity of tidal marshes, this function will only be provided when tidal marsh plants are able to grow and survive under exposure to the hydrodynamic forces of waves and currents. Especially along the shoreward marsh edges, mechanical stress from waves and currents (and wind to a lesser extend at low water, (Denny and Gaylord 2002; Anten et al. 2005)) can alter the growth of marsh plants (Schoelynck et al. 2015) and the surrounding geomorphology, e.g. cliff formation (Cao et al. 2021). Moving water will generate drag forces on the submerged vegetation. Moreover, the presence of a shoot will deform the flow around the stem (Kitsikoudis et al. 2017), creating turbulent currents which might result in scouring (i.e. local erosion around the stem), uprooting and eventually dislodgement of the entire shoot (Bouma et al. 2009a; Bywater-Reyes et al. 2015). Interestingly, studies on freshwater macrophytes found that some species avoid the mechanical stress, e.g. reconfiguration of the stems or leaves reduce contact surface by bending in the direction of the flow, while other species tend to tolerate the stress by standing stiff, i.e. plants develop strategies to either avoid or tolerate stress from hydrodynamic forces (Puijalon et al. 2011). However, growing plant traits that favor avoidance of mechanical stress from waves and currents, i.e. smaller, more flexible shoots, results in a lower capacity to attenuate hydrodynamic forces. While in contrast, plant traits favoring a good hydrodynamic attenuation capacity, i.e. taller and stiffer shoots, result in a lower capacity to cope with hydrodynamic forces. Hence there seems to be a trade-off between plant traits that benefit the wave and flow attenuation capacity of tidal marsh plants and plant traits that allow the species to grow in exposed conditions (Bouma et al. 2005). Moreover, when similar plant traits are responsible for both the ability to grow under hydrodynamic forces and the capacity to attenuate these hydrodynamic forces, the question is raised what implications such a trade-off has for the shoreline protection function of the tidal marsh.

Shoreline protection is most needed during extreme conditions, e.g. storm surges. Although many of the above-mentioned studies stress the potential of tidal marshes as effective and sustainable addition to existing shoreline protection measures, limited research focusses on such extreme events (Möller et al. 2014; Rupprecht et al. 2017). Previous studies, e.g. on wave attenuation by tidal marsh vegetation, are often conducted over relatively short time periods of days to weeks during peak biomass in summer. In NW Europe however, most extreme conditions occur during the winter storms, when aboveground biomass is reduced. Additionally, past storm events have shown that dikes are not infallible and recent historical analysis of dike breaches prove that tidal marshes do not fully prevent dike breaches (Zhu et al. 2020). Nevertheless, the analysis showed that dike breaches were smaller and less deep when high tidal marshes were present shoreward of the dike breach revealing a potential new shoreline protection mechanism of tidal marshes. Although the extreme hydrodynamic

events bring the highest risks of flood hazards, many uncertainties remain on the persistence and stability of shoreline protection capacity by tidal marshes during such extreme conditions. Yet, this knowledge is needed to understand the long-term effectiveness and resilience of shoreline protection by tidal marshes.

1.4 Species distribution

Spatial distribution patterns of tidal marsh vegetation is often observed along a cross-shore gradient, i.e. from the shoreward marsh edge towards the landward marsh edge. In the landward located marsh zones, species distribution is mainly driven by competitive growth capacity, while in lower, more shoreward located marsh zones, the species' capacity to tolerate longer tidal inundation and higher sediment salinity are considered the dominant drivers in existing literature (Bertness 1991; Pennings et al. 2005; Silvestri et al. 2005). However, a study in two NW European estuaries found that in wave-exposed pioneer marshes, there is a clear spatial separation between species growing in different zones, while in wave-sheltered marshes all species can grow in the same, most seaward zone (Heuner et al. 2018). In line with these observations, laboratory flume experiments found that species growing in the most wave-exposed zones have aboveground plant traits that favors survival from wave stress (i.e., they experience less drag force from waves by having less stem surface area and more flexible stems) (Heuner et al. 2015; Carus et al. 2016; Silinski et al. 2016). Although these studies indicate that growth and survival capacity under hydrodynamic forcing varies with species-specific plant traits, it is unknown to what extend this extra mechanical stress might enforce the growth response to tidal inundation stress. Nevertheless, this knowledge is crucial to successfully implement tidal marshes as shoreline protection.

1.5 Aim of this thesis

There is an urge to adapt our traditional shoreline protection infrastructure to global changes in order to mitigate the risk of coastal flood hazards. Nature-based shoreline protection strategies provide multiple opportunities of combined benefits. For instance, they can consist of conservation, restoration or creation of tidal marshes in front of dikes, as such contributing to attenuate the landward propagation of waves and currents, and reducing the impacts of waves, currents and erosion risks on dikes behind marshes. However crucial uncertainties on their effectiveness remain. A better understanding on the driving processes of marsh establishment, species growth and marsh stability will help to support the implementation of tidal marshes as nature-based climate mitigation by conservation, restoration and creation of tidal marsh habitats. The focus of this thesis is on mutual plant-wave-sediment interactions with specific attention for the role of species-specific plant-traits in how they determine the spatial-temporal variation in shoreline protection capacity of tidal marshes (Fig. 1.1).
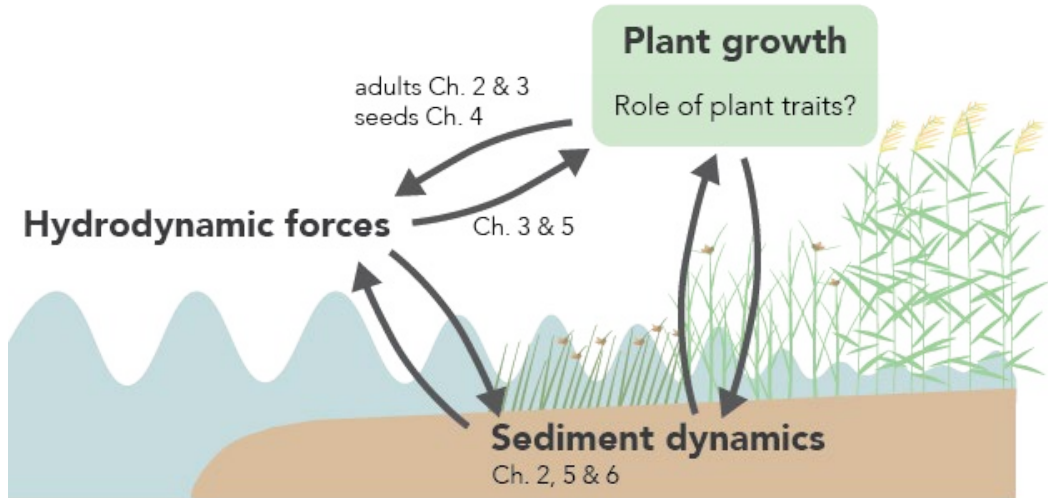
Figure 1.1: Bio-physical interaction have an important impact on the nature-based shoreline protection function of tidal marshes. This scheme of a cross-shore sea-to-land transect of a tidal marsh illustrates the mutual interactions between the three main components, i.e. hydrodynamic forces, plant growth and sediment dynamics. It also illustrates which parts of the bio-physical interactions are investigated in the different chapters of this thesis.

Wave and flow attenuation capacity is typically measured on healthy vegetation during peak biomass. Nevertheless in NW Europe, the pioneer tidal marsh vegetation dies-off in winter which is the period with the strongest hydrodynamic forces and most chance of storm surges. During this time of year, the additional shoreline protection by tidal marshes is most wanted. In **chapter 2**, the shoreline protection capacity of the pioneer tidal marsh zone is explored throughout an entire season of field monitoring, including the winter season.

In **chapter 3**, the trade-off between wave and flow attenuation capacity of the plants on the one hand and the capacity to cope with and grow under exposure to waves and flow is explored. Based on field observations of two tidal marsh species, a conceptual model was proposed to explain how the interaction between species-specific plant traits and the hydrodynamic forces might result in a spatial species distribution.

Tidal marsh restoration and creation involves (re)establishment of vegetation in a (created) suitable habitat. In this case, plant colonization can be the result of (i) clonal expansion, (ii) seedling growth or (iii) settling of adult propagules. **Chapter 4** elaborates on the seedling survival after germination, needed for successful and long-term survival of the tidal marsh. Therefore it is crucial that seedlings survive the first growing season which might involve exposure to extreme wave events. Plant trait dependent survival was tested on four pioneer species with a distinct morphology exposed to extreme waves in a flume.

Chapter 3 and 4 investigate a plant trait dependent survival to hydrodynamic exposure from waves and flow and its potential consequences on the spatial species distribution in tidal marsh pioneer zones. Species specific growth and survival capacity in tidal marshes is suggested to create a species distribution which is often ascribed to tidal inundation stress. However, in exposed fringing marshes where shoreline protection is most wanted, there is a cross-shore gradient in exposure to waves and currents too. Altered plant growth and survival will have implications for the shoreline protection capacity of tidal marshes, therefore, a better understanding of species-specific growth responses is needed. In **chapter 5** the growth response to wave exposure and tidal inundation in relation to species-specific plant traits, is quantified through a field transplantation experiment with in situ manipulation of hydrodynamic exposure to waves and currents in combination with different levels of tidal inundation.

Although the shoreline protection functions of tidal marshes reduce the risk of dike breaches, recent analysis of historical dike breach events have learned that the risk of dike breaching and flood hazards during extreme storm surges remains. In **chapter 6**, a new, additional mechanism of shoreline protection by tidal marshes is explored, i.e. do well-developed tidal marshes in front of a dike breach function as an extra natural barrier against flood water discharge towards the embanked hinterland? Within a flume experiment, the stability of winter-state vegetation and the sediment bed are quantified under extreme flow velocities, which can be expected on the marsh platform during a dike breach.

1.6 Reference

Adams, J. B., J. L. Raw, T. Riddin, J. Wasserman, and L. Van Niekerk. 2021. Salt Marsh Restoration for the Provision of Multiple Ecosystem Services. Diversity **13**. doi:doi.org/10.3390/d13120680

Allen, J. 2000. Morphodynamics of Holocene salt marshes: a review sketch from the Atlantic and Southern North Sea coasts of Europe. Quat. Sci. Rev. **19**: 1155–1231. doi:10.1016/S0277-3791(99)00034-7

Anderson, M. E., and J. M. Smith. 2014. Wave attenuation by flexible, idealized salt marsh vegetation. Coast. Eng. **83**: 82–92. doi:10.1016/j.coastaleng.2013.10.004

Anten, N. P. R., R. Casado-Garcia, and H. Nagashima. 2005. Effects of Mechanical Stress and Plant Density on Mechanical Characteristics, Growth, and Lifetime Reproduction of Tobacco Plants. Am. Nat. **166**: 650. doi:10.2307/3491228

Arkema, K. K., G. Guannel, G. Verutes, and others. 2013. Coastal habitats shield people and property from sea-level rise and storms. Nat. Clim. Chang. **3**: 913–918. doi:10.1038/nclimate1944

Van Asselen, S., P. H. Verburg, J. E. Vermaat, and J. H. Janse. 2013. Drivers of wetland conversion: A global meta-analysis. PLoS One **8**: 1–13. doi:10.1371/journal.pone.0081292

Augustin, L. N., J. L. Irish, and P. Lynett. 2009. Laboratory and numerical studies of wave damping by emergent and near-emergent wetland vegetation. Coast. Eng. **56**: 332–340. doi:10.1016/j.coastaleng.2008.09.004

De Baets, S., J. Poesen, G. Gyssels, and A. Knapen. 2006. Effects of grass roots on the erodibility of topsoils during concentrated flow. Geomorphology **76**: 54–67. doi:10.1016/j.geomorph.2005.10.002

Barber, D. C., S. C. Neubauer, S. C. Hagen, and others. 2016. Contributions of organic and inorganic matter to sediment volume and accretion in tidal wetlands at steady state. Earth's Futur. **4**: 110–121. doi:10.1002/2015ef000334

Barbier, E. B., S. D. Hacker, C. Kennedy, E. W. Koch, A. C. Stier, and B. R. Silliman. 2011. The value of estuarine and coastal ecosystem services. Ecol. Monogr. **81**: 169–193. doi:10.1890/10-1510.1

Bertness, M. D. 1991. Zonation of *Spartina patens* and *Spartina alterniflora* in a New England Salt Marsh. Ecology **72**: 138–148.

Boettle, M., D. Rybski, and J. P. Kropp. 2016. Quantifying the effect of sea level rise and flood defence - A point process perspective on coastal flood damage. Nat. Hazards Earth Syst. Sci. **16**: 559–576. doi:10.5194/nhess-16-559-2016

Bouma, T. J., J. van Belzen, T. Balke, and others. 2016. Short-term mudflat dynamics drive long-term cyclic salt marsh dynamics. Limnol. Oceanogr. 2261–2275. doi:10.1002/lno.10374

Bouma, T. J., M. Friedrichs, P. Klaassen, and others. 2009a. Effects of shoot stiffness, shoot size and current velocity on scouring sediment from around seedlings and propagules. Mar. Ecol. Prog. Ser. **388**: 293–297. doi:10.3354/meps08130

Bouma, T. J., M. Friedrichs, B. K. van Wesenbeeck, S. Temmerman, G. Graf, and P. M. J. Herman. 2009b. Density-dependent linkage of scale-dependent feedbacks: a flume study on the intertidal macrophyte *Spartina anglica*. Oikos **118**: 260–268. doi:10.1111/j.1600-0706.2008.16892.x

Bouma, T. J., M. B. De Vries, and P. M. J. Herman. 2010. Comparing ecosystem engineering efficiency of two plant species with contrasting growth strategies. Ecol. Soc. Am. **91**: 2696–2704. doi:10.1890/09-0690.1

Bouma, T. J., M. B. De Vries, E. Low, G. Peralta, I. C. Tánczos, J. van de Koppel, and P. M. J. Herman. 2005. Trade-offs related to ecosystem engineering: a case study on stiffness of emerging macrophytes. Ecology **86**: 2187–2199. doi:10.1890/04-1588

Van De Broek, M., S. Temmerman, R. Merckx, and G. Govers. 2016. Controls on soil organic carbon stocks in tidal marshes along an estuarine salinity gradient.
Biogeosciences **13**: 6611–6624. doi:10.5194/bg-13-6611-2016

Brooks, H., I. Möller, S. Carr, C. Chirol, E. Christie, B. Evans, K. L. Spencer, and T. Spencer. 2021. Resistance of salt marsh substrates to near-instantaneous hydrodynamic forcing. Earth Surf. Process. Landforms **88**: 67–88. doi:10.1002/esp.4912

Burden, A., R. A. Garbutt, C. D. Evans, D. L. Jones, and D. M. Cooper. 2013. Carbon sequestration and biogeochemical cycling in a saltmarsh subject to coastal managed realignment. Estuar. Coast. Shelf Sci. **120**: 12–20. doi:10.1016/j.ecss.2013.01.014

Bywater-Reyes, S., C. A. Wilcox, C. J. Stella, and A. F. Lightbody. 2015. Flow and scour constraints on uprooting of pioneer woody seedlings. Water Resour. Res. **51**: 9190–9206. doi:doi:10.1002/2014WR016641

Cahoon, D. R., K. L. McKee, and J. T. Morris. 2020. How Plants Influence Resilience of Salt Marsh and Mangrove Wetlands to Sea-Level Rise. Estuaries and Coasts. doi:10.1007/s12237-020-00834-w

Cao, H., Z. Zhu, P. M. J. Herman, S. Temmerman, J. de Smit, L. Zhang, L. Yuan, and T. J. Bouma. 2021. Plant traits determining biogeomorphic landscape dynamics: a study on clonal expansion strategies driving cliff formation at marsh edges. Limnol. Oceanogr. 6–82. doi:10.1002/lno.11915

Carus, J., M. Paul, and B. Schröder. 2016. Vegetation as self-adaptive

coastal protection: Reduction of current velocity and morphologic plasticity of a brackish marsh pioneer. Ecol. Evol. **6**: 1579–1589. doi:10.1002/ece3.1904

Chen, Y., C. E. L. Thompson, and M. B. Collins. 2012. Saltmarsh creek bank stability: Biostabilisation and consolidation with depth. Cont. Shelf Res. **35**: 64–74. doi:10.1016/j.csr.2011.12.009

Cheong, S.-M., B. Silliman, P. P. Wong, B. van Wesenbeeck, C.-K. Kim, and G. Guannel. 2013. Coastal adaptation with ecological engineering. Nat. Clim. Chang. **3**: 787–791. doi:10.1038/nclimate1854

Chirol, C., K. L. Spencer, S. J. Carr, I. Möller, B. Evans, J. Lynch, H. Brooks, and K. R. Royse. 2021. Effect of vegetation cover and sediment type on 3D subsurface structure and shear strength in saltmarshes. Earth Surf. Process. Landforms **46**: 2279–2297. doi:10.1002/esp.5174

Christiansen, T., P. L. Wiberg, and T. G. Milligan. 2000. Flow and Sediment Transport on a Tidal Salt Marsh. Estuaries and Coasts **50**: 315–331. doi:10.1006/ecss.2000.0548

Cloern, J. E., S. Q. Foster, and A. E. Kleckner. 2014. Phytoplankton primary production in the world's estuarine-coastal ecosystems. Biogeosciences **11**: 2477–2501. doi:10.5194/bg-11-2477-2014

Costanza, R., R. D'Arge, R. de Groot, and others. 1997. The value of the world's ecosystem services and natural capital. Nature **387**: 253–260. doi:10.1038/387253a0

Costanza, R., R. de Groot, P. Sutton, S. van der Ploeg, S. J. Anderson, I. Kubiszewski, S. Farber, and R. K. Turner. 2014. Changes in the global value of ecosystem services. Glob. Environ. Chang. **26**: 152–158. doi:10.1016/j.gloenvcha.2014.04.002

Dalrymple, R. A., and R. G. Dean. 1991. Water wave mechanics for engineers and scientists (Vol. 2), Prentice-Hall.

Denny, M. W., and B. Gaylord. 2002. Review the mechanics of wave-swept algae. J. Exp. Biol. **205**: 1355–1362.

Duarte, C. M. 2009. Introduction: Global Loss of Coastal Habitats Rates, Causes and Consequences, p. 14–24. *In* Global Loss of Coastal Habitats Rates, Causes and Consequences.

Feagin, R. a, S. M. Lozada-Bernard, T. M. Ravens, I. Möller, K. M. Yeager, and A. H. Baird. 2009. Does vegetation prevent wave erosion of salt marsh edges? Proc. Natl. Acad. Sci. U. S. A. **106**: 10109–13. doi:10.1073/pnas.0901297106

Feser, F., M. Barcikowska, O. Krueger, F. Schenk, R. Weisse, and L. Xia. 2015. Storminess over the North Atlantic and northwestern Europe-A review. Q. J. R. Meteorol. Soc. **141**: 350–382. doi:10.1002/qj.2364

Ford, H., A. Garbutt, C. Ladd, J. Malarkey, and M. W. Skov. 2016. Soil stabilization linked to plant diversity and environmental

context in coastal wetlands. J. Veg. Sci. **27**: 259–268. doi:10.1111/jvs.12367

Francalanci, S., M. Bendoni, M. Rinaldi, and L. Solari. 2013. Ecomorphodynamic evolution of salt marshes: Experimental observations of bank retreat processes. Geomorphology **195**: 53–65. doi:10.1016/j.geomorph.2013.04.026

French, J. 2006. Tidal marsh sedimentation and resilience to environmental change: Exploratory modelling of tidal, sea-level and sediment supply forcing in predominantly allochthonous systems. Mar. Geol. **235**: 119–136. doi:10.1016/j.margeo.2006.10.009

Garzon, J. L., M. Maza, C. M. Ferreira, J. L. Lara, and I. J. Losada. 2019a. Wave Attenuation by Spartina Saltmarshes in the Chesapeake Bay Under Storm Surge Conditions. J. Geophys. Res. Ocean. **124**: 5220–5243. doi:10.1029/2018JC014865

Garzon, J. L., T. Miesse, and C. M. Ferreira. 2019b. Field-based numerical model investigation of wave propagation across marshes in the Chesapeake Bay under storm conditions. Coast. Eng. **146**: 32–46. doi:10.1016/j.coastaleng.2018.11.001

de Groot, R., L. Brander, S. van der Ploeg, and others. 2012. Global estimates of the value of ecosystems and their services in monetary units. Ecosyst. Serv. **1**: 50–61.

doi:10.1016/j.ecoser.2012.07.005

Gyssels, G., J. Poesen, E. Bochet, and Y. Li. 2005. Impact of plant roots on the resistance of soils to erosion by water: a review. Prog. Phys. Geogr. **29**: 189–217. doi:10.1191/0309133305pp443ra

Hanson, S., R. Nicholls, N. Ranger, S. Hallegatte, J. Corfee-Morlot, C. Herweijer, and J. Chateau. 2011. A global ranking of port cities with high exposure to climate extremes. Clim. Change **104**: 89–111. doi:10.1007/s10584-010-9977-4

Heuner, M., B. Schröder, U. Schröder, and B. Kleinschmit. 2018. Contrasting elevational responses of regularly flooded marsh plants in navigable estuaries. Ecohydrol. Hydrobiol. **19**: 38–53. doi:10.1016/j.ecohyd.2018.06.002

Heuner, M., A. Silinski, J. Schoelynck, and others. 2015. Ecosystem Engineering by Plants on Wave-Exposed Intertidal Flats Is Governed by Relationships between Effect and Response Traits. PLoS One **10**: e0138086. doi:10.1371/journal.pone.0138086

Hinkel, J., D. Lincke, A. T. Vafeidis, and others. 2014. Coastal flood damage and adaptation costs under 21st century sea-level rise. Proc. Natl. Acad. Sci. U. S. A. **111**: 3292–3297. doi:10.1073/pnas.1222469111

Hu, Z., T. Suzuki, T. Zitman, W. Uittewaal, and M. Stive. 2014. Laboratory study on wave

dissipation by vegetation in combined current-wave flow. Coast. Eng. **88**: 131–142. doi:10.1016/j.coastaleng.2014.02.009

Hughes, R. G. 2004. Climate change and loss of saltmarshes: Consequences for birds. Ibis (Lond. 1859). **146**: 21–28. doi:10.1111/j.1474-919X.2004.00324.x

Jonkman, S. N., M. M. Hillen, R. J. Nicholls, W. Kanning, and M. van Ledden. 2021. Costs of Adapting Coastal Defences to Sea-Level Rise — New Estimates and Their Implications. J. Coast. Conserv. **29**: 1212–1226. doi:10.2112/JCOASTRES-D-12-00230.1

Joyeux, E., A. Carpentier, F. Corre, S. Haie, and J. Pétillon. 2017. Impact of salt-marsh management on fish nursery function in the bay of Aiguillon (French Atlantic coast), with a focus on European sea bass diet. J. Coast. Conserv. **21**: 435–444. doi:10.1007/s11852-017-0501-0

Kirezci, E., I. R. Young, R. Ranasinghe, S. Muis, R. J. Nicholls, D. Lincke, and J. Hinkel. 2020. Projections of global-scale extreme sea levels and resulting episodic coastal flooding over the 21st Century. Sci. Rep. **10**: 1–12. doi:10.1038/s41598-020-67736-6

Kirwan, M. L., and J. P. Megonigal. 2013. Tidal wetland stability in the face of human impacts and sea-level rise. Nature **504**: 53–60. doi:10.1038/nature12856

Kirwan, M. L., S. Temmerman, E. E. Skeehan, G. R. Guntenspergen, S. Fagherazzi, and S. Faghe. 2016. Overestimation of marsh vulnerability to sea level rise. Nat. Clim. Chang. **6**: 253–260. doi:10.1038/nclimate2909

Kitsikoudis, V., V. S. O. Kirca, O. Yagci, and M. F. Celik. 2017. Clear-water scour and flow field alteration around an inclined pile. Coast. Eng. **129**: 59–73. doi:10.1016/j.coastaleng.2017.09.001

Koch, E. W., E. B. Barbier, B. R. Silliman, and others. 2009. Non-linearity in ecosystem services: temporal and spatial variability in coastal protection. Front. Ecol. Environ. **7**: 29–37. doi:10.1890/080126

Van de Koppel, J., D. Van der Wal, J. P. Bakker, and P. M. J. Herman. 2005. Self-Organization and Vegetation Collapse in Salt Marsh Ecosystems. Am. Nat. **165**: 1–12.

Lefeuvre, J. C., V. Bouchard, E. Feunteun, S. Grare, P. Laffaille, and A. Radureau. 2000. European salt marshes diversity and functioning: The case study of the Mont Saint-Michel bay, France. Wetl. Ecol. Manag. **8**: 147–161. doi:10.1023/a:1008440401950

Lenk, S., D. Rybski, O. Heidrich, R. J. Dawson, and J. P. Kropp. 2016. Costs of sea dikes &amp;ndash; regressions and uncertainty estimates. Nat. Hazards Earth Syst. Sci. Discuss. 1–21. doi:10.5194/nhess-2016-270

Leonardi, N., N. K. Ganju, and S. Fagherazzi. 2015. A linear

relationship between wave power and erosion determines salt-marsh resilience to violent storms and hurricanes. Proc. Natl. Acad. Sci. **113**: 64–68. doi:10.1073/pnas.1510095112

van Loon-Steensma, J. M., and H. A. Schelfhout. 2017. Wide Green Dikes: A sustainable adaptation option with benefits for both nature and landscape values? Land use policy **63**: 528–538. doi:10.1016/j.landusepol.2017.02.002

Lotze, H. K., H. S. Lenihan, B. J. Bourque, and others. 2006. Depletion, Degradation, and Recovery Potential of Estuaries and Coastal Seas. Science (80-.). **312**: 1806–1809. doi:10.1126/science.1128035

MacManus, K., D. Balk, H. Engin, G. McGranahan, and R. Inman. 2021. Estimating Population and Urban Areas at Risk of Coastal Hazards, 1990–2015: How data choices matter,.

Macreadie, P. I., Q. R. Ollivier, J. J. Kelleway, and others. 2017. Carbon sequestration by Australian tidal marshes. Sci. Rep. **7**: 1–10. doi:10.1038/srep44071

Marijnissen, R., P. Esselink, M. Kok, C. Kroeze, and J. M. van Loon-Steensma. 2020. How natural processes contribute to flood protection - A sustainable adaptation scheme for a wide green dike. Sci. Total Environ. **739**: 139698. doi:10.1016/j.scitotenv.2020.139698

McGranahan, G., D. Balk, and B. Anderson. 2007. The rising tide: Assessing the risks of climate change and human settlements in low elevation coastal zones. Environ. Urban. **19**: 17–37. doi:10.1177/0956247807076960

Mcluskey, D. S., and M. Elliott. 2004. The estuarine ecosystem: Ecology, threats and management, Third. Oxford University Press.

Mcowen, C. J., L. V. Weatherdon, J. W. Van Bochove, and others. 2017. A global map of saltmarshes. Biodivers. Data J. **5**. doi:10.3897/BDJ.5.e11764

Mendez, F. J., and I. J. Losada. 2004. An empirical model to estimate the propagation of random breaking and nonbreaking waves over vegetation fields. Coast. Eng. **51**: 103–118. doi:10.1016/j.coastaleng.2003.11.003

Möller, I. 2006. Quantifying saltmarsh vegetation and its effect on wave height dissipation: Results from a UK East coast saltmarsh. Estuar. Coast. Shelf Sci. **69**: 337–351. doi:10.1016/j.ecss.2006.05.003

Möller, I. 2019. Applying uncertain science to nature-based coastal protection: Lessons from shallow wetland-dominated shores. Front. Environ. Sci. **7**. doi:10.3389/fenvs.2019.00049

Möller, I., M. Kudella, F. Rupprecht, and others. 2014. Wave attenuation over coastal salt marshes under storm surge conditions. Nat. Geosci. **7**: 727–731. doi:10.1038/ngeo2251

Möller, I., and T. Spencer. 2002. Wave dissipation over macro-tidal

saltmarshes: Effects of marsh edge typology and vegetation change. J. Coast. Res. **36**: 506–521. doi:10.2112/1551-5036-36.sp1.506

Morris, R. L., A. Boxshall, and S. E. Swearer. 2020. Climate-resilient coasts require diverse defence solutions. Nat. Clim. Chang. **10**: 485–487. doi:10.1038/s41558-020-0798-9

Mudd, S. M., A. D'Alpaos, and J. T. Morris. 2010. How does vegetation affect sedimentation on tidal marshes? Investigating particle capture and hydrodynamic controls on biologically mediated sedimentation. J. Geophys. Res. Earth Surf. **115**: 1–14. doi:10.1029/2009JF001566

Mury, A., A. Collin, T. Houet, E. Alvarez-Vanhard, and D. James. 2020. Using multispectral drone imagery for spatially explicit modeling of wave attenuation through a salt marsh meadow. Drones **4**: 1–12. doi:10.3390/drones4020025

Narayan, S., M. W. Beck, B. G. Reguero, and others. 2016. The Effectiveness, Costs and Coastal Protection Benefits of Natural and Nature-Based Defences. PLoS One **11**: e0154735. doi:10.1371/journal.pone.0154735

Neumann, B., A. T. Vafeidis, J. Zimmermann, and R. J. Nicholls. 2015. Future coastal population growth and exposure to sea-level rise and coastal flooding - A global assessment. PLoS One **10**. doi:10.1371/journal.pone.0118571

Nicholls, R. J., and A. Cazenave. 2010. Sea-Level Rise and Its Impact on Coastal Zones. Science (80-.). **328**: 1517–1520. doi:10.1126/science.1185782

Van Niekerk, L., J. B. Adams, G. C. Bate, and others. 2013. Country-wide assessment of estuary health: An approach for integrating pressures and ecosystem response in a data limited environment. Estuar. Coast. Shelf Sci. **130**: 239–251. doi:10.1016/j.ecss.2013.05.006

Oppenheimer, M., B. Glavovic, J. Hinkel, and others. 2019. Sea Level Rise and Implications for Low Lying Islands, Coasts and Communities. IPCC Spec. Rep. Ocean Cryosph. a Chang. Clim. **355**: 126–129. doi:10.1126/science.aam6284

Paquier, A. E., J. Haddad, S. Lawler, and C. M. Ferreira. 2016. Quantification of the Attenuation of Storm Surge Components by a Coastal Wetland of the US Mid Atlantic. Estuaries and Coasts 1–17. doi:10.1007/s12237-016-0190-1

Pennings, S. C., M. Grant, and M. D. Bertness. 2005. Plant zonation in low-latitude salt marshes : disentangling the roles of flooding , salinity and competition. J. Coast. Res. **93**: 159–167. doi:10.1111/j.1365-2745.2004.00959.x

Prahl, B. F., M. Boettle, L. Costa, J. P. Kropp, and D. Rybski. 2018. Data Descriptor: Damage and protection cost curves for coastal floods within the 600 largest European cities. Sci. Data

5: 1–18. doi:10.1038/sdata.2018.34

Prosser, D. J., T. E. Jordan, J. L. Nagel, R. D. Seitz, D. E. Weller, and D. F. Whigham. 2019. Impacts of Coastal Land Use and Shoreline Armoring on Estuarine Ecosystems: an Introduction to a Special Issue. Estuaries and Coasts **42**: 912. doi:10.1007/s12237-018-00505-x

Puijalon, S., T. J. Bouma, C. J. Douady, J. van Groenendael, N. P. R. Anten, E. Martel, and G. Bornette. 2011. Plant resistance to mechanical stress: evidence of an avoidance-tolerance trade-off. New Phytol. **191**: 1141–9. doi:10.1111/j.1469-8137.2011.03763.x

Reed, D., B. Van Wesenbeeck, P. M. J. Herman, and E. Meselhe. 2018. Tidal flat-wetland systems as flood defenses : Understanding biogeomorphic controls. Estuar. , Coast. Shelf Sci. **213**: 269–282. doi:10.1016/j.ecss.2018.08.017

Reguero, B. G., M. W. Beck, D. N. Bresch, J. Calil, and I. Meliane. 2018. Comparing the cost effectiveness of nature-based and coastal adaptation: A case study from the Gulf Coast of the United States. PLoS One **13**: 1–24. doi:10.1371/journal.pone.0192132

van Rooijen, A. A., J. S. M. van Thiel de Vries, R. T. McCall, A. R. van Dongeren, J. A. Roelvink, and A. J. H. M. Reniers. 2015. Modeling of wave attenuation by vegetation with XBeach. E-proceedings 36th IAHR World Congr. 7.

Rupprecht, F., I. Möller, M. Paul, and others. 2017. Vegetation-wave interactions in salt marshes under storm surge conditions. Ecol. Eng. **100**: 301–315. doi:10.1016/j.ecoleng.2016.12.030

Schoelynck, J., T. de Groote, K. Bal, W. Vandenbruwaene, P. Meire, and S. Temmerman. 2012. Self-organised patchiness and scale-dependent bio-geomorphic feedbacks in aquatic river vegetation. Ecography (Cop.). **35**: 760–768. doi:10.1111/j.1600-0587.2011.07177.x

Schoelynck, J., S. Puijalon, P. Meire, and E. Struyf. 2015. Thigmomorphogenetic responses of an aquatic macrophyte to hydrodynamic stress. Front. Plant Sci. **6**: 1–7. doi:10.3389/fpls.2015.00043

Schoonees, T., A. Gijón Mancheño, B. Scheres, T. J. Bouma, R. Silva, T. Schlurmann, and H. Schüttrumpf. 2019. Hard Structures for Coastal Protection, Towards Greener Designs. Estuaries and Coasts **42**: 1709–1729. doi:10.1007/s12237-019-00551-z

Schuerch, M., T. Spencer, and B. Evans. 2019. Coupling between tidal mudflats and salt marshes affects marsh morphology. Mar. Geol. **412**. doi:10.1016/j.margeo.2019.03.008

Schuerch, M., T. Spencer, S. Temmerman, and others. 2018. Future response of global coastal wetlands to sea-level rise. Nature **561**: 231–234.

doi:10.1038/s41586-018-0476-5

Schulze, D., F. Rupprecht, S. Nolte, and K. Jensen. 2019. Seasonal and spatial within - marsh differences of biophysical plant properties : implications for wave attenuation capacity of salt marshes. Aquat. Sci. **81**: 1–11. doi:10.1007/s00027-019-0660-1

Shepard, C. C., C. M. Crain, and M. W. Beck. 2011. The protective role of coastal marshes: A systematic review and meta-analysis. PLoS One **6**. doi:10.1371/journal.pone.0027374

Silinski, A., M. Heuner, P. Troch, and others. 2016. Effects of contrasting wave conditions on scour and drag on pioneer tidal marsh plants. Geomorphology **255**: 49–62. doi:10.1016/j.geomorph.2015.11.021

Silinski, A., K. Schoutens, S. Puijalon, J. Schoelynck, D. Luyckx, P. Troch, P. Meire, and S. Temmerman. 2018. Coping with waves: Plasticity in tidal marsh plants as self-adapting coastal ecosystem engineers. Limnol. Oceanogr. **63**: 799–815. doi:10.1002/lno.10671

Silvestri, S., A. Defina, and M. Marani. 2005. Tidal regime, salinity and salt marsh plant zonation. Estuar. Coast. Shelf Sci. **62**: 119–130. doi:10.1016/j.ecss.2004.08.010

Small, C., and R. J. Nicholls. 2003. A global analysis of human settlement in coastal zones. J. Coast. Res. **19**: 584–599. doi:10.2307/4299200

Smolders, S., Y. Plancke, S. Ides, P. Meire, and S. Temmerman. 2015. Role of intertidal wetlands for tidal and storm tide attenuation along a confined estuary: A model study. Nat. Hazards Earth Syst. Sci. **15**: 1659–1675. doi:10.5194/nhess-15-1659-2015

Stark, J., T. Van Oyen, P. Meire, and S. Temmerman. 2015. Observations of tidal and storm surge attenuation in a large tidal marsh. Limnol. Oceanogr. **60**: 1371–1381. doi:10.1002/lno.10104

Sutton-Grier, A. E., K. Wowk, and H. Bamford. 2015. Future of our coasts: The potential for natural and hybrid infrastructure to enhance the resilience of our coastal communities, economies and ecosystems. Environ. Sci. Policy **51**: 137–148. doi:10.1016/j.envsci.2015.04.006

Taherkhani, M., S. Vito, P. L. Barnar, N. Frazer, T. R. Anderson, and C. H. Fletcher. 2020. Sea-level rise exponentially increases coastal flood frequency. Sci. Rep. **10:6466**: 1–17. doi:10.1038/s41598-020-62188-4

Temmerman, S., T. J. Bouma, J. Van de Koppel, D. Van der Wal, M. B. De Vries, and P. M. J. Herman. 2007. Vegetation causes channel erosion in a tidal landscape. Geology **35**: 631. doi:10.1130/G23502A.1

Temmerman, S., and M. L. Kirwan. 2015. Building land with a rising sea. Science (80-.). **349**: 588–9. doi:10.1126/science.aac8312

Temmerman, S., P. Meire, T. J. Bouma, P. M. J. Herman, T. Ysebaert, and H. J. De Vriend. 2013. Ecosystem-based coastal defence in the face of global change. Nature **504**: 79–83. doi:10.1038/nature12859

Tempest, J. A., I. Möller, and T. Spencer. 2015. A review of plant-flow interactions on salt marshes: the importance of vegetation structure and plant mechanical characteristics. Wiley Interdiscip. Rev. Water **2**: 669–681. doi:10.1002/wat2.1103

Townend, I., C. Fletcher, M. Knappen, and K. Rossington. 2011. A review of salt marsh dynamics. Water Environ. J. **25**: 477–488. doi:10.1111/j.1747-6593.2010.00243.x

Vitousek, S., P. L. Barnard, C. H. Fletcher, N. Frazer, L. Erikson, and C. D. Storlazzi. 2017. Doubling of coastal flooding frequency within decades due to sea-level rise. Sci. Rep. **7**: 1–9. doi:10.1038/s41598-017-01362-7

Vousdoukas, M. I., L. Mentaschi, E. Voukouvalas, A. Bianchi, F. Dottori, and L. Feyen. 2018. Climatic and socioeconomic controls of future coastal flood risk in Europe. Nat. Clim. Chang. **8**: 776–780. doi:10.1038/s41558-018-0260-4

Vuik, V., B. W. Borsje, P. W. J. M. Willemsen, and S. N. Jonkman. 2019. Salt marshes for flood risk reduction: Quantifying long-term effectiveness and life-cycle costs. Ocean Coast. Manag. **171**: 96–110. doi:10.1016/j.ocecoaman.2019.01.010

Vuik, V., S. N. Jonkman, B. W. Borsje, and T. Suzuki. 2016. Nature-based flood protection: The efficiency of vegetated foreshores for reducing wave loads on coastal dikes. Coast. Eng. **116**: 42–56. doi:10.1016/j.coastaleng.2016.06.001

Wang, H., D. van der Wal, X. Li, and others. 2017. Zooming in and out: Scale dependence of extrinsic and intrinsic factors affecting salt marsh erosion. J. Geophys. Res. Earth Surf. **122**: 1455–1470. doi:10.1002/2016JF004193

Willemsen, P. W. J. M., B. W. Borsje, V. Vuik, T. J. Bouma, J. M. Suzanne, and H. Hulscher. 2020. Field-based decadal wave attenuating capacity of combined tidal flats and salt marshes. Coast. Eng. **156**. doi:10.1016/j.coastaleng.2019.103628

Wu, W. C., G. Ma, and D. T. Cox. 2016. Modeling wave attenuation induced by the vertical density variations of vegetation. Coast. Eng. **112**: 17–27. doi:10.1016/j.coastaleng.2016.02.004

Xin, P., B. Gibbes, L. Li, Z. Song, and D. Lockington. 2010. Soil saturation index of salt marshes subjected to spring-neap tides a new variable for describing marsh soil aeration condition. Hydrol. Process. **24**: 2564–2577.

Xue, L., X. Li, B. Shi, B. Yang, S. Lin, Y. Yuan, Y. Ma, and Z. Peng. 2021. Pattern-regulated wave attenuation by salt marshes in the Yangtze Estuary, China. Ocean Coast. Manag. **209**: 105686. doi:10.1016/j.ocecoaman.2021.105686

Yang, S. L., B. W. Shi, T. J. Bouma, T. Ysebaert, and X. X. Luo. 2012. Wave attenuation at a salt marsh margin : A case study of an exposed coast on the Yangtze Estuary. Estuaries and Coasts **35**: 169–182. doi:10.1007/s12237-011-9424-4

Young, I. R., and A. Ribal. 2019. Multiplatform evaluation of global trends in wind speed and wave height. Science (80-.). **364**: 548–552. doi:10.1126/science.aav9527

Ysebaert, T., S. Yang, L. Zhang, Q. He, T. J. Bouma, and P. M. J. Herman. 2011. Wave attenuation by two contrasting ecosystem engineering salt marsh macrophytes in the intertidal pioneer zone. Wetlands **31**: 1043–1054. doi:10.1007/s13157-011-0240-1

van Zelst, V. T. M., J. T. Dijkstra, B. K. van Wesenbeeck, D. Eilander, E. P. Morris, H. C. Winsemius, P. J. Ward, and M. B. de Vries. 2021. Cutting the costs of coastal protection by integrating vegetation in flood defences. Nat. Commun. **12**: 1–11. doi:10.1038/s41467-021-26887-4

Zhang, X., P. Lin, Z. Gong, B. Li, and X. Chen. 2020. Wave Attenuation by Spartina alterniflora under Macro-Tidal and Storm Surge Conditions. Wetlands **40**: 2151–2162. doi:10.1007/s13157-020-01346-w

Zhu, Z., V. Vuik, P. J. Visser, and others. 2020. Historic storms and the hidden value of coastal wetlands for nature-based flood defence. Nat. Sustain. doi:10.1038/s41893-020-0556-z

2

How effective are tidal marshes as nature-based shoreline protection throughout seasons?

Ken Schoutens, Maike Heuner, Vanessa Minden, Tilla Schulte Ostermann, Alexandra Silinski, Jean-Philippe Belliard, Stijn Temmerman

2.1 Abstract

Nature-based mitigation is increasingly proposed as a strategy to cope with global change and related risks for coastal flooding and erosion. Tidal marshes are known to provide shoreline protection as their aboveground biomass attenuates waves and their belowground biomass contributes to reducing erosion rates. The aim of this study was to quantify how effectively wave attenuation rates and erosion reduction rates are sustained throughout seasons in pioneer tidal marshes in the Elbe estuary (Germany). Changes in hydrodynamics and sediment dynamics were measured during 17 months along three sea-to-land transects of 50 m length. Simultaneously, changes in biomass of the monospecific pioneer vegetation (*Bolboschoenus maritimus)* were measured monthly. This study shows that wave and flow attenuation rates positively correlate with seasonal variations in aboveground biomass, that is: in summer, aboveground biomass and associated wave and flow attenuation rates are highest; while aboveground biomass is washed away during the first storms in autumn or winter, resulting in low wave and flow attenuation rates. Contrastingly, maximum incoming wave heights and flow velocities occur during winter, indicating that wave and flow attenuation is most needed then. However, hibernating root biomass assures low erosion rates in winter, especially at sandy sites. Although wave attenuation by pioneer marshes is highly variable throughout seasons and pioneer marshes alone are not so effective, they might facilitate the survival of higher marshes. Therefore, it is important to conserve or restore a gradual sea-to-land gradient from tidal flats, over pioneer marsh to high marsh to provide nature-based shoreline protection.

2.2 Introduction

Coastal societies are experiencing an increasing risk of flooding and shoreline erosion. Recent storm events including cyclone Haiyan in the Philippines (2013) and hurricanes Irma and Maria in the Caribbean (2017) highlight the vulnerability of coastal societies. As a result of climate change, such extreme storm surges are expected to increase in frequency and intensity over the coming decades (Allison et al. 2009; Bender et al. 2010; Woolf and Wolf 2013). Sea level rise (from the seaward side) and increasing human activities (from the landward side) in the coastal zone amplify the pressure on shorelines even more. Hence, global change necessitates novel, long-term sustainable approaches to protect coasts, deltas, and estuaries against flood and shoreline erosion risks induced by sea level rise, storm surges, and human activities.

Apart from traditional coastal protection by hard structures, such as seawalls and dikes only, nature-based solutions are increasingly proposed as an additional, sustainable shoreline protection strategy (Cheong et al. 2013; Temmerman et al. 2013; Sutton-Grier et al. 2015). In this context, the conservation or creation of tidal marsh ecosystems between the sea and the hard defenses in front of coastal communities provides protective functions (Costanza et al. 2008; Duarte et al. 2013; Temmerman and Kirwan 2015) such as wave attenuation (Ysebaert et al. 2011; Yang et al. 2012; Möller et al. 2014), sediment stabilization and accretion (French 2006; Mudd et al. 2010; Kirwan and Megonigal 2013; Ma et al. 2014), and storm surge attenuation (Wamsley et al. 2010; Smolders et al. 2015; Stark et al. 2015; Van Coppenolle et al. 2018). Apart from flood and erosion risk reduction, tidal marsh ecosystems provide other valuable ecosystem services, including water quality regulation, carbon sequestration, contribution to fisheries production and recreation (Barbier et al. 2011), which is why nature-based solutions have multiple benefits in addition to traditional hard structures (Turner et al. 2007; Narayan et al. 2016, 2017; Arkema et al. 2017). Furthermore, combining nature-based and hard defense structures, e.g., by restoring or conserving tidal marshes in front of dikes or breakwaters forms a cost-effective measure due to the self-sustaining character of tidal marshes which have the ability to adapt to sea level rise by sediment accretion (Temmerman and Kirwan 2015; Kirwan et al. 2016).

Marsh vegetation exerts friction to the water motion and thereby attenuates currents and waves (Yang et al. 2012; Möller et al. 2014; Carus et al. 2016; Vuik et al. 2016). Even narrow fringes at the seaward edge of dikes have a stabilizing effect since the majority of incoming wave height, and thereby wave energy, is reduced in the first few meters of the pioneer marsh (80% over <50 m, Ysebaert et al. 2011; 20–40% over 12 m, Silinski et al. 2017). Although water depth on marshes is higher during storm surge conditions and the rate of wave attenuation is known to be reduced with greater water depth (Gedan et al. 2011; Yang et al. 2012), flume studies under simulated storm conditions show that up to 60% of wave height reduction can be attributed to marsh

vegetation (Möller et al. 2014). Reduced hydrodynamic forces decrease the risk of sediment erosion and stimulate sediment deposition on the marsh surface (Mudd et al. 2010). In the pioneer zone (i.e., the gradually sloping transition zone between bare tidal flats and densely vegetated marshes, which is vegetated by pioneer plant species), however, vegetation density-dependent processes such as turbulence around single shoots or increased current speed around vegetation patches might also cause local scouring or erosion (Bouma et al. 2009; Silinski et al. 2016*b*).

The efficiency of wave attenuation and erosion risk reduction by vegetation depends on the plant morphological traits (Barbier et al. 2008; Tempest et al. 2015). Both field and flume studies showed that higher standing biomass, higher shoot densities, and higher stiffness enhance wave attenuation (Bouma et al. 2010; Ysebaert et al. 2011; Silinski et al. 2017). Most studies focused on the effects of aboveground biomass on wave and current attenuation, while the role of belowground biomass in erosion risk reduction has long been neglected (Bouma et al. 2014). Recently, a mesocosm experiment showed that the presence of a belowground root network can enhance the stability and reduce the erodibility of the sediment (Wang et al. 2017). Additionally, field and flume studies emphasize the function of belowground biomass for reducing erosion of the sediment surface of tidal marshes (Coops et al. 1996; Chen et al. 2012; Francalanci et al. 2013). Even after harsh storm conditions in winter, the marsh surface has been observed to remain stable (Spencer et al. 2015).

Most above-mentioned field studies on wave attenuation and erosion risk reduction by tidal marshes are based on observations during relatively short periods in summer when vegetation biomass is maximal. However, in temperate climate regions, where tidal marsh vegetation depicts seasonal growth cycles, these results cannot be extrapolated to a full year. In particular, in regions where plants die back in winter and standing biomass diminishes (e.g., Charpentier and Stuefer 1999; Coulombier et al. 2012; Silinski et al. 2016*a*), marshes may be less effective in wave and erosion risk reduction in winter. In many cases, the winter period is associated with a higher storm activity. Historical records of storm surges along the coast of northwest Europe show that most severe events occurred during winter (e.g., Saint Marcellus flood 1219 and 1362, North Sea flood 1953, but also more recent floods such as cyclone Xavier in 2013 and cyclone Burglind in 2018) which coincide with most historical dike failures (van Baars and van Kempen 2009) as a result of wave overtopping (Stanczak et al. 2007; Morris et al. 2009; Steendam et al. 2011; Le Hai and Verhagen 2014). Therefore, existing studies on wave attenuation in marshes during summer peak-biomass conditions give an overestimation of year-round wave attenuation capacity of temperate zone tidal marshes.

The aim of this article is to quantify the impact of seasonal differences of both aboveground and belowground tidal marsh plant biomass on wave attenuation and

erosion-sedimentation rates. This research was conducted in a temperate-zone tidal marsh in the Elbe estuary (Germany) during a 17 months period from December 2015 to April 2017. We address the following research questions: Are wave attenuation rates (i.e., the reduction of wave height with distance traveled through the marsh) (1) directly related to temporal (seasonal) changes in aboveground biomass and (2) lowest in winter when aboveground biomass is minimal? In other words, how effective is the marsh in attenuating waves in winter? To what extend is the sediment stabilizing effect induced by the vegetation reduced in winter compared to summer? Are erosion rates on the marsh still lower compared to the adjacent tidal flat as a result of stabilization by below-ground hibernating biomass?

2.3 Methods

2.3.1 Study sites

Field work was conducted in the Elbe estuary (Germany, 53° 47° N, 9° 22° E) which is one of the principal waterways in Western Europe of high economic and natural value. It is both geomorphologically and ecologically comparable to other NW European estuaries. Intertidal marsh sites were chosen based on the following criteria: (1) presence of monospecific stands of *Bolboschoenus maritimus* (L.) Palla, which is the dominant pioneer species in brackish marshes in NW European estuaries; (2) continuous marsh edge, parallel to the estuarine subtidal channel; (3) gently sloping transition between bare tidal flat and marsh (slope $\leq 1^{\circ}$); and (4) absence of obstructions (e.g., riprap) on the seaward side of the marsh (Fig. 2.1). The halophyte *B. maritimus* forms clonal stands of fast growing aboveground shoots, which can reach stem heights of up to 2 m (Silinski et al. 2017) and which die off and are flushed away in autumn and winter (*see* supplementary Fig. 2.1). Belowground tubers and a dense root network ensure the survival in winter and the regrowth of new shoots in spring. Three sampling sites (Balje: $53^{\circ}51^{\circ}23.5^{\circ\circ}$N, $9^{\circ}4^{\circ}9.2^{\circ\circ}$E; Hollerwettern: $53^{\circ}49^{\circ}55.5^{\circ\circ}$N, $9^{\circ}22^{\circ}17.4^{\circ\circ}$E; and Krautsand: $53^{\circ}46^{\circ}32.3^{\circ\circ}$N, $9^{\circ}22^{\circ}5.9^{\circ\circ}$E) were selected in the brackish part of the estuary. The salinity ranges from 0.3 PSU to 4.0 PSU and the semidiurnal tidal range is on average 2.8 m (1.6 m during neap tide and 3.8 m during spring tide) in all three sites (2015–2017). Mean freshwater discharge of the Elbe (1926–2014) is 712 m^3 s^{-1} ranging from 560 m^3 s^{-1} in summer to 866 m^3 s^{-1} in winter (Strotmann 2014). Suspended sediment concentration varies as a positive function of freshwater discharge between 0.3 kg m^{-3} and 1.0 kg m^{-3} (Bundesanstalt für Gewässerkunde, Blasi et al. 2014). The wind climate is shown in supplementary Fig. 2.2, and it is characterized by winds predominantly blowing from the southwest (DWD Climate Data Center 2019).
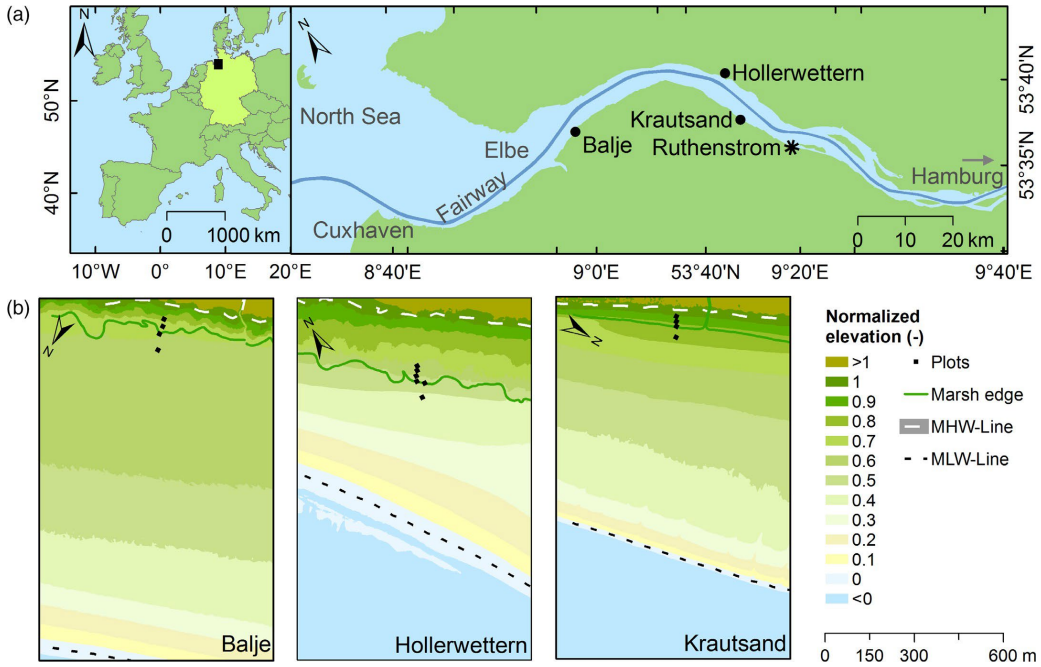
Figure. 2.1: Location and characteristics of the study sites along the Elbe estuary in Germany. (a) Location of the Elbe estuary in Europe and of the three study sites: Balje, Hollerwettern, Krautsand together with Ruthenstrom weather station. (b) The elevation maps for all sites showing the marsh edge and width of the tidal flat as well as the mean low and high water level (MLW and MHW). The elevations are normalized by tidal range as (Elevation − Mean low water)/(Mean high water − Mean low water).

2.3.2 Monitoring plots

At each study site, a cross-shore transect of 40 m length, starting at the bare tidal flat 20 m in front of the seaward marsh edge and reaching 20 m into the marsh, was set up. Elevations ranged between −1.0 m MSL (relative to local mean sea level) on the tidal flat and −0.2 m MSL in the marsh at Balje, between −1.5 m MSL and −0.5 m MSL at Hollerwettern, and between −0.6 m MSL and 0.0 m MSL at Krautsand. Within the marsh, the measurement plots were set up at an interval of 10 m (Fig. 2.2). At each plot wave heights, sedimentation-erosion rates, sediment properties, and vegetation biomass (within the marsh over a 15 m stretch parallel to the marsh edge) were monitored.

2.3.3 Measurements

2.3.3.1 Hydrodynamics

Waves

Wave heights were measured continuously over 17 months from December 2015 until April 2017. We deployed three pressure sensors along the transect at each of the three sites (i.e., nine wave sensors in total), i.e., at the marsh edge, 10 m into the marsh and 20 m into the marsh. Wave attenuation on the tidal flat (representing nonvegetated conditions with only bed friction) was measured during three measurement campaigns of 1–2 weeks in March, August, and January by deploying an additional pressure sensor 20 m from the marsh on the tidal flat (Fig. 2.2). The automated pressure sensors (P-Log3021-MMC, Driesen & Kern) sampled at a frequency of 8 Hz. Pressure data were then converted into water surface elevation with a Matlab routine. Raw data (absolute pressure) were first corrected for atmospheric pressure (DWD Climate Data Center, Ruthenstrom: 7.0 m above ground surface) and then converted into meters of water. Resulting water levels were corrected for depth-dependent pressure attenuation based on linear wave theory (Dalrymple and Dean 1991). Next, a low-pass filter with a cutoff frequency of 0.002 Hz was used to separate the tidal signal (i.e., slow water level changes with a semidiurnal period) from the wave signal (i.e., fast water level fluctuations with a period in the order of seconds). Waves resulted from both wind-generated and ship-generated waves; however, no distinction was made for further analyses. From the processed wave data, we calculated significant wave height (H_s, mean of the highest third of recorded waves) and $H_{1/100}$ (mean of the highest 1% of recorded waves) over 10 min time intervals. The relative wave attenuation rate (R) was calculated as $R = (H_{in} - H_{10m})/H_{in} \times 100$ (%), where H_{in} are the incoming significant wave heights at the seaward edge of the *B. maritimus*-zone and H_{10m} are the significant wave heights at 10 m into the *B. maritimus*-zone.
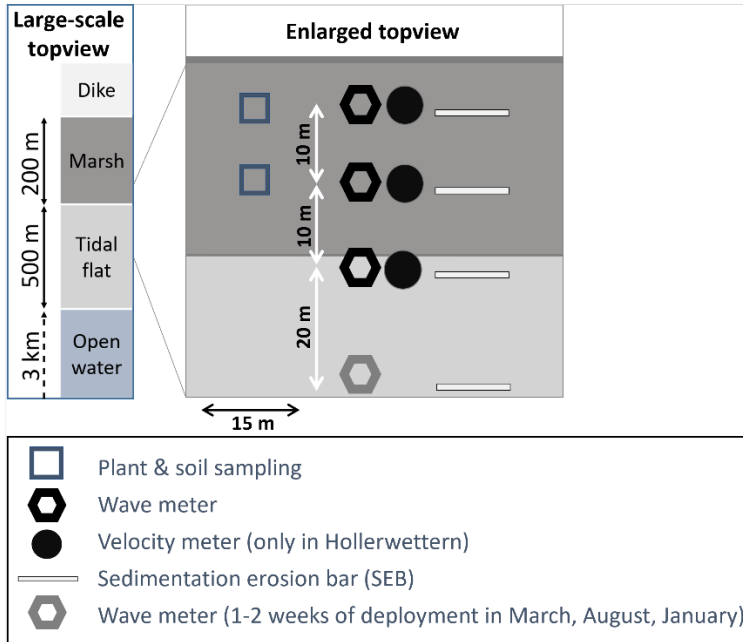
Figure 2.2: Top view of the monitoring setup along the cross-shore transect at each of the three sites. At each plot, wave heights, sedimentation-erosion rates, sediment properties, and vegetation biomass were measured.

Flow velocity

Flow velocities were measured with three ADVs (Acoustic Doppler Velocity sensors, Nortek) at one of the transects (Hollerwettern, Figs. 2.1, 2.2). They were positioned horizontally with the central beam at 0.10 m above the sediment surface. Raw data were filtered for beam correlations below 70% after which the planar velocity was calculated as $U = u^2 + v^2$ (m s^{-1}) with u and v being the two horizontal flow velocities (m s^{-1}) perpendicular to each other. Flow attenuation rate was calculated in the same way as the wave attenuation rate (see above). Wave and flow data were compared with hourly wind data of the Ruthenstrom station (Fig. 2.1) obtained from the German Meteorological Office (DWD Climate Data Center 2019).

2.3.3.2 Sediment properties and dynamics

The erosion-sedimentation rates at each plot along the transects were monitored next to the pressure sensors (Fig. 2.2), so that elevation changes could be correlated to wave heights. By monitoring elevation changes on the tidal flat and in the marsh, we could compare elevation changes without and with presence of belowground biomass. Monthly measurements were conducted with sedimentation erosion bars (SEBs), each consisting of two vertically positioned poles 2.0 m apart and inserted 1.0 m into the sediment bed, on top of which a horizontal bar was placed as reference level to measure

sediment surface elevation changes (van Wijnen and Bakker 2001; Nolte et al. 2013; Silinski et al. 2016*a*). The SEBs were installed parallel to the marsh edge and for each SEB, the sediment surface elevation was measured at 10 replicate locations at 10 cm horizontal distance intervals with a vertical accuracy in the order of 1.5 mm. Additionally, site-specific sediment characteristics were quantified monthly on three replicate samples per plot. Samples from the sediment bed were taken with a Kopecky ring (4.6 cm in diameter and 5.2 cm high) and used to determine dry bulk density and water contents (after drying at 70°C for 72 h). Next, the same samples were used to perform grain size analyses with a Mastersizer 2000 (Malvern) after a combined H_2O_2 and HCl treatment to remove organic compounds and disperse aggregates. Organic matter content was determined with loss on ignition, i.e., by ashing the samples at 550°C for 6 h.

2.3.3.3 Plant biomass
Biomass of *B. maritimus* was measured monthly from February 2016 until February 2017. Aboveground biomass was sampled by clipping all shoots in 0.2 m × 0.2 m quadrants (if needed this was repeated until a minimum of 20 shoots was reached). To derive the aboveground biomass per square meter, shoot densities were determined per plot by counting the number of shoots (i.e., dead and living) within three permanent quadrats of 0.4 m × 0.4 m. Belowground plant biomass was quantified three times, i.e., in April, August, and December 2016 by taking three replicate soil cores per plot with a diameter of 0.1 m up to a depth of 0.45 m. After rinsing, biomass was quantified as dry weight (drying at 70°C for 72 h) per square meter of soil.

2.3.4 Data analyses
All analyses were performed in R 3.3.1. (R Core Team, 2016) and significance was assumed at $p < 0.05$ for all tests. Prior to statistical analyses, the data were checked for normality based on visual inspection of histograms and normal Q-Q plots. If needed, transformations (logarithmic or square root) of the data were applied to approximate normal distribution. We explored if temporal variations in significant wave height were correlated with wind speed (hourly intervals) and sedimentation-erosion rates (monthly intervals). Wind directions were taken into account by making the correlation for different classes of wind direction (every class represents 45°, e.g., the "North" direction corresponds to all wind speeds ranging in between 337.5° and 22.5°). We tested correlations between wave attenuation rate, water depth (temporal, 10 min intervals), and aboveground biomass (spatial and temporal, monthly intervals) as well as between sedimentation-erosion rates (temporal, monthly intervals) and aboveground biomass (temporal, monthly intervals). For correlations with wave attenuation rates, we used the nonparametric Spearman's rank coefficient (rho, i.e., ρ). The Pearson correlation coefficients (*r*) were calculated for all other correlations. The

variables tested for correlation were recast where necessary for a matter of data consistency. The temporal and spatial effect of aboveground biomass on wave attenuation was explored by multiple linear regression taking into account the sites and time of the year (month). Visualizing the wave, wind, and current velocity data by applying a simple moving average (over one tide) reveals the potential seasonal trends in the time series. Comparisons of the mean flow and wave attenuation rates in summer (defined as the period May–August) and winter (defined as the period December–March) were performed using a Wilcoxon signed-rank test. Local polynomial regression (LOESS) was applied to the monthly measurements (time series) of aboveground biomass and sedimentation-erosion rates.

2.4 Results

2.4.1 Incoming waves and flow velocities at the marsh edges

Wave heights entering the *B. maritimus* vegetation are shown throughout the seasons from December 2015 until May 2017 (Fig. 2.3). Over the whole monitoring period, the average significant wave height was 0.09 m and the average maximum wave height was 0.30 m (Table 2.1). In winter, time periods were measured with significant wave heights up to 1.0 m and maximum wave heights up to 1.5 m (based on the 10 min interval data). These extremes were observed during three distinct tides (26 December 2016, 04 January 2017, and 12 January 2017) and coincided with high-wind speeds coming from the west and northwest (Fig. 2.3). Overall, Hollerwettern was the most exposed site with longer and more frequent inundation periods and Krautsand the least exposed site as a result of its higher elevation (Table 2.1). Median wave heights are comparable between the three sites. Gaps in the data resulted from removing the wave or ADV sensors from the field to prevent frost damage, from battery failure or from non-inundated periods. Highest flow velocities coincided with highest wind speeds (from December 2016 to mid-March 2017). Wind speeds and significant wave heights were well correlated with the longest wind fetch directions per site, i.e., NW directions in Balje; Spearman's ρ = 0.60; $p < 0.05$, SW, NW and SE directions in Hollerwettern; Spearman's ρ = 0.74, 0.64, and 0.50, respectively; $p < 0.05$ and NW directions in Krautsand; Spearman's ρ = 0.70; $p < 0.05$.

2.4.2 Wave and flow attenuation over the marsh transects

The seasonal effect of vegetation as physical buffer for waves is clearly demonstrated by the change in wave attenuation rates from winter to summer and back to winter (Fig. 2.4). Over a 10 m stretch of *B. maritimus* vegetation, wave heights were attenuated up to 50% in summer while in winter a maximum attenuation of only 10% was reached. The wave attenuation rate decreased with increasing water depth over the course of individual tidal cycles ($F_{21;37,576}$ = 1383, R^2 = 0.44, $p < 0.05$). Moreover, at water depths higher than 1.5 m, no seasonal change in wave attenuation rate was observed. In Balje,

wave attenuation rates were >10% higher than in the other two sites during the whole year. Although there was a clear summer-peak of wave attenuation rate in all sites, the decline in Balje and Hollerwettern started in August until September, while in Krautsand wave attenuation rate only decreased in December 2016. Wave attenuation rates within the marsh during winter are in the same range as on the bare tidal flat. Here, wave attenuation rates stay below 10% all year long (based on short term measurement periods of 1–2 weeks in March and August 2016 and January 2017). Flow attenuation rates were significantly higher in summer and spring situations (>15% higher attenuation rates) than during the two winter periods (Fig. 2.5).

2.4.3 Sediment characteristics and dynamics

The changes in sediment surface elevation varied between sites and between the tidal flat and the tidal marsh. Median grain sizes are all <125 µm and differ between the sites (Fig. 2.6b). Balje has the finest grain size (34% sand, 63% silt, and 3% clay) with mainly silt while Krautsand (69% sand, 30% silt, and 1% clay) is dominated by sandy sediments and Hollerwettern (56% sand, 42% silt, and 2% clay) has an intermediate grain size distribution. Over the entire measurement period, the tidal flat in Krautsand experienced periods of severe erosion (Fig. 2.6a), in particular during the winter of 2016. In Hollerwettern, there was some erosion in winter, but a net sedimentation was observed over the entire measurement period. In contrast, elevation changes on the tidal flat in Balje were limited. In the tidal marsh, the patterns for Hollerwettern and Balje are comparable to the ones on the tidal flat with an overall net sedimentation. In Krautsand, however, a strong sedimentation up to >15 cm was observed. During the field campaigns, benthic biofilms were only visually observed on the tidal flat in Balje and Hollerwettern. Significant incoming wave heights increased erosion risk in Krautsand ($F_{1,74}$ = 15.34, p < 0.05), but no effect was found for Hollerwettern and Balje ($F_{1,102}$ = 2.41, p > 0.05 and $F_{1,87}$ = 0.49, p > 0.05, respectively). Wave attenuation and elevation change were only correlated in Krautsand (Spearman's ρ = 0.53, p < 0.05).
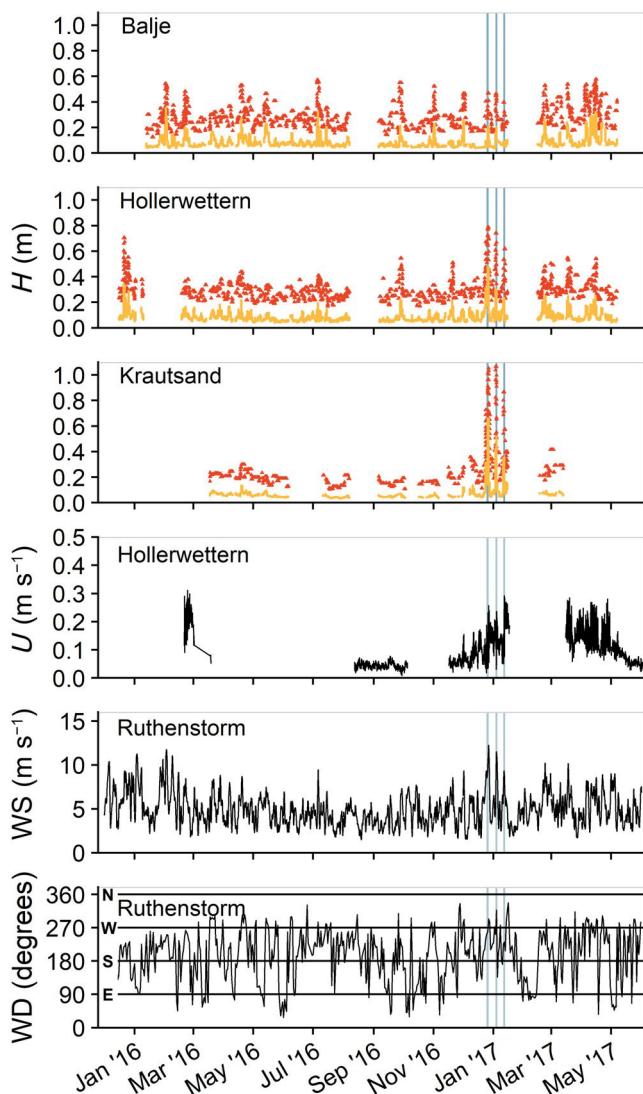
Figure 2.3: Significant wave height (H_s, yellow squares) and $H_{1/100}$ (mean of the highest 1% of recorded waves, red triangles) are represented as the moving average over one tide and are shown for the three study sites. Planar flow velocity (U; m s^{-1}) at the marsh edge in Hollerwettern, wind speed (WS; m s^{-1}) and wind direction (WD; degree) at the weather station Ruthenstrom are represented as a moving average (calculated over 3 h from 10 min interval flow data and calculated over 24 h from hourly interval wind data). These data are shown from December 2015 until May 2017. Storm days in winter are marked with vertical (blue) lines.

2.4.4 Plant biomass

Aboveground plant biomass was lowest during the winter months with only small dead shoot stumps remaining (<50 g m^{-2}) (Fig. 2.7a). The biomass increased rapidly in May

and growth continued until peak biomass (700–900 g m^{-2}) was reached in mid-August. Hollerwettern showed a slightly lower peak biomass (500–700 g m^{-2}). After peak biomass was reached in summer, it started to decrease earlier in Balje and Hollerwettern (August) while the high biomass in Krautsand remained longer before the decrease started (September–October). Concerning the belowground biomass, no significant temporal or site specific differences were observed (Fig. 2.7b). Closer to the marsh edge, belowground biomass is consistently lower compared to 20 m into the marsh.

2.4.5 Relation between biomass and wave attenuation and erosion-sedimentation rates

Aboveground biomass correlated positively with wave attenuation rates at all sites (Fig. 2.8). Furthermore, from this figure, it can be seen that observations during periods of low-water depths lie above the regression lines and observations during periods of higher water depths lie mainly below the regression lines. Multiple linear regression shows that wave attenuation rate is explained by aboveground biomass (partial R^2 = 0.42) and there is indeed an important effect of water depth (partial R^2 = 0.28) ($F_{5,84}$ = 42.94, $p < 0.05$, R^2 = 0.70). The friction effect of the bed topography is shown by the intercept which is similar in Balje and Hollerwettern and slightly higher in Krautsand. No relation was found between aboveground biomass and sedimentation-erosion rates (R^2 = 0.02, $p > 0.05$) nor between belowground biomass and wave attenuation rates (R^2 = 0.03, $p > 0.05$).

Table 2.1: Overview of the main hydrodynamic variables per site over the entire monitoring campaign measured at the marsh edge of each respective study site; mean inundation depth (I_{depth}, m), mean inundation time per tide (I_{time}, min), percentage of time inundated (I_{perc}, %), median of the significant wave heights (H_s, m), median maximum wave height ($H_{1/100}$, m), highest wave (H_{max}, m), median planar flow velocity (U, m s^{-1}), and normalized elevation at the marsh edge (Z_{norm}).

Site	I_{depth} (m)	I_{time} (min)	I_{perc} (%)	H_s (m)	$H_{1/100}$ (m)	H_{max} (m)	U (m s^{-1})	Z_{norm}
Balje	0.70	263	35	0.09	0.15	0.91	0.11	0.66
Hollerwettern	1.14	374	50	0.10	0.17	1.28	0.09	0.50
Krautsand	0.43	177	21	0.09	0.16	1.72	0.07	0.83
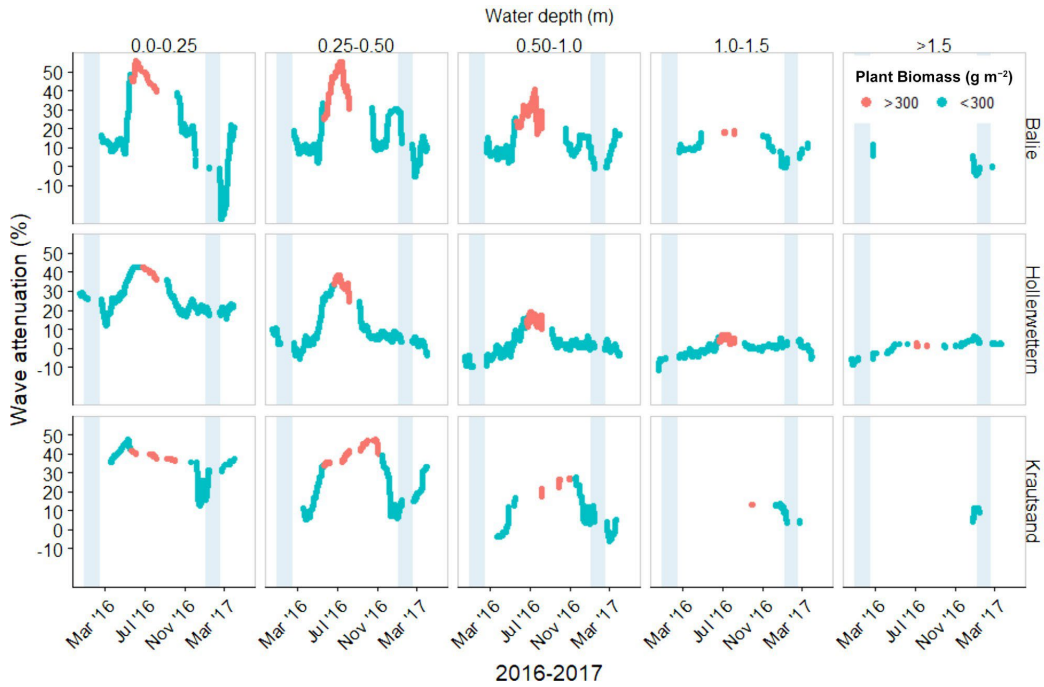
Figure 2.4: Wave attenuation rate over 10 m of *B. maritimus* at the three study sites from winter 2015 to spring 2017 for different water depths during the tidal inundated periods. Lines represent a moving average of the wave attenuation rate (calculated over windows of 3 d, based on 10 min interval data) and red colors represent the period of high standing biomass (>300 g m^{-2}, *see* Fig. 2.7) while blue colors represent the low biomass conditions during winter (<300 g m^{-2}). The periods indicated by blue background are periods of frost and potential ice formation, which is likely to affect the wave data and therefore these periods were excluded from the data analysis.
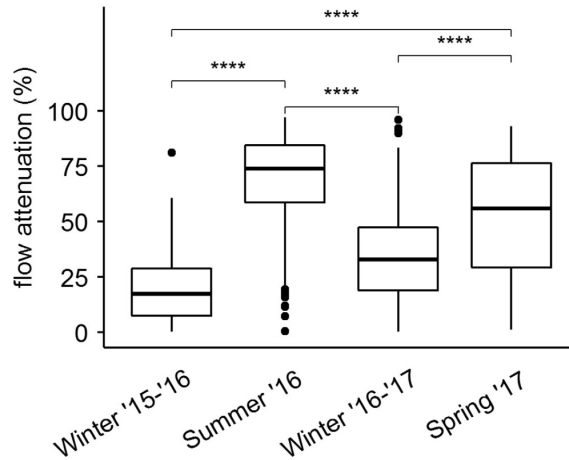
Figure 25: Flow attenuation rates over 10 m of *B. maritimus* in Hollerwettern. The boxplots represent the summer and winter periods (10 min intervals). Comparisons of the medians were performed using a Wilcoxon rank sum test with the asterisks representing the significance level of $\alpha = 0.001$.

2.5 Discussion

Tidal pioneer marshes in the temperate climate regions may lose much of their aboveground biomass in winter which temporarily reduces the efficiency of the marsh for shoreline protection. Although the general processes of wave attenuation (Ysebaert et al. 2011; Yang et al. 2012; Möller et al. 2014; Silinski et al. 2017) and erosion reduction (Chen et al. 2012; Francalanci et al. 2013; Wang et al. 2017) by tidal marshes are well studied, studies are mostly done under peak-biomass (summer) conditions while studies under lower biomass (winter) conditions are sparse (Coulombier et al. 2012; Spencer et al. 2015; Vuik et al. 2016). In this study, we quantify seasonal changes in wave attenuation rates and sedimentation-erosion rates in pioneer marsh vegetation. We showed that the wave attenuation capacity of the pioneer tidal marsh vegetation is strongly reduced in winter, when incoming wave heights are highest during storms, and hence when marsh-induced shoreline protection is most needed. In contrast, sediment stabilization is maintained due to the presence of hibernating belowground biomass especially at sandy sites.

At our field sites, strongest hydrodynamic conditions (both significant wave heights and flow velocities) occur during winter. This is a combined effect of higher wind speeds (Fig. 2.3) and higher river discharge (560 m^3 s^{-1} in summer vs. 866 m^3 s^{-1} in winter) (Bundesanstalt für Gewässerkunde 2014; Kappenberg et al. 2016). Along the coast of northwest Europe, the most severe storm events and dike failures typically occurred during winter (see above-mentioned historical records). This highlights that shoreline protection in northwest Europe is most needed during the winter period.

Although Krautsand has the lowest median wave heights throughout the year (Table 2.1), highest wave heights were recorded here during three distinct storm tides in the winter of 2016–2017. This can be explained by the morphological characteristics of the tidal flat and marsh. It has an overall higher elevation as compared to the two other study sites, which reduces the inundation depth and therefore limits the wave heights during normal tides. However, the concave cross-sectional shape of the tidal flat creates a short and steep slope right in front of the marsh edge, which during storm surge conditions (i.e., higher water depths) allows the landward propagation of higher waves (*see* supplementary Fig. 2.3 on cross-sectional profiles of the three study sites).
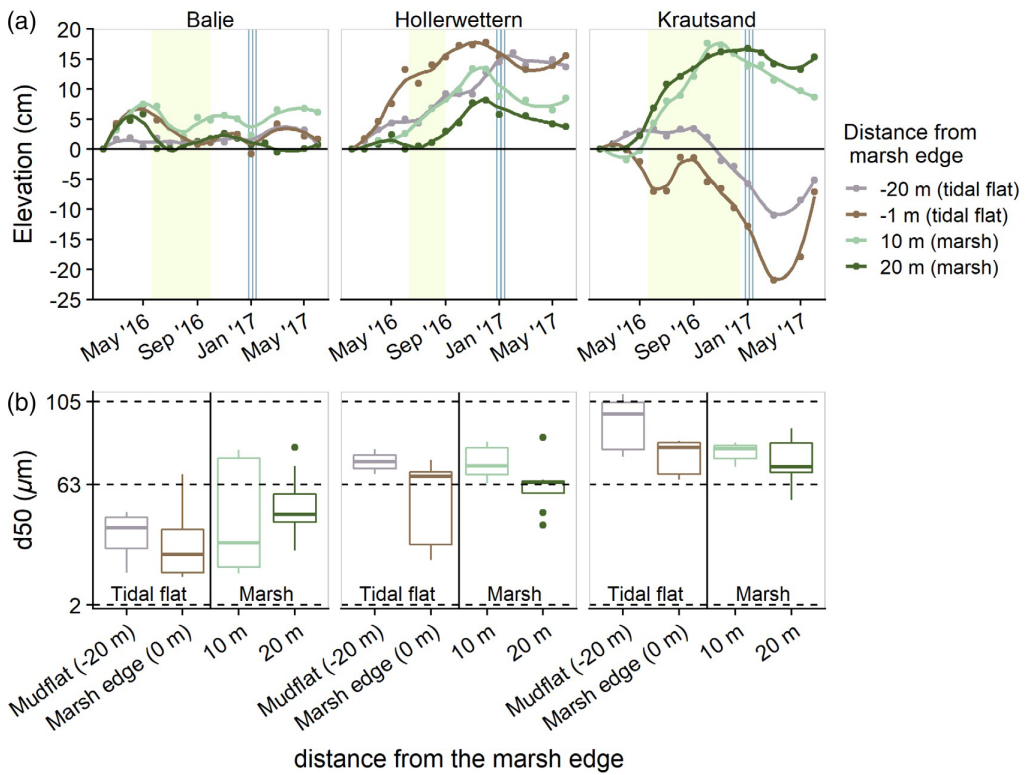
Figure 2.6: (a) Elevation (cm) relative to the first measurement at the three study sites from February 2016 to June 2017 for different distances from the marsh edge. Negative distances are on the tidal flat and positive distances are at the landward side of the marsh edge (monthly measurements; $n = 10$). The green shaded areas delineate the period of high biomass (>300 g m^{-2}, see Fig. 2.7). Storm days in winter are marked with vertical blue lines. (b) Median sediment grain size (d50 in µm) for the three sites and for different distances from the marsh edge ($n = 9$).

The wave and flow attenuation rates that are reported in the literature, and that were typically measured during summer peak-biomass conditions (Leonard and Croft 2006; Ysebaert et al. 2011; Silinski et al. 2017), are in the same range as our measurements

for summer peak biomass. However in the present study, wave and flow attenuation rates were measured throughout the season. In contrast to the rates in summer, wave and flow attenuation rates were almost negligible in winter (Figs. 2.4, 2.5). Regarding flow attenuation rates, these findings are supported by the measurements done by Carus et al. (2016) who covered two sites along the brackish part of the Elbe and measured flow attenuation rates in *B. maritimus* both under unvegetated (April) and vegetated (August) conditions. These contrasting attenuation rates between summer and winter emphasize the necessity to evaluate the shoreline protection capacity of tidal marshes throughout a full yearly cycle, taking into account the low-biomass periods of the pioneer zone during winter. In addition, wave attenuation rates decrease with water depth (Figs. 2.4, 2.8) and when water depths exceed 1.5 m the attenuation effect of pioneer marshes is negligible even during the summer season with peak biomass. This observation highlights the importance of wave attenuation in higher marshes landwards of the pioneer zone. Even though pioneer marshes lose their wave attenuation capacity during deeper inundation periods, it may be expected that the higher marshes will take over this function.

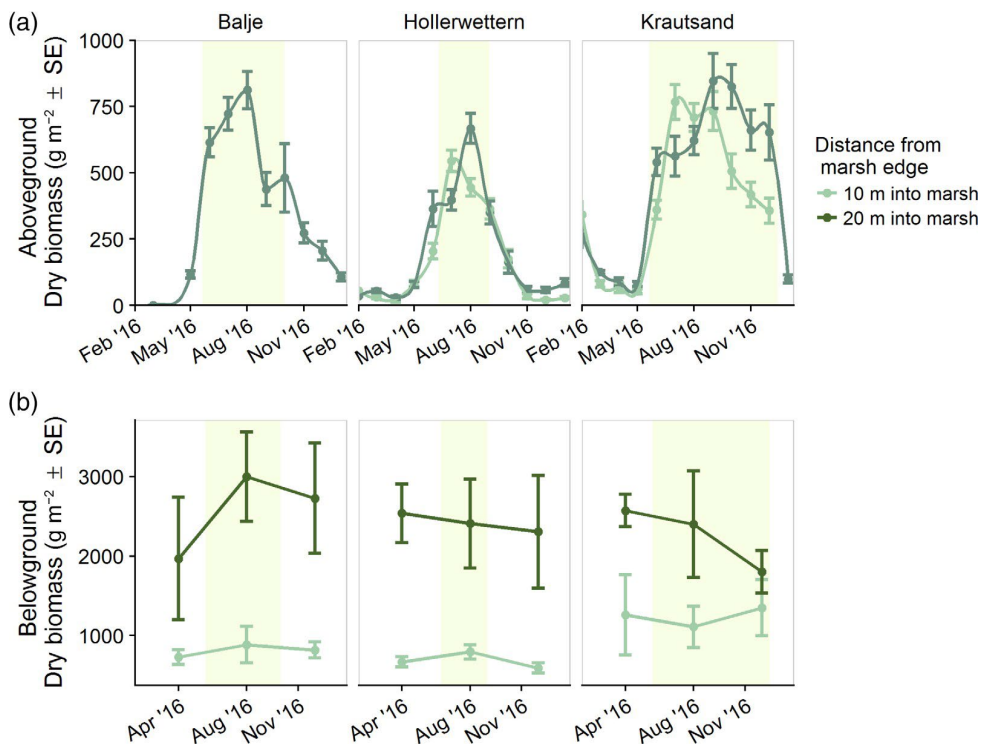Figure 2.7: Time series of (a) aboveground (n >20) and (b) belowground (n = 3) dry biomass/m^2 per site in the period between February 2016 and January 2017 for two distances in the marsh. The green shaded area indicates the period of high aboveground biomass (>300 g m^{-2}). Data of aboveground biomass at 10 m into the marsh in Balje are left out of the graph because *B. maritimus* was dominated by another

species (*Schoenoplectus tabernaemontani*) after 2–3 months in the growing season of 2016.

Under average inundation depths, the wave attenuation rates reflect the seasonal changes in aboveground biomass as they increase rapidly at the start of the growing season beginning of May, reaching a peak in August, and decreasing simultaneously at the end of the growing season (compare Figs. 2.4, 2.7). At the marsh sites of Balje and Hollerwettern, the aboveground biomass starts to decrease already directly after August from September to December (Fig. 2.7). At the marsh of Krautsand, the aboveground biomass is not washed away immediately in autumn and thus wave attenuation rates remain high in autumn and only drop after the first winter storms have removed this biomass (i.e., after the stormy days of 26 December 2016, 27 December 2016, 04 January 2017, and 12 January 2017; compare Figs. 2.3, 2.7). The reason why biomass is washed away later in Krautsand as compared to the other two marsh sites, is probably because of the higher location of the marsh edge, i.e., causing a shorter inundation time and lower inundation frequency (Table 2.1) in combination with low incoming wave heights during fall (Fig. 2.3) which allows the decaying vegetation to remain without being washed away. Only when significant wave heights start to increase (December 2016– January 2017 at Krautsand), the aboveground biomass starts to decrease (Figs. 2.3, 2.7). This suggests that waves play a role in breaking off the decaying vegetation and subsequently washing away the broken stems (Vuik et al. 2018). As a result, biomass removal happens earlier at sites exposed to stronger wave conditions.
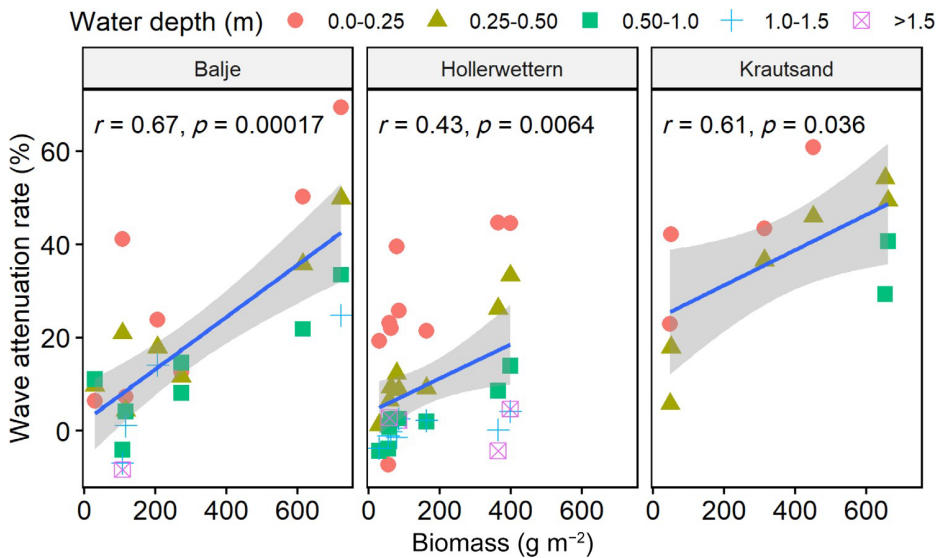

Figure 2.8: The relation between aboveground plant biomass (g m^{-2}) and the wave attenuation rate (%) (average calculated over 1 week time period, i.e., 5 d before until 1 d after sampling of the biomass) for the three sites. Linear regression lines with

confidence intervals (95%) are displayed. The different symbols refer to water depths (m) at which the wave attenuation rate was measured.

Although aboveground biomass of the pioneer vegetation is washed away, the belowground biomass persists throughout winter (Fig. 2.7). The role of the belowground biomass for reducing erosion risk is not straightforward to interpret from our results as the biomass-effect seems to interact with other variables that influence the erosion-sedimentation rates. The sediment composition seems to be an important variable. At the more sandy site (Krautsand), the roots within the marsh seem to protect the sediment from erosion during the winter period, in contrast to the eroding unvegetated tidal flat (Fig. 2.6). However, this discrepancy between eroding tidal flat and protected marsh was not visible at the other two sites which are characterized by finer sediments that are expected to be more cohesive and thus less vulnerable to erosion by hydrodynamic forcing (Hjulstrom 1935). Furthermore, the presence of benthic diatoms probably enhanced the sediment stability in the latter two sites (Sutherland et al. 1998). For these two sites, the hydrodynamic forcing might not have been strong enough to see any response. This suggests that especially in areas with sandy sediment, which typically has a noncohesive nature and is less prone to developing a diatom film, the presence of belowground biomass contributes most to increased sediment cohesion and hence to erosion reduction (Vannoppen et al. 2017). Although the stabilizing effect of belowground biomass for soil erosion reduction in terrestrial landscapes is known (De Baets et al. 2008; Francalanci et al. 2013; Vannoppen et al. 2015), the functional role in reducing erosion throughout all seasons has not been described yet.

We highlight that our study focused on pioneer tidal marshes, i.e., at the seaward edge of marshes (first 20 m), where in temperate climate zones the aboveground decaying biomass is washed away in winter due to incoming waves and tidal currents. In contrast to pioneer tidal marshes, we observed that the aboveground biomass in the more landward and higher portions of the studied marshes (>100 m landwards) remains relatively unchanged during winter. Although the vegetation in the high marshes deteriorates, not all dead stems are flushed away and a considerable part of the aboveground biomass remains standing even during winter. This might be the combined consequence of lower wave heights and less frequent inundation as a result of the higher elevation and friction with the bottom and a change in species composition. For instance, the higher marshes in this brackish part of the Elbe are often dominated by *Phragmites australis*, which might have a different response to hydrodynamic forces. When marshes are broad and high enough, the wave attenuation function of the whole marsh is thus not necessarily lost in winter. Furthermore, the low pioneer tidal marshes sustain erosion risk reduction during winter and as such contribute to the erosion protection of the more landward, higher located marsh portions. Our results showed the role of belowground biomass in reducing erosion

risks under sandy conditions; however, we could not observe erosion events at sites with finer sediments. These findings especially emphasize the importance of a sequence of marsh developmental stages over the sea-to-land gradient, consisting of a minimal width of low pioneer tidal marshes to ensure the erosion protection and persistence of a high marsh in the more landward direction. Hence, we argue that it is important to have a gradually sloping sea-to-land sequence from tidal flat, over low pioneer tidal marsh, to high marsh, to provide effective nature-based shoreline protection. Future research on the wave attenuation capacity and sediment stability (and other shoreline protection functions such as reduced wave reflection and storm surge attenuation) during the winter period, including the more landward located higher portions of marshes, should give better insights in seasonal changes to predict threshold marsh widths that ensure the shoreline protection function throughout seasons.

Our findings show that nature-based shoreline protection by conserving, restoring, or creating tidal marshes should take into account the seasonal dependency of the protection function of tidal marshes in terms of wave attenuation and erosion reduction. In winter, during the main storm season, wave attenuation rates in pioneer tidal marshes are reduced due to the annual biological cycle of these plants. Management and policy makers should take into account that the width of tidal marshes and a sequence of gradually sloping low to high marshes are crucial to ensure sufficient wave attenuation and by extend, shoreline protection throughout the year.

2.6 Acknowledgments

2.7 References

Allison, I., and others. 2009. The Copenhagen Diagnosis, 2009: Updating the World on the Latest Climate Science. The Univ. of New South Wales Climate Change Research Centre, Sydney, Australia, 60pp.

Arkema, K. K., R. Griffin, S. Maldonado, J. Silver, J. Suckale and A. D. Guerry. 2017. Linking social, ecological, and physical science to advance natural and nature-based protection for coastal communities. Ann. N. Y. Acad. Sci. 1399: 5–26. doi:10.1111/nyas.13322

Barbier, E. B., and others. 2008. Coastal ecosystem-based management with nonlinear ecological functions and values supporting material. Science 319: 321–323. doi:10.1126/ science.1150349

Barbier, E. B., S. D. Hacker, C. Kennedy, E. W. Koch, A. C. Stier, and B. R. Silliman. 2011. The value of estuarine and coastal ecosystem services. Ecol. Monogr. 81: 169–193. doi: 10.1890/10-1510.1

Blasi, C., Winterscheid, A. and others, Bundesanstalt für Gewässerkunde. 2014. Sediment management Tideelbe Strategien und Potenziale - Systemstudie II- Ökologische Auswirkungen der Unterbringung von Feinmaterial. Im Auftrag des Wasser- und Schifffahrtsamtes Hamburg. doi:10.5675/BfG-1763

Bender, M. A., T. R. Knutson, R. E. Tuleya, J. J. Sirutis, G. A. Vecchi, S. T. Garner, and I. M. Held. 2010. Modeled impact of anthropogenic warming on the frequency of intense Atlantic hurricanes. Science 327: 454–458. doi:10.1126/ science.1180568

Bouma, T. J., M. Friedrichs, B. K. van Wesenbeeck, S. Temmerman, G. Graf, and P. M. J. Herman. 2009. Density- dependent linkage of scale-dependent feedbacks: A flume study on the intertidal macrophyte *Spartina anglica*. Oikos 118: 260–268. doi:10.1111/j.1600-0706.2008.16892.x

Bouma, T. J., M. B. De Vries, and P. M. J. Herman. 2010. Comparing ecosystem engineering efficiency of two plant species with contrasting growth strategies. Ecol. Soc. Am. 91: 2696–2704. doi:10.1890/09-0690.1

Bouma, T. J., and others. 2014. Identifying knowledge gaps hampering application of intertidal habitats in coastal protection: Opportunities & steps to take. Coast. Eng 87: 147–157. doi:10.1016/j.coastaleng.2013.11.014

Carus, J., M. Paul, and B. Schröder. 2016. Vegetation as self-adaptive coastal protection: Reduction of current velocity and morphologic plasticity of a brackish marsh pioneer. Ecol. Evol. 6: 1579–1589. doi:10.1002/ece3.1904

Charpentier, A., and J. F. Stuefer. 1999. Functional specialization of ramets in *Scirpus maritimus* - splitting the tasks of sexual

reproduction, vegetative growth, and resource storage. Plant Ecol 141: 129–136. doi:10.1023/A:1009825905117

Chen, Y., C. E. L. Thompson, and M. B. Collins. 2012. Saltmarsh creek bank stability: Biostabilisation and consolidation with depth. Cont. Shelf Res. 35: 64–74. doi: 10.1016/j.csr.2011.12.009

Cheong, S.-M., B. Silliman, P. P. Wong, B. van Wesenbeeck, C.-K. Kim, and G. Guannel. 2013. Coastal adaptation with ecological engineering. Nat. Clim. Chang. 3: 787–791. doi: 10.1038/nclimate1854

Coops, H., N. Geilen, H. J. Verheij, R. Boeters, and G. Van der Velde. 1996. Interactions between waves, bank erosion and emergent vegetation: An experimental study in a wave tank. Aquat. Bot. 53: 187–198. doi:10.1016/0304-3770(96)01027-3

Costanza, R., O. Pérez-Maqueo, M. L. Martinez, P. Sutton, S. J. Anderson, and K. Mulder. 2008. The value of coastal wetlands for hurricane protection. Ambio 37: 241–248. doi: 10.1579/0044-7447(2008)37[241:tvocwf]2.0.co;2

Coulombier, T., U. Neumeier, and P. Bernatchez. 2012. Sediment transport in a cold climate salt marsh (St. Lawrence Estuary, Canada), the importance of vegetation and waves. Estuar. Coast. Shelf Sci. 101: 64–75. doi:10.1016/j.ecss.2012.02.014

Dalrymple, R. A., and R. G. Dean. 1991. Water wave mechanics for engineers and scientists, v. 2. Prentice-Hall. doi: 10.1142/1232

De Baets, S., J. Poesen, B. Reubens, K. Wemans, J. De Baerdemaeker, and B. Muys. 2008. Root tensile strength and root distribution of typical Mediterranean plant species and their contribution to soil shear strength. Plant Soil 305: 207–226. doi:10.1007/s11104-008-9553-0

Duarte, C. M., I. J. Losada, I. E. Hendriks, I. Mazarrasa, and N. Marbà. 2013. The role of coastal plant communities for climate change mitigation and adaptation. Nat. Clim. Chang. 3: 961–968. doi:10.1038/nclimate1970

DWD Climate Data Center. 2019. Ftp://Ftp-Cdc.Dwd.de/Pub/CDC/Observations_germany/Climate/Hourly/Pressure/Recent/.

Francalanci, S., M. Bendoni, M. Rinaldi, and L. Solari. 2013. Ecomorphodynamic evolution of salt marshes: Experimental observations of bank retreat processes. Geomorphology 195: 53–65. doi:10.1016/j.geomorph.2013.04.026

French, J. 2006. Tidal marsh sedimentation and resilience to environmental change: Exploratory modelling of tidal, sea level and sediment supply forcing in predominantly allochthonous systems. Mar. Geol. 235: 119–136. doi: 10.1016/j.margeo.2006.10.009

Gedan, K. B., M. L. Kirwan, E. Wolanski, E. B. Barbier, and R. Silliman.

2011. The present and future role of coastal wetland vegetation in protecting shorelines: Answering recent challenges to the paradigm. Clim. Change 106: 7–29. doi:10.1007/s10584-010-0003-7

Hjulstrom, F. 1935. Studies of the morphological activity of rivers as illustrated by the River Fyris. Bull. Geol. Inst. Upsalsa 25: 221–527.

Kappenberg, J., M. Berendt, N. Ohle, R. Riethmüller, D. Schuster, and T. Strotmann. 2016. Seasonal, spring-neap and tidal variation of hydrodynamics and water constituents in the mouth of the Elbe Estuary, Germany. Ocean Sci. Discuss. doi:10.5194/os-2016-7

Kirwan, M. L., and J. P. Megonigal. 2013. Tidal wetland stability in the face of human impacts and sea-level rise. Nature 504: 53–60. doi:10.1038/nature12856

Kirwan, M. L., S. Temmerman, E. E. Skeehan, G. R. Guntenspergen, and S. Faghe. 2016. Overestimation of marsh vulnerability to sea level rise. Nat. Clim. Chang. 6: 253–260. doi:10.1038/ nclimate2909

Le Hai, T., and H. J. Verhagen. 2014. Damage to grass covered slopes due to overtopping. Coast. Eng. 56: 21. ISBN 978-0- 9896611-2-6.

Leonard, L. A., and A. L. Croft. 2006. The effect of standing biomass on flow velocity and turbulence in *Spartina alterniflora* canopies. Estuar. Coast. Shelf Sci. 69: 325–336. doi:10.1016/j.ecss.2006.05.004

Ma, Z., T. Ysebaert, D. van der Wal, D. J. de Jong, X. Li, and P. M. J. Herman. 2014. Long-term salt marsh vertical accretion in a tidal bay with reduced sediment supply. Estuar. Coast. Shelf Sci. 146: 14–23. doi:10.1016/j.ecss.2014.05.001

Möller, I., and others. 2014. Wave attenuation over coastal salt marshes under storm surge conditions. Nat. Geosci 7: 727–731. doi:10.1038/ngeo2251

Morris, M., M. Hassan, A. Kortenhaus, and P. Visser. 2009. Breaching processes: A state of the art review. FLOODsite Publ. 70. T06-06-03.

Mudd, S. M., A. D'Alpaos, and J. T. Morris. 2010. How does vegetation affect sedimentation on tidal marshes? Investigating particle capture and hydrodynamic controls on biologically mediated sedimentation. J. Geophys. Res. Earth Surf 115: 1–14. doi:10.1029/2009JF001566

Narayan, S., and others. 2016. The effectiveness, costs and coastal protection benefits of natural and nature-based defences. PLoS One 11: e0154735. doi:10.1371/journal. pone.0154735

Narayan, S., and others. 2017. The value of coastal wetlands for flood damage reduction in the northeastern USA. Sci. Rep 7: 1–12. doi:10.1038/s41598-017-09269-z

Nolte, S., E. C. Koppenaal, P. Esselink, K. S. Dijkema, M. Schuerch, A. V. De Groot, J. P. Bakker, and S. Temmerman. 2013. Measuring sedimentation in tidal marshes: A review on methods and their applicability in biogeomorphological studies. J. Coast. Conserv. 17: 301–325. doi:10.1007/ s11852-013-0238-3

R Core Team, R: A Language and Environment for Statistical Computing, Vienna, Austria, 2016.

Silinski, A., E. Fransen, T. J. Bouma, P. Meire, and S. Temmerman. 2016*a*. Unravelling the controls of lateral expansion and elevation change of pioneer tidal marshes. Geomorphology 274: 106–115. doi:10.1016/j.geomorph.2016.09.006

Silinski, A., and others. 2016*b*. Effects of contrasting wave conditions on scour and drag on pioneer marsh plants. Geomorphology 255: 49–62. doi:10.1016/j.geomorph.2015.

Silinski, A., K. Schoutens, S. Puijalon, J. Schoelynck, D. Luyckx, P. Troch, P. Meire, and S. Temmerman. 2017. Coping with waves: Plasticity in tidal marsh plants as self-adapting coastal ecosystem engineers. Limnol. Oceanogr. 63: 799–815. doi:10.1002/lno.10671

Smolders, S., Y. Plancke, S. Ides, P. Meire, and S. Temmerman. 2015. Role of intertidal wetlands for tidal and storm tide attenuation along a confined estuary: A model study. Nat. Hazards Earth Syst. Sci. 15: 1659–1675.

doi:10.5194/nhess- 15-1659-2015

Spencer, T., S. M. Brooks, B. R. Evans, J. A. Tempest, and Möller. 2015. Earth-science reviews southern North Sea storm surge event of 5 December 2013 : Water levels, waves and coastal impacts. Earth Sci. Rev 146: 120–145. doi: 10.1016/j.earscirev.2015.04.002

Stanczak, G., H. Oumeraci, and A. Kortenhaus. 2007. Laboratory tests on the erosion of clay revetment of sea dike with and without a grass cover induced by breaking wave impact. FLOODsite, 935, T04-07-11.

Stark, J., T. Van Oyen, P. Meire, and S. Temmerman. 2015. Observations of tidal and storm surge attenuation in a large tidal marsh. Limnol. Oceanogr. 60: 1371–1381. doi: 10.1002/lno.10104

Steendam, G. J., P. Peeters, J. W. van der Meer, K. Van Doorslaer, and K. Trouw. 2011. Destructive wave overtopping tests on Flemish dikes, p. 49–50. *In* International Conference on Coastal Structures 2011, September 5–9, 2011, Yokohama, Japan: Book of abstracts. doi:10.1142/ 9789814412216_0016

Strotmann, T. 2014. Deutsches Gewässerkundliches Jahrbuch, Elbegebiet Teil 3. Freie und Hansestadt Hamburg HPA Hamburg Port Authority AöR: ISSN 0949-3654.

Sutherland, T. F., J. Grant, and C. L. Amos. 1998. The effect of carbohydrate production by the

diatom *Nitzschia curvilineata* on the erodibility of sediment. Limnol. Oceanogr. 43: 65–72.

Sutton-Grier, A. E., K. Wowk, and H. Bamford. 2015. Future of our coasts: The potential for natural and hybrid infrastructure to enhance the resilience of our coastal communities, economies and ecosystems. Environ. Sci. Policy 51: 137–148. doi:10.1016/j.envsci.2015.04.006

Temmerman, S., P. Meire, T. J. Bouma, P. M. J. Herman, T. Ysebaert, and H. J. De Vriend. 2013. Ecosystem-based coastal defence in the face of global change. Nature 504: 79–83. doi:10.1038/nature12859

Temmerman, S., and M. L. Kirwan. 2015. Building land with a rising sea: Cost-efficient nature-based solutions can help to sustain coastal societies. Science 349: 588–589. doi: 10.1126/science.aac8312

Tempest, J. A., I. Möller, and T. Spencer. 2015. A review of plant-flow interactions on salt marshes: The importance of vegetation structure and plant mechanical characteristics. Wiley Interdiscip. Rev. Water 2: 669–681. doi:10.1002/ wat2.1103

Turner, R. K., D. Burgess, D. Hadley, E. Coombes, and N. Jackson. 2007. A cost-benefit appraisal of coastal managed realignment policy. Glob. Environ. Chang. 17:397–407. doi:10.1016/j.gloenvcha.2007.05.006

van Baars, S., and I. M. van Kempen. 2009. The causes and mechanisms of historical dike failures in The Netherlands. E-WAter: ISSN 1994-8549.

Van Coppenolle, R., C. Schwarz, and S. Temmerman. 2018. Contribution of mangroves and salt marshes to nature-based mitigation of coastal flood risks in major deltas of the world. Estuaries Coast. 41: 1699–1711. doi:10.1007/s12237-018-0394-7

van Wijnen, H. J., and J. P. Bakker. 2001. Long-term surface elevation change in salt marshes: A prediction of marsh response to future sea-level rise. Estuar. Coast. Shelf Sci. 52: 381–390. doi:10.1006/ecss.2000.0744

Vannoppen, W., M. Vanmaercke, S. De Baets, and J. Poesen. 2015. A review of the mechanical effects of plant roots on concentrated flow erosion rates. Earth Sci. Rev. 150: 666–678. doi:10.1016/j.earscirev.2015.08.011

Vannoppen, W., S. De Baets, J. Keeble, Y. Dong, and J. Poesen. 2017. How do root and soil characteristics affect the erosion-reducing potential of plant species? Ecol. Eng. 109: 186–195. doi:10.1016/j.ecoleng.2017.08.001

Vuik, V., S. N. Jonkman, B. W. Borsje, and T. Suzuki. 2016. Nature-based flood protection: The efficiency of vegetated foreshores for reducing wave loads on coastal dikes. Coast. Eng. 116: 42–56. doi:10.1016/j.coastaleng.2016.06.001

Vuik, V., H. Y. Suh Heo, Z. Zhu, B. W. Borsje, and S. N. Jonkman. 2018. Stem breakage of salt marsh

vegetation under wave forcing: A field and model study. Estuar. Coast. Shelf Sci. 200: 41–58. doi:10.1016/j.ecss.2017.09.028

Wamsley, T. V., M. A. Cialone, J. M. Smith, J. H. Atkinson, and J. D. Rosati. 2010. The potential of wetlands in reducing storm surge. Ocean Eng. 37: 59–68. doi:10.1016/j. oceaneng.2009.07.018

Wang, H., D. Van Der Wal, X. Li, and others. 2017. Zooming in and out: Scale-dependence of extrinsic and intrinsic factors affecting salt marsh erosion. J. Geophys. Res. Earth Surf 122: 1455–1470. doi:10.1002/2016JF004193

Woolf, D., and J. Wolf. 2013. Impacts of climate change on storms and waves. MCCIP Sci. Rev 2013: 20–26. doi: 10.14465/2013.arc03.020-026.

Yang, S. L., B. W. Shi, T. J. Bouma, T. Ysebaert, and X. X. Luo. 2012. Wave attenuation at a salt marsh margin: A case study of an exposed coast on the Yangtze Estuary. Estuaries Coast. 35: 169–182. doi:10.1007/s12237-011-9424-4

Ysebaert, T., S. Yang, L. Zhang, Q. He, T. J. Bouma, and P. M. J. Herman. 2011. Wave attenuation by two contrasting ecosystem engineering salt marsh macrophytes in the intertidal pioneer zone. Wetlands 31: 1043–1054. doi: 10.1007/s13157-011-0240-1

3

Nature-based shoreline protection by tidal marsh plants depends on trade-offs between avoidance and attenuation of hydrodynamic forces

Ken Schoutens, Maike Heuner, Elmar Fuchs, Vanessa Minden, Tilla Schulte-Ostermann, Jean-Philippe Belliard, Tjeerd J. Bouma, Stijn Temmerman

3.1 Abstract

In face of growing land-flooding and shoreline-erosion risks along coastal and estuarine shorelines, tidal marshes are increasingly proposed as part of nature-based protection strategies. While the effect of plant species traits on their capacity to attenuate waves and currents has been extensively studied, the effect of species traits on their capacity to cope with and grow under wave and current forces has received comparatively less attention. We studied the relationships between species zonation and the associated two-way interactions between species traits and hydrodynamics, by quantifying the effectiveness of avoidance and attenuation of hydrodynamic forces under field conditions. Measurements were done for two pioneer tidal marsh species in the brackish part of the Elbe estuary (Germany). *Schoenoplectus tabernaemontani* (*S. tabernaemontani*), which grows as a single stem without leaves and *Bolboschoenus maritimus* (*B. maritimus*) which grows as a triangular stem with multiple leaves. Our results reveal that *S. tabernaemontani* grows more seaward being exposed to stronger hydrodynamic forces than *B. maritimus*. The stems of *S. tabernaemontani* have, in comparison to *B. maritimus*, a lower flexural stiffness and less biomass, which decrease the experienced drag forces, thereby favoring its capacity to avoid hydrodynamic stress. At the same time, these plant traits which favor such avoidance capacity, were shown to also result in a lower capacity to attenuate waves and currents. Hence this implies there are trade-offs between avoiding and attenuating hydrodynamic forces. Most efficient attenuation of waves and currents is thus only reached when species have the ability to grow under the prevailing hydrodynamic forces. Therefore, we argue that the two-way interaction between plants and hydrodynamics contributes to species zonation. The presence of this species zonation in turn enhances the overall efficiency of nature-based shoreline protection in pioneer tidal marshes.

3.2 Introduction

Climate change increases the need for sustainable strategies to cope with projected sea level rise, increasing storm intensity, and associated growing risks of shoreline erosion and flooding of coastal and estuarine lowlands (Nicholls et al. 2008; Hallegatte et al. 2013; Woodruff et al. 2013; Tessler et al. 2015; Schipper et al. 2017). Additionally, regional to local human impacts have altered many estuarine and coastal landscapes. For example, dredging for navigation and conversion of natural floodplains into human land use protected by engineered flood defenses contribute to tidal wave amplification, which further increases the vulnerability of shorelines to flood and erosion risks (Pethick and Orford 2013; Auerbach et al. 2015; Temmerman and Kirwan 2015). In this context, it is increasingly proposed that conservation and restoration of natural ecosystems, such as tidal marshes, can provide a sustainable nature-based contribution to shoreline protection (Gedan et al. 2011; Temmerman et al. 2013; Bouma et al. 2014). Tidal marshes have the capacity to temporally store water, attenuate hydrodynamic forces and reduce erosion risks on more landward located human flood defences and infrastructures, even under extreme storm conditions (Möller et al. 2014; Stark et al. 2015; Vuik et al. 2016). In pioneer tidal marshes, which grow at the shoreward edge of marshes, friction induced by the physical presence of vegetation attenuates incoming hydrodynamic forces such as wave energy and current velocities. This well-studied mechanism shows that the majority of wave energy is reduced in the first meters of the pioneer marsh (Koch et al. 2009; Anderson and Smith 2014). Wave heights can be reduced by 20-40% over 12 m of pioneer marshes (Silinski et al. 2017) and up to 80% over <50 m (Ysebaert et al. 2011) while current velocities can be reduced by more than 50% after 15 m (Nepf 1999; Leonard and Croft 2006; Tempest et al. 2015; Carus et al. 2016).

3.2.1 Plant strategies: avoidance versus resistance traits?

Plants in tidal marshes not only attenuate waves and currents, but they also have to cope with these incoming hydrodynamic forces. Mechanical stress from waves, currents and wind can alter the growth and survival of plant species (Biddington 1986; Butler et al. 2012; Hamann and Puijalon 2013; Schoelynck et al. 2015). Apart from waves and currents, plants in the intertidal area are exposed to wind generated mechanical stress during low water (Denny 1994; Anten et al. 2017). However in tidal marshes, the wind generated stress is relatively low compared to the stress generated by hydrodynamic forces (Denny and Gaylord 2002). The main causes of mechanical plant failure by waves and currents are excessive drag forces acting on the plant shoots (Miler et al. 2012; Henry et al. 2015; Paul et al. 2016) and erosion (e.g. uprooting) around plants (Bouma et al. 2009; Friess et al. 2012). Nevertheless, plants developed adaptations to mitigate stress from drag induced by hydrodynamic forces. Morphological adaptations such as shape reconfiguration, compact size or simple architecture reduce or avoid drag (Sand-Jensen 2003; Albayrak et al. 2012; Puijalon

and Bornette 2013), while increased rigidity or anchoring enables the plant to resist drag (Puijalon et al. 2008; Miler et al. 2012). Multiple studies from different research fields point out a trade-off between the plant traits that favour an avoidance or a resistance strategy against mechanical stress (Puijalon et al. 2011; Anten and Sterck 2012; Starko et al. 2015; Starko and Martone 2016). This trade-off could have consequences for the growth, performance and ecology of a species (Denny et al. 2003; Puijalon and Bornette 2013; Feagin et al. 2019). Moreover, growth strategies at the level of individual plants (i.e. plant traits) can thus have implications at the landscape scale for e.g. the shoreline protection capacity of a tidal marsh (Bouma et al. 2008, 2014; Vuik et al. 2016). However, studies on how species-specific marsh plant traits determine the plants' ability to cope with and survive hydrodynamic stress are rather sparse (Miler et al. 2014; Silinski et al. 2015, 2017).

3.2.2 Hydrodynamic avoidance VS attenuation capacity

Multiple studies have shown that the effectiveness of wave and flow attenuation within marshes is dependent on plant traits such as standing biomass, vegetation canopy height and stem stiffness, with higher, stiffer and denser vegetation canopies being more effective on flow and wave attenuation (Bouma et al. 2010; Callaghan et al. 2010; Paul et al. 2016; Rupprecht et al. 2017). Additionally, the species-specific capacity to avoid hydrodynamic stress was recently suggested to play a role in the spatial distribution (zonation) of two pioneer tidal marsh species in the wave-exposed parts of the brackish zone of NW European estuaries. More specifically, Heuner et al. (2018) showed that *Schoenoplectus tabernaemontani* (C.C.Gmel.) Palla is highly dominant in the pioneer zone, while *Bolboschoenus maritimus* (L.) Palla grows more landward at a farther distance from the marsh edge. Moreover, laboratory flume experiments, showed that plants sampled from the *Schoenoplectus*-zone had aboveground plant traits that favor avoidance of wave-induced stress: i.e., low frontal surface area and flexible stems, so that lower drag forces from waves were measured on the plants (Heuner et al. 2015; Silinski et al. 2016). In contrast, plants from the *Bolboschoenus*-zone had aboveground plant traits that result in less effective avoidance of wave-induced stress: i.e., higher stem surface area and stiffer stems, causing higher drag forces from waves. An additional flume experiment showed that wave attenuation rates were smaller for the more flexible plants sampled and grown from the *Schoenoplectus*-zone as compared to the stiffer plants from the *Bolboschoenus*-zone. Overall, these findings were interpreted as a cost-benefit trade-off as suggested in Bouma et al. (2005) for other intertidal plant species. They described a trade-off between stress-avoidance capacity (i.e. the more flexible species have a higher capacity to avoid wave-induced drag forces) versus ecosystem-engineering capacity (i.e. the more flexible species have less wave attenuation capacity). We emphasize here that these findings are based on experiments in laboratory flumes, where both species are exposed to similar wave conditions. In the field, however, both species grow in sequential zones, and hence most

likely experience different physical forcing from waves and currents. This raises the question how a trade-off between stress-avoidance capacity versus ecosystem-engineering capacity applies to *in-vivo* field conditions, accounting for the fact that each species has its own unique habitat. We further hypothesize that similar plant traits are responsible for both the ability to grow under hydrodynamic forces and the capacity to attenuate these hydrodynamic forces.

In this study, we aim to further deepen our insights into the two-way interaction between plant traits and hydrodynamics, by *i)* relating the observed plant species zonation to field measurements of species-specific traits and physical forcing by waves and currents in the different zones and *ii)* analyzing how these species-specific traits imply trade-offs between the effectiveness of hydrodynamic-stress-avoidance vs. attenuation of hydrodynamic forces. To our knowledge, there is no literature that discusses the implications of this trade-off for the attenuation capacity of hydrodynamic forces (and hence for nature-based shoreline protection capacity) of pioneer tidal marshes.

3.3 Methods

3.3.1 Study sites

Two sites were selected along the brackish part of the Elbe estuary, Germany: Balje (53°51'23.5"N, 9°4'9.2"E) and Hollerwettern (53°49'55.5"N, 9°22'17.4"E) (Fig. 3.1a). These two sites are characterized by a gentle transition between bare tidal flat and marsh, and a spatial zonation of plant species (see section 'Studied species' below) growing in distinct zones that run parallel to the estuarine tidal channel (Fig. 3.1b). The semidiurnal tide is on average 2.8 m (1.6 m during neap tide and 3.8 m during spring tide, data for 2015-2017). Mean freshwater discharge of the Elbe (1926–2014) is 712 m^3 s^{-1} ranging from 560 m^3 s^{-1} in summer to 866 m^3 s^{-1} in winter (Strotmann 2014). The water salinity measured using the Practical Salinity Scale at the two sites ranges between 0.3 – 4.0.
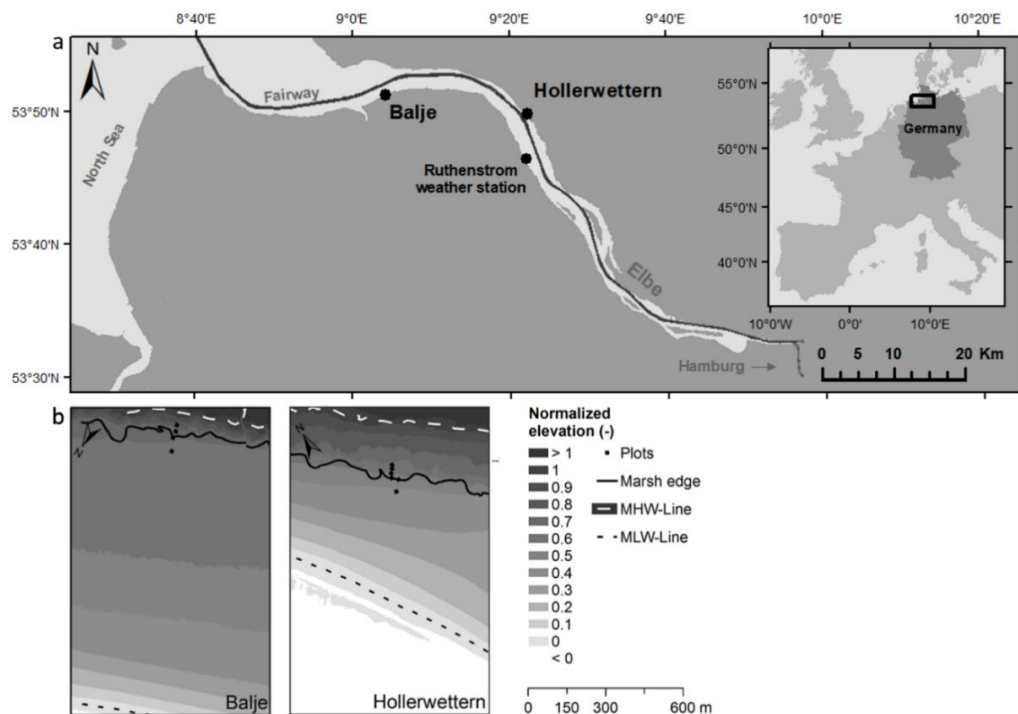
Figure 3.1: Location of the Elbe estuary in Europe and of the study sites Balje and Hollerwettern (1a). The location of Ruthenstrom weather station is marked. The fairway (black line) goes to the harbour of Hamburg. The elevation maps for both sites show the measurement plots, the marsh edge and width of the tidal flat as well as the mean low and high water level (MLW and MHW). The elevations are normalized by tidal range as (Elevation – Mean low water)/(Mean high water – Mean low water) (1b).

3.3.2 Studied species

Along the brackish parts of NW European estuaries *Schoenoplectus tabernaemontani* (C.C.Gmel.) Palla (formerly *Scirpus tabernaemontani*) and *Bolboschoenus maritimus* (L.) Palla (formerly *Scirpus maritimus*), both members of the Cyperaceae-family, are the most common pioneer plant species. In tidal marshes, both species typically reproduce by clonal outgrowth resulting in rhizomatous root networks. In winter the aboveground biomass of both species dies off and is flushed away while the roots hibernate (chapter 2: Schoutens et al. 2019)*. S. tabernaemontani* shoots grow as single stems with a circular cross-section, a diameter around 15 mm, and a height up to 2.0 m (own measurements) (Fig. 3.2). At the base there are a few small leaf sheaths embracing the round stem. In contrast*, B. maritimus* has leaves along the full length of a triangular stem that can grow up to 2.5 m in height and have a base length of the triangular cross-section up to 17 mm (own measurements). Both species form dense monospecific zones in belts that run parallel to the marsh edge. They both grow at

overlapping elevations relative to mean sea level in which *S. tabernaemontani* typically grows directly adjacent to the shoreward edge of marshes, while *B. maritimus* grows in a more landward located zone (Heuner et al. 2018).
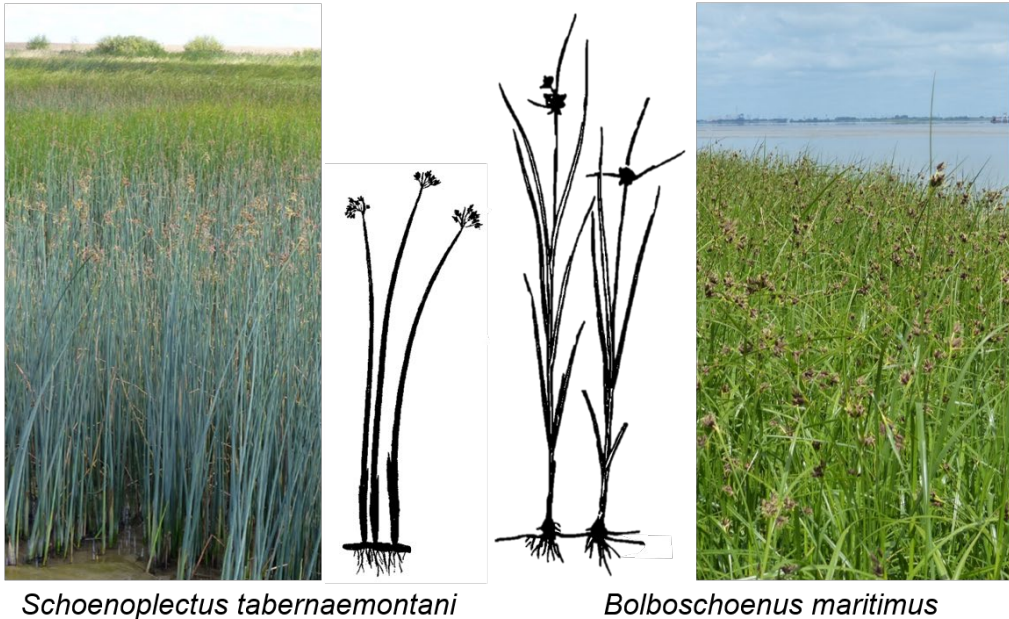
Figure 3.2: Marsh vegetation of the brackish parts of the Elbe estuary is composed of two dominant pioneer marsh species: *Schoenoplectus tabernaemontani* (C.C.Gmel.) Palla which typically grows at the shoreward edge, and *Bolboschoenus maritimus* (L.) Palla which typically grows more landward.

3.3.3 Overall description of the field measurements

This study investigated how species zonation is determined by the two-way interaction of plant traits and hydrodynamic forces. The resulting trade-offs between the effectiveness of avoidance and attenuation of hydrodynamic forces were assessed under field conditions. First, the spatial distribution in terms of species zonation was illustrated using maps of the Elbe estuary. Next, the hydrodynamic conditions acting upon the two species (i.e. exposed or sheltered from waves and currents) were measured locally at the two study sites throughout the growing season with wave height and current velocities as proxies. These measurements were accompanied by quantification of wave and flow attenuation rates per species zone to illustrate their capacity to attenuate hydrodynamics at peak biomass. We then coupled the two way interactions with field measurements of species-specific plant traits that play a role in the interaction with the hydrodynamics. Therefore, aboveground biomass, flexural stiffness and frontal plant area were used as proxies for drag forces exerted on the plant shoots (Vogel 1996; Silinski et al. 2016). Combining these measurements allowed us to construct a conceptual mechanism of how species-specific plants traits play a key role

in the spatial distribution of pioneer marsh plant species and what the consequences for nature-based shoreline protection might be.

3.3.4 Plant zonation

The frequency distribution of surface elevations at which both species are growing, was quantified for both study sites. This was compared to a similar analysis for all marshes in the Elbe estuary, see Fig. 3.1a), to demonstrate that the elevation range of both species in our two study sites is representative for what is generally found in the Elbe estuary. The analysis was based on vegetation maps, aerial pictures and digital elevation models (DEM) made in summer 2016. The vegetation maps were generated from aerial pictures (0.20 m resolution) (WSA 2017). In both estuaries, 140 random sampling points were generated of which the elevation above MHW was extracted from the DEM (1.0 m grid and 0.5 m position accuracy) (Zentrales Datenmanagement der GDWS Standort Kiel 2017). For more details on this method, we refer to Heuner et al. 2018. The elevations were normalized by tidal range as (Elevation – Mean low water)/(Mean high water – Mean low water), in order to be comparable between the datasets for the two sites and the whole Elbe estuary.

3.3.5 Plant exposure to and attenuation of hydrodynamic forces

3.3.5.1 Waves

During a six-month field campaign in the growing season from May to October 2016, wave heights were measured. Automated pressure sensors (P-Log3021-MMC, Driesen & Kern) were deployed at three distances along one cross-shore transect at every site (i.e. 2 x 3 sensors; Fig. 3.3) to record absolute pressure at 8 Hz. The 1st sensor was placed in front of the marsh edge for measuring incoming waves just before they enter the marsh vegetation. The 2nd sensor was placed at 10 m distance from the marsh edge, coinciding with the transition from the *S. tabernaemontani* zone to the *B. maritimus* zone. Together with sensor 1, this set-up enabled quantifying wave attenuation over 10 m of *S. tabernaemontani* marsh. A third sensor was placed another 10 m further within the *B. maritimus* vegetation. Comparing sensor 2 and 3 allowed quantification of wave attenuation over 10 m of *B. maritimus* marsh.

To quantify wave heights, pressure data were converted into water surface elevation using a Matlab routine. After correction for atmospheric pressure (obtained from the DWD Climate Data Center), the resulting water levels were then corrected for depth-dependent pressure attenuation based on the linear wave theory (Dalrymple and Dean 1991), i.e. the water motion of passing waves and hereby the hydrostatic pressure is attenuated with increasing water depth. Next, the tidal signal was extracted from the wave signal using a low-pass filter and zero-down crossing method was then applied on the resulting time series of wave fluctuations to determine individual waves (Vanlierde et al. 2011; Belliard et al. 2019). Significant wave height (H_s, mean of the

highest third of recorded waves) and maximum wave height (H_{max}, mean of the 99th percentile of recorded waves) were calculated over 10 minute time intervals. The relative wave attenuation rate (R_w) was calculated for *S. tabernaemontani* as $R_w = (H_1 - H_2)/H_1 \times 100(\%)$ where H_1 is the incoming significant wave height at sensor location 1 at the seaward edge of the vegetation zone and H_2 is the significant wave height at 10 m into the *S. tabernaemontani* zone. Similarly, the relative wave attenuation rate (R_w) was calculated for *B. maritimus* as $R_w = (H_2 - H_3)/H_2 \times 100(\%)$ where H_3 is the significant wave height at 10 m into the *B. maritimus* zone. For comparison with plant traits, the wave attenuation capacity was calculated during the period of peak biomass. With increasing water depth, the inundated frontal area of the plants increases and consequently the interaction of the waves with the vegetation increases until the water depth exceeds the canopy height. Since both species are growing at different surface elevations, wave attenuation rates were calculated and compared for water depth classes of 0.25 m intervals to enable a species comparison. A similar comparison between wave attenuation rates and wave height classes of 0.1 m intervals was made to take into account the wave transformation in front of the respective vegetation zone.

3.3.5.2 Flow velocity

As sensor availability was limited, flow velocities were only measured at Hollerwettern during the growing season from May to October 2016 (Figs. 3.1 and 3.3). Next to the pressure sensors, flow velocities were measured at 4 Hz with ADVs (Acoustic Doppler Velocity sensors, Nortek) measuring at 0.10 m above the sediment bed. Raw data were removed for beam correlations below 70% after which the planar velocity (m/s) was calculated as $U = \sqrt{u^2 + v^2}$ with u and *v* being the mean flow velocities (m/s) in the two horizontal dimensions perpendicular to each other calculated over 10 minute time intervals. Flow attenuation rate (R_f) was calculated similarly to the wave attenuation rate (see above: $R_f = (U_1 - U_2)/U_1 \times 100(\%)$ and $R_f = (U_2 - U_3)/U_2 \times 100(\%)$ respectively with U_1, U_2 and U_3 are now mean flow velocities instead of wave heights at the respective measurement locations).
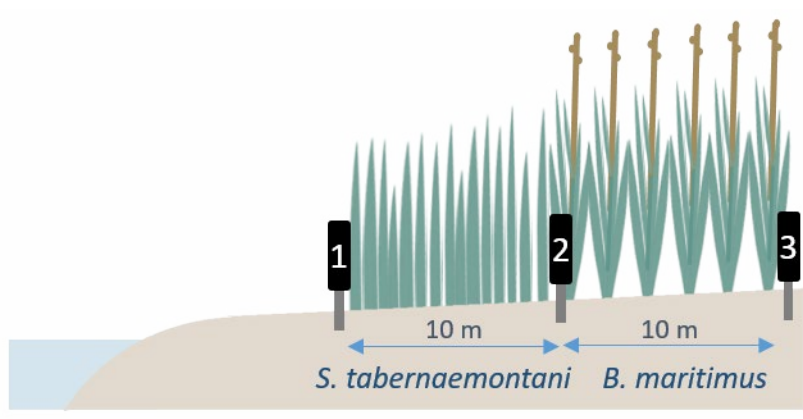
Figure 3.3: Schematic cross section of the field monitoring setup. Along the sea-to-land transect sensors were installed at 3 locations to measure hydrodynamic conditions (waves and currents). Wave attenuation was measured over a 10 m vegetation belt between sensor 1 and sensor 2 for *S. tabernaemontani* and between sensor 2 and 3 for *B. maritimus* vegetation. Flow velocities were measured in a similar way but only at site Hollerwettern. Plant traits were measured in every respective species zone.

3.3.6 Plant traits

Quantification of species-specific plant traits was conducted at peak biomass in August 2016. Based on a literature study, we selected to focus on the principal plant traits responsible for (i) avoiding mechanical stress from waves and currents (e.g. Puijalon et al. 2011; Henry et al. 2015; Paul et al. 2016; Silinski et al. 2016b; Chen et al. 2018) and (ii) the capacity to attenuate hydrodynamic forces. These plant traits can be grouped into shoot morphological traits (i.e., aboveground biomass density and frontal shoot area) and stem biomechanical traits (i.e., Young's modulus and flexural stiffness) (e.g. Bouma et al. 2010; Anderson et al. 2011; Shepard et al. 2011; Vuik et al. 2016; Rupprecht et al. 2017; Silinski et al. 2017; Schulze et al. 2019).

3.3.6.1 Plant morphological traits

Shoot densities were determined per species by counting the number of shoots within three permanent quadrats of 0.4 m x 0.4 m. Aboveground biomass of both species was sampled by clipping all shoots in a 0.2 m x 0.2 m quadrat (if needed this was repeated until a minimum of 20 shoots was reached). Aboveground biomass density (kg/m^2) was quantified by multiplying counted shoot densities (number of shoots/m^2) and dried shoot weight (g/number of shoots) of the clipped quadrats (drying at 70 °C for 72h) (Pérez-Harguindeguy et al. 2013). Before drying the harvested samples, the shoot length was measured and pictures were made to calculate the frontal area of the entire plants. Therefore, aboveground plant material was spread on a white background to make high contrast pictures (> 8 Mega pixels). Using ArcMap (Environmental Systems

Research Institute (ESRI), ArcGIS release 10.3, Redlands, CA) the surface area was determined through an Iso Cluster Unsupervised classification. This process was automated with a Python code.

3.3.6.2 Stem biomechanical traits

Mechanical properties of the lowest 0.20 m of the stems were measured with a three-point bending test at the Royal Netherlands Institute of Sea Research (NIOZ). The measuring method and calculations are based on Usherwood et al. (1997) and Silinski et al. (2016). The universal testing machine Instron EMSYSL7049 (precision ± 0.5%) with a 10 kN load cell was used (Instron Corporation, Canton, MA, USA). Force was applied at a displacement rate of 10 mm min^{-1} to the centre of a 0.20 m long stem section resting on two supports. The supports are separated from each other at a distance of 15 times the stem diameter which reduces the effect of shear stress (Usherwood et al. 1997). From the resulting stress-strain curve the Young's modulus (E in N/m^2) was calculated based on the slope of the elastic deformation zone, as a measure of the stress that can be applied on the stem before permanent deformation occurs (i.e. before the stem breaks). Higher values for Young's modulus mean lower flexibility of the stems. Second moment of area (I in m^4) was calculated based on a triangular stem geometry for *B. maritimus* $I=bh^3/36$ and based on a round stem geometry for *S. tabernaemontani* $I=\pi r^4/64$ where b is the base and h is the height of the triangular cross section, and r is the diameter of the circular cross section (m). The flexural stiffness or stem flexibility, which is a measure of the resistance of the stem against breaking, was then calculated as EI (Nm^2). Higher values for flexural stiffness indicate higher stiffness and therefore lower flexibility. The stress experienced by the plants can be expressed by the drag forces acting on the shoots. Drag forces could not be measured directly in the field but proxies were used to give an idea of the relative differences between drag forces experienced by the two species. From the Morison equation adapted by Vogel (1996) we used the frontal plant area and flexural stiffness as proxies for drag force F (N):

Eq. (1) $F = \frac{1}{2}\rho a A U^{2+d}$

where ρ is the density of the fluid [kg m^{-3}], A is the wet frontal area of the shoot [m^2] and a and d are the species-specific constants that depend on the flexibility of the plant shoot.

3.3.7 Data analysis

Statistical analyses were performed in R 3.3.1. (R Core Team, 2016) and significance was assumed at $p < 0.05$ for all tests (exceptions are indicated). Normality was tested based on visual inspection with histograms and Q-Q plots and homogeneity of variance was tested with the F-test where needed. The species comparison was done with the

Welch two sample t-test when the data was normally distributed or the unpaired two-sample Wilcoxon rank sum test (also named Mann-Whitney U test) for non-parametric data which both take into account the different origins (marsh sites) of the samples. The hydrodynamics in both species zones were compared using linear mixed models with time as a random factor.

3.4 Results

3.4.1 Plant zonation

The elevation distribution of *S. tabernaemontani* lies lower in the tidal frame compared to *B. maritimus*. This observation was consistent in the present study sites and in throughout the brackish part of the Elbe estuary (Fig. 3.4). *S. tabernaemontani* grows in the small fringe between the mean water level and the *B. maritimus* zone.
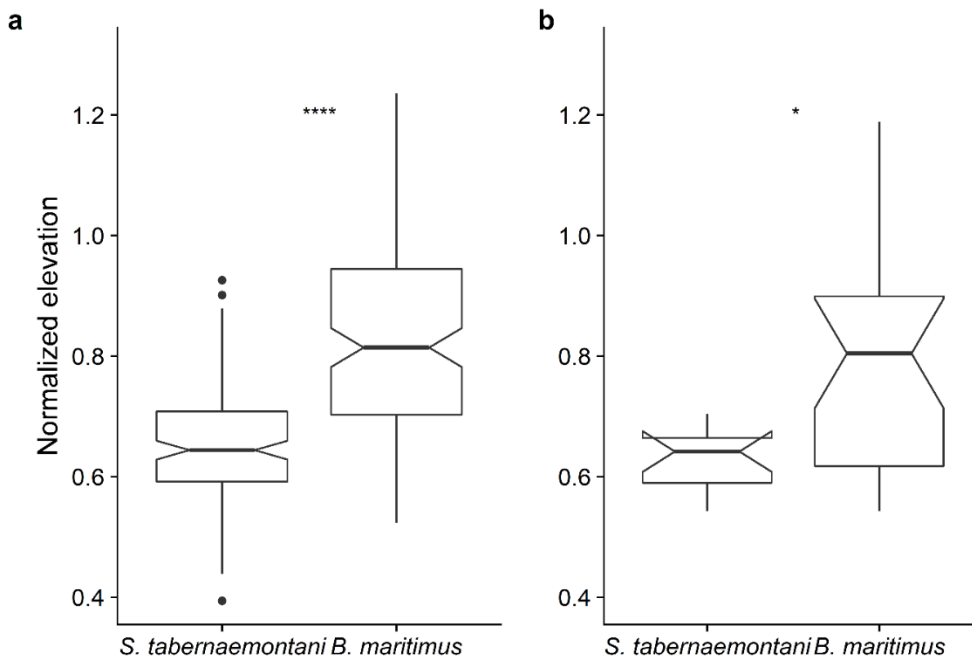
Figure 3.4: The elevation niche of both *B. maritimus* and *S. tabernaemontani* for (a) the Elbe estuary (n = 140 for both *S. tabernaemontani* and *B. maritimus*) and (b) for the study plots Balje and Hollerwettern (n = 12 for *S. tabernaemontani* and n = 24 for *B. maritimus*). The elevations are normalized by tidal range as (Elevation – Mean low water)/(Mean high water – Mean low water). Significance of differences was tested with the non-parametric Wilcoxon test (**** represents $p<0.001$, * represents $p<0.05$).

3.4.2 Hydrodynamic forces of the *S. tabernaemontani* and *B. maritimus* zones

S. tabernaemontani is exposed to stronger hydrodynamic forces as compared to *B. maritimus* (Fig. 3.5). During the growing season of 2016, peak values for the maximum

wave heights over 10 minute intervals were found to be up to 0.5 m in the *B. maritimus* zone and up to 0.6 m in the *S. tabernaemontani* zone (Chi-square (1) = 54.18, p < 0.001). The median incoming significant wave height was 0.06 m in the *B. maritimus* zone and 0.08 m in the *S. tabernaemontani* zone which was up to 25 % higher (Chi-square (1) = 20623, p < 0.001; not shown in the figure). This difference in incoming wave heights is consistent over the measurement period (see supplementary Fig. S3.1 for a time series). Median planar flow velocity in Hollerwettern was 0.025 ms^{-1} in the *B. maritimus* zone and 0.040 ms^{-1} in the *S. tabernaemontani* zone (Chi-square (1) = 534.42, p < 0.001). The 99th percentile of planar flow velocities reached 0.16 ms^{-1} in *B. maritimus* and 0.19 ms^{-1} in *S. tabernaemontani*. The different exposure to hydrodynamic forces was found consistent over the different elevation gradients of both study sites (see Fig. S3.2 in supplementary info).
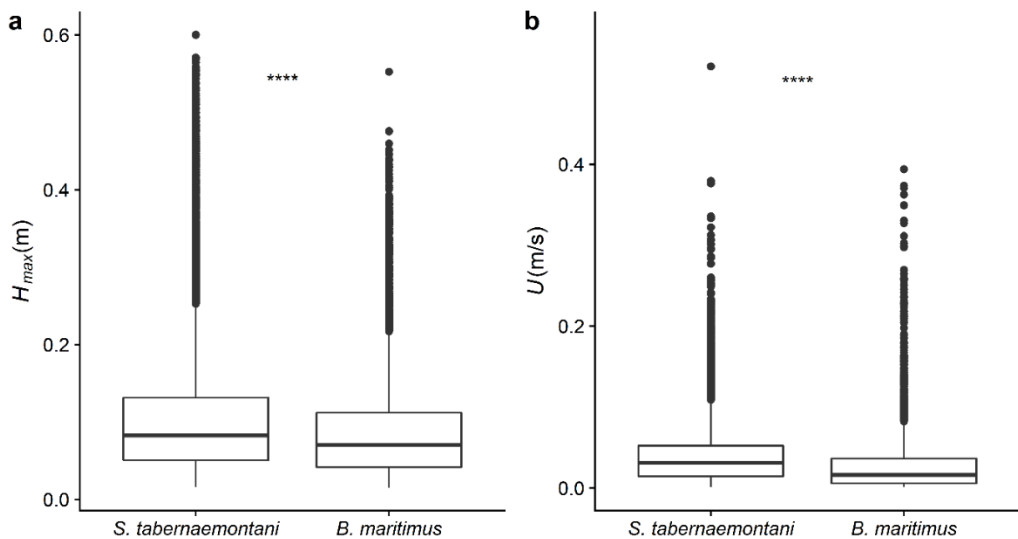
Figure 3.5: The boxplots show the maximum wave height (H_{max}; m) calculated over 10 minute time intervals (n = 96552 and n = 80410 for the *S. tabernaemontani* and *B. maritimus* zones respectively) and planar flow velocity (*U*; m/s) averaged over 10 minute time intervals for the two pioneer species during the growing season from May to October 2016 (n = 9629 and n = 7020 for *S. tabernaemontani* and *B. maritimus* respectively). Incoming wave heights and flow velocities for *S. tabernaemontani* were significantly higher compared to *B. maritimus*. Flow velocities were solely measured at the site Hollerwettern due to limited sensor availability. Significance of differences was tested with the non-parametric Wilcoxon test (**** represents p<0.001).

3.4.3 Plant species traits

The two species show different plant traits measured at peak biomass in August 2016. This trend is visible at both study sites. The aboveground dry biomass (AGB, kg/m^2) of *S. tabernaemontani* is more than seven times smaller compared to *B.* maritimus (Fig.

3.6a, table 3.1). In addition, *S. tabernaemontani* produces less frontal area compared to *B. maritimus*, both per soil surface area and per shoot (Fig. 3.6b, table 3.1)*.* The shoot tissue of *S. tabernaemontani* is more flexible, i.e. low Young's modulus, and less resistant against bending, i.e. low flexural stiffness, compared to *B. maritimus* (Fig. 3.6c and 3.6d, table 3.1).

Table 3.1: Overview of the plant traits measured for both *S. tabernaemontani* and *B. maritimus*. Per species, the mean and standard error are given in addition to the p-value of the Wilcoxon rank sum test which indicates the difference between the two species. The variables presented are aboveground dry biomass (*AGB* kg/m²), frontal area per soil surface area (*FA*, m²/m²) and frontal area per shoot (*FA$_{sh}$*, m²/shoot), Young's modulus (*E*, N/m²) and Flexural stiffness (*EI*, Nm²).

	AGB (kg/m²)	*FA* (m²/m²)	*FA$_{sh}$* (m²/shoot)	*E* (N/m²)	*EI* (Nm²)
S. tabernaemontani	0.19 ± 0.02	0.99 ± 0.13	3e-3 ± 4e-4	1.3e8 ± 9e6	0.013 ± 0.001
B. maritimus	0.89 ± 0.06	2.34 ± 0.13	8e-3 ± 4e-4	9.7e8 ± 1e8	0.047 ± 0.004
p-value	< 0.001	< 0.001	< 0.001	< 0.001	< 0.001
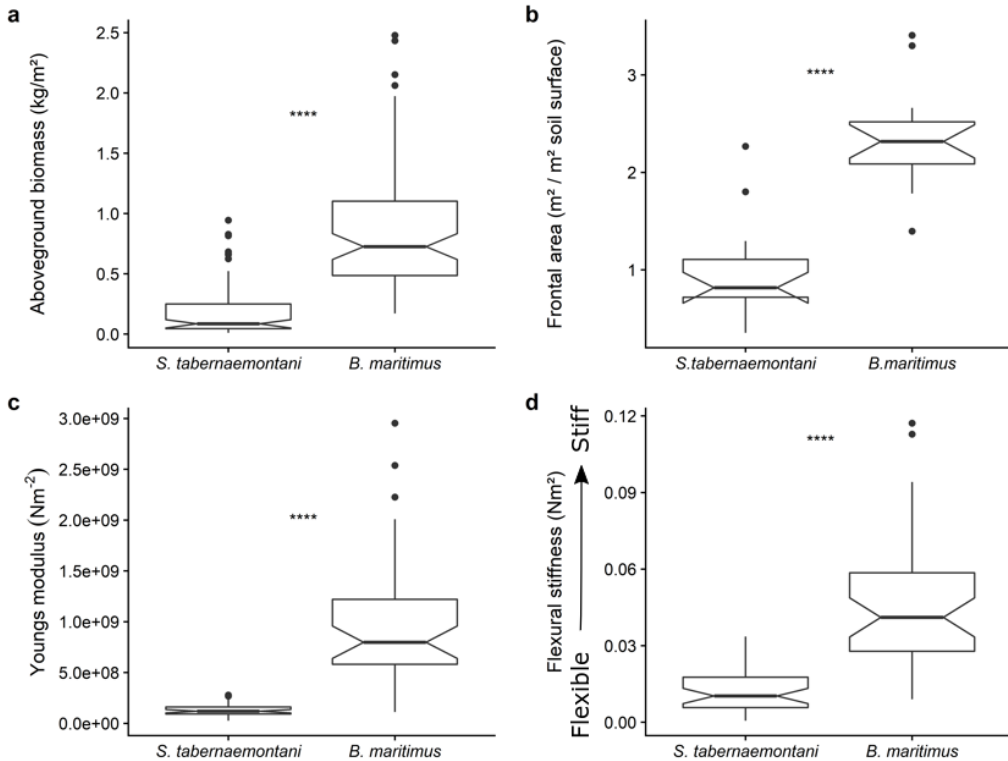
Figure 3.6: Aboveground biomass (kg/m²) (a) and frontal area (m²/m² soil surface) (b) show the shoot morphological traits and Young's modulus (N/m²) (c) and flexural stiffness (Nm²) (d) show the stem biomechanical traits. All traits are represented in boxplots as a descriptive statistic per species at peak biomass in summer 2016 (n = 83 for a, 16 for b and n = 40 for c and d). Significance of differences was tested with the non-parametric Wilcoxon test (**** represents p<0.001).

3.4.4 Species-dependent attenuation of hydrodynamic forces

Attenuation rates of waves and flow velocities were compared for the same water depth classes (Fig. 3.7). Especially for the shallow water depths, wave attenuation was stronger in the *B. maritimus* zone. With increasing water depth, wave attenuation decreased in both species zones. Moreover, the difference between the species-zones reduces when water depths increased. Yet for all water depth classes the differences in attenuation rates between both species-zones were statistically significant (Fig. 3.7). In the *S. tabernaemontani* zone, the wave attenuation rate dropped to almost zero at a water depth higher than 1.5 m. Planar flow attenuation rates were significantly higher in *B. maritimus* compared to *S. tabernaemontani*. In contrast to the wave attenuation, the flow attenuation did not change with increasing water depth (Fig. 3.7). For water depths over 1.5 m (not shown in Fig. 3.7) no significant difference in flow attenuation

rate between both species was found which might be attributed to the low sample size (n = 14).

Figure 3.7: Boxplots of wave and planar flow attenuation rates over 10 m stretches of *S. tabernaemontani* and *B. maritimus* measured during peak biomass (August 2016). Wave attenuation rates (number of measurements is indicated per water depth) and flow attenuation rate (n is indicated per water depth, for water depths >1.5 m the number of data points was too low and therefore data are not shown) are grouped per class of water depth. Significance of differences was tested with the non-parametric Wilcoxon test (**** represents p<0.001).

In the set-up of this study (Fig. 3.3), *S. tabernaemontani* grows in front of *B. maritimus* so that incoming wave heights in the *B. maritimus* zone are affected by wave transformation in front of that vegetation zone, i.e. within the *S. tabernaemontani* zone. In order to compare the wave attenuation rates of both the *S. tabernaemontani* and *B. maritimus* zones, we therefore compared wave attenuation rates for categories of the same incoming wave heigths. Within each incoming wave height category, we find then that there is a significantly higher wave height attenuation rate within the *B. maritimus* zone as compared to the *S. tabernaemontani* zone (Fig. 3.8).
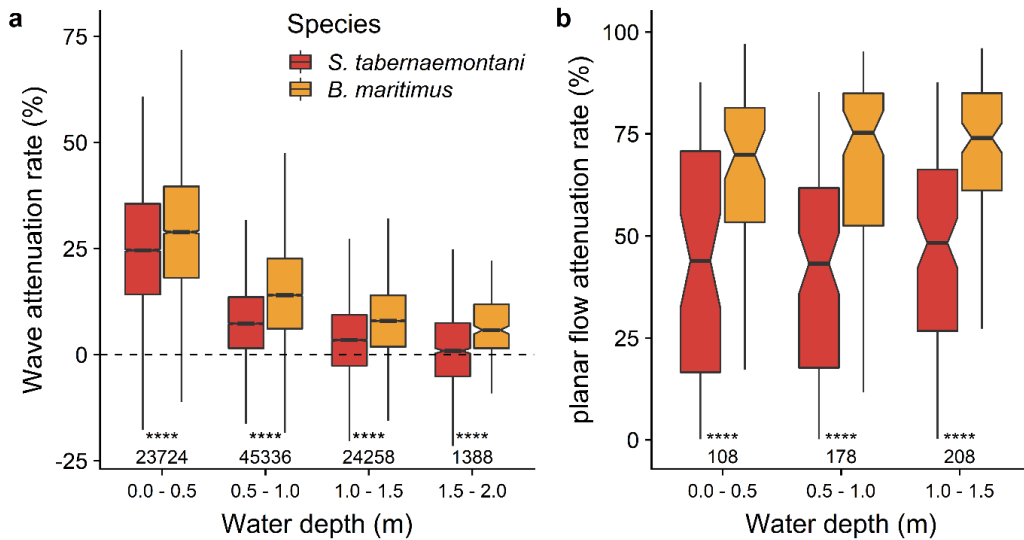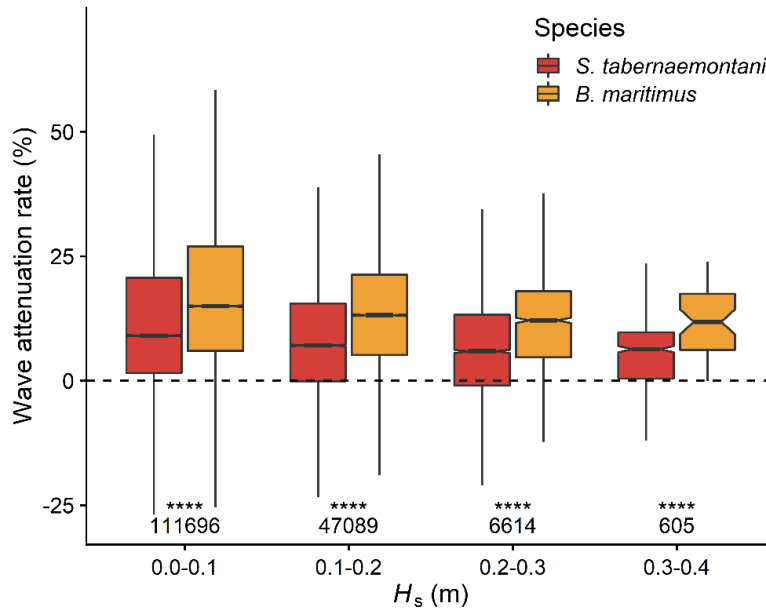
Figure 3.8: Boxplots of wave attenuation rates over 10 m stretches of *S. tabernaemontani* and *B. maritimus* measured during the growing season (May 2016 – October 2016). Wave attenuation rates (n is indicated per H_s class of 0.10 m) are grouped in classes of significant wave heights entering the specific vegetation zone. This allows a comparison of wave attenuation rates for both species zones independent of their location/distance from the marsh edge. Significance of differences was tested with the non-parametric Wilcoxon test (**** represents p<0.001).

3.5 Discussion

Nature-based mitigation of coastal flood and erosion risks is increasingly studied in the context of growing risks associated with global and local changes, and in light of growing demand for novel, sustainable risk mitigation strategies (Duarte et al. 2013; Cheong et al. 2013; Temmerman et al. 2013; Vuik et al. 2016). Accordingly, conservation and restoration of tidal marshes that contribute to wave, flow and erosion reduction, is increasingly proposed and implemented (Narayan et al. 2016; Gracia et al. 2018; Rangel-buitrago et al. 2018). A large amount of studies have focused on how plant species traits determine the effectiveness of wave, flow and erosion reduction (Bouma et al. 2005, 2010; Yang et al. 2012; Tempest et al. 2015; Carus et al. 2016), while fewer knowledge exists on how species traits determine their capacity to cope with and grow under wave and flow conditions (Coops and Van der Velde 1996; Heuner et al. 2015; Silinski et al. 2017). Here we demonstrate under field conditions that plant species zonation is associated with trade-offs between species traits that allow coping with wave and flow exposure versus attenuation of these hydrodynamic forces (Figs. 3.6 and 3.7): (1) pioneer species growing at the exposed marsh front have plant traits

that are better suited to avoid wave and current-induced stress compared to species growing more landward; (2) the same plant traits induce less effective attenuation of hydrodynamic forces in the exposed marsh front zone as compared to the more landward marsh zone. In the following, the trade-off involving species specific plant traits and hydrodynamic forces will be discussed more in details.

3.5.1 Avoidance capacity of species-specific plant traits

S. tabernaemontani and *B. maritimus* are pioneer plant species in brackish tidal marshes that grow in a similar elevation range, yet often in separate spatial zones, with *S. tabernaemontani* growing in the zone directly adjacent to the marsh front and *B. maritimus* in a more landward zone (Heuner et al. 2018; Fig. 3.4). Under exposed conditions we found that incoming wave heights and flow velocities were higher in the *S. tabernaemontani* zone compared to the *B. maritimus* zone independently from site elevation, distance from the marsh edge or incoming wave height (Figs. 3.4 and 3.8). The results show that on local scales the capacity to cope with such hydrodynamic forces is plant trait dependent. Under strong mechanical stress, plants are more vulnerable to mechanical failure such as uprooting, toppling and even breaking of the stem (Read and Stokes 2006). Therefore, plants developed morphological and biomechanical adaptations (amongst others) (Albayrak et al. 2012; Puijalon and Bornette 2013). *S. tabernaemontani* has a simple morphology of a single leafless stem creating vegetation with low biomass per square meter (Figs. 3.1 and 3.6). Especially the lack of leaves reduces the frontal area which is important to minimize the drag experienced by the plant (e.g. up to 60 %, Bal et al. 2011a).

In addition to the simple morphology, *S. tabernaemontani* has more flexible shoot bases (Fig. 3.6) which allows it to bend with passing waves or tidal currents. This flexibility enables the plants to reduce the experienced drag forces even more (Puijalon et al. 2005; Paul et al. 2016). Since drag forces were not measured directly in the field, the proxies used in this study (frontal plant area, flexural stiffness) indicate that drag forces exerted on *S. tabernaemontani* should be lower than on *B. maritimus* (Rupprecht et al. 2015). In terrestrial (wind driven) ecosystems however, some authors point out that high flexibility could increase the experienced drag as a result of the so-called flagging of the plant and turbulent flows created (Anten and Sterck 2012; Butler et al. 2012). Nevertheless, they stress that under hydrodynamic forces a turbulent flow regime is less likely to fully develop as a result of lower flow velocities and the higher density of water compared to air. The morphological and biomechanical traits of *S. tabernaemontani* favor an efficient avoidance of mechanical stress. This may allow them to grow directly adjacent to the marsh front under the prevailing hydrodynamic forces (Henry et al. 2015; Paul and Gillis 2015).

In contrast, *B. maritimus* grows leaves along the full length of the stem and thus produces high biomass with a high frontal area (Figs. 3.1 and 3.6). The morphological

traits of *B. maritimus* results in higher drag forces which make them more vulnerable to mechanical failure if they would grow under high wave and current exposure. The biomechanical traits measured for *B. maritimus* and *S. tabernaemontani* were in the same range of values found in literature (Silinski et al. 2015, 2016; Vuik et al. 2018). The flexural stiffness of *S. tabernaemontani* was 4-5 times smaller compared to values for *B. maritimus* (Fig. 3.6). The consequence of the stiffer shoots is that they do not reconfigure by elastic deformation to avoid the mechanical stress. Instead, they experience even more drag forces by keeping their rigid standing shoots (Bouma et al. 2005). Consequently, the growth of *B. maritimus* might be more limited by hydrodynamic forces, compared to *S. tabernaemontani*, which may be the reason why the first species grows landwards in more sheltered conditions. The ability to cope with hydrodynamic forces from waves and currents may thus be considered as a driver for species distribution (spatial zonation) along the sea-to-land gradient in pioneer tidal marshes. Although there is no experimental data available so far, future research with e.g. translocation experiments could give empirical proof for this mechanism. By growing both species under the same exposed and sheltered hydrodynamic conditions, insights on the survival chances of the species under the prevailing hydrodynamic conditions can be gained. Combining field data on plant survival chances and shoreline protection capacity of species in a model, could enable to make large scale (e.g. estuarine scale) assessments on the suitability of different intertidal areas for marsh restoration or conservation projects aiming at nature-based shoreline protection. This upscaling of the shoreline protection potential of an area is especially crucial for policy makers and environmental management agencies.

3.5.2 Wave and flow attenuation capacity of species-specific plant traits

As pointed out above, the two different species exert different frictions on the water motion and by this, attenuate rate of wave heights and current velocities in contrasting ways. When friction with the vegetation increases, the wave and flow attenuation becomes higher (Möller 2006; Suzuki et al. 2012; Paul et al. 2016). *S. tabernaemontani* did not attenuate waves and water flows as much as *B. maritimus* did (Fig. 3.7) due to differences of the morphological and biomechanical properties of the two species (Fig. 3.6). High shoot stiffness and high shoot density are mentioned as the main drivers for wave attenuation (Feagin et al. 2011; Shepard et al. 2011), however biomass should be taken into account (Bouma et al. 2010; Ysebaert et al. 2011). The biomass per square meter accounts for both the shoots density and morphological properties of the shoots (e.g. stems, leaves, flowers). Nevertheless, when stems are highly flexible and bend away with passing waves and water flow, the effective biomass and frontal plant area under hydrodynamic forcing is reduced (Verschoren et al. 2016). Therefore, both stem flexibility and standing biomass are important drivers of the wave and flow attenuation capacity of a species. In general, species that avoid the mechanical stress, such as *S. tabernaemontani* will have a less effect on attenuation of hydrodynamic forces

compared to species that resist the mechanical stress such as *B. maritimus*. It can be argued that the presented wave attenuation rates of *B. maritimus* are higher than for *S. tabernaemontani* because of the smaller incoming waves and lower water depths, and additionally several studies showed that the wave attenuation capacity of tidal marshes is strongest in the first few meters (Möller and Spencer 2002; Koch et al. 2009; Carus et al. 2016). Nevertheless, we showed that under similar water depths (Fig. 3.7) and wave heights (Fig. 3.8) the wave attenuation rates in *B. maritimus* are consequently higher. This result shows that the difference in attenuation capacity is mainly caused by the difference in vegetation properties.

3.5.3 Avoiding or attenuating hydrodynamic forces: a trade-off

Based on our results, we formulate a conceptual model describing the trade-offs between coping with and attenuating hydrodynamics (Fig. 3.9). This means that species that can cope with hydrodynamic stress such as *S. tabernaemontani* have plant traits that limit the drag forces exerted on the plant, which in consequence results in a lesser attenuation capacity. However, landwards of such species, the hydrodynamic conditions become more favourable for other species that have a lower capacity to avoid the hydrodynamic stress due to their plant traits (e.g. *B. maritimus*). Such plant traits enhance the attenuation capacity of the species. In other words, avoiding the hydrodynamic stress reduces the attenuation capacity, but allows plants to grow in more hydrodynamic conditions. While in contrast, species that have less avoidance capacity enhance their attenuation capacity, but limit the hydrodynamic exposure that these species can handle to survive. *B. maritimus* has a higher ecosystem engineering capacity compared to *S. tabernaemontani* (Heuner et al. 2015) which gives them a competitive advantage when conditions are mild enough for their establishment and survival (Wilson and Keddy 1986; Keddy 2001; Heuner et al. 2018). When hydrodynamic forces limit the expansion of the *B. maritimus* zone, *S. tabernaemontani* might still be able to grow out in front of the *B. maritimus* zone. This is only possible when there is enough space for *S. tabernaemontani* to grow, which is often not the case and might force *S. tabernaemontani* into a stressful situation of both seaward stress coming from hydrodynamic forces and inundation stress as well as landward stress coming from competition with *B. maritimus*. Consequently, the trade-off between attenuation capacity and mechanical stress resistance presented in this field study might eventually create a zonation of species in exposed pioneer tidal marshes. Nevertheless, caution is needed as this study is descriptive and based on field observations, hence further experimental evidence is needed to come to causal conclusions.
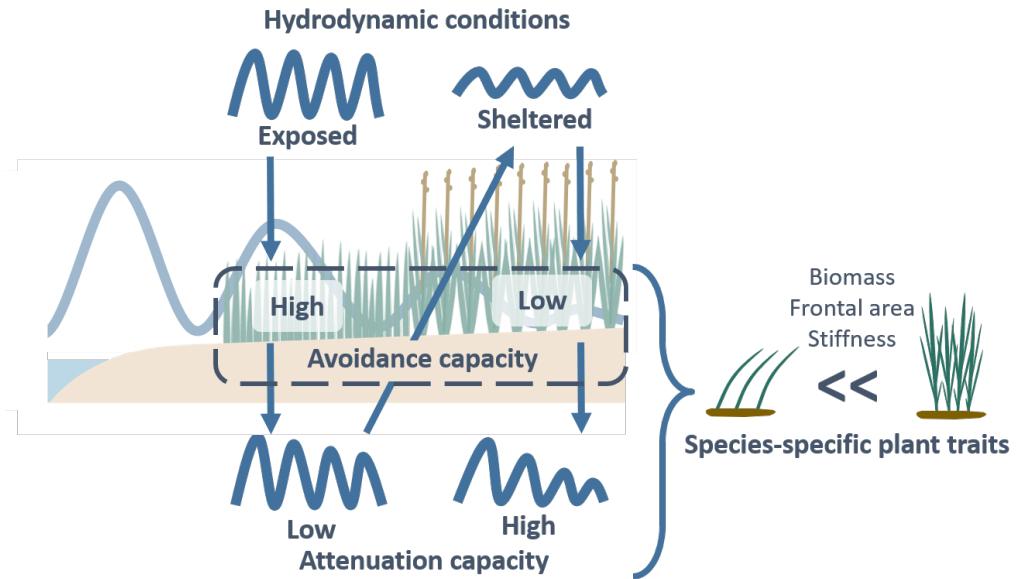
Figure 3.9: Schematisation of the relationships between spatial plant species zonation, hydrodynamic forces in which the species grow, plant traits of the species, and the trade-off between the plants' capacity to avoid and to attenuate the hydrodynamic forces. Pioneer species growing at the marsh front are exposed to the strongest hydrodynamics. Accordingly, they have a high capacity to avoid mechanical stress as a result of species-specific plant traits that reduce the drag forces exerted on the shoot. As a consequence of these plant traits, the wave attenuation capacity of such species is low. The slightly sheltered conditions that are created more landward facilitate the growth of other species which have a lower capacity to cope with strong hydrodynamic stress. Corresponding species-specific plant traits result in higher drag forces, hence creating a stronger hydrodynamic attenuation capacity.

3.5.4 Implications for natural shoreline protection

The trade-off described in this paper (Fig. 3.9) has consequences for bringing nature-based shoreline protection into practice: when conservation or restoration/creation of tidal marshes are proposed for shoreline protection, conditions might be unsuitable for the species that provide most efficient attenuation of hydrodynamic forces. In such case, shoreline protection capacity (here attenuation of hydrodynamics) is determined by the plant traits of the species that are able to grow under the prevailing hydrodynamic conditions. Hence, artificially creating slightly sheltered conditions (e.g. small man-made reefs in front of the shore or shallow willow fences) might facilitate the establishment and growth of species with a higher hydrodynamic attenuation capacity (e.g. *B. maritimus*) in an environment that normally would have been too exposed for such species. Nevertheless, the establishment of species that are able to cope with hydrodynamic exposure (e.g. *S. tabernaemontani*) can result already in some

degree of wave attenuation and therefore can naturally create these slightly sheltered conditions where growth of other, less wave tolerant species can be facilitated. Provided that there is enough space (perpendicular to the dike/shipping channel) to allow the development of such a species zonation in the pioneer zones of marshes, the overall efficiency of shoreline protection will increase as the result of this natural species zonation.

3.6 Acknowledgements

3.7 References

Albayrak, I., V. Nikora, O. Miler, and M. O'Hare. 2012. Flow-plant interactions at a leaf scale: Effects of leaf shape, serration, roughness and flexural rigidity. Aquat. Sci. **74**: 267–286. doi:10.1007/s00027-011-0220-9

Anderson, M. E., and J. M. Smith. 2014. Wave attenuation by flexible, idealized salt marsh vegetation. Coast. Eng. **83**: 82–92. doi:10.1016/j.coastaleng.2013.10.004

Anderson, M. E., J. M. Smith, and S. K. McKay. 2011. Wave dissipation by vegetation. Coastal and Hydraulics Engineering Technical Note ERDC/CHL CHETN-I-82. Vicksburg, MS US Army Corps Eng. Eng. Res. Dev. Center. 22.

Anten, N. P. R., and F. J. Sterck. 2012. Terrestrial vs aquatic plants: How general is the drag tolerance-avoidance trade-off? New Phytol. **193**: 6–8. doi:10.1111/j.1469-8137.2011.03994.x

Anten, N. P. R., Casado-Garcia, R. and Nagashima, H. 2017. Effects of Mechanical Stress and Plant Density on Mechanical Characteristics, Growth, and Lifetime Reproduction of Tobacco Plants. Am. Nat. **166**: 650. doi:10.2307/3491228

Auerbach, L. W., S. L. Goodbred, D. R. Mondal, and others. 2015. Flood risk of natural and embanked landscapes on the Ganges-Brahmaputra tidal delta plain. Nat. Clim. Chang. **5**: 153–157. doi:10.1038/nclimate2472

Bal, K. D., T. J. Bouma, K. Buis, E. Struyf, J. Schoelynck, H. Backx, and P. Meire. 2011. Trade-off between drag reduction and light interception of macrophytes: Comparing five aquatic plants with contrasting morphology. Funct. Ecol. **25**: 1197–1205. doi:10.1111/j.1365-2435.2011.01909.x

Belliard, J. P., A. Silinski, D. Meire, G. Kolokythas, Y. Levy, A. Van Braeckel, T. J. Bouma, and S. Temmerman. 2019. High-resolution bed level changes in relation to tidal and wave forcing on a narrow fringing macrotidal flat: Bridging intra-tidal, daily and seasonal sediment dynamics. Mar. Geol. **412**: 123–138. doi:10.1016/j.margeo.2019.03.001

Biddington, N. L. 1986. The effects of mechanically-induced stress in plants - a review. Plant Growth Regul. **4**: 103–123. doi:10.1007/BF00025193

Bouma, T., M. Friedrichs, P. Klaassen, and others. 2009. Effects of shoot stiffness, shoot size and current velocity on scouring sediment from around seedlings and propagules. Mar. Ecol. Prog. Ser. **388**: 293–297. doi:10.3354/meps08130

Bouma, T. J., J. van Belzen, T. Balke, and others. 2014. Identifying knowledge gaps hampering application of intertidal habitats in coastal protection: Opportunities & steps to take. Coast. Eng. **87**: 147–157. doi:10.1016/j.coastaleng.2013.11.014

Bouma, T. J., M. Friedrichs, B. K. van Wesenbeeck, F. G. Brun, S. Temmerman, M. B. de Vries, G. Graf, and P. M. J. Herman. 2008. Plant growth strategies directly affect biogeomorphology of estuaries, p. 292. *In* River, Coastal and Estuarine Morphodynamics: RCEM 2007, Two Volume Set.

Bouma, T. J., M. B. De Vries, and P. M. J. Herman. 2010. Comparing ecosystem engineering efficiency of two plant species with contrasting growth strategies. Ecol. Soc. Am. **91**: 2696–2704. doi:10.1890/09-0690.1

Bouma, T. J., M. B. De Vries, E. Low, G. Peralta, I. C. Tánczos, J. van de Koppel, and P. M. J. Herman. 2005. Trade-offs related to ecosystem engineering: a case study on stiffness of emerging macrophytes. Ecology **86**: 2187–2199. doi:10.1890/04-1588

Butler, D. W., S. M. Gleason, I. Davidson, Y. Onoda, and M. Westoby. 2012. Safety and streamlining of woody shoots in wind: An empirical study across 39 species in tropical Australia. New Phytol. **193**: 137–149. doi:10.1111/j.1469-8137.2011.03887.x

Callaghan, D. P., T. J. Bouma, P. Klaassen, D. van der Wal, M. J. F. Stive, and P. M. J. Herman. 2010. Hydrodynamic forcing on salt-marsh development: Distinguishing the relative importance of waves and tidal flows. Estuar. Coast. Shelf Sci. **89**: 73–88. doi:10.1016/j.ecss.2010.05.013

Carus, J., M. Paul, and B. Schröder. 2016. Vegetation as self-adaptive coastal protection: Reduction of current velocity and morphologic plasticity of a brackish marsh pioneer. Ecol. Evol. **6**: 1579–1589. doi:10.1002/ece3.1904

Chen, H., Y. Ni, Y. Li, and others. 2018. Deriving vegetation drag coefficients in combined wave-current flows by calibration and direct measurement methods. Adv. Water Resour. **122**: 217–227. doi:10.1016/j.advwatres.2018.10.008

Cheong, S.-M., B. Silliman, P. P. Wong, B. van Wesenbeeck, C.-K. Kim, and G. Guannel. 2013. Coastal adaptation with ecological engineering. Nat. Clim. Chang. **3**: 787–791. doi:10.1038/nclimate1854

Coops, H., and G. Van der Velde. 1996. Effects of waves on helophyte stands : mechanical characteristics of stems of Phragmites australis and Scirpus lacustris. Aquat. Bot. **53**: 175–185. doi:10.1016/0304-3770(96)01026-1

Dalrymple, R. A., and R. G. Dean. 1991. Water wave mechanics for engineers and scientists (Vol. 2), Prentice-Hall.

Denny, M. W. 1994. Extreme drag forces and the survival of wind- and water-swept organisms. J. Exp. Bot. **194**: 97–115.

Denny, M. W., and B. Gaylord. 2002. Review the mechanics of wave-swept algae. J. Exp. Biol. **205**: 1355–1362.

Denny, M. W., L. P. Miller, M. D. Stokes, L. J. H. Hunt, and B. S. T. Helmuth. 2003. Extreme water velocities: Topographical amplification of wave-induced flow in the surf zone of rocky shores. Limnol. Oceanogr. **48**: 1–8. doi:10.4319/lo.2003.48.1.0001

Duarte, C. M., I. J. Losada, I. E. Hendriks, I. Mazarrasa, and N. Marbà. 2013. The role of coastal plant communities for climate change mitigation and adaptation. Nat. Clim. Chang. **3**: 961–968. doi:10.1038/nclimate1970

DWD Climate Data Center, (CDC). 2019. Recent hourly station observations of wind speed and wind direction for Germany, quality control not completed yet. Ftp://Ftp-Cdc.Dwd.de/Pub/ CDC/Observations_germany/Climate/Hourly/.

Feagin, R. A., M. Furman, K. Salgado, and others. 2019. The role of beach and sand dune vegetation in mediating wave run up erosion. Estuar. Coast. Shelf Sci. **219**: 97–106. doi:10.1016/j.ecss.2019.01.018

Feagin, R. a., J. L. Irish, I. Möller, A. M. Williams, R. J. Colón-Rivera, and M. E. Mousavi. 2011. Short communication: Engineering properties of wetland plants with application to wave attenuation. Coast. Eng. **58**: 251–255. doi:10.1016/j.coastaleng.2010.10.003

Friess, D. a, K. W. Krauss, E. M. Horstman, T. Balke, T. J. Bouma, D. Galli, and E. L. Webb. 2012. Are all intertidal wetlands naturally created equal?

Bottlenecks, thresholds and knowledge gaps to mangrove and saltmarsh ecosystems. Biol. Rev. Camb. Philos. Soc. **87**: 346–66. doi:10.1111/j.1469-185X.2011.00198.x

Gedan, K. B., M. L. Kirwan, E. Wolanski, E. B. Barbier, and B. R. Silliman. 2011. The present and future role of coastal wetland vegetation in protecting shorelines: answering recent challenges to the paradigm. Clim. Change **106**: 7–29. doi:10.1007/s10584-010-0003-7

Gracia, A., N. Rangel-Buitrago, J. A. Oakley, and A. T. Williams. 2018. Use of ecosystems in coastal erosion management. Ocean Coast. Manag. **156**: 277–289. doi:10.1016/j.ocecoaman.2017.07.009

Hallegatte, S., C. Green, R. J. Nicholls, and J. Corfee-Morlot. 2013. Future flood losses in major coastal cities. Nat. Clim. Chang. **3**: 802–806. doi:10.1038/nclimate1979

Hamann, E., and S. Puijalon. 2013. Biomechanical responses of aquatic plants to aerial conditions. Ann. Bot. **112**: 1869–1878. doi:10.1093/aob/mct221

Henry, P. Y., D. Myrhaug, and J. Aberle. 2015. Drag forces on aquatic plants in nonlinear random waves plus current. Estuar. Coast. Shelf Sci. **165**: 10–24. doi:10.1016/j.ecss.2015.08.021

Heuner, M., B. Schröder, U. Schröder, and B. Kleinschmit. 2018. Contrasting elevational responses of regularly flooded

marsh plants in navigable estuaries. Ecohydrol. Hydrobiol. **19**: 38–53. doi:10.1016/j.ecohyd.2018.06.002

Heuner, M., A. Silinski, J. Schoelynck, and others. 2015. Ecosystem Engineering by Plants on Wave-Exposed Intertidal Flats Is Governed by Relationships between Effect and Response Traits. PLoS One **10**: e0138086. doi:10.1371/journal.pone.0138086

Keddy, P. A. 2001. Modelling Competition Chapter 9, p. 333–404. *In* Competition. Kluwer Academic Publishers.

Koch, E. W., E. B. Barbier, B. R. Silliman, and others. 2009. Non-linearity in ecosystem services: temporal and spatial variability in coastal protection. Front. Ecol. Environ. **7**: 29–37. doi:10.1890/080126

Leonard, L. A., and A. L. Croft. 2006. The effect of standing biomass on flow velocity and turbulence in Spartina alterniflora canopies. Estuar. Coast. Shelf Sci. **69**: 325–336. doi:10.1016/j.ecss.2006.05.004

Miler, O., I. Albayrak, V. Nikora, and M. O'Hare. 2012. Biomechanical properties of aquatic plants and their effects on plant-flow interactions in streams and rivers. Aquat. Sci. **74**: 31–44. doi:10.1007/s00027-011-0188-5

Miler, O., I. Albayrak, V. Nikora, and M. O'Hare. 2014. Biomechanical properties and morphological characteristics of lake and river plants: implications for adaptations to flow conditions.
Aquat. Sci. doi:10.1007/s00027-014-0347-6

Möller, I. 2006. Quantifying saltmarsh vegetation and its effect on wave height dissipation: Results from a UK East coast saltmarsh. Estuar. Coast. Shelf Sci. **69**: 337–351. doi:10.1016/j.ecss.2006.05.003

Möller, I., M. Kudella, F. Rupprecht, and others. 2014. Wave attenuation over coastal salt marshes under storm surge conditions. Nat. Geosci. **7**: 727–731. doi:10.1038/ngeo2251

Möller, I., and T. Spencer. 2002. Wave dissipation over macro-tidal saltmarshes: Effects of marsh edge typology and vegetation change. J. Coast. Res. **36**: 506–521. doi:10.2112/1551-5036-36.sp1.506

Narayan, S., M. W. Beck, B. G. Reguero, and others. 2016. The Effectiveness, Costs and Coastal Protection Benefits of Natural and Nature-Based Defences. PLoS One **11**: e0154735. doi:10.1371/journal.pone.0154735

Nepf, H. M. 1999. Drag, turbulence, and diffusion in flow through emergent vegetation. Water Resour. Res. **35**: 479–489. doi:10.1029/1998WR900069

Nicholls, R. J., S. Hanson, C. Herweijer, N. Patmore, S. Hallegatte, J. Corfee-Morlot, J. Chateau, and R. Muir-Wood. 2008. Ranking Port Cities with High Exposure and Vulnerability to Climate Extremes: Exposure Estimates. OECD Environ. Work. Pap. **1**. doi:10.1787/011766488208

Paul, M., and L. G. Gillis. 2015. Let it flow: How does an underlying current affect wave propagation over a natural seagrass meadow? Mar. Ecol. Prog. Ser. **523**: 57–70. doi:10.3354/meps11162

Paul, M., F. Rupprecht, I. Möller, and others. 2016. Plant stiffness and biomass as drivers for drag forces under extreme wave loading: A flume study on mimics. Coast. Eng. **117**: 70–78. doi:10.1016/j.coastaleng.2016.07.004

Pérez-Harguindeguy, N., S. Díaz, E. Garnier, and others. 2013. New handbook for standardised measurement of plant functional traits worldwide. Aust. J. Bot. **61**: 167–234. doi:10.1071/BT12225

Pethick, J., and J. D. Orford. 2013. Rapid rise in effective sea-level in southwest Bangladesh: Its causes and contemporary rates. Glob. Planet. Change **111**: 237–245. doi:10.1016/j.gloplacha.2013.09.019

Puijalon, S., and G. Bornette. 2013. Multi-Scale Macrophyte Responses to Hydrodynamic Stress and Disturbances: Adaptive Strategies and Biodiversity Patterns, p. 261–270. *In* Ecohydraulics: an integrated approach.

Puijalon, S., G. Bornette, and P. Sagnes. 2005. Adaptations to increasing hydraulic stress: morphology, hydrodynamics and fitness of two higher aquatic plant species. J. Exp. Bot. **56**: 777–86. doi:10.1093/jxb/eri063

Puijalon, S., T. J. Bouma, C. J. Douady, J. van Groenendael, N. P. R. Anten, E. Martel, and G. Bornette. 2011. Plant resistance to mechanical stress: evidence of an avoidance-tolerance trade-off. New Phytol. **191**: 1141–9. doi:10.1111/j.1469-8137.2011.03763.x

Puijalon, S., T. J. Bouma, J. Van Groenendael, and G. Bornette. 2008. Clonal plasticity of aquatic plant species submitted to mechanical stress: Escape versus resistance strategy. Ann. Bot. **102**: 989–996. doi:10.1093/aob/mcn190

R Core Team, 2016. A Language and Environment for Statistical Computing. R, Vienna, Austria.

Rangel-buitrago, N., V. N. De Jonge, and W. Neal. 2018. How to make Integrated Coastal Erosion Management a reality. Ocean Coast. Manag. **156**: 290–299. doi:10.1016/j.ocecoaman.2018.01.027

Read, J., and A. Stokes. 2006. Plant biomechanics in an ecological context. Am. J. Bot. **93**: 1546–1565. doi:10.3732/ajb.93.10.1546

Rupprecht, F., I. Möller, B. Evans, T. Spencer, and K. Jensen. 2015. Biophysical properties of salt marsh canopies — Quantifying plant stem flexibility and above ground biomass. Coast. Eng. **100**: 48–57. doi:10.1016/j.coastaleng.2015.03.009

Rupprecht, F., I. Möller, M. Paul, and others. 2017. Vegetation-wave interactions in salt marshes under storm surge conditions.

Ecol. Eng. **100**: 301–315. doi:10.1016/j.ecoleng.2016.12.030

Sand-Jensen, K. 2003. Drag and reconfiguration of freshwater macrophytes. Freshw. Biol. **48**: 271–283. doi:10.1046/j.1365-2427.2003.00998.x

Schipper, C. A., H. Vreugdenhil, and M. P. C. De Jong. 2017. A sustainability assessment of ports and port-city plans : Comparing ambitions with achievements. Transp. Res. Part D **57**: 84–111. doi:10.1016/j.trd.2017.08.017

Schoelynck, J., S. Puijalon, P. Meire, and E. Struyf. 2015. Thigmomorphogenetic responses of an aquatic macrophyte to hydrodynamic stress. Front. Plant Sci. **6**: 1–7. doi:10.3389/fpls.2015.00043

Schoutens, K., M. Heuner, V. Minden, T. Schulte Ostermann, A. Silinski, J.-P. Belliard, and S. Temmerman. 2019. How effective are tidal marshes as nature-based shoreline protection throughout seasons? Limnol. Oceanogr. **64**: 1750–1762. doi:10.1002/lno.11149

Schulze, D., F. Rupprecht, S. Nolte, and K. Jensen. 2019. Seasonal and spatial within - marsh differences of biophysical plant properties : implications for wave attenuation capacity of salt marshes. Aquat. Sci. doi:10.1007/s00027-019-0660-1

Shepard, C. C., C. M. Crain, and M. W. Beck. 2011. The protective role of coastal marshes: A systematic review and meta-analysis. PLoS One **6**. doi:10.1371/journal.pone.0027374

Silinski, A., M. Heuner, J. Schoelynck, and others. 2015. Effects of wind waves versus ship waves on tidal marsh plants: A flume study on different life stages of *Scirpus maritimus*. PLoS One **10**: e0118687. doi:10.1371/journal.pone.0118687

Silinski, A., M. Heuner, P. Troch, and others. 2016. Effects of contrasting wave conditions on scour and drag on pioneer tidal marsh plants. Geomorphology **255**: 49–62. doi:10.1016/j.geomorph.2015.11.021

Silinski, A., K. Schoutens, S. Puijalon, J. Schoelynck, D. Luyckx, P. Troch, P. Meire, and S. Temmerman. 2017. Coping with waves: Plasticity in tidal marsh plants as self-adapting coastal ecosystem engineers. Limnol. Oceanogr. **63**: 799–815. doi:10.1002/lno.10671

Stark, J., T. Van Oyen, P. Meire, and S. Temmerman. 2015. Observations of tidal and storm surge attenuation in a large tidal marsh. Limnol. Oceanogr. **60**: 1371–1381. doi:10.1002/lno.10104

Starko, S., B. Z. Claman, and P. T. Martone. 2015. Biomechanical consequences of branching in flexible wave-swept macroalgae. New Phytol. **206**: 133–140. doi:10.1111/nph.13182

Starko, S., and P. T. Martone. 2016. Evidence of an evolutionary-developmental trade-off between drag avoidance and tolerance strategies in wave-swept intertidal kelps (Laminariales, Phaeophyceae). J. Phycol. **52**: 54–63. doi:10.1111/jpy.12368

Strotmann, T. 2014. Deutsches Gewässerkundliches Jahrbuch, Elbegebiet Teil 3, Untere Elbe ab der Havelmündung.

Suzuki, T., M. Zijlema, B. Burger, M. C. Meijer, and S. Narayan. 2012. Wave dissipation by vegetation with layer schematization in SWAN. Coast. Eng. **59**: 64–71. doi:10.1016/j.coastaleng.2011.07.006

Temmerman, S., and M. L. Kirwan. 2015. Building land with a rising sea: Cost-efficient nature-based solutions can help to sustain coastal societies. Science **349**: 588–589. doi:10.1126/science.aac8312

Temmerman, S., P. Meire, T. J. Bouma, P. M. J. Herman, T. Ysebaert, and H. J. De Vriend. 2013. Ecosystem-based coastal defence in the face of global change. Nature **504**: 79–83. doi:10.1038/nature12859

Tempest, J. A., I. Möller, and T. Spencer. 2015. A review of plant-flow interactions on salt marshes: the importance of vegetation structure and plant mechanical characteristics. Wiley Interdiscip. Rev. Water **2**: 669–681. doi:10.1002/wat2.1103

Tessler, Z. D., C. J. Vörösmarty, M. Grossberg, I. Gladkova, H. Aizenman, J. P. M. Syvitski, and E. Foufoula-Georgiou. 2015. Profiling risk and sustainability in coastal deltas of the world. Science (80-.). **349**: 638–643. doi:10.1126/science.aab3574

Usherwood, J. R., A. R. Ennos, and D. J. Ball. 1997. Mechanical and anatomical adaptations in terrestrial and aquatic buttercups to their respective environments. J. Exp. Bot. **48**: 1469–1475. doi:10.1093/jxb/48.7.1469

Vanlierde, E., S. Michielsen, K. Vereycken, R. Hertoghs, D. Meire, M. Deschamps, T. Verwaest, and F. Mostaert. 2011. Onderzoek naar de invloedsfactoren van golfbe-lasting en de morfologische effecten op slikken en schorren in de Beneden Zeeschelde, meer specifiek op het Galgeschoor: Deelrapport 2: Verslag testmeting van 29/11/2010 - 01/12/2010. Technical Report. Waterb.

Verschoren, V., D. Meire, J. Schoelynck, K. Buis, K. D. Bal, P. Troch, P. Meire, and S. Temmerman. 2016. Resistance and reconfiguration of natural flexible submerged vegetation in hydrodynamic river modelling. Environ. Fluid Mech. **16**: 245–265. doi:10.1007/s10652-015-9432-1

Vogel, S. 1996. Life in moving fluids: the physical biology of flow, 2nd ed. Princeton University Press.

Vuik, V., S. N. Jonkman, B. W. Borsje, and T. Suzuki. 2016. Nature-based flood protection: The efficiency of vegetated foreshores for reducing wave loads on coastal

dikes. Coast. Eng. **116**: 42–56. doi:10.1016/j.coastaleng.2016.06.001

Vuik, V., H. Y. Suh Heo, Z. Zhu, B. W. Borsje, and S. N. Jonkman. 2018. Stem breakage of salt marsh vegetation under wave forcing: A field and model study. Estuar. Coast. Shelf Sci. **200**: 41–58. doi:10.1016/j.ecss.2017.09.028

Wilson, S. D., and P. A. Keddy. 1986. Species Competitive Ability and Position Along a Natural Stress / Disturbance Gradient. Ecology **67**: 1236–1242. doi:10.2307/1938679

Woodruff, J. D., J. L. Irish, and S. J. Camargo. 2013. Coastal flooding by tropical cyclones and sea-level rise. Nature **504**: 44–52. doi:10.1038/nature12855

WSA, H. 2017. Außenelbe Nordsee und Tideelbe | DGM-W 2016 | verschiedene Teilgebiete | Modelldaten.

Yang, S. L., B. W. Shi, T. J. Bouma, T. Ysebaert, and X. X. Luo. 2012. Wave attenuation at a salt marsh margin : A case study of an exposed coast on the Yangtze Estuary. Estuaries and Coasts **35**: 169–182. doi:10.1007/s12237-011-9424-4

Ysebaert, T., S. Yang, L. Zhang, Q. He, T. J. Bouma, and P. M. J. Herman. 2011. Wave attenuation by two contrasting ecosystem engineering salt marsh macrophytes in the intertidal pioneer zone. Wetlands **31**: 1043–1054. doi:10.1007/s13157-011-0240-1

Zentrales Datenmanagement der GDWS Standort Kiel, W. H. 2017. Digitale Orthophotos Unter- und Außenelbe (DOP020) WSA Hamburg 2016.

4

Survival of the thickest?
Impacts of extreme wave-forcing on marsh seedlings are mediated by species morphology

Ken Schoutens, Svenja Reents, Stefanie Nolte, Ben Evans, Maike Paul, Matthias Kudella, Tjeerd J. Bouma, Iris Möller, Stijn Temmerman

4.1 Abstract

Although tidal marshes are known for their coastal defense function during storm surges, the impact of extreme wave forcing on tidal marsh development is poorly understood. Seedling survival in the first season after germination, which may involve exposure to extreme wave events, is crucial for the natural establishment and human restoration of marshes. We hypothesize that species-specific plant traits plays a significant role in seedlings survival and response to wave induced stress, i.e. through stem bending and uprooting. To test this hypothesis, seedlings of pioneer species (*Bolboschoenus maritimus*, *Schoenoplectus tabernaemontani*, *Spartina anglica* and *Puccinellia maritima*) with contrasting biophysical traits were placed in the Large Wave Flume in Hannover (Germany) and exposed to storm wave conditions.

Seedlings of *P. maritima* and *S. anglica* experienced a lower loss rate and bending angle after wave exposure compared to *S. tabernaemontani* and especially *B. maritimus*. The higher loss rates of *B. maritimus* and *S. tabernaemontani* result from deeper scouring around the stem base. Scouring depth was larger around stems of greater diameter and higher resistance to bending. Here, *B. maritimus* and *S. tabernaemontani* have both thicker and stiffer stems than *S. anglica* and *P. maritima*. Our results show that especially seedlings with thicker stems suffer from erosion and scouring, and have the highest risk of being lost during extreme wave events. This implies that for successful seedling establishment and eventually the establishment of a mature tidal marsh vegetation, the species composition and their capacity to cope with storm wave disturbances is crucial.

4.2 Introduction

Understanding the mechanisms that facilitate or hinder plant establishment on tidal flats is fundamental for successful tidal marsh restoration and creation, which is increasingly implemented for delivery of a multitude of ecosystem services, including the nature-based mitigation of coastal hazards related to global change (Narayan et al. 2016; van der Nat et al. 2016; Oppenheimer et al. 2019). Despite being the focus of this increased attention, tidal marsh ecosystems are still under threat due to environmental change and anthropogenic pressures, such as sea level rise, and local factors, such as marsh conversion to human land use (Lotze et al., 2006; Nicholls and Cazenave, 2010; Van Asselen et al., 2013).

To counteract loss or create new tidal marshes as nature based solutions, a variety of methods are used to (re-)establish ecological functioning. In practice, tidal marsh (re-)establishment requires the presence of a suitable habitat for marsh development, such as suitable bed elevation (i.e. tidal inundation frequency) and hydrodynamic conditions that allow seedling establishment and growth (Wolters et al., 2008; Zhao et al., 2020). There are several options to initiate the growth of marsh vegetation, i.e. (i) by adult propagule settlement, (ii) lateral clonal expansion of existing marsh plants or (iii) seedling establishment (Balke et al., 2014; Hu et al., 2015). Aside from a detailed understanding of the conditions under which seeds of tidal marsh plants can germinate and establish (Hu et al., 2015), it might be even more important to know how seedlings can survive energetic environments to facilitate and ensure successful marsh restoration and creation.

Studies on seedling survival often focus on the initial establishment phase, i.e. the phase where the seedlings become independent of the resources in the seed (Balke et al., 2014; Zhu et al., 2014). After initial seedling establishment in calm growing conditions, potential storm events in the course of the growing season might exert strong mechanical stress on the developing seedlings (Paul et al., 2016; Rupprecht et al., 2017) and may limit their survival. Yet many studies on seedling survival are conducted under relatively low levels of hydrodynamic exposure (Cao et al., 2020, 2018; Silinski et al., 2015; Xie et al., 2019). In contrast, little is known about survival in the period between initial seedling establishment and fully grown, patch forming pioneer vegetation, when the plants could still be vulnerable to more extreme hydrodynamic disturbances. On the one hand storm surges are difficult to investigate in the field due to their sporadic nature and relative unpredictability in terms of timing of occurrence, magnitude and precise meteorological characteristics (Hansen et al., 2019). On the other hand storm surges and storm waves are difficult to simulate in lab conditions without encountering significant scaling issues (Masselink et al., 2016; Spencer et al., 2015).

Fundamental knowledge on the processes that determine seedling survival under storm conditions is required to support the implementation of successful restoration

of tidal marshes and their valuable ecosystem services. Structural failure of plants due to hydrodynamic stress is initiated by (1) drag forces acting on the plant shoots (Henry et al., 2015; Paul et al., 2016) and can be facilitated by (2) sediment scour around the stem base (Friess et al., 2012). Drag forces result from friction between the water flow and the plant shoot (e.g. Dalrymple and Dean 1991; Denny 1994), which is known to be a function of hydrodynamic forces (i.e. flow velocities), plant morphology (i.e. shoot surface area) and stem biomechanical properties (i.e. stem stiffness) (Paul et al., 2016; Vuik et al., 2018). Recent studies highlight that such species-specific plant traits also affect the plant's capacity to cope with mechanical stress from hydrodynamic forces (chapter3: Schoutens et al., 2020; Silinski et al., 2018). For example, if the drag forces exceed the shoots' resistance against breakage, the stem will buckle or will break which can be fatal for the survival of the plant (Vuik et al., 2018). Moreover, when drag forces exceed the root anchoring strength, the seedling will be dislodged and will be flushed away by waves and currents. For the anchoring strength of the seedling, the root growth and structure are crucial (Peralta et al., 2006; Szmeja and Galka, 2008). Additionally, anchoring strength decreases through the development of scour holes around the stem base resulting from turbulence, leading to reduced contact area between roots and soil. Scour hole volume around single shoots has been shown to be a function of hydrodynamic forces, morphological and biomechanical plant properties (Bouma et al., 2009a), and sediment properties (Lo et al., 2017). Additionally, scouring around patches of multiple shoots growing close to each other, has been reported to depend also on the shoot density within the patch (e.g. Bouma et al. 2009b; Duggan-Edwards et al. 2020). When scour decreases the anchoring strength up to a point where drag forces can dislodge the complete plant, it will be flushed away and lost (Bywater-Reyes et al., 2015). The role of plant traits on drag forces and scouring processes during storm wave conditions remains unclear.

In the present study we experimentally assess the survival rates of four different species of pioneer tidal marsh seedlings with distinct morphologies, under storm wave conditions. More specifically, we examine the cause of structural failure, i.e. stem bending and uprooting by storm waves and how this relates to species-specific plant traits. Drag force proxies and scouring were quantified. Plant morphological and biomechanical properties were measured to support discussion of potential explanations of species differences in survival, damage, scouring and drag forces. With this discussion we aim to increase insights into the link between species-specific plant traits and the capacity of the seedlings to survive storm wave conditions.

4.3 Methods

4.3.1 Studied species

To test the hypothesis that plant traits exert a significant influence on the survival of pioneer marsh seedlings under storm wave conditions, four NW European pioneer marsh species with distinct morphologies were selected: *Bolboschoenus maritimus* (L.) Palla, *Schoenoplectus tabernaemontani* (C.C.Gmel.) Palla, *Spartina anglica* C.E. Hubb. and *Puccinellia maritima* (Huds.) Parl. *B. maritimus* and *S. tabernaemontani* are pioneer species in brackish marshes, while *P. maritima* and *S. anglica* are found in pioneer salt marshes. All four species can spread by clonal outgrowth (via rhizomes or stolons) of existing adult plants but can also colonize bare mudflats by seed dispersal. After flowering in summer, seeds can spread by the wind or tide in autumn followed by germination in spring. *B. maritimus* is often found as pioneer species in brackish marshes forming monospecific patches/zones parallel to the marsh shoreline. They form tall, thick shoots (up to 2.5 m high) with leaves. *S. tabernaemontani* can be found in the same brackish environment of pioneer marshes (Elsen et al., 2019; Heuner et al., 2018). It grows in monospecific stands and produces tall and thick stems (up to 2.0 m high) without leaves. *P. maritimus* is typically found in pioneer (to mid-successional) salt marshes characterised by sheltered conditions. It forms dense tufts (up to 0.7 m high) of thin flexible stems with leaves spread over the soil surface. The salt marsh coloniser *S. anglica* is a pioneer that grows in dense tussocks of thin stems with leaves (up to 1.5 m high) under highly dynamic conditions often covering the lowest parts of the marsh.

4.3.2 Experimental setup

4.3.2.1 Preparation of experimental plant units

Upon stratification (4 °C during the night and room temperature during the day), germination of seeds was initiated on moist substrate. Three weeks after the start of the stratification (mid-June 2018), the seedlings were first planted in fertilised (slow release Osmocote, Substral) sand from the Scheldt estuary (SW Netherlands) and grown in greenhouse conditions. Five weeks later, the seedlings were transplanted in large sediment boxes (120cm by 80cm, 40 cm soil depth) that were later placed in the flume. The sediment in the boxes was composed of 32% silt and clay (< 63 μm), and 31%, 11%, 24%, and 2% very fine (63 – 125 μm), fine (125 – 200 μm), medium (200 – 630 μm), and coarse sand (> 630 μm), respectively, with a mean grainsize of 152.02 μm. As the sediment comes from the intertidal zone of the Scheldt estuary, this particle size distribution is representative for tidal marshes and mudflats in this estuary. Seedlings were planted 15 cm apart in a grid of 4 by 6 with a distance of 20 cm from the front and the back and 15 cm from the sides of the sediment box to minimize interference between the individuals and still enabling plantation of a reasonable amount of individuals (24 per sediment box) in the available space of the sediment

boxes to allow statistical analyses (Fig. 4.1). Throughout the entire preparation period, the boxes were stored outside and the substrate was kept moist by irrigation with freshwater. The seedlings were 10 to 14 weeks old during the experiment.

4.3.2.2 Spatial and temporal setup

The experiment was carried out over a three week period (13-31 August 2018) in the Large Wave Flume (Grosser Wellenkanal, GWK) of the Forschungszentrum Küste (FZK), Hannover, Germany. In the middle of the wave flume (310 m long, 5 m wide and 7 m deep), an elevated platform (40 m long) was split over its length into separate zones (Fig. 4.1). The zones (horizontally separated by 10 m of platform) consisted of lowered gaps in the platform in which sediment boxes with plants were placed so that the surface of the sediment boxes was level with the platform surface. In addition to the experiment with seedlings described in this paper, which was performed in one such zone, other sediment boxes in other zones contained parallel experiments of which the results will be reported in other manuscripts. In the seedling zone, four sediment boxes were placed, each box contained 24 individual seedlings (pseudo replicates) of one of the four different plant species. This set-up with sediment boxes excludes flume wall-edge erosion effects (Möller et al., 2014). One set of four boxes was placed in the flume for a whole week and then replaced by a new set of four boxes in the next week. Hence, for the three week period of the experiment, three sets of four sediment boxes filled with seedlings were prepared.

We highlight that the three consecutive weeks do not represent three replicate runs with the same wave conditions. Instead, over the three-week course of the experiment, a sequence of different wave conditions was applied (further called wave runs). Every week, four different wave runs were applied on day 2, 3, 4 and 5, with a daily increase in the intensity of simulated wave conditions (Table 4.1). This set-up gave us a total of 12 different wave runs covering a wide range of (extreme) hydrodynamic wave conditions. We chose this design to limit the risk of having a too narrow range of wave conditions for which either (i) all wave conditions would be too harsh and all seedlings would flush away after the first wave run or (ii) all wave conditions would be not harsh enough and none of the species would show any response. Instead, applying a wide range of wave conditions allowed us to identify species-dependent differences in seedling response. However, this choice and practical limitations (oa. in terms of time and resources) implied that we could not do replicate wave runs under exactly the same wave and plant conditions. Every daily wave run consisted of a JONSWAP wave spectrum of 1000 random waves (i.e. waves of different height and period as experienced typically on the shores of the North Sea) with an inundation depth of 1.5 m approximating storm surge conditions in temperate regions (Table 4.2). Wave and water depth conditions were selected to mimic conditions that (a) are typical of those experienced at marsh margins around the North Sea basin (e.g. Spencer et al. 2015)), (b) generate high bed shear stresses, but also (c) maintain relative uniformity of

hydrodynamic forcing along the individual successive experimental zones on the raised platform. Only during the last wave run (on day 4 of week 3) were monochromatic waves used to allow higher time-averaged wave induced bed stresses to be simulated (see Table 4.1), which could not be achieved through an irregular wave spectrum. In between the daily wave runs the flume was drained slowly over several hours in order to prevent erosion on the sediment surface and drag on the seedlings. Once the flume was drained, in between every daily wave run, the effects of the preceding inundation and wave conditions on the plant seedlings and sediment surface were measured, but the same boxes with sediments and plants were kept in the flume for 5 days. Hence, for four days (days 2-5), the seedlings and sediment surfaces were exposed to an accumulating load of wave energy resulting from the four consecutive wave runs.

Table 4.1. Incoming wave conditions measured at the start of the experimental platform. Significant wave height (H_s, m) and significant wave period (T_s, s) are shown per week and per wave run. Every wave run consisted of 1000 waves. Note that apart from the monochromatic waves during wave run 4 of week 3 (italics), all wave runs had randomly generated waves representative for North Sea conditions (JONSWAP spectrum).

		H_s (m)			T_s (s)		
		Week 1	Week 2	Week 3	Week 1	Week 2	Week 3
Wave run	1	0.30	0.68	0.68	2.58	3.80	4.02
	2	0.40	0.68	0.77	4.22	3.80	5.63
	3	0.58	0.78	0.78	3.56	5.66	5.63
	4	0.69	0.78	*0.71*	5.23	5.63	*6.00*

Table 4.2. Field studies with recordings of a maximum significant wave height (H_s, m) and inundation depths (h, m) at the marsh edge as compared to the conditions in this flume experiment.

Publication	H_s (m)	h (m)	Study site
This flume study	**0.78**	**1.5**	
Möller et al. 1999	0.58	1.39	North Norfolk Coast, UK
Ysebaert et al. 2011	0.64	1.86	Yangtze, CN
Yang et al. 2012	0.73	1.71	Yangtze, CN
Vuik et al. 2016	0.69	1.90	Western Scheldt, NL
Chapter 2: Schoutens et al. 2019	1.00	3.85	Elbe, GE
Zhu et al. 2020	0.87	2.20	Wadden Sea Coast, NL

4.3.3 Hydrodynamic measurements

Wave-induced current velocities were recorded directly in front (0.30 m) of the seedling zone (Fig. 4.1). High-frequency (25 Hz) flow velocity measurements were conducted with Acoustic Doppler Velocimeters (ADVs) positioned in the middle of the flume width at 0.05 m above the bottom of the experimental platform. Wave gauge arrays mounted against the flume side wall were installed at the start of the experimental platform (Fig. 4.1). From these measurements, the significant wave height and period (mean of the highest third of recorded wave heights, H_s or wave periods T_s respectively) were derived (Table 4.1). Over the course of the four days for which individual seedling boxes were retained in the flume, the wave exposure of the seedlings and sediment surfaces progressively increased. The plant and sediment surface responses recorded on each day thus represent change induced through the previous day's wave run, but, for days 3, 4, and 5, the reported change is that which has resulted from all preceding wave runs during that week, i.e. is relative to day 1 of the experiment. The accumulated wave load (action, S) for each wave run was calculated from the orbital flow velocities as the kinetic energy times the exposure time (i.e. number of wave oscillations times the representative wave period) and has the unit Joules-second (Js) (see supplementary info for the full method).

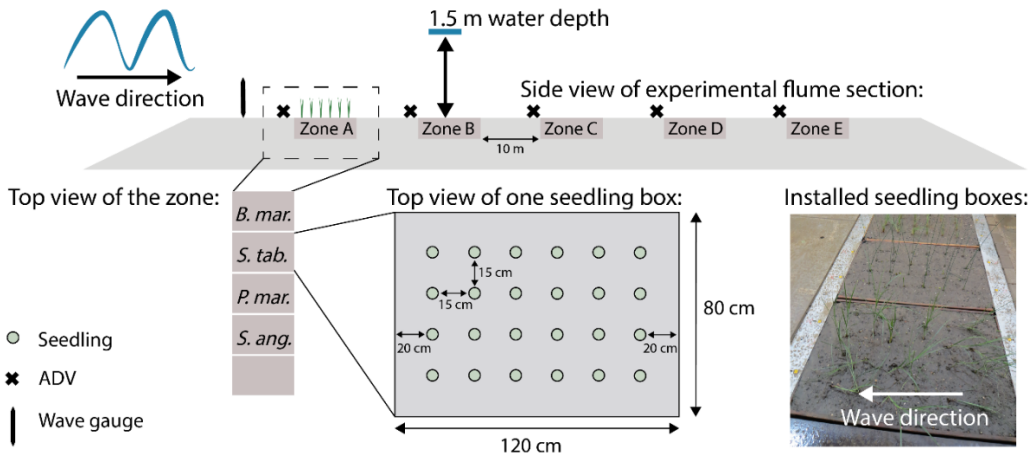
Figure 4.1: Schematic overview of the experimental setup in the Large Wave Flume (GWK, Hannover, Germany). On the elevated platform, installed in the flume, one zone was used to install four boxes with seedlings (the fifth box was part of another experiment). Each box contained 24 seedlings of one species. The picture on the right illustrates the seedling boxes installed in the flume platform.

4.3.4 Plant trait dependent response to storm waves

4.3.4.1 Plant damage and vitality

Seedling response to storm wave exposure was quantified daily after each wave run and was compared to the initial seedling condition before the first wave run of the week. Remaining seedlings were counted and the angle, perpendicular to the sediment bed, of the standing stem was measured in categories ranging from '<18°', '18°-36°', '36°-54°', '54°-72°' and '72°-90°' (the latter representing the seedlings that were almost completely bent over on the sediment bed). Seedlings that were missing were categorised as 'lost shoot'. When a shoot was lost, the cause (uprooting, i.e. including loss of below-ground roots; or stem breakage, i.e. below-ground roots still present) was noted.

4.3.4.2 Damage resulting from drag forces and erosion

Scouring and erosion features

Structure from motion (SFM) photogrammetry of the sediment surfaces was used to quantify the degree of erosion, including local scouring around the individual shoots, and in certain cases larger-scale erosion features in the sediment boxes. Pictures (ca. 300) were taken daily from various angles in between wave runs, after which they were processed in Agisoft Photoscan Professional software to produce three-dimensional point clouds. For the processing of the SFM photographs to accurate ground geometry and the spatial co-registration of successive point clouds, self-adhesive fiducial markers were placed at fixed positions on metal fixings around the experimental zone. Point clouds were scaled and co-registered to a reference cloud (Day 1 of the week, before any wave run) that had previously been scaled and registered to a lower resolution (5 mm) point cloud derived from an overhead laser scanner. Comparisons between clouds were conducted using the M3C2 plugin for Cloud Compare (Lague et al., 2013). The M3C2 distances, projected onto the reference cloud, were then rasterized on a 1 mm grid prior to further analysis in R (R Core Team, 2020). From this raster, the sediment elevation was extracted as rings of 2 mm thickness designated here by their outer radius. Differentiation between scour features and pallet erosion was achieved through visual inspection of images.

Drag forces on plants

Hydrodynamic drag forces can initiate severe mechanical stresses when applied to plant structures. It is known that such hydrodynamic drag forces depend on flow velocities, shoot biomass and shoot stiffness (Vogel, 1996). In this paper, shoot biomass, shoot length and flexural stiffness were used as proxies for drag forces experienced by the four species.

4.3.5 Plant morphology and biomechanics

Plant morphological properties (shoot biomass, shoot length, basal stem diameter) were quantified for all four species as follows. Aboveground biomass was harvested for every surviving seedling after the last wave run of each week. Belowground biomass, as proxy for anchoring capacity, was sampled on 5 replicate seedlings per species by digging up all the roots and rinsing the sediment off. After biomass collection, the samples were dried for 72h at 70 °C and weighed. Root:shoot ratios were calculated as the mean belowground biomass divided by the mean aboveground biomass and the error bars were obtained through a propagation formula. Shoot lengths and basal stem diameters were measured on all 24 seedlings of every species each week.

Biomechanical properties (second moment of area, Young's modulus and flexural stiffness) were quantified for all four species by three-point bending tests (Niklas, 1992; Rupprecht et al., 2015). Per week, 5 seedlings per species were harvested after the last wave run to test for flexural strength of the shoots. The tests were performed using a universal testing machine (Instron 5942, precision ± 0.5%) with a 10 kN load cell (Instron Corporation, Canton, MA, USA). Prior to testing, the diameters of the stems were measured with a caliper. The supports of the machine, on which the plant shoots were horizontally placed, were fixed at a distance of 15 times the stem diameter to diminish shear stress on the supports during the tests (Usherwood et al., 1997). The most basal part of the stem was placed on the two supports after which a force was applied on the center of the stems at a displacement rate of 10 mm min^{-1}. The Instron Bluehill 3.0 software accompanied by the device creates a stress-strain curve, i.e. a graph describing the relation between vertical deflection of the stem (D; on the X-axis) and the bending force of the stem (F; on the Y-axis) which enables the calculation of the slope from the elastic deformation zone on the curve (F/D) (see supplementary figure S4.2 for an example of the stress-strain curve). From this slope, the flexural stiffness (EI in Nm^2) was calculated as:

(eq 1.) $EI = (s^3\,F)/(48D)$,

where s is the distance between the supports. Next, the second moment of area (I in m4), a measure for the structural geometry (i.e. shape) of the stem, was calculated. The formula used for round stems (*S. tabernaemontani*, *P. maritima* and *S. anglica*) is:

(eq 2.) $I = \pi r^4/64$,

where r is the diameter of the stem's cross section, and the formula for the triangular stems of *B. maritimus* is:

(eq 3.) $I = bh^3/36$,

where *b* is the base and *h* is the height of the triangular cross section. Using the flexural stiffness and the second moment of area, we calculated Young's modulus (E in Nm^{-2}), which is a measure for the strength of the stem material, as $E = EI/I$.

4.3.6 Data analysis

Probabilities of damage were compared between species with two-proportion z-tests. Species-specific differences in scouring depth in response to storm wave conditions as well as species differences in plant traits (morphological and biomechanical properties) were tested with one-way ANOVAs or the non-parametric alternative Kruskal-Wallis test. These were followed by a multiple pairwise comparison with a post-hoc Tukey honest significant difference test or with a non-parametric pairwise comparison using Wilcoxon rank sum test with Bonferroni correction. Linear regression was applied to check for a relationship between scour depth and stem diameter and Pearson correlation coefficient was calculated. To test if shoot length is important for the risk of getting damaged we used a logistic mixed effect model with 'damage' after the 4th wave run of the week as the response variable ('damaged' and 'not damaged'), the 'week' of the experiment was added as random variable and 'species' was added as random variable nested in 'week'. The significance of the shoot length was tested with a Likelihood Ratio test (Zuur et al., 2009). All statistical analyses were performed in R 3.5.3 (R Core Team, 2020) applying a significance level of $p < 0.05$ for all tests. Normality of the residuals was tested based on visual inspection with histograms and Q-Q plots and homogeneity of variance was tested with scale-location plots. To meet normality assumptions, a log transformation was applied to the aboveground biomass data.

4.4 Results

4.4.1 Storm wave induced damage

Simulated storm waves had an increasing significant wave height H_s every consecutive wave run in a week (Table 4.1). The waves had an H_s ranging from 0.30 m up to 0.78 m and a significant wave period T_s ranging between 2.6 s and 6.0 s. As seedlings were exposed to 4 consecutive wave runs in one week, the experienced stress on any specific day was the result of the effect of all preceding wave runs that week, including the run on the day of, and preceding, the measurement of plant characteristics. Thus, the accumulated wave load was calculated (Fig. 4.2). With an accumulated wave load of 819 Js, the first week represented the calmest storm conditions of the experiment. The accumulated wave load in week 2 (1667 Js) and week 3 (1454 Js) were similar to each other, although the specific wave characteristics differed (Table 4.1).

After exposure to storm-wave conditions, the damage (i.e. stem bending angle and seedling loss) observed was highest for the *B. maritimus* and *S. tabernaemontani*

seedlings (Fig. 4.2). Seedlings of *S. anglica* and *P. maritima* hardly showed noticeable damage, while up to 100 % of the *B. maritimus* seedlings showed damage from wave exposure. The main damage in *B. maritimus* were bent shoots and over the three weeks less than 15 % of the shoots were lost. *S. tabernaemontani* seedlings had better survival rates and after four wave runs, the *S. tabernaemontani* seedlings had more than 57 % chance to remain upright in contrast to 26 % for *B. maritimus* seedlings (z-test Chi-squared = 13.18, df = 1, p < 0.05). Most damage in *S. tabernaemontani* seedlings only started from wave run 3 onwards, but was still limited, i.e. after the fourth wave run, *S. tabernaemontani* seedlings had less than 15 % chance of being bent by > 72° while this was more than 40 % for *B. maritimus* seedlings (z-test Chi-squared = 10.04, df = 1, p < 0.05). Interestingly, all seedlings that were lost suffered from stem breakage, mainly at the base of the stem. No cases were observed of seedlings that were uprooted, i.e. completely eroded and washed away including their roots. Apart from some exceptions, the stems bent or broke at the stem-root connection.
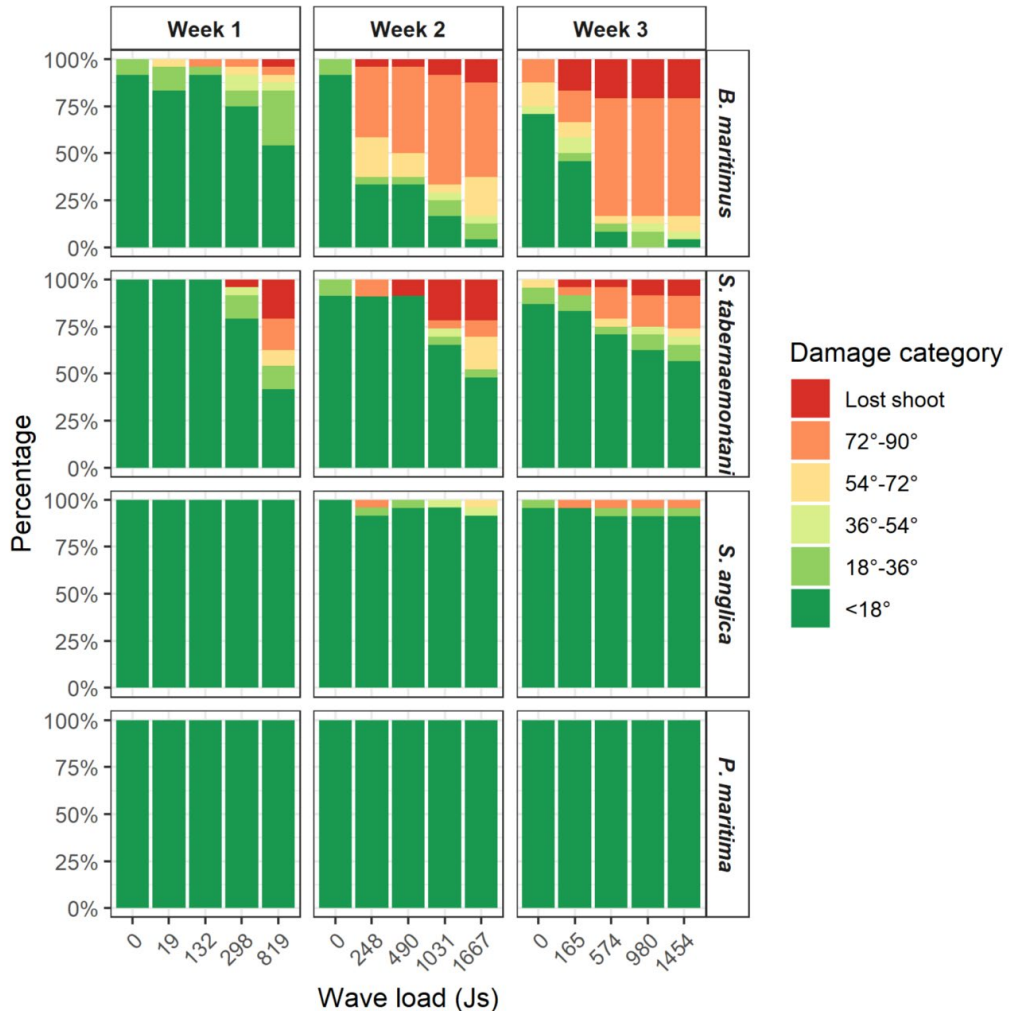
Figure 4.2: Percentage of seedlings (n = 24) that experienced damage caused by storm-wave exposure for the four species. Damage is quantified in six categories ranging from < 18° (i.e. no or negligible damage), to higher bending angles (increasing damage), to completely lost shoots (due to breakage at the stem base). The first day represents the initial starting situation before any wave exposure (wave load is zero). The accumulated wave load (Js) after each daily wave run is indicated on the x-axis.

4.4.2 Scouring processes

To gain insights in why damage differs between the species, we investigated two groups of processes that can generate wave-induced damage to the plants: (1) proxies for drag forces and (2) erosion processes such as scouring. Measurements of sediment scouring around individual plant stems, induced by turbulence, indicate a difference between species (Kruskal-Wallis Chi-squared = 128.5, df = 1, p < 0.05) that is in line with the observed species differences in seedling damage (Fig. 4.3). Especially close to

the seedling stems, *B. maritimus* and *S. tabernaemontani* produced deeper scour holes (median values of 1.0 cm) compared to *P. maritima* and *S. anglica* (only a few millimeter). The scour holes around *P. maritima* were shallower and narrower compared to the scour holes around *B. maritimus* and *S. tabernaemontani*. Least scour was observed around *S. anglica*. Around some of the seedlings, the sediment was slightly elevated (in the order of magnitude of a few millimeters), which may be within registration errors, due to small deposition of elsewhere eroded sediments or due to slight swelling of the clay and silt rich sediment surface during the experiment.
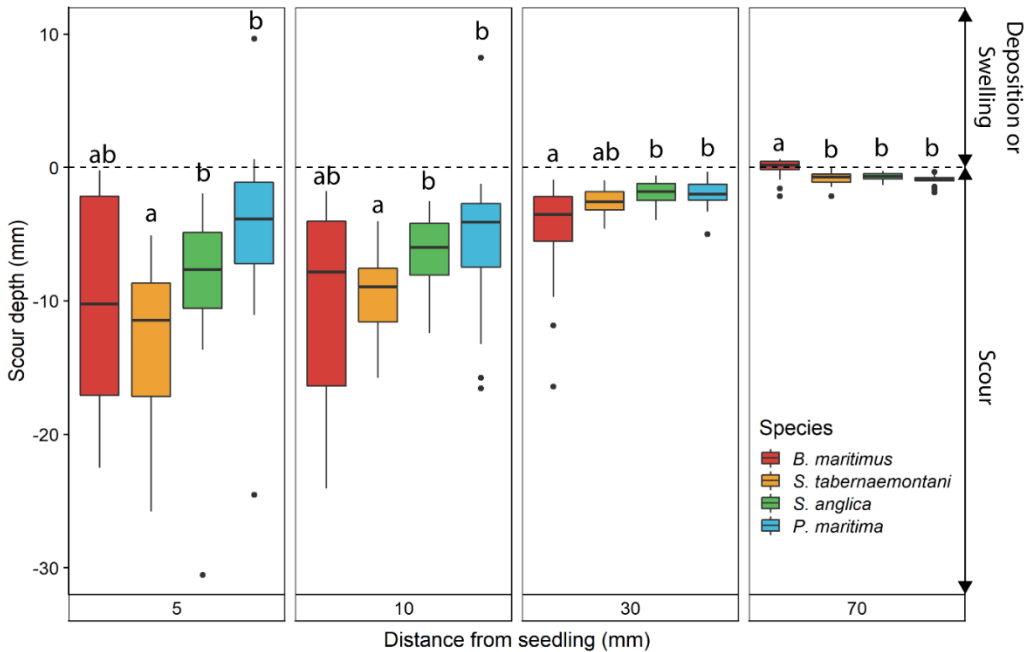
Figure 4.3: Median scour depth at four circular distances from the seedlings plotted as boxplots per species at the end of the 4th wave run of week 3 (i.e. the week with most extreme wave conditions) (n = 72). Erosion features, not linked to scour around the seedlings, are not shown in this figure, i.e. edge erosion induced from the edge of the sediment box or erosion induced by a pebble in the sediment. Different letters indicate significant differences as obtained by a non-parametric pairwise comparison using Wilcoxon rank sum test with Bonferroni correction.

4.4.3 Link between damage and erosion processes

In general, the seedlings that were not damaged did not suffer from strong erosion features, even after several wave runs (Fig. 4.4). *B. maritimus* seedlings that were lost due to shoot breakage at the stem base showed relatively shallow (< 10 mm) erosion features in contrast to the seedlings of *S. tabernaemontani* (> 10 mm) that were lost also due to shoot breakage. The deeper erosion features around *B. maritimus* seedlings were observed around seedlings that suffered from damage by stem bending but where

the shoot was still attached. Each successive wave run resulted in higher bending angles which were also corresponding with deeper erosion features. This pattern was less pronounced in *S. tabernaemontani*, however it should be noted that the number of seedlings suffering from damage by bending were low for this species. The *S. tabernaemontani* seedlings that did suffer damage, showed an increase in erosion depth in the last wave run of the week. In general, when a shoot started to show damage, this coincided with a step-wise change to much higher bending angles (bending angle > 18°) bypassing intermediate bending angle categories. Partial uprooting was observed for multiple seedlings, however all roots remained anchored in the sediment and hence no complete root dislodgement was recorded (see supplementary figure S4.1).
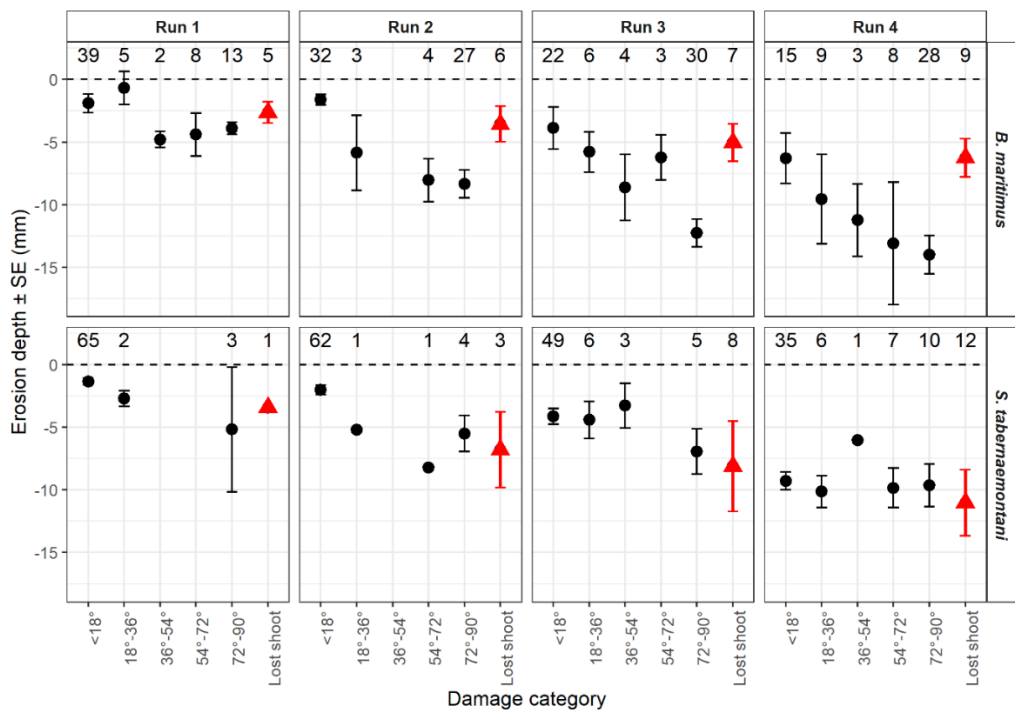
Figure 4.4: Mean erosion depth (mm ± SE) at 10 mm from the seedling per damage category for *B. maritimus* and *S. tabernaemontani* plotted per wave run, pooled over the three weeks to increase the number of observations in every damage category. The numbers indicate the count of seedlings per calculated mean. Shoots that were lost by breakage at the stem base are indicated with red triangles.

In order to explore species differences in scouring depth, we further investigated species differences in plant traits that were expected to affect the scour intensity around plants, i.e. basal stem diameter and stem flexibility. Basal stem diameters of *B. maritimus* and *S. tabernaemontani* were similar to each other and significantly larger

than for the other two species (Fig. 4.5a). *P. maritima* had the lowest stem diameter (mean of 0.9 mm), however it should be noted that seedlings of *P. maritima* sprout multiple stems and leaves from the crown. Three-point-bending tests showed that in agreement with these thicker diameters for *B. maritimus* and *S. tabernaemontani*, their second moment of area was significantly bigger than for *S. anglica* and *P. maritima* (Fig. 4.6c). Since no species differences in Young's modulus were found except for the higher values of *P. maritimus* during the three-point bending test, the flexural stiffness of *B. maritimus* and *S. tabernaemontani* was higher, causing higher resistance against bending with the flow (Fig. 4.6a-b).

4.4.4 Proxies for drag force and anchoring capacity

Plant traits were used as proxy for drag force to explain species differences in damage. Shoot length was highest for *S. tabernaemontani* seedlings followed by *B. maritimus* (Fig. 4.5b). Both species had a significantly longer shoot length (almost double the length) compared to *S. anglica* and *P. maritima*. Seedlings that suffered from damage had significantly longer shoots compared to the seedlings that remained upstanding (damage category < 18°) (Likelihood ratio test: Chi-squared = 5.07, df = 1 p < 0.05). Aboveground dry biomass of *B. maritimus* seedlings collected after the 4th wave run of the week was more than twice as high (average of 0.52 ± 0.04 g per seedling) as compared to the other species (Fig. 4.5c). There was a non-significant difference in aboveground biomass between *S. tabernaemontani* and *S. anglica* (Tukey HSD p = 0.1). The aboveground biomass of *P. maritima* was lowest compared to the other species. Both shoot length and aboveground biomass indicate a higher drag force for *B. maritimus* and *S. tabernaemontani* and lowest drag force for *P. maritima*. In addition to the morphological proxies for drag force, the biomechanical proxy, i.e. flexural stiffness (described above), are in line with this result (Fig. 4.6a). Higher resistance against breaking (i.e. higher flexural stiffness) of *B. maritimus* and *S. tabernaemontani* indicate higher drag forces compared to *S. anglica* and *P. maritima* that both have low resistance against bending (low flexural stiffness).
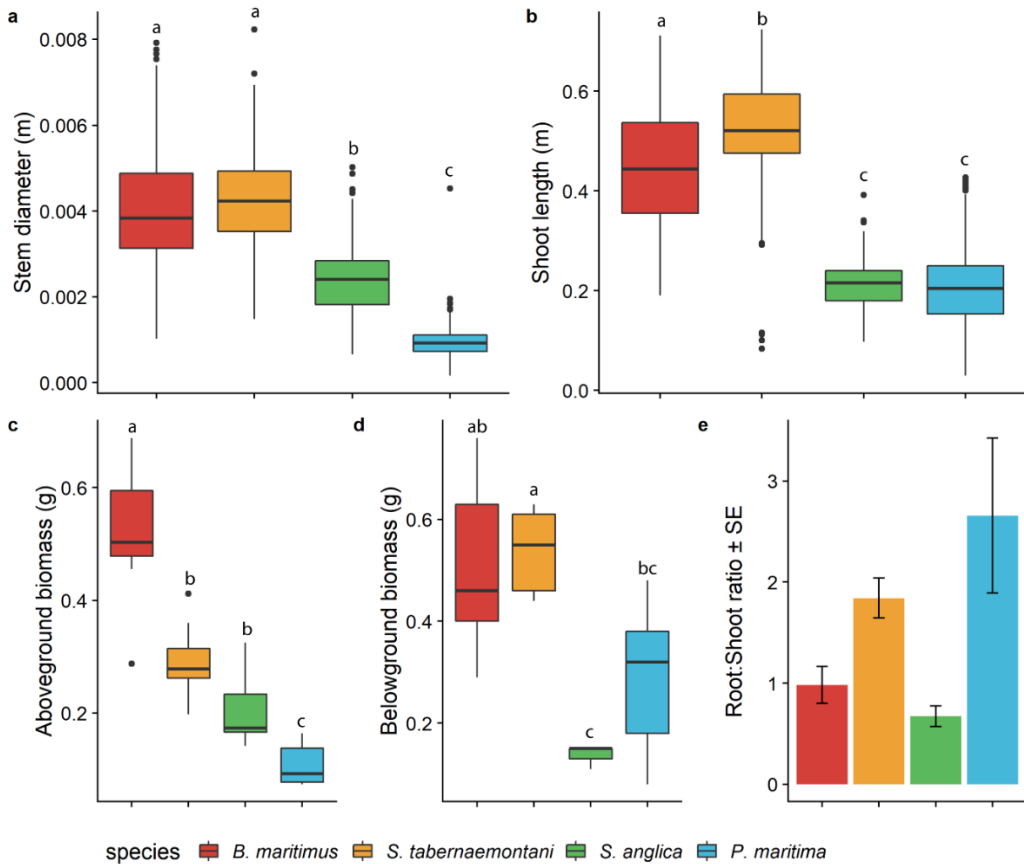
Figure 4.5: Plant morphogical properties as proxy for drag forces and driving force for scour. (a) Basal stem diameter and (b) shoot length per species (n = 72) are plotted as boxplots. (c) Aboveground dry biomass per seedling (n=8) and (d) belowground dry biomass per seedling (n=5) are plotted as boxplots and (e) root:shoot ratios per species ± SE (n = 1). Letters indicate the significant differences obtained by one-way ANOVAs followed by a post-hoc Tukey HSD test.

Belowground biomass was biggest for *B. maritimus* and *S. tabernaemontani* (Fig. 4.5d). Root:Shoot ratios indicate highest investment in root biomass for *S. tabernaemontani* and *P. maritima* seedlings which invested twice as much biomass in belowground parts compared to investments in shoots (Fig. 4.5e). In contrast to the absolute values for dry belowground biomass, *B. maritimus* invested a similar amount of biomass in its aboveground and belowground parts. *S. anglica* seedlings invested less in belowground biomass as the root:shoot ratio was below one.
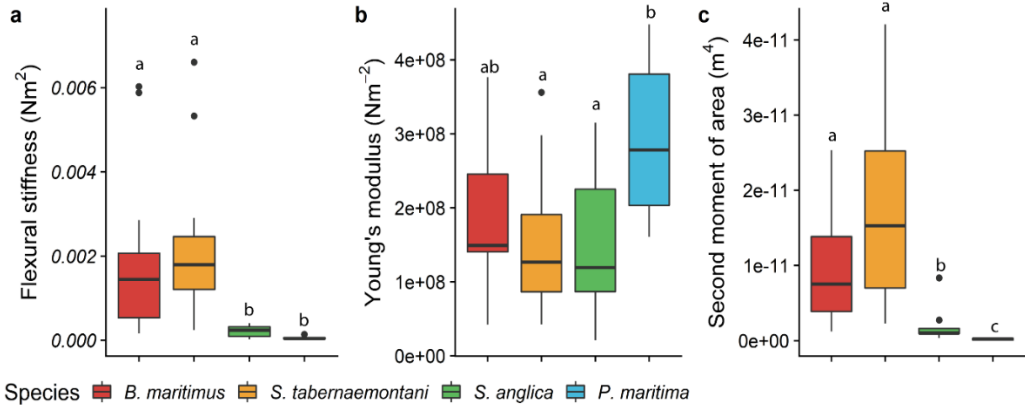
Figure 4.6: Biomechanical properties per species sampled over the three weeks represented as boxplots (n is, respectively, 15 for *B. maritimus* and *S. tabernaemontani* and 13 for *S. anglica* and *P. maritima*). Letters indicate the significant differences between species tested with a one-way ANOVA followed by a Tukey HSD test.

Despite the spread, a significant trend of deeper scour holes with increasing stem diameter was observed over all three species characterized by a single stem (Regression analysis: $F_{3,114}$ = 31.08, p < 0.05, R^2 = 0.45, non-scour-related erosion features were excluded from the analysis) (Fig. 4.7). Due to the multiple stems of *P. maritima*, which act more as a tussock, this species was excluded from the analysis. *S. anglica* had the smallest stem diameters. Therefore, scour depth was generally lower compared to *B. maritimus* and *S. tabernaemontani.*
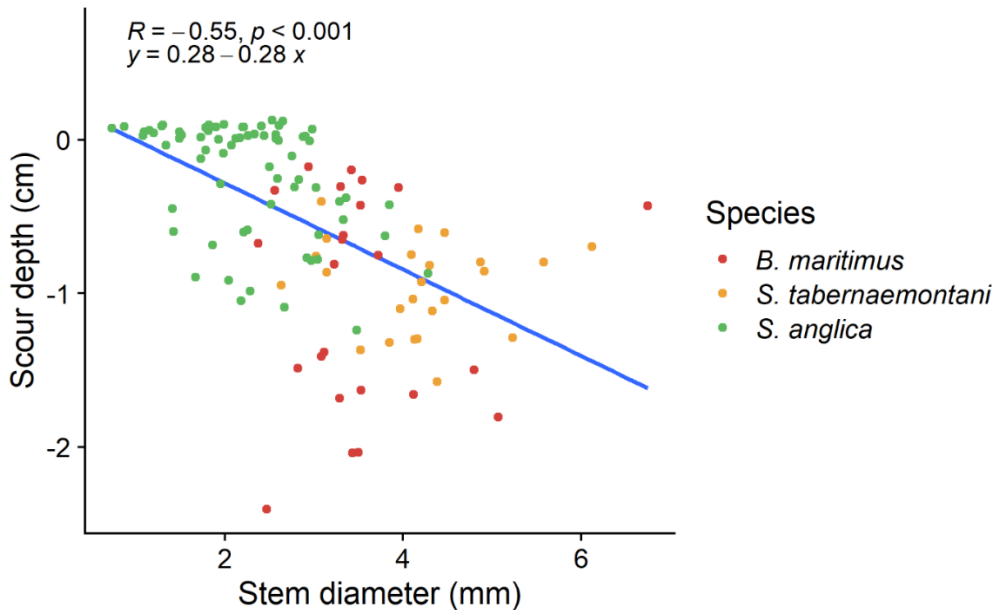
Figure 4.7: Scour depth (m) plotted against basal stem diameter (mm) across the three single-stem species (*B. maritimus*, *S. tabernaemontani* and *S. anglica*) showed a negative correlation indicated by the Pearson correlation coefficient (*R*).

4.5 Discussion

The results of this large wave-flume experiment show that the survival rate of seedlings in response to storm waves is plant trait dependent. More specifically, seedling survival decreases when the seedling has plant traits that increase the potential drag force and scouring around the stem. This knowledge has multiple implications for marsh (re-)establishment and should be taken into consideration when modeling and planning tidal marsh restoration and creation projects.

4.5.1 Plant-trait dependent loss of seedling shoots

Both *B. maritimus* and *S. tabernaemontani* showed a similarly high loss of shoots, while this was negligible for *S. anglica* and *P. maritima* (Fig. 4.2). Dislodgement is considered the main cause of death for young seedlings during germination and the initial establishment phase, even under calm wave conditions (Balke et al., 2013; Cao et al., 2018; Zhu et al., 2014). However, in this study we did not observe complete dislodgment of seedlings, including their roots, under storm wave conditions. All observed losses of *B. maritimus* and *S. tabernaemontani* shoots happened through basal stem breakage, predominantly at the connection between the stem and the roots. It is known from previous studies that long shoots increase the drag forces pulling on the stems which makes them more vulnerable to breaking (Albayrak et al., 2014). Hence

our results confirm that the higher loss rate by stem breakage for *B. maritimus* and *S. tabernaemontani* seedlings (Fig. 4.2), is related to their significantly higher shoot lengths as compared to the two other species in our experiments (Fig. 4.5). Stem breakage of adult shoots of these two species mainly occurs several centimeters above the sediment surface at the end of the growing season when the shoots are deteriorating as part of the seasonal growth cycle (chapter 2: Schoutens et al., 2019; Vuik et al., 2018; Zhu et al., 2020b). Our experiments show that seedling stems typically first bend and then break at the shoot-root interface. It should be noted that the question of whether shoot breakage leads to permanent loss of the seedlings, cannot be confirmed from our experiments. The ability of a shoot to break close to the root connection may be seen as a strategy to avoid drag forces and scouring, while the remaining root network might prevent the sediment surface from eroding (Spencer et al., 2016; Wang et al., 2017). Hence, damage by stem breakage in the short term could reduce the risk for complete root dislodgement, thus allowing regrowth of shoots from the roots and facilitating seedling survival over the longer term. Such a survival strategy by stem breaking under storm waves and regrowth from surviving roots was also suggested by Rupprecht et al. (2017) for an adult canopy of the high marsh species *Elymus athericus*. Fast regrowth of shoots is also what we observed from the cut-off outgrown shoots of *B. maritimus* and *S. tabernaemontani* (see supplementary figure S4.1).

4.5.2 Plant trait dependent bending of shoots

Applying a wide range of different wave runs with different wave conditions allowed us to demonstrate that species-specific responses also depend on the wave conditions (Fig. 4.2). The calmest wave conditions in this experiment show very small (or no) differences in species response while heavier wave conditions show increaslingly larger species-specific responses. This proves that it are the more extreme wave conditions that are most selective in terms of species response. *B. maritimus* suffered the most among all studied species with bent shoots or shoots lying flat on the sediment surface after an accumulative wave loading of ≥ 132 Js (Fig. 4.2). Here, we argue that this species-dependent difference in shoot bending may be the result of two mechanisms: scouring around stems and drag forces exerted by the waves on the stems. First, the seedlings of *B. maritimus,* with greatest bending angles (Fig. 4.2), also had the deepest scour holes (Fig. 4.3), which resulted in partial uprooting. This suggests that the loss of the anchoring strength of the roots may have contributed to reduced ability of the shoots to keep an upstanding position. Although scour holes around *S. tabernaemontani* were of similar dimensions (Fig. 4.3), no uprooting was observed indicating that the root system of this species develops at several centimeters below the sediment surface. As *S. tabernaemontani* did not experience uprooting, this may partly explain why it also experienced less bending as compared to *B. maritimus* seedlings. *S. anglica* and *P. maritima* showed least percentages of shoot bending (Fig.

4.2) and lowest scouring depths (Fig. 4.3). Overall, this suggests that shoot bending is positively related to the depth of scouring holes across the studied species.

Moreover, our results showed that across the studied species, the scouring depth is deeper around stems with a larger diameter (Fig. 4.7). Here, it should be noted that although *S. anglica* had thicker stem diameters, the seedlings of *P. maritima* form grass clumps with multiple stems sprouting from the crown which will likely act as one entity causing more turbulence and thus more scour compared to *S. anglica*. Scour is the result of the interaction between hydrodynamics (wave induced currents in this experiment) and a physical obstacle (seedlings in this experiment) that creates turbulent flow. Although in this study design sediments were all the same, the sediment characteristics in the field can play a major role in the susceptibility of the sediment to erosion and how it will interact with the plant traits (De Battisti et al., 2019; Lo et al., 2017). Furthermore, hydrodynamic forces were the same for all seedlings, and therefore the stem shape was the key variable to explain the observed differences in scouring depth. It has been shown that the dimensions of scour holes are related to the diameter of the obstacle (Bouma et al., 2009a). Additionally and in accordance with literature, thicker stems were found to have a higher flexural stiffness, which limits their tendency to bend over with the flow. Interestingly, studies on scouring around engineered structures, like bridge pillars, showed that when the angle of the obstacle to the incoming flow is wider, i.e. the obstacle is bent over in the direction of the flow, the turbulence generated around the object changes and creates less deep scouring compared to objects of the same dimensions that stand perpendicular against the flow (Kitsikoudis et al., 2017). Applying this to plant shoots, stiffer stems, that have more tendency to stand perpendicular against the flow, will generate deeper scour holes compared to more flexible stems that bend over to reduce the angle with respect to the flow direction (Bouma et al., 2009a; Yagci et al., 2016).

Secondly, to explain why *B. maritimus* suffers much more from structural bending of the stem compared to *S. tabernaemontani*, we also consider the expected drag forces acting on the seedlings. Both stem diameters and stem lengths are similar for both species, however, an important difference is the aboveground biomass, which is almost double for *B. maritimus* as compared to the biomass of *S. tabernaemontani* (Fig. 4.5). The absence of leaves in *S. tabernaemontani* lowers their aboveground biomass which reduces the frontal area and hence, is expected to reduce the experienced drag (Paul et al., 2016; Silinski et al., 2016). *S. anglica* and *P. maritima* do have leaves, but these were small (Figs. 4.5 and 4.6) and thus contribute little to the expected drag forces (Paul et al., 2016; Vuik et al., 2018). Apart from aboveground biomass, a higher shoot stiffness is also expected to result in increased drag force and to induce more wave-induced damage on the stem (Rupprecht 2017). Our results also indicate that flexural stem stiffness was highest for the *B. maritimus* and *S. tabernaemontani* (Fig. 4.6a), which were the species that showed the highest percentages of stem bending (Fig. 4.2).

Overall, our result confirm that plant traits responsible for an increase of drag forces, also increase the damage experienced by the seedling.

4.5.3 The role of a root network

All four species in this experiment are able to grow clonally by producing an extended root network of rhizomes or, in the case of *P. maritima*, aboveground stolons (Charpentier and Stuefer, 1999; Silinski et al., 2016; Sosnová et al., 2010). During the experiment, the seedlings were between 10 and 14 weeks old which for *B. maritimus* and *S. tabernaeomontani* had resulted in clonal outgrowth and well developed roots (Figs. 4.5d and 4.5e). Although outgrown shoots were cut off prior to the wave runs, the belowground network of rhizomes was able to maintain an anchoring capacity that was strong enough to avoid complete uprooting during the experiment. Hence, despite their age which results in a more developed shoot that increases the drag forces, a more developed belowground biomass (Fig. 4.5e) seems to compensate this increased stress (Balke et al., 2013; Cao et al., 2020). It is known from other ecosystems that anchoring capacity is positively correlated with root properties such as rooting depth, structural complexity and root biomass (Edmaier et al., 2014; Peralta et al., 2006; Schwarz et al., 2010), but research on root networks in tidal marsh vegetation remains sparse (Friess et al., 2012). Apart from the root properties of the seedlings, the cohesiveness of the sediment bed plays a role in the anchoring capacity and resistance against dislodgement of the seedlings (Edmaier et al., 2014; Lo et al., 2017; Schwarz et al., 2015). Highly cohesive sediments have a higher shear strength which prevents erosion (e.g. scouring) and potential uprooting, even under storm wave conditions (Möller et al., 2014; Spencer et al., 2016). The sediment used in this experiment was fairly cohesive (32% < 63 μm), implying that erosion and uprooting might have been more prominent in less cohesive, more sandy sediment. Fast developing belowground root networks are likely to be an important survival strategy of developing seedlings, which may facilitate marsh establishment. Moreover, root development is regulated by multiple environmental variables such as oxygen limitation (Bouma et al., 2001), bioturbation and salt stress, which are conditions that were not varied in this study. Therefore, detailed studies of the root development in the first growing season with a focus on rooting depth and outgrowth by rhizomes can provide crucial insights into spatial and temporal patterns of colonisation and survival of marsh plant seedlings (Balke et al., 2014; Cao et al., 2020, 2018).

4.5.4 Simulated storm-wave and local environmental conditions

The hydrodynamics created in this experiment were simulating storm waves that matched or exceeded most severe wave conditions measured in the field in marsh pioneer zones (Table 4.1). Important to note is that storm wave exposure under field conditions has a duration of multiple hours which is longer than the short term exposure in this experiment. Moreover, water depths in this study (1.5 m) were rather

deep. Although such water depths may indeed typically occur during storm surges at the moment of peak water level (Table 4.2), tidal water level variations in marsh pioneer zones may also lead to storm wave conditions coinciding with much shallower water depths. Therefore, it should be noted that even higher shear stress can be expected under storm conditions coinciding with more shallow water and breaking wave conditions (Fagherazzi and Wiberg, 2009; Leonardi et al., 2015; Pascolo et al., 2018).

Interestingly, the two species that were most damaged (i.e. *S. tabernaemontani* and *B. maritimus)*, grow in the brackish water zone of estuaries. Along estuarine salt gradients, the brackish water zone is more upstream, where open water surfaces are typically smaller, and thus wind fetch length and wave loading during storms are expected to be smaller. The two species that were least affected in our experiments (i.e. *P. maritima* and *S. anglica*), grow in the salt water zone, in what are often more exposed areas closer to the mouth of estuaries where storms energies are higher (Callaghan et al., 2010; Van der Wal et al., 2008; Yang et al., 2012). This suggests that the natural hydrodynamic growth conditions of the species may have played a role in the selection of species traits that allow salt marsh plants to cope better with storm waves as compared to brackish marsh species, althoug many other factors such as tolerance to salt stress will play a role, and more research is needed to further investigate this hypothesis. For example, studies on adult plants have already shown different responses to hydrodynamic forces in relation to their species-specific plant traits (e.g. Bouma et al. 2010; Silinski et al. 2016a; Rupprecht et al. 2017; Vuik et al. 2018; Zhu et al. 2019; chapter 3: Schoutens et al. 2020).

4.5.5 Implications for planning of marsh restoration and creation

Our results indicate that, depending on the pioneer marsh species, storm wave events can be a bottleneck for the success of marsh establishment in the first growing season. This has implications for the selection and design of suitable marsh restoration or creation sites, a practice that is frequently adopted to enhance or increase the delivery of valuable ecosystem services such as biodiversity conservation, coastal defense, and carbon sequestration (Barbier et al., 2011). Apart from well-documented site characteristics, such as suitable intertidal elevation and soil conditions (Wolters et al., 2008; Zhao et al., 2020), and proximity to existing marshes for seed dispersal (Morzaria-Luna and Zedler, 2007; Zhu et al., 2014), our findings stress that site exposure to risks of storm waves is one of the factors that should be taken into account in marsh restoration or creation projects. The latter is expected to become increasingly relevant, as in many coastal areas, storm activity is expected to increase over the coming decades due to climate change (Bender et al., 2010; Habel et al., 2020; Vitousek et al., 2017),

From our findings it becomes evident that, when planning and designing sites for marsh restoration and creation projects, it is important to evaluate the risk of damage and disturbance caused by storm waves beyond an initial window of opportunity for seed dispersal and germination (Bouma et al., 2014). For example, tidal marsh creation in a brackish water environment, where the pioneer species are *B. maritimus* and *S. tabernaemontani*, will be more vulnerable to storm waves in the first growing season. In contrast, the seedlings of pioneer salt water species such as *S. anglica* and *P. maritima* are better able to withstand the storm waves. Moreover we argue that, depending on the location, a low disturbance period for seed germination (i.e. previously identified to be 3 days up to 4 weeks, Hu et al. 2015) might not be sufficient for successful marsh establishment, as marsh seedlings (here grown for 10 – 14 weeks) can still be disrupted by storm waves. Furthermore, the increased storminess due to global climate change might affect the frequency and duration of windows of opportunity for seedling survival and therefore the chance of marsh establishment (Balke et al., 2014). To mitigate the risk for potential disturbance such as through storm wave events, artificial wave damping structures (such as wood branch fences; Dao et al. 2018) can be used to create temporary sheltered conditions, which can facilitate the growth of seedlings into mature plants and improve the success of the restoration. Indeed, over time, the clonal outgrowth and the formation of a root network seems to secure the survival chance of marsh plants. This type of density-dependent feedback through clonal outgrowth and tussock formation is known to contribute importantly to the stability of more mature marshes (Bouma et al., 2009b; Bricker et al., 2018). Hence, temporary fences constructed to create wave sheltered environments so as to facilitate seedling establishment, may be removed after several years once dense vegetation patches have formed.

Finally, knowledge on the impact of extreme wave events on the probability of seedling establishment is often a big uncertainty in predicting marsh establishment, and is consequently not considered in existing marsh evolution models (Hu et al., 2015; Mariotti and Fagherazzi, 2010; Poppema et al., 2019). Large scale flume experiments such as reported in this study, can help to better define processes and parameters that need to be included in marsh development models to improve their predictive capability. As pointed out by Hanley et al. (2020), knowledge on the scale of individual plants is crucial to optimize the succes rate of large scale marsh restoration and creation projects that are key to adapt our coastal areas to the predictions of increased storminess.

4.6 Acknowledgements

4.7 References

Albayrak, I., Nikora, V., Miler, O., O'Hare, M.T., 2014. Flow-plant interactions at leaf, stem and shoot scales: Drag, turbulence, and biomechanics. Aquat. Sci. 76, 269–294. https://doi.org/10.1007/s00027-013-0335-2

Balke, T., Herman, P.M.J., Bouma, T.J., 2014. Critical transitions in disturbance-driven ecosystems : identifying Windows of Opportunity for recovery. J. Ecol. 102, 700–708. https://doi.org/10.1111/1365-2745.12241

Balke, T., Webb, E.L., van den Elzen, E., Galli, D., Herman, P.M.J.J., Bouma, T.J., 2013. Seedling establishment in a dynamic sedimentary environment: A conceptual framework using mangroves. J. Appl. Ecol. 50, 740–747. https://doi.org/10.1111/1365-2664.12067

Barbier, E.B., Hacker, S.D., Kennedy, C., Koch, E.W., Stier, A.C., Silliman, B.R., 2011. The value of estuarine and coastal ecosystem services. Ecol. Monogr. 81, 169–193. https://doi.org/10.1890/10-1510.1

Bender, M.A., Knutson, T.R., Tuleya, R.E., Sirutis, J.J., Vecchi, G.A., Garner, S.T., Held, I.M., 2010. Modeled Impact of Anthropogenic Warming on the Frequency of Intense Atlantic Hurricanes. Science (80-.). 327, 454–458. https://doi.org/10.1126/science.1180568

Bouma, T.J., De Vries, M.B., Herman, P.M.J., 2010. Comparing ecosystem engineering efficiency of two plant species with contrasting growth strategies. Ecol. Soc. Am. 91, 2696–2704. https://doi.org/10.1890/09-0690.1

Bouma, T.J., Friedrichs, M., Klaassen, P., van Wesenbeeck, B.K., Brun, F.G., Temmerman, S., Van Katwijk, M.M., Graf, G., Herman, P.M.J., 2009a. Effects of shoot stiffness, shoot size and current velocity on scouring sediment from around seedlings and propagules. Mar. Ecol. Prog. Ser. 388, 293–297. https://doi.org/10.3354/meps08130

Bouma, T.J., Friedrichs, M., van Wesenbeeck, B.K., Temmerman, S., Graf, G., Herman, P.M.J., 2009b. Density-dependent linkage of scale-dependent feedbacks: a flume study on the intertidal macrophyte *Spartina anglica*. Oikos 118, 260–268. https://doi.org/10.1111/j.1600-0706.2008.16892.x

Bouma, T.J., Michel, B.P.K., Nielsen, K.L., 2001. Coping with low nutrient availability and inundation : root growth responses of three halophytic grass species from different elevations along a flooding gradient 472–481. https://doi.org/10.1007/s0044420000545

Bouma, T.J., van Belzen, J., Balke, T., Zhu, Z., Airoldi, L., Blight, A.J., Davies, A.J., Galvan, C., Hawkins, S.J., Hoggart, S.P.G., Lara, J.L., Losada, I.J., Maza, M., Ondiviela,

B., Skov, M.W., Strain, E.M., Thompson, R.C., Yang, S., Zanuttigh, B., Zhang, L., Herman, P.M.J., 2014. Identifying knowledge gaps hampering application of intertidal habitats in coastal protection: Opportunities & steps to take. Coast. Eng. 87, 147–157. https://doi.org/10.1016/j.coastaleng.2013.11.014

Bricker, E., Calladine, A., Virnstein, R., Waycott, M., 2018. Mega clonality in an aquatic plant—a potential survival strategy in a changing environment. Front. Plant Sci. 9, 1–8. https://doi.org/10.3389/fpls.2018.00435

Bywater-Reyes, S., Wilcox, C.A., Stella, C.J., Lightbody, A.F., 2015. Flow and scour constraints on uprooting of pioneer woody seedlings. Water Resour. Res. 51, 9190–9206. https://doi.org/doi:10.1002/2014WR016641

Callaghan, D.P.P., Bouma, T.J.J., Klaassen, P., van der Wal, D., Stive, M.J.F.J.F., Herman, P.M.J.M.J., 2010. Hydrodynamic forcing on salt-marsh development: Distinguishing the relative importance of waves and tidal flows. Estuar. Coast. Shelf Sci. 89, 73–88. https://doi.org/10.1016/j.ecss.2010.05.013

Cao, H., Zhu, Z., Balke, T., Zhang, L., Bouma, T.J., 2018. Effects of sediment disturbance regimes on Spartina seedling establishment: Implications for salt marsh creation and restoration. Limnol. Oceanogr. 63, 647–659.

https://doi.org/10.1002/lno.10657

Cao, H., Zhu, Z., James, R., Herman, P.M.J.J., Liquan, Z., Yuan, L., Bouma, T.J., Zhang, L., Yuan, L., Bouma, T.J., 2020. Wave effects on seedling establishment of three pioneer marsh species: survival, morphology and biomechanics. Ann. Bot. 125, 345–352. https://doi.org/10.1093/aob/mcz136

Charpentier, A., Stuefer, J.F., 1999. Functional specialization of ramets in *Scirpus maritimus* - Splitting the tasks of sexual reproduction, vegetative growth, and resource storage. Plant Ecol. 141, 129–136. https://doi.org/https://doi.org/10.1023/A:1009825905117

Dalrymple, R.A., Dean, R.G., 1991. Water wave mechanics for engineers and scientists (Vol. 2). Prentice-Hall. https://doi.org/https://doi.org/10.1142/1232

Dao, T., Stive, M.J.F., Hofland, B., Mai, T., 2018. Wave Damping due to Wooden Fences along Mangrove Coasts. J. Coast. Res. 34, 1317. https://doi.org/10.2112/jcoastres-d-18-00015.1

De Battisti, D., Fowler, M.S., Jenkins, S.R., Skov, M.W., Rossi, M., Bouma, T.J., Neyland, P.J., Griffin, J.N., 2019. Intraspecific Root Trait Variability Along Environmental Gradients Affects Salt Marsh Resistance to Lateral Erosion. Front. Ecol. Evol. 7, 1–11. https://doi.org/10.3389/fevo.2019.00150

Denny, M.W., 1994. Extreme drag forces and the survival of wind- and water-swept organisms. J. Exp. Bot. 194, 97–115.

Duggan-Edwards, M.F., Pagès, J.F., Jenkins, S.R., Bouma, T.J., Skov, M.W., 2020. External conditions drive optimal planting configurations for salt marsh restoration. J. Appl. Ecol. 57, 619–629. https://doi.org/10.1111/1365-2664.13550

Edmaier, K., Crouzy, B., Ennos, R., Burlando, P., Perona, P., 2014. Influence of root characteristics and soil variables on the uprooting mechanics of Avena sativa and Medicago sativa seedlings. Earth Surf. Process. Landforms 39, 1354–1364. https://doi.org/10.1002/esp.3587

Elsen, R., Van Braeckel, A., Vanoverbeke, J., Vandevoorde, B., Van den Berg, E., 2019. Habitatmapping Sea Scheldt supralittoral: Partim pioneer club-rush species. Brussels. https://doi.org/doi.org/10.21436/inbor.16164273

Fagherazzi, S., Wiberg, P.L., 2009. Importance of wind conditions, fetch, and water levels on wave-generated shear stresses in shallow intertidal basins. J. Geophys. Res. Earth Surf. 114, 1–12. https://doi.org/10.1029/2008JF001139

Friess, D. a, Krauss, K.W., Horstman, E.M., Balke, T., Bouma, T.J., Galli, D., Webb, E.L., 2012. Are all intertidal wetlands naturally created equal? Bottlenecks, thresholds and knowledge gaps to mangrove and saltmarsh ecosystems. Biol. Rev. Camb. Philos. Soc. 87, 346–66. https://doi.org/10.1111/j.1469-185X.2011.00198.x

Habel, S., Fletcher, C.H., Anderson, T.R., Thompson, P.R., 2020. Sea-Level Rise Induced Multi-Mechanism Flooding and Contribution to Urban Infrastructure Failure. Sci. Rep. 10, 1–12. https://doi.org/10.1038/s41598-020-60762-4

Hanley, M.E., Bouma, T.J., Mossman, H.L., 2020. The gathering storm : optimizing management of coastal ecosystems in the face of a climate-driven threat. Ann. Bot. 125, 197–212. https://doi.org/10.1093/aob/mcz204

Hansen, F., Kruschke, T., Greatbatch, R.J., Weisheimer, A., 2019. Factors Influencing the Seasonal Predictability of Northern Hemisphere Severe Winter Storms. Geophys. Res. Lett. 46, 365–373. https://doi.org/10.1029/2018GL079415

Henry, P.Y., Myrhaug, D., Aberle, J., 2015. Drag forces on aquatic plants in nonlinear random waves plus current. Estuar. Coast. Shelf Sci. 165, 10–24. https://doi.org/10.1016/j.ecss.2015.08.021

Heuner, M., Schröder, B., Schröder, U., Kleinschmit, B., 2018. Contrasting elevational responses of regularly flooded marsh plants in navigable estuaries. Ecohydrol. Hydrobiol. 19, 38–53. https://doi.org/10.1016/j.ecohyd.2018.06.002

Hu, Z., van Belzen, J., van der Wal, D., Balke, T., Wang, Z.B., Stive, M., Bouma, T.J., 2015. Windows of opportunity for salt marsh vegetation establishment on bare tidal flats: The importance of temporal and spatial variability in hydrodynamic forcing. J. Geophys. Res. Biogeosciences 120. https://doi.org/10.1002/2014JG002870.Received

Kitsikoudis, V., Kirca, V.S.O., Yagci, O., Celik, M.F., 2017. Clear-water scour and flow field alteration around an inclined pile. Coast. Eng. 129, 59–73. https://doi.org/10.1016/j.coastaleng.2017.09.001

Lague, D., Brodu, N., Leroux, J., 2013. Accurate 3D comparison of complex topography with terrestrial laser scanner: Application to the Rangitikei canyon (N-Z). ISPRS J. Photogramm. Remote Sens. 82, 10–26. https://doi.org/10.1016/j.isprsjprs.2013.04.009

Leonardi, N., Ganju, N.K., Fagherazzi, S., 2015. A linear relationship between wave power and erosion determines salt-marsh resilience to violent storms and hurricanes. Proc. Natl. Acad. Sci. 113, 64–68. https://doi.org/10.1073/pnas.1510095112

Lo, V.B., Bouma, T.J., van Belzen, J., Van Colen, C., Airoldi, L., 2017. Interactive effects of vegetation and sediment properties on erosion of salt marshes in the Northern Adriatic Sea. Mar. Environ. Res. 131, 32–42. https://doi.org/10.1016/j.marenvres.2017.09.006

Lotze, H.K., Lenihan, H.S., Bourque, B.J., Bradbury, R.H., Cooke, R.G., Kay, M.C., Kidwell, S.M., Kirby, M.X., Peterson, C.H., Jackson, J.B.C., Bay, M., 2006. Depletion, Degradation, and Recovery Potential of Estuaries and Coastal Seas. Science (80-.). 312, 1806–1809. https://doi.org/10.1126/science.1128035

Mariotti, G., Fagherazzi, S., 2010. A numerical model for the coupled long-term evolution of salt marshes and tidal flats. J. Geophys. Res. 115, F01004. https://doi.org/10.1029/2009JF001326

Masselink, G., Scott, T., Poate, T., Russell, P., Davidson, M., Conley, D., 2016. The extreme 2013/2014 winter storms: Hydrodynamic forcing and coastal response along the southwest coast of England. Earth Surf. Process. Landforms 41, 378–391. https://doi.org/10.1002/esp.3836

Möller, I., Kudella, M., Rupprecht, F., Spencer, T., Paul, M., van Wesenbeeck, B.K., Wolters, G., Jensen, K., Bouma, T.J., Miranda-Lange, M., Schimmels, S., 2014. Wave attenuation over coastal salt marshes under storm surge conditions. Nat. Geosci. 7, 727–731. https://doi.org/10.1038/ngeo2251

Möller, I., Spencer, T., French, J.R., Leggett, D.J., Dixond, M., 1999. Wave Transformation Over Salt Marshes: A Field and Numerical Modelling Study from North Norfolk, England. Estuar. Coast. Shelf Sci. 49, 411–426.

https://doi.org/10.1006/ecss.1
999.0509

Morzaria-Luna, H.N., Zedler, J.B., 2007. Does seed availability limit plant establishment during salt marsh restoration? Estuaries and Coasts 30, 12–25. https://doi.org/10.1007/BF02782963

Narayan, S., Beck, M.W., Reguero, B.G., Losada, I.J., van Wesenbeeck, B., Pontee, N., Sanchirico, J.N., Ingram, J.C., Lange, G.-M., Burks-Copes, K.A., 2016. The Effectiveness, Costs and Coastal Protection Benefits of Natural and Nature-Based Defences. PLoS One 11, e0154735. https://doi.org/10.1371/journal.pone.0154735

Nicholls, R.J., Cazenave, A., 2010. Sea-Level Rise and Its Impact on Coastal Zones. Science (80-.). 328, 1517–1520. https://doi.org/10.1126/science.1185782

Niklas, K.J., 1992. Plant biomechanics: An engineering approach to plant form and function, The University of Chicago Press. The University of Chicago Press, Chicago & London. https://doi.org/10.1016/0169-5347(93)90072-W

Oppenheimer, M., Glavovic, B., Hinkel, J., van de Wal, R., Magnan, A.K., Abd-Elgawad, A., Cai, R., Cifuentes-Jara, M., DeConto, R.M., Ghosh, T., Hay, J., Isla, F., Marzeion, B., Meyssignac, B., Sebesvari, Z., 2019. Sea Level Rise and Implications for Low Lying Islands, Coasts and Communities. IPCC Spec. Rep. Ocean Cryosph. a Chang. Clim. 355, 126–129.

https://doi.org/10.1126/science.aam6284

Pascolo, S., Petti, M., Bosa, S., 2018. On the wave bottom shear stress in shallow depths: The role of wave period and bed roughness. Water (Switzerland) 10, 1348–1367. https://doi.org/10.3390/w10101348

Paul, M., Rupprecht, F., Möller, I., Bouma, T.J., Spencer, T., Kudella, M., Wolters, G., van Wesenbeeck, B.K., Jensen, K., Miranda-Lange, M., Schimmels, S., 2016. Plant stiffness and biomass as drivers for drag forces under extreme wave loading: A flume study on mimics. Coast. Eng. 117, 70–78. https://doi.org/10.1016/j.coastaleng.2016.07.004

Peralta, G., Brun, F.G., Pérez-Lloréns, J.L., Bouma, T.J., 2006. Direct effects of current velocity on the growth, morphometry and architecture of seagrasses: A case study on *Zostera noltii*. Mar. Ecol. Prog. Ser. 327, 135–142. https://doi.org/10.3354/meps327135

Poppema, D.W., Willemsena, P.W.J.M., de Vries, M.B., Zhu, Z., Borsje, B.W., Hulscher, S.J.M.H., 2019. Experiment - supported modelling of salt marsh establishment. Ocean Coast. Manag. 168, 238–250.

R Core Team, 2020. R: A language and environment for statistical computing.

Rupprecht, F., Möller, I., Evans, B., Spencer, T., Jensen, K., 2015. Biophysical properties of salt marsh canopies — Quantifying plant stem flexibility and above

ground biomass. Coast. Eng. 100, 48–57. https://doi.org/10.1016/j.coastaleng.2015.03.009

Rupprecht, F., Möller, I., Paul, M., Kudella, M., Spencer, T., van Wesenbeeck, B.K., Wolters, G., Jensen, K., Bouma, T.J., Miranda-Lange, M., Schimmels, S., 2017. Vegetation-wave interactions in salt marshes under storm surge conditions. Ecol. Eng. 100, 301–315. https://doi.org/10.1016/j.ecoleng.2016.12.030

Schoutens, K., Heuner, M., Fuchs, E., Minden, V., Schulte-Ostermann, T., Belliard, J.P., Bouma, T.J., Temmerman, S., 2020. Nature-based shoreline protection by tidal marsh plants depends on trade-offs between avoidance and attenuation of hydrodynamic forces. Estuar. Coast. Shelf Sci. 236, 11. https://doi.org/10.1016/j.ecss.2020.106645

Schoutens, K., Heuner, M., Minden, V., Schulte Ostermann, T., Silinski, A., Belliard, J.-P., Temmerman, S., 2019. How effective are tidal marshes as nature-based shoreline protection throughout seasons? Limnol. Oceanogr. 64, 1750–1762. https://doi.org/10.1002/lno.11149

Schwarz, C., Bouma, T.J., Zhang, L.Q., Temmerman, S., Ysebaert, T., Herman, P.M.J., 2015. Interactions between plant traits and sediment characteristics influencing species establishment and scale-dependent feedbacks in salt marsh ecosystems. Geomorphology 250, 298–307.

https://doi.org/10.1016/j.geomorph.2015.09.013

Schwarz, M., Cohen, D., Or, D., 2010. Root-soil mechanical interactions during pullout and failure of root bundles. J. Geophys. Res. Earth Surf. 115, 1–19. https://doi.org/10.1029/2009JF001603

Silinski, A., Fransen, E., van Belzen, J., Bouma, T.J.T.J., Troch, P., Meire, P., Temmerman, S., Fransen, E., Bouma, T.J.T.J., Troch, P., Meire, P., Temmerman, S., 2016. Quantifying critical conditions for seaward expansion of tidal marshes: A transplantation experiment. Estuar. Coast. Shelf Sci. 169, 227–237. https://doi.org/10.1016/j.ecss.2015.12.012

Silinski, A., Heuner, M., Schoelynck, J., Puijalon, S., Schröder, U., Fuchs, E., Troch, P., Bouma, T.J., Meire, P., Temmerman, S., 2015. Effects of wind waves versus ship waves on tidal marsh plants: A flume study on different life stages of *Scirpus maritimus*. PLoS One 10, e0118687. https://doi.org/10.1371/journal.pone.0118687

Silinski, A., Schoutens, K., Puijalon, S., Schoelynck, J., Luyckx, D., Troch, P., Meire, P., Temmerman, S., 2018. Coping with waves: Plasticity in tidal marsh plants as self-adapting coastal ecosystem engineers. Limnol. Oceanogr. 63, 799–815. https://doi.org/10.1002/lno.10671

Sosnová, M., van Diggelen, R., Klimešová, J., 2010. Distribution of clonal growth forms in

wetlands. Aquat. Bot. 92, 33–39. https://doi.org/10.1016/j.aquabot.2009.09.005

Spencer, T., Brooks, S.M., Evans, B.R., Tempest, J.A., Möller, I., 2015. Southern North Sea storm surge event of 5 December 2013 : Water levels , waves and coastal impacts. Earth Sci. Rev. 146, 120–145. https://doi.org/10.1016/j.earscirev.2015.04.002

Spencer, T., Möller, I., Rupprecht, F., Bouma, T.J., van Wesenbeeck, B.K., Kudella, M., Paul, M., Jensen, K., Wolters, G., Miranda-Lange, M., Schimmels, S., 2016. Salt marsh surface survives true-to-scale simulated storm surges. Earth Surf. Process. Landforms 41, 543–552. https://doi.org/10.1002/esp.3867

Szmeja, J., Galka, A., 2008. Phenotypic responses to water flow and wave exposure in aquatic plants. Acta Soc. Bot. Pol. 77, 59–65. https://doi.org/https://doi.org/10.5586/asbp.2008.009

Van Asselen, S., Verburg, P.H., Vermaat, J.E., Janse, J.H., 2013. Drivers of wetland conversion: A global meta-analysis. PLoS One 8, 1–13. https://doi.org/10.1371/journal.pone.0081292

van der Nat, A., Vellinga, P., Leemans, R., van Slobbe, E., 2016. Ranking coastal flood protection designs from engineered to nature-based. Ecol. Eng. 87, 80–90. https://doi.org/10.1016/j.ecoleng.2015.11.007

Van der Wal, D., Wielemaker-Van den Dool, A., Herman, P.M.J., 2008.

Spatial patterns, rates and mechanisms of saltmarsh cycles (Westerschelde, The Netherlands). Estuar. Coast. Shelf Sci. 76, 357–368. https://doi.org/10.1016/j.ecss.2007.07.017

Vitousek, S., Barnard, P.L., Fletcher, C.H., Frazer, N., Erikson, L., Storlazzi, C.D., 2017. Doubling of coastal flooding frequency within decades due to sea-level rise. Sci. Rep. 7, 1–9. https://doi.org/10.1038/s41598-017-01362-7

Vogel, S., 1996. Life in moving fluids: the physical biology of flow, 2nd ed. Princeton University Press, New Jersey, USA.

Vuik, V., Jonkman, S.N., Borsje, B.W., Suzuki, T., 2016. Nature-based flood protection: The efficiency of vegetated foreshores for reducing wave loads on coastal dikes. Coast. Eng. 116, 42–56. https://doi.org/10.1016/j.coastaleng.2016.06.001

Vuik, V., Suh Heo, H.Y., Zhu, Z., Borsje, B.W., Jonkman, S.N., 2018. Stem breakage of salt marsh vegetation under wave forcing: A field and model study. Estuar. Coast. Shelf Sci. 200, 41–58. https://doi.org/10.1016/j.ecss.2017.09.028

Wang, H., van der Wal, D., Li, X., van Belzen, J., Herman, P.M.J., Hu, Z., Ge, Z., Zhang, L., Bouma, T.J., 2017. Zooming in and out: Scale dependence of extrinsic and intrinsic factors affecting salt marsh erosion. J. Geophys. Res. Earth Surf. 122, 1455–1470. https://doi.org/10.1002/2016JF004193

Wolters, M., Garbutt, A., Bekker, R.M., Bakker, J.P., Carey, P.D., 2008. Restoration of salt-marsh vegetation in relation to site suitability, species pool and dispersal traits. J. Appl. Ecol. 45, 904–912. https://doi.org/10.1111/j.1365-2664.2008.01453.x

Xie, T., Cui, B., Li, S., Bai, J., 2019. Topography regulates edaphic suitability for seedling establishment associated with tidal elevation in coastal salt marshes. Geoderma 337, 1258–1266. https://doi.org/10.1016/j.geoderma.2018.07.053

Yagci, O., Celik, M.F., Kitsikoudis, V., Ozgur Kirca, V.S., Hodoglu, C., Valyrakis, M., Duran, Z., Kaya, S., 2016. Scour patterns around isolated vegetation elements. Adv. Water Resour. 97, 251–265. https://doi.org/10.1016/j.advwatres.2016.10.002

Yang, S.L., Shi, B.W., Bouma, T.J., Ysebaert, T., Luo, X.X., 2012. Wave attenuation at a salt marsh margin : A case study of an exposed coast on the Yangtze Estuary. Estuaries and Coasts 35, 169–182. https://doi.org/10.1007/s12237-011-9424-4

Ysebaert, T., Yang, S., Zhang, L., He, Q., Bouma, T.J., Herman, P.M.J., 2011. Wave attenuation by two contrasting ecosystem engineering salt marsh macrophytes in the intertidal pioneer zone. Wetlands 31, 1043–1054. https://doi.org/10.1007/s13157-011-0240-1

Zhao, Z., Yuan, L., Li, W., Tian, B., Zhang, L., 2020. Re-invasion of Spartina alterniflora in restored saltmarshes: Seed arrival, retention, germination, and establishment. J. Environ. Manage. 266, 110631. https://doi.org/10.1016/j.jenvman.2020.110631

Zhu, Z., Bouma, T.J., Ysebaert, T., Zhang, L., Herman, P.M.J., 2014. Seed arrival and persistence at the tidal mudflat: Identifying key processes for pioneer seedling establishment in salt marshes. Mar. Ecol. Prog. Ser. 513, 97–109. https://doi.org/10.3354/meps10920

Zhu, Z., Vuik, V., Visser, P.J., Soens, T., van Wesenbeeck, B., van de Koppel, J., Jonkman, S.N., Temmerman, S., Bouma, T.J., 2020a. Historic storms and the hidden value of coastal wetlands for nature-based flood defence. Nat. Sustain. https://doi.org/10.1038/s41893-020-0556-z

Zhu, Z., Yang, Z., Bouma, T.J., 2020b. Biomechanical properties of marsh vegetation in space and time: effects of salinity, inundation and seasonality. Ann. Bot. https://doi.org/10.1046/j.1365-2087.1998.00089.x

Zuur, A.F., Ieno, E.N., Walker, N.J., Saveliev, A.A., Smith, G.M., 2009. Mixed effects models and extensions in ecology with R. Springer, New York, USA, New York, NY.

5

Traits of tidal marsh plants determine survival and growth response to hydrodynamic forcing: implications for nature-based shoreline protection

Ken Schoutens, Pieter Luys, Maike Heuner, Elmar Fuchs, Vanessa Minden, Tilla Schulte-Ostermann, Tjeerd J. Bouma, Jim Van Belzen, Stijn Temmerman

5.1 Abstract

Tidal marshes are increasingly valued for their nature-based shoreline protection function, as they reduce waves, currents and erosion. The effectiveness of this function depends on the ability of tidal marsh plants to grow and survive under waves and currents. However, how this varies with species-dependent plant traits is poorly understood. We performed a field transplantation experiment to quantify species-specific growth responses to different levels of hydrodynamic exposure and tidal inundation for three NW European marsh species: *Schoenoplectus tabernaemontani*, *Bolboschoenus maritimus* and *Phragmites australis*. In this order, these species show increasing shoot stiffness, length and biomass, which are plant traits known to increase hydrodynamic drag forces experienced by plants. Increased exposure to tidal inundation and hydrodynamics reduced the growth of all three species, but species with lower biomass, shorter, thinner and more flexible shoots could better cope with higher hydrodynamic exposure and tidal inundation. Furthermore, transplants of *S. tabernaemontani* (i.e. the species with the lowest shoot stiffness, length and biomass that survived under all tested conditions) developed smaller, thinner and more flexible shoots in response to higher hydrodynamic exposure and inundation. Hence our study indicates that similar inter- and intra-specific plant traits drive plant growth in response to hydrodynamics and inundation. This suggests that the spatial species distribution, typically observed in tidal marshes, does not only result from species-specific tolerance to tidal inundation gradients but also from hydrodynamic gradients. Allowing enough space for development of species zonation may be important to increase the efficiency of nature-based shoreline protection by tidal marshes.

5.2 Introduction

Climate change induced sea level rise and increasing storminess emphasize the need for sustainable shoreline protection strategies for often densely populated low-lying coastal zones, river deltas and estuaries (Hallegatte et al. 2013, Temmerman et al. 2013, Auerbach et al. 2015, Tessler et al. 2015). Conservation and restoration of coastal vegetated wetlands, such as tidal marshes and mangroves, is increasingly proposed and implemented as a nature-based climate adaptation strategy to complement man-made shoreline protection infrastructure such as dikes, common across the NW European coast (Schoonees et al. 2019, Smith et al. 2020). Tidal marshes in front of dikes have been shown to attenuate waves (Vuik et al. 2016, Chapter 2: Schoutens et al. 2019), tidal currents (Carus et al. 2016, Chapter 2: Schoutens et al. 2019), storm surges (Smolders et al. 2015, Stark et al. 2016) and erosion (Lo et al. 2017), thereby reducing wave loads on dikes, lowering the risk of dike failure during storms and even limiting the damage of the hinterland when dikes breach (Zhu et al. 2020a). Not only do tidal marshes provide this protection function, they also deliver a multitude of other valuable ecosystem services that benefit nature and society (Barbier et al. 2011).

The capacity of marsh plant species for nature-based shoreline protection depends on (1) their effectiveness to temper waves, currents and erosion, but also (2) their ability to grow and persist under the effects of waves and currents. The hydrodynamic attenuation has been the subject of multiple studies, showing that the effectiveness of wave and current attenuation depends on plant morphological traits such as high biomass (Paul & Amos 2011, Shepard et al. 2011, chapter 3: Schoutens et al. 2020), high density of shoots (Shepard et al. 2011, Vuik et al. 2016), high shoot lengths (Garzon et al. 2019) and stiff shoots (Rupprecht et al. 2017, Schulze et al. 2019, chapter 3: Schoutens et al. 2020). These plant traits increase friction (i.e. hydraulic resistance) on waves and tidal currents, hence contributing to decrease the hydrodynamic forces and reduce the risk of erosion in marshes and on the dikes behind marshes (Möller et al. 2014, chapter 2: Schoutens et al. 2019). Concerning the plant growth, fewer studies have identified the mechanisms determining the ability of marsh plants to withstand waves and tidal currents. Recent studies suggest that a trade-off exists between the capacity of plants to attenuate hydrodynamic forces and their capacity to cope with and grow under hydrodynamic forces (Heuner et al. 2015, chapter 3: Schoutens et al. 2020). These studies suggest that plant traits that enhance the reduction of hydrodynamic forces, such as having a high biomass and stiff shoots, also lead to higher drag forces exerted by the flow on the plants and thus higher mechanical stress experienced by the plants (Bouma et al. 2005).

The growth responses to mechanical stress from hydrodynamic forces have been studied in multiple aquatic ecosystems (e.g. Gaylord et al. 2003 and Demes et al. 2013 on kelp vegetation; Puijalon et al. 2008 and Schoelynck et al. 2015 on freshwater macrophytes; Nafie et al. 2012 and Peralta et al. 2006 on seagrasses). In tidal marshes,

key knowledge gaps on species-specific plant growth response to wave exposure remain. A limited number of short-term (minutes to hours) flume studies showed that drag forces on plants and dislodgement of plants in response to hydrodynamic forces increased with species-specific plant traits such as shoot stiffness (Bouma et al. 2005, Silinski et al. 2016b, chapter 4: Schoutens et al. 2021). Only few experimental studies have shown the longer-term (months) implications of hydrodynamic forces on intra-specific variations in plant growth during at most one summer growing season (Coops et al. 1996a, Silinski et al. 2016a, 2018, Cao et al. 2020). These studies revealed that stronger hydrodynamic forces resulted in seedling mortality, reduced growth and an increased shoot flexibility. There are however to our knowledge no experimental studies showing growth responses to hydrodynamic forces over multiple growing seasons. In particular, there are no field experiments in temperate-climate marshes that identified how hydrodynamic forces from waves and currents affect plant survival during winter seasons, when plants are largely dormant, and then affect regrowth of shoots from the roots and rhizomes during the subsequent growing seasons. Yet, such knowledge is key if we want to understand under which wave and current conditions tidal marshes can be conserved, restored, or created by plantings, e.g., for nature-based shoreline protection. Further, such knowledge is essential for developing models enabling the prediction of the biogeomorphic evolution of marshes (Schwarz et al. 2018, Gourgue et al. 2021) and their nature-based contribution to shoreline protection (Marijnissen et al. 2020, Willemsen et al. 2020).

Marshes that are most vulnerable to shoreline erosion are often the small fringes (i.e. 10-100 m) along embanked shorelines of estuaries and coasts, where hydrodynamic forces are dominant. These smaller fringing marshes in front of embankments are however of particular interest to policymakers and shoreline managers, because of their function as nature-based shoreline protection in addition to man-made structure like dikes landward of the fringing marshes (van der Nat et al. 2016, van Loon-Steensma & Schelfhout 2017, Schoonees et al. 2019). Whereas in wide marshes (i.e. several hundreds to several thousands of meters wide) the presence of a less-effective wave-attenuating species may be compensated for by the large width of the marsh providing significant wind wave attenuation (Shepard et al. 2011, Li et al. 2013, Xue et al. 2021). The species composition and their spatial distribution might play an important role in determining the capacity to attenuate hydrodynamic forces such as waves and currents (van Loon-Steensma et al. 2016, chapter 3: Schoutens et al. 2020). Moreover, increasing storminess and sea level rise might increase landward marsh edge erosion, reducing the width of the marsh in front of the dike (Torio & Chmura 2013, Borchert et al. 2018).

Apart from waves and currents, other environmental stress factors are known to affect plant growth in tidal marshes, e.g. tidal inundation, salinity, pollutants, sediment grainsize, competition, grazing. In particular, spatial species distribution has been

related to spatial variation in environmental stressors, as the capacity of a species to cope with these stress factors determines where they survive (Pennings et al. 2005, Silvestri et al. 2005, Rasser et al. 2013, Bang et al. 2018, Veldhuis et al. 2019). Most research on tidal marsh plant zonation has focused on the role of abiotic drivers such as species tolerance to salt gradients (Engels et al. 2011) and inundation frequency and time (Castillo et al. 2000, Farina et al. 2009), and how this affects biotic interactions via competition or facilitation between species (Bertness 1991). How species-dependent tolerance of marsh plants to waves and currents contributes to spatial plant zonation, in addition to other factors like tolerance to tidal inundation time, is much less studied (Heuner et al. 2018). That is, the ability of tidal marsh vegetation to cope with waves and tidal currents might play a role in the species zonation along a hydrodynamic exposure gradient from high exposure close to the shore towards lower exposure further inland (Bruno 2000, chapter 3: Schoutens et al. 2020). This means that some species might have plant properties that allow them to grow in more wave exposed conditions compared to other species that lack these properties. Phenotypic plasticity to waves and currents may further affect the growth and alter plant traits (Carus et al. 2016, Silinski et al. 2018) and thus modify their ability to withstand hydrodynamic forces. Although knowledge on the phenotypic plasticity, long-term growth and survival is crucial for marsh management and restoration projects, little is known on how co-occurring species differing in traits respond to gradients in contrasting hydrodynamic exposures.

The present study aims to quantify experimentally the relative effects of hydrodynamic forces from waves and currents, in addition to tidal inundation, on the growth and morphology of three different co-occurring pioneer species of temperate-climate brackish tidal marshes. We investigate over two subsequent growing seasons, including the winter dormant season, how species responses differ in relation to species-specific plant traits through a field transplantation experiment, in which we applied in-situ manipulation of the hydrodynamic forces along an inundation gradient. Based on the findings from this experiment we aim to enhance insight in the role of hydrodynamic forces, in addition to tidal inundation, on species-specific plant growth.

5.3 Materials and Methods

5.3.1 Study area and species description

This study took place in the brackish zone of the Elbe Estuary, Germany (Fig. 5.1), where soil water salinity is ranging between 0.3 and 1.2 PSU (Schulte Ostermann et al. 2021a) and the semi-diurnal tide has an average tidal range of 2.8 m (data for 2018–2019 for the tide gauge station of Brokdorf, Küstendaten, Federal Waterways and Shipping Administration). Transplantation locations were selected on an intertidal flat using following selection criteria: A first criterion was absence of vegetation, so that

transplanted plants were not affected by existing vegetation. Secondly, we searched for a tidal flat location with similar surface elevations (i.e. similar tidal inundation frequency and time) as to where pioneer vegetation was present in adjacent areas. Thirdly, the tidal flat should be exposed to incoming waves at high tides. Along the marshes of Hollerwettern, a location with these conditions was found (53° 50' 0.7"N, 9° 22' 6.0"E). The tidal flat at this location has a gentle slope of ≤ 1° perpendicular to the estuary tidal channel with a median grainsize < 125 μm. There was a trend of larger grainsizes with increasing inundation depth, where hydrodynamic exposure is larger (table S5.1). The tidal flat is exposed to the dominant wind and wave direction coming from West to South as illustrated by the windrose diagram in Fig. 5.1b, with a wind fetch length at high tide of ca. 3 km.
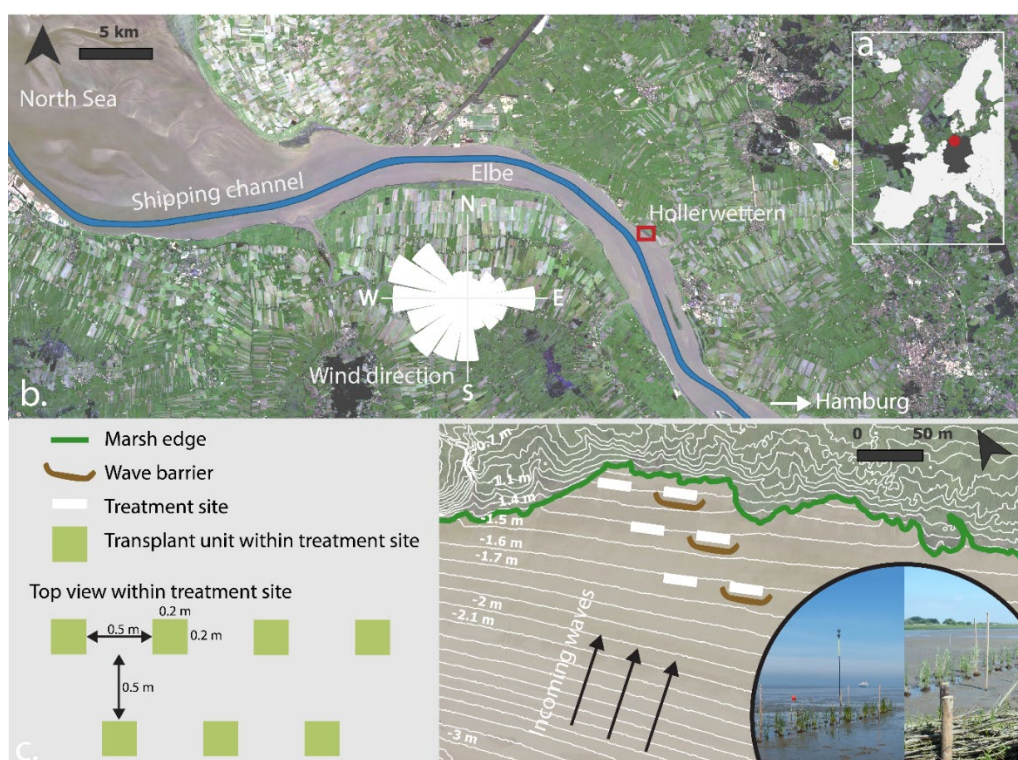
Figure 5.1: (a) The study area in the Hollerwettern marshes was situated in the brackish part of the Elbe estuary in NW Germany. (b) The shape of the estuary in combination with the dominant wind directions illustrate that the Hollerwettern marsh is a wave exposed site. Wind conditions are shown on the wind rose diagram during the experimental period in 2018-2019. (c) The experimental setup was a factorial design of two hydrodynamic exposure treatments spread over three elevations (i.e. inundation treatments) representing 6 treatment sites. Sheltered wave and flow conditions were created with wooden wave barriers which were placed outside each other's wake zones. In every treatment site, 20 transplant units of each species were

installed in two staggered rows and in random order. Elevations relative to MHW are visualized with contour lines.

The species selected for this study are *Schoenoplectus tabernaemontani* (C.C.Gmel.) Palla (formerly *Scirpus tabernaemontani*), *Bolboschoenus maritimus* (L.) Palla (formerly *Scirpus maritimus*) and *Phragmites australis* (Cav.) Trin. ex Steud (Fig. S5.1). Those three species are typically found along the brackish zone of the Elbe estuary and other NW European estuaries, growing in distinct zones parallel to the marsh edge in which they are the dominant species in their respective zones: *S. tabernaemontani* typically grows in a zone at the waterfront of marshes, followed in landward direction by a zone of *B. maritimus* and then *P. australis* (chapter 3: Schoutens et al. 2020). Apart from seed dispersal, the three species reproduce by clonal outgrowth through rhizomes or by dispersal of root fragments, e.g. released from marsh erosion. During the winter period, the aboveground biomass of the three species dies back and can get washed away by the waves and tides. Next growing season, new shoots sprout from the surviving belowground biomass. *S. tabernaemontani* produces round, leafless stems up to 2.0 m and grows from thick rhizomes that form a sparce root network. *B. maritimus* grows as a triangular shoot up to 2.5 m tall and forms a dense root network of rhizomes and tubers. The hollow stems of *P. australis* can reach up to 4.0 m in brackish marshes and are supported by a densely branched network of rhizomes.

5.3.2 Set-up of transplantation experiment

Sites for transplantation of the three species were selected on three different intertidal elevations (corresponding to different tidal inundation times and depths), and in each elevation zone two sites were established of which one site was exposed to and the other one was sheltered from incoming waves. The three elevations represent inundation depths under which at least one of the three species can be found in natural marshes. During two growing seasons, from March 2018 until August 2019, three wave barriers of 24 m wide and 0.7 m high were installed, one at each of the three selected elevations (Fig. 5.1), to create wave sheltered conditions at the naturally wave exposed site. The barriers were made from horizontally piled wooden branches that were fixed in between two rows of poles which were hammered vertically in the soil (Fig. 5.1). The orientation of the barriers was perpendicular to the dominant incoming wave direction from the Southwest. Edge effects were limited by extending the barrier 2 m further than the transplanted vegetation. The outer ends of the barrier were placed under a slight angle to provide an even better protection from incoming waves with a direction that slightly deviates from the Southwest. Large deviation in wave direction is not expected due to wave refraction over the tidal flat, which is expected to result in dominant Southwestern wave directions more or less perpendicular to the tidal flat slope (Fig. 5.1). Apart from the three wave sheltered sites, three wave exposed sites (i.e. without wave barrier) were installed at the same elevations. Although the sites were positioned nearby each other to ensure similar conditions, they were positioned far enough (at

least 30 m) from each other to ensure the wave barriers did not affect the plant growth on the wave exposed treatment sites (without barriers) (Fig. 5.1).

Transplantation took place in April 2018 at the start of the growing season. In order to excavate a consistent amount of marsh soil for every transplant, a metal clump-extractor was used to create marsh soil transplant units with a surface area of 0.20 x 0.20 m and a depth of 0.30 m. At each of the six treatment sites, 20 transplants from each of the three species were planted equally spaced at 0.50 m from the adjacent transplant unit. The total of 60 transplant units per treatment site were transplanted in two spatially staggered rows parallel to the wave barrier (Fig. 5.1). All 360 transplant units were taken from the adjacent marsh and directly planted at the experimental sites. In December 2018, when aboveground vegetation was low, the wave barriers were washed away. The barriers were rebuild in March 2019, before the start of the next growing season.

5.3.3 Growth response and species-specific plant traits

The following plant traits were quantified, which are known to affect the capacity of the plants for nature-based attenuation of waves and currents. For each transplant, the number of shoots were counted monthly from March 2018 until August 2019. In all six sites, canopy height (average of the three highest shoots per transplant) was measured monthly at ten transplant units per species and was used as a measure for average shoot length of the transplant. Basal shoot diameters were measured monthly at every site for ten shoots from different transplant units per species. Spatial outgrowth was quantified as the largest horizontal distance between shoots grown from the transplanted unit and was measured at every site for ten transplant units per species. In August 2019, at the end of the experiment, aboveground biomass was harvested from all treatments in case they survived. Upon drying at 70 °C for 72h, biomechanical properties were quantified on 20 individuals per species and per treatment. For more details on the methods to quantify biomechanical properties we refer to chapter 4: Schoutens et al. (2021).

5.3.4 Hydrodynamics and sediment dynamics

Hydrodynamic conditions were measured at the different sites to make sure that the barriers created an environment sheltered from waves and currents as compared to the sites without barriers. Tides, waves and current velocities were measured with automated pressure sensors (P-Log3021-MMC, Driesen & Kern) and acoustic doppler velocity sensors (Vector ADV, Nortek).

The pressure sensors were placed in front of the transplanted vegetation at an elevation of 0.07 m above the sediment surface and recording at 8 Hz. The pressure data was converted into water surface elevation using a Matlab routine, accounting for corrections for atmospheric pressure and depth-dependent pressure, followed by

calculations of the following wave characteristics: significant wave height (H_s, mean of the highest third of recorded waves) and $H_{1/100}$ (mean of the highest 1% of recorded waves) over 10 min time intervals. For more details on this method, we refer to Belliard et al. (2019). The water surface elevation data were also used to calculate tidal inundation characteristics such as inundation time per tide (I_{time}), mean inundation depth at high water (I_{depth}), and inundation frequency (i.e. proportion of high tides inundating the sites).

The ADV sensors measured flow velocities at 1 Hz at 0.10 m above the sediment surface. After filtering out low quality data based on the signal to noise ratio and the beam correlations, the planar flow velocity (U, m/s) was calculated as $U = \sqrt{u^2 + v^2}$ with u and v being the mean flow velocities (m/s) in the two horizontal dimensions perpendicular to each other, calculated over 10 min time intervals.

Hydrodynamic exposure or the presence of a barrier can alter the sediment dynamics. Therefore, sediment bed level changes were quantified with a combination of an RTK-GPS and laser leveler over the first growing period in 2018, revealing a vertical accuracy in the order of +/- 2 cm. At the start of the second growing season in March 2019, a triangular SEB (sedimentation erosion bar) setup was installed in every site (i.e. six in total) to increase the vertical accuracy of the bed level change measurements up to an order of +/- 2 mm (van Wijnen & Bakker 2001, Nolte et al. 2013). Monthly SEB measurements were done from March 2019 until the end of the experiment in August 2019.

5.3.5 Data analysis

Survival and growth response quantified through shoot counts were compared using a generalized linear model with negative binomial distribution to account for the many 'zero' counts (glm.nb function of the MASS package, R-project). Both treatments, i.e. the hydrodynamic treatments and the tidal inundation treatments were added as independent variables. The date of sampling was added to include the effect of seasonal variation. Separate models were made for each species since comparing shoot counts between the different species would not be meaningful without normalizing against typical shoot densities observed in the natural marsh populations. The factorial design of this transplantation experiment allowed us to test the effect of inundation and wave exposure on shoot morphological properties such as shoot length, stem diameter and aboveground shoot biomass and whether the size of the effect differs among the three species. To make interspecific comparisons, shoot length, stem diameter and above-ground biomass were normalized for the mean value of the respective property in the adjacent natural marsh population (table 5.1, data used from Schulte Ostermann et al. (2021a)), i.e., values >1 indicate a higher performance and values <1 indicate a lower performance of the respective variable compared to the natural population. The responses at the end of the growing season in 2019 were compared in a three-way

ANOVA including the species, wave exposure and inundation stress as independent variables. Within every species, the ANOVA was followed by a post-hoc comparison between the combined treatments using Tukey HSD. All statistical analyses were performed in R 4.0.3 (R Core Team 2020) and significance was assumed at $p < 0.05$ for all tests. All p-values < 0.001 were reported as '<0.001', p-values < 0.1 were reported with the exact number and p-values > 0.1 were reported as 'ns'. Assumptions were checked based on visual inspection with histograms and Q-Q plots.

Table 5.1: General description of the growth conditions where the three transplanted species are naturally growing in the adjacent tidal marshes of Hollerwettern. Elevations relative to the tidal range and distance to the marsh edge (± SD) indicate that the sampling of all three natural populations occurred on locations which were sheltered from incoming waves and currents. Data on shoot length, stem diameter and above-ground biomass measured on these populations were published in Schulte Ostermann et al. (2021b) and were used here to normalize the data measured from the transplants.

	Elevation (relative to tidal range)	Distance to marsh edge (m)
S. tabernaemontani	0.70 ± 0.13	5.7 ± 3.0
B. maritimus	0.88 ± 0.11	38.1 ± 15.1
P. australis	1.08 ± 0.05	86.6 ± 35.2

5.4 Results

5.4.1 Hydro- and morphodynamic conditions within the experimental treatments

Hydrodynamic forces from waves and currents were stronger in the exposed sites (table 5.2 and Fig. S5.2 and S5.3). Significant wave heights and mean flow velocities were higher in the exposed sites as compared to the sheltered sites, and this difference increased with decreasing tidal inundation depths (i.e. up to a maximum of 16 % higher significant wave heights and 21 % higher flow velocity). The deepest inundated sites had an inundation time which was approximately 1.5 h longer and a mean high-water depth that was around 0.40 m deeper than the shallowest inundated sites (table 5.2). Inundation frequency was > 98 % for all sites, meaning that they were inundated nearly every high tide. Over the entire period of the experiment, all sites experienced both periods of erosion and accretion (table 5.2 and Fig. S5.4). Erosion mainly occurred during the winter period when waves were largest, and accretion in spring and summer as waves were smaller. It is important to note that during the winter period from December 2018 – March 2019, the wave barriers were damaged during storms, and this was associated with erosion up to 15 cm observed on several of the sheltered and exposed sites (Fig S5.4).

Table 5.2: Summary of the main hydrodynamic properties per treatment combination over the entire monitoring campaign; mean of the significant wave heights ($H_s \pm$ SD, m), mean maximum wave height ($H_{1/100} \pm$ SD, m), single maximum wave height (H_{max}, m), mean planar flow velocity ($U \pm$ SD, m s^{-1}), mean inundation depth at high water (I_{depth}, m), mean inundation time per tide (I_{time}, min), elevation relative to MHW (E_{MHW}, m) and elevation variation (E_{var}, m) calculated as the maximum elevation – minimum elevation over the time period.

Inun.	Wave	H_s (m)	$H_{1/100}$ (m)	H_{max} (m)	U (m/s)	I_{depth} (m)	I_{time} (min)	E_{MHW} (m)	E_{var} (cm)
Shallow	Exp.	0.088 ± 0.06	0.11 ± 0.08	0.71	0.06 ± 0.05	1.15	379	-1.17	13.6
	Shelt.	0.085 ± 0.05	0.10 ± 0.07	0.7	0.06 ± 0.04	1.13	373	-1.18	14.0
Mid	Exp.	0.084 ± 0.06	0.11 ± 0.08	0.68		1.38	425	-1.35	7.6
	Shelt.	0.071 ± 0.05	0.09 ± 0.07	0.5		1.29	405	-1.39	17.4
Deep	Exp.	0.085 ± 0.06	0.11 ± 0.08	0.89	0.19 ± 0.09	1.58	462	-1.62	5.9
	Shelt.	0.078 ± 0.06	0.10 ± 0.08	0.78	0.15 ± 0.08	1.52	451	-1.63	14.8

5.4.2 Effects of hydrodynamic exposure and inundation on shoot numbers

Transplantation on deeper and longer inundated sites, i.e. with higher inundation time (> 405 min) and depth (>1.29 m) (table 5.1), reduced the number of shoots per transplant in the three species (Fig. 5.2, p < 0.001). Interestingly, there was a big difference in shoot numbers between the two growing seasons (Fig. 5.2). In the second growing season, in the shallow inundation sites, the *S. tabernaemontani* and *B. maritimus* plants produced more shoots, while *P. australis* formed a similar amount of shoots compared to the first season. In the deep inundation treatments, the seasonal difference diminishes as shoot numbers of all species were strongly reduced. The number of shoots was highest in *S. tabernaemontani*, followed by *B. maritimus*. In the second growing season, *S. tabernaemontani* grew less than 50 shoots per transplant when inundated more than 1.29 m and more than 405 min per tide, i.e. deep inundation treatment, while the other species hardly grew any shoot starting from an intermediate inundation stress. Already in the first growing season, *P. australis* transplants died off in the intermediately and deeply inundated sites. Hydrodynamic exposure decreased the number of shoots in *B. maritimus* and *S. tabernaemontani* (p < 0.05). The low number of shoots for *P. australis* did not allow the detection of significant differences between the exposed and sheltered sites. The different responses of shoot numbers to hydrodynamic exposure was only visible when the stress from tidal inundation was low enough.
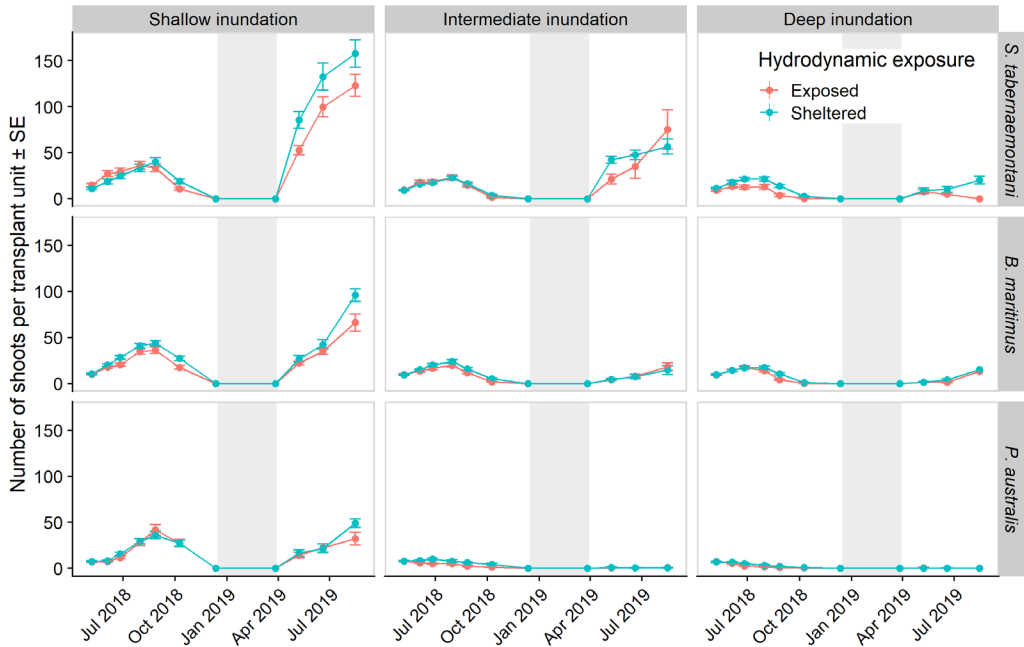
Figure 5.2: Number of shoots per transplant unit for both hydrodynamic exposure treatments and three inundation treatments. The shoots were counted over two growing seasons (2018-2019). Grey boxes indicate the winter season when aboveground biomass dies-off and was flushed away by the tides.

5.4.3 Effects of hydrodynamic exposure and inundation on shoot diameter, shoot length and biomechanical properties

In the natural marsh of Hollerwettern, from where plant material was collected for the transplantation, plant morphological measurements of the natural population showed a clear species-specific difference in plant traits (Fig. 5.3).
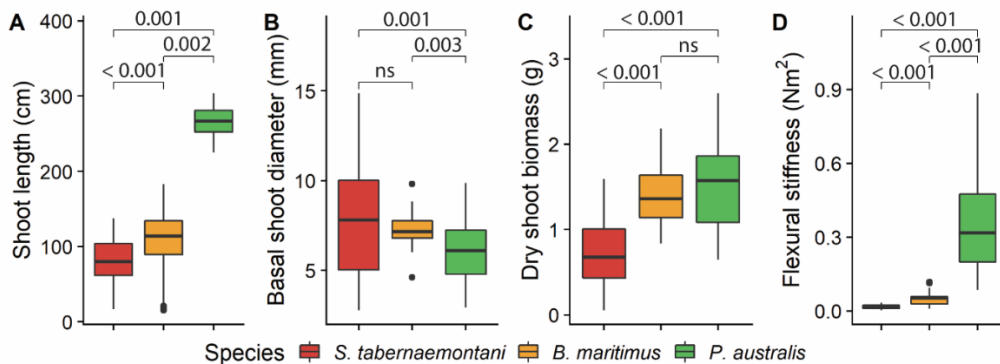

Figure 5.3: Plant morphological traits in the adjacent natural marsh (Hollerwettern) for *S. tabernaemontani*, *B. maritimus* and *P. australis*. Shoot length (m), basal shoot diameter (mm), dry shoot biomass (g) and shoot flexural stiffness (Nm^2) were

quantified at peak biomass (data from Schulte Ostermann et al. (2021a)). Differences between the species are indicated with significance levels obtained with ANOVA.

Both the inundation stress and the hydrodynamic exposure had a negative effect on the basal shoot diameter and the shoot length (Fig. 5.4 and 5.5). Nevertheless, the response to these stressors was species-specific (table 5.3), i.e. *S. tabernaemontani* was able to cope better with the combined stressors from tidal inundation and hydrodynamic exposure, followed by *B. maritimus* and *P. australis* which had a strongly reduced growth compared to the natural population. In *S. tabernaemontani* transplants, increased inundation stress and increased hydrodynamic exposure resulted in thinner basal stem diameters and shorter shoots. Except for the exposed, deep inundation treatment, *S. tabernaemontani* transplants grew shoots that were consistently thicker and longer compared to the natural population. *B. maritimus* grew thinner and shorter shoots with increasing inundation stress, however, no significant differences between the hydrodynamic exposure treatments were found. Under shallow inundation, shoot of *B. maritimus* were up to twice as thick and 1.3 times longer compared to the natural population. In the two deeper inundation treatments, the basal shoot diameters of *B. maritimus* were more comparable to the natural population, however the shoot lengths were shorter compared to the natural population. In *P. australis*, no differences in treatment response were observed and compared to the natural population, the basal stem diameter of the remaining shoots was halved and the shoot lengths were less than half of the normal length.

Figure 5.4: Shoot basal diameter normalized by shoot diameters in the natural marsh (see Fig. 5.3) at peak biomass for the two hydrodynamic exposure treatments and the three inundation treatments. Significance of differences between the combined treatments was tested with ANOVA for every species and followed by a post-hoc Tukey's HSD, indicated by different letters.
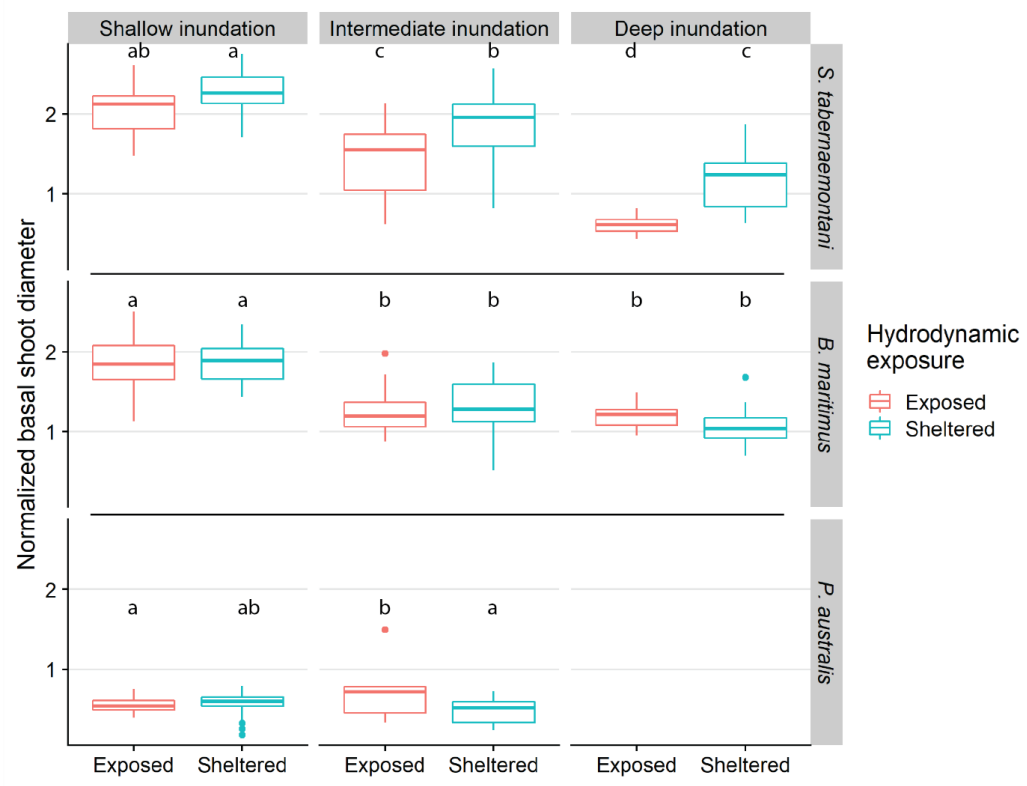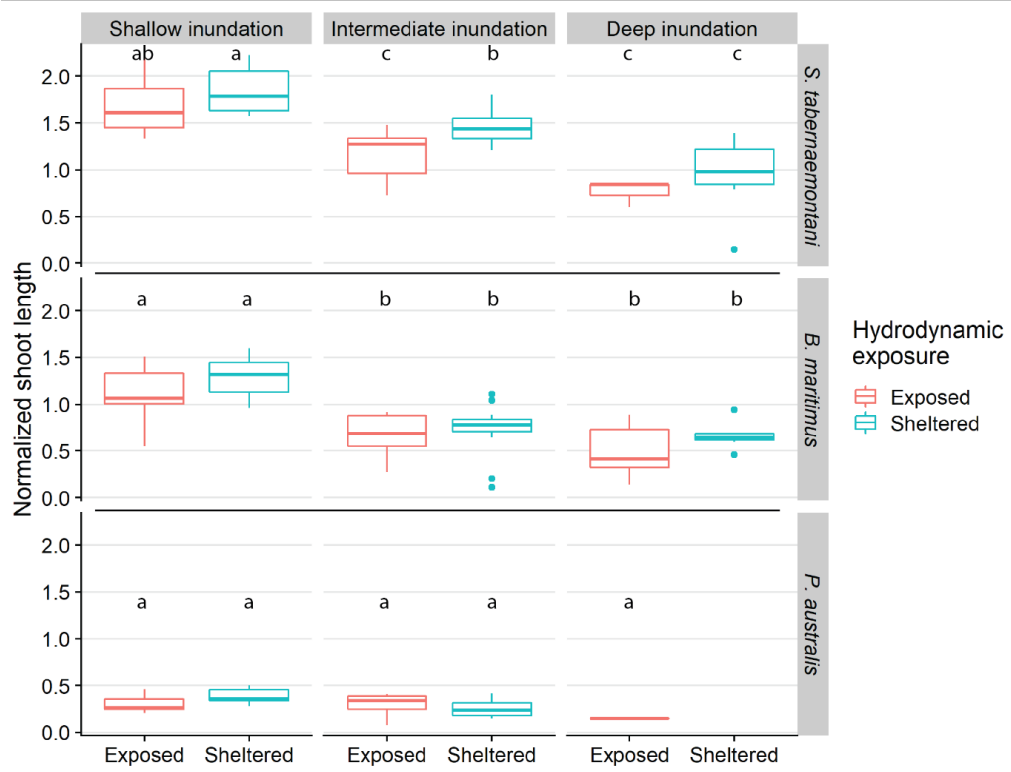
Figure 5.5: Shoot lengths normalized by shoot lengths in the natural marsh (see Fig. 5.3) at peak biomass for the two hydrodynamic exposure treatments and the three inundation treatments. Significance of differences between the combined treatments was tested with ANOVA for every species and followed by a post-hoc Tukey's HSD, indicated by different letters.

Table 5.3: The ANOVA table for the linear model made for normalized shoot diameters, normalized shoot lengths and normalized stem biomass at peak biomass in August 2019. Both the hydrodynamic exposure treatment (exposed - sheltered) and the inundation treatment (shallow – intermediate – deep) were tested across the three species (*S. tabernaemontani, B. maritimus, and P. australis*). Significant variables are indicated with a **bold** p-value.

Variable		df	*F*	p		df	*F*	p		df	*F*	p
Wave		1	26.6	**< 0.001**		1	19.6	**< 0.001**		1	22.0	**< 0.001**
Inundation		2	134.8	**< 0.001**		2	129.5	**< 0.001**		2	13.9	**< 0.001**
Species	Diameter	2	553.5	**< 0.001**	Length	2	537.2	**< 0.001**	Shoot biomass	2	71.1	**< 0.001**
Wave*inundation		2	1.8	0.2		2	0.4	0.7		2	4.5	**< 0.05**
Wave*species		2	8.8	**< 0.001**		2	1.8	0.2		2	4.6	**< 0.05**
Inundation*species		3	8.8	**< 0.001**		3	9.0	**< 0.001**		3	4.3	**< 0 .05**
Wave*inundation*species		1	0.4	0.5		1	0.004	0.9		1	1.7	0.2

Biomechanical properties such as Young's modulus and flexural stiffness were not affected by the inundation treatment nor the hydrodynamic exposure treatment, except for *S. tabernaemontani* shoots in the shallow inundation sites, which were stiffer on the sheltered sites as compared to the exposed shoots (ANOVA, $F_{1,77}$ = 15.3; p < 0.001). More details are given in table S5.2.

5.4.4 Effects of hydrodynamic exposure and inundation on lateral expansion and overall biomass

The three species in this transplantation experiment reproduce primarily by clonal outgrowth, which is important for the long-term survival of the species. Outgrowth of the transplants in the second growing season was reduced with increasing stress from inundation while no significant response to hydrodynamic exposure was observed. Outgrowth of the transplants in the second growing season did show a species-specific response and was highest in *S. tabernaemontani* which expanded in multiple directions forming a star-like pattern of shoots (Fig. 5.6). The transplants of *B. maritimus* were also expanding, however to a lesser extent compared to *S. tabernaemontani*. *P. australis* hardly expanded and the few surviving transplants had the same diameter as when the experiment started (Fig. 5.6).
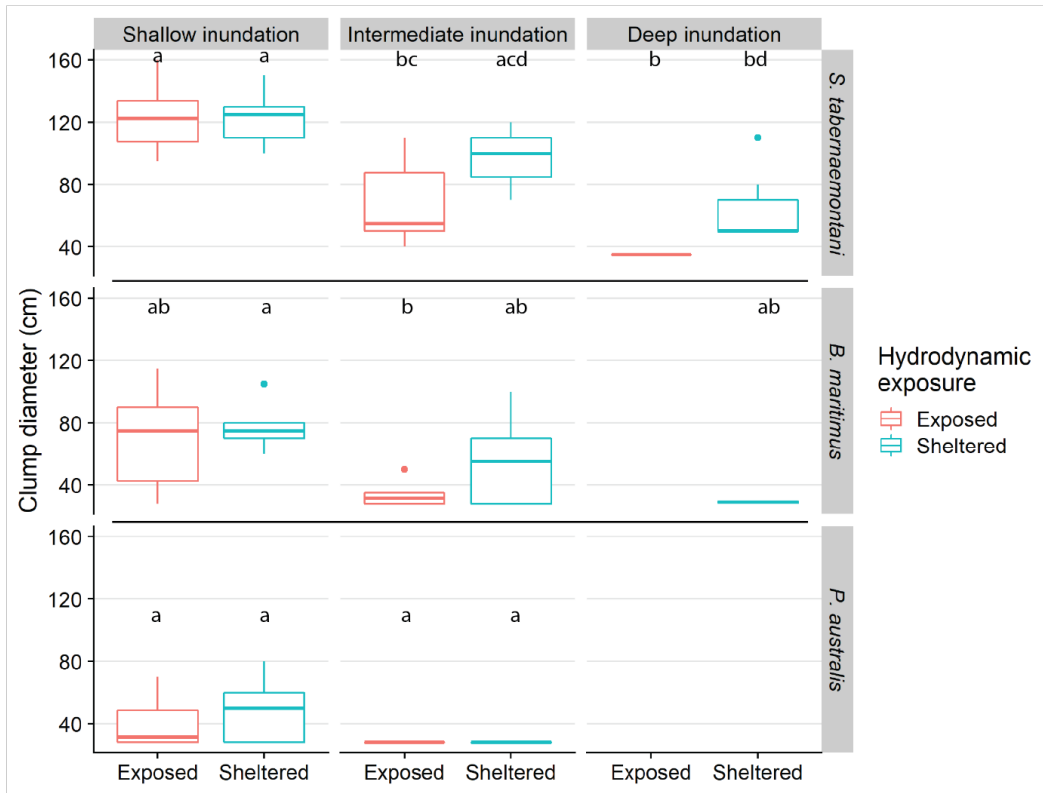
Figure 5.6: Outgrowth of the transplants in the 2nd growing season, expressed as clump diameter (i.e. biggest diameter of the transplant unit) at peak biomass for the two hydrodynamic exposure treatments and the three inundation treatments. Significance of differences between the combined treatments was tested with ANOVA for every species and followed by a post-hoc Tukey's HSD, indicated by different letters.

Although there seems to be a trend of decreasing shoot biomass with increasing inundation stress (table 5.3), this trend was not consistent for all species with remaining shoots (Fig. 5.7). Nevertheless, biomass die-off in the deep inundation treatment for B. maritimus and in both the intermediate and deep inundation treatment for P. australis do show a negative effect on the survival and hence shoot biomass production as a result of increased inundation stress. Hydrodynamic exposure had a similar negative effect on the shoot biomass, however this was not significant for S. tabernaemontani and only significant in the intermediate inundation treatment for B. maritimus shoots. The remaining P. australis biomass in the shallow inundation treatments did not differ either. Shoot biomass of the transplants was lower in all treatments compared to the natural population, except for the shallow inundation and sheltered, intermediate inundation treatments of S. tabernaemontani and B. maritimus which had a similar biomass compared to the natural population. Only the sheltered, shallow inundated transplants of S. tabernaemontani grew a higher (by 1.5) shoot biomass.
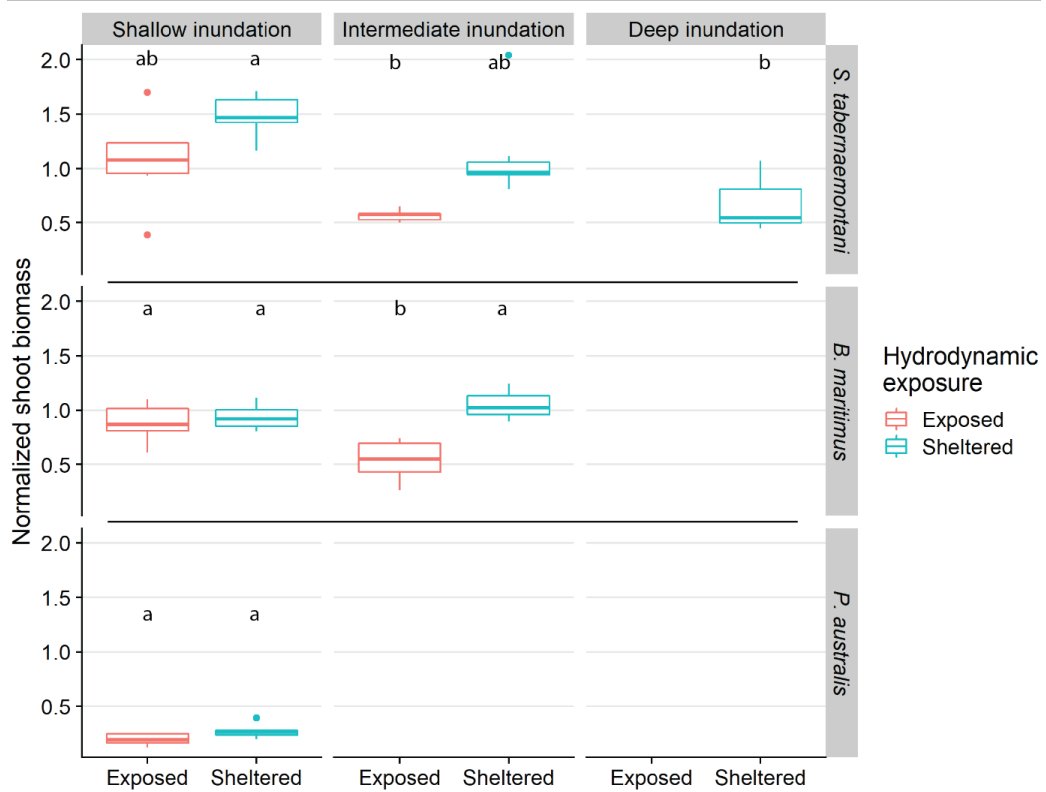
Figure 5.7: Dry shoot biomass harvested in August 2019, normalized by shoot biomass in the natural marsh at peak biomass (see Fig. 5.3) for the two hydrodynamic exposure treatments and the three inundation treatments. Significance of differences between the combined treatments was tested with ANOVA for every species and followed by a post-hoc Tukey's HSD, indicated by different letters.

5.5 Discussion

Our findings highlight that plants with a higher capacity to grow under hydrodynamic forces, have inter- and intraspecific traits that are known to reduce mechanical stress from waves and currents. Species-specific growth responses to wave and current exposure is likely to contribute to spatial species zonation. Previous studies on nature-based shoreline protection by tidal marsh plants have identified species traits that increase their effectiveness to attenuate waves and currents (Bouma et al. 2005, 2010, Vuik et al. 2016, Schulze et al. 2019, chapter 3: Schoutens et al. 2020). In contrast, relatively little is known about how species traits affect the capacity of species to survive and grow under the influence of different levels of exposure to waves and currents. Yet, such knowledge on species-dependent growth responses to wave and current exposure is crucial to manage and restore marshes for nature-based shoreline protection. Here, we showed by a 2-year field transplantation experiment, that in

addition to tidal inundation, exposure to waves and currents also decreases the growth of three tidal marsh species, with the magnitude of growth reduction being species specific.

5.5.1 Species-specific response to tidal inundation and hydrodynamic forces

Tidal inundation had a negative effect on the shoot numbers, but with a species-specific magnitude (Fig. 5.2). Apart from limited light availability during inundation, water submergence creates anaerobic conditions which can suppress the growth of vegetation, e.g. by anaerobic formation of phytotoxic compounds surrounding the roots (Hellings et al. 1992, Coops et al. 1996a, Engloner 2009). Many tidal marsh species developed morphological adaptations to these anaerobic conditions of which oxygen supply to their root system is most common, i.e. species grow aerenchym tissue that allows oxygen transport from aerated organs such as leaves towards the root system (Armstrong et al. 2006, Lemoine et al. 2012). The thicker stems of *S. tabernaemontani* and *B. maritimus* provided structural rigidity in this study which might result from more aerenchyma tissue in response to oxygen deprivation (Albert et al. 2013). In contrast, more aerenchyma and thicker stems are also linked to a softer and thinner epidermic layer, i.e. resulting in less strength molecules and structural rigidity which increases the stem flexibility (Shah et al. 2017, Silinski et al. 2018). Growing shoots that stay emerged during flooding, facilitate and ensure the oxygen supply to the roots (Maricle & Lee 2002) and hence help to cope with increased tidal inundation (Colmer & Flowers 2008). However, this strategy can only work when shoots do not break due to hydrodynamic forces.

In addition to the tidal inundation treatments, plant growth and development were hampered in the wave and current exposed sites for *B. maritimus* and especially for *S. tabernaemontani,* compared to the sheltered sites, but the plants were still able to survive (Fig. 5.4, 5.5, 5.7). This result suggests that both species were, to some extent, able to grow under the increased mechanical stress from waves and currents which is most likely a result of species-specific plant morphological traits (Fig. 5.3). Plant traits such as small, flexible shoots found in the natural population of *S. tabernaemontani* and to a lesser extend *B. maritimus* reduce drag, hence increasing the capacity to cope with waves and currents (Bouma et al. 2005, Puijalon et al. 2011, Paul et al. 2016, chapter 3: Schoutens et al. 2020, Schulte Ostermann et al. 2021a). These are plant morphological traits that are often found in species growing under mechanical stress (Anten et al. 2005, Anten & Sterck 2012). For some wetland species, shoot elongation in response to inundation stress was described as part of a so called escape strategy, i.e. the shoots grow to stay emerged from the water (Garssen et al. 2015). This suggests that inundation stress and mechanical stress from hydrodynamic forces might have contrasting effects on plant growth.

For *P. australis*, the observed response to tidal inundation stress might be enhanced by an indirect response to damage from hydrodynamic exposure. *P. australis* grows relatively stiff stems in natural populations (see Fig. 5.3 and Coops et al. 1996b, chapter 3: Schoutens et al. 2020, Zhu et al. 2020b, Zhang & Nepf 2021), but shoots with a higher stiffness are more susceptible to stem breakage (Shah et al. 2017, Zhu et al. 2020b). Immediately from the first growing season after transplantation, *P. australis* produced little shoot numbers, which could suggest a mechanical growth restriction by breakage of young sprouting stiff shoots. It is known that *P. australis* is prone to drowning when shoots are cut during the growing season as a result of an impaired oxygen supply to the roots and the loss of photosynthetic activity (Hellings et al. 1992, Rolletschek et al. 2000, Asaeda et al. 2003). For the shoot that did survive, growth was hampered, e.g. by mechanical stress. Hence, the amount of photosynthetic active leave surface is reduced which might increase the susceptibility to other stressors, such as oxygen deprivation by tidal inundation stress.

Apart from direct stress responses induced by the experimental treatments in this study, the observed stress responses of the species could be the result of a species-specific capacity to cope with the stress from the transplantation itself, e.g. change of local sediment properties or damage to the roots. Transplantation success of marsh plants is typically optimized by providing enough belowground biomass of nearby populations from species that have a high capacity to expand clonally (Thomsen et al. 2005, Ott et al. 2019, Popoff et al. 2021). Although no control transplantation was performed, it is known from literature, on previous transplantation treatments, that the three species in this study are well able to handle the disturbance of a transplantation (Coops et al. 1996b, Amsberry et al. 2000, Silinski et al. 2016a, Taylor et al. 2019). Indirect effects of the applied treatments might play an important role in the growth response too. For example, the hydrodynamically driven grainsize distribution (table S5.1) results in coarser sediments on places with increased hydrodynamic exposure, more inundation alters the redox potential of the soil, and sheltered conditions might increase sediment accretion and potential burial of young shoots. Although sediment dynamics in this experiment were mostly limited outside the period of the growing season, we acknowledge that sediment dynamics and sediment characteristics can alter the growth of the root network which is important for the long term survival of the marsh plants (Bradley & Morris 1990, Chen et al. 2012, Jafari et al. 2019). Moreover, both direct and indirect effects of synergetic stressors should be considered (Veldhuis et al. 2019), e.g. the presence of grazers will reduce aboveground biomass and wave attenuation capacity, however it was shown that it promotes belowground biomass production which could increase the stability of the sediment bed (Pagès et al. 2019). Although changes in belowground biomass were not measured in this experiment, including belowground biomass dynamics should be considered in future research.

5.5.2 Phenotypic plasticity in response to tidal inundation and hydrodynamic forces

Apart from plant trait differences between species, a similar trend of intraspecific varying plant traits was also found in response to the different inundation and hydrodynamic exposure treatments. Within the species that was able to survive and grow under all tested conditions (i.e. *S. tabernaemontani*), the transplants developed smaller, thinner and more flexible shoots in response to higher exposure to waves and currents and increasing tidal inundation, which was similar to the response in interspecific variation in plant traits. Interestingly, when comparing morphological traits in the transplantation experiment with the natural population, *S. tabernaemontani* grew thicker and taller shoots on the sites with shallow and intermediate inundation (Fig. 5.4, 5.5), which resulted in a stronger stem geometry (i.e., high moment of area, see table S5.2) and stiffer shoots. This suggests that in these treatments stress from hydrodynamic exposure and tidal inundation where relatively low for *S. tabernaemontani*. Since all transplant units were evenly spaced from each other to limit potential competition between them, this enhanced growth capacity compared to the natural population might result from better resource availability and less competition between shoots in the transplants (Shen et al. 2020). Phenotypic plasticity as a growth response to waves or currents has been previously reported for *B. maritimus*, as it grows shorter and more flexible shoots with thicker stem diameters in response to increasing exposure to waves and currents (Carus et al. 2016, Silinski et al. 2018). Interestingly, this response can vary depending on the species and habitat-specific conditions, e.g. for *Juncus roemerianus* and *Spartina alterniflora* thinner stem diameters in response to wave exposure were reported (Temple et al. 2021).

Variation of plant traits in response to environmental stress creates variation in the functional role of the plants and their bio-physical interactions within the environment (Heuner et al. 2015, Renzi et al. 2019, Battisti 2021). The intra- and interspecific variation of plant traits generate different ecosystem engineering capacities, e.g. plant traits that generate more friction with the water, have a stronger wave attenuation effect which will promote sedimentation and limit erosion risk (Silinski et al. 2018, chapter 3: Schoutens et al. 2020). In this context, plant traits are linked to species habitat, i.e. seagrasses benefit from being flexible, limiting their capacity to accrete sediments, but maintaining the submerged conditions (Bouma et al. 2005). Variability in plant traits will therefore generate spatial variability in bio-physical interactions which is important for the geomorphology of the marsh, e.g. sedimentation-erosion processes (Bouma et al. 2009, Corenblit et al. 2015). The balance between the strength of the bio-physical interactions, generated through the plant traits, and the environmental stressors will therefore create large-scale geomorphological patterns such as cliffs and channels (Van de Koppel et al. 2005, Brückner et al. 2019).

Interestingly, the adaptive nature of tidal marsh plants and their plant trait-based variation in functionality can improve the resilience of the ecosystem to a range of environmental settings (Battisti 2021).

5.5.3 Consequences for spatial species distribution in pioneer tidal marshes

Spatial species distribution within tidal marshes is traditionally thought as being predominantly the result of the balance between competition and species tolerance to environmental stress factors, typically tidal inundation and salinity (Pennings & Callaway 1992, Wang et al. 2010, Janousek & Mayo 2013, Rasser et al. 2013). This study indicates that species-specific tolerance to waves and currents can play an additional role in the spatial distribution of pioneer tidal marsh plants. The high capacity of *S. tabernaemontani* to grow under hydrodynamic forces allows this species to colonize areas where other species might not be able to grow. The establishment of *S. tabernaemontani* leads to attenuation of waves and currents within and behind patches of *S. tabernaemontani* (chapter 3: Schoutens et al. 2020) and as such is expected to create more sheltered conditions that may facilitate the establishment of other species, less tolerant to waves and currents, such as *B. maritimus*. Subsequently the presence of those two species zones can create even more wave and current attenuation and hence create the environmental conditions that allow the establishment of species such as *P. australis*. Wave-induced species distribution in pioneer tidal marshes has been suggested in other studies (Heuner et al. 2018, chapter 3: Schoutens et al. 2020, Zhu et al. 2020b). Although the growth response to waves and currents was less clear for *B. maritimus* and *P. australis,* tidal inundation is likely to be the dominant stressor which diminishes the potential effects of wave exposure on survival or growth. To make the growth response to hydrodynamic exposure more apparent, future research should consider increasing the elevation range towards higher sites, reducing the tidal inundation stress, and/or increasing the differences between the hydrodynamic exposure treatments.

5.5.4 Species-specific survival chances determine the shoreline protection capacity of tidal marshes

Nature-based shoreline protection capacity of tidal marshes depends on (1) the wave and current attenuation capacity of marsh plants and (2) their ability to cope with the exposure to waves and currents. Our results emphasize there is an apparent trade-off between these two aspects, i.e. that species growing at the wave exposed marsh edge have plant traits (smaller, more flexible shoots) that reduce the drag forces on their shoots, but the same plant traits reduce their wave attenuation capacity, which has been hypothesis before (chapter 3: Schoutens et al. 2020). Studies on wave and current attenuation use plant traits of natural populations or plants that were grown under ideal conditions (Suzuki et al. 2012, Möller et al. 2014, Vuik et al. 2016, Garzon et al. 2019, Willemsen et al. 2020). The effectiveness of attenuating hydrodynamics is then

described based on the plant traits of idealized species. However, when considering tidal marsh restoration and (re-)establishment, the new environmental conditions (e.g. in case of strong hydrodynamic exposure and high tidal inundation stress) might alter the growth and plant traits of some species, which also changes the expected wave- and current attenuation capacity of the newly formed marsh. Nevertheless, we argue here that the traits that allow plants to grow in more exposed sites create more sheltered conditions in the landward direction and facilitate there the growth of species that otherwise would not have been able to cope with the stronger hydrodynamic forces. Such facilitation implies that tidal marshes might be able to survive more exposed conditions than previously thought. Nevertheless, growth facilitation between different marsh species zones will only work when there is enough space for the marsh to develop different vegetation zones. At many shorelines all over the world, land use change has reduced the spatial extent of tidal marshes drastically (Duarte 2009, Davidson 2014, Crosby et al. 2016, Spencer et al. 2016). Moreover, sea level rise and increased hydrodynamics (e.g. shipping) will enhance the so called coastal squeeze, increasing hydrodynamic exposure of tidal marshes (Torio & Chmura 2013, Borchert et al. 2018, Valiela et al. 2018). This trend will make the existing space for interspecific growth facilitation and tidal marsh development even smaller. However, we argue that providing enough space for tidal marsh development and species facilitation is important to ensure shoreline protection throughout changes in the hydrodynamic conditions which as a result may improve marsh resilience to environmental change (Renzi et al. 2019).

Our findings have practical implications for restoration and conservation of natural shorelines, a measure that is often applied to improve the ecosystem service functions of tidal marshes, such as biodiversity conservation, water quality improvement, carbon sequestration and coastal defense (Barbier et al. 2011). Firstly we argue that, when space allows, interspecific facilitation of plant growth and survival results in a species distribution which increases the effectiveness of the hydrodynamic attenuation function of the marsh. Secondly, the presented results can help to identify sites that are suitable for tidal marsh restoration in terms of suitable site exposure to waves and currents and tidal inundation. This type of data is also highly useful for improving models that predict species occurrence and that can be used in restoration projects (Gourgue et al. 2021). More specifically, species-specific growth rates under a range of hydrodynamic conditions could be used to calibrate and validate such models (Van de Koppel et al. 2005, Mariotti & Fagherazzi 2010, Hu et al. 2015, Carus et al. 2017). Rather than e.g. planting seedlings, creating enough space for a suitable environment where species with the right plant traits can grow, might be even more important for long term survival of tidal marshes and therefore their shoreline protection capacity.

5.6 Acknowledgements

5.7 References

Albert DA, Cox DT, Lemein T, Yoon HD (2013) Characterization of schoenoplectus pungens in a great lakes Coastal Wetland and a Pacific Northwestern Estuary. Wetlands 33:445–458.

Amsberry L, Baker M a., Ewanchuk PJ, Bertness MD (2000) Clonal integration and the expansion of *Phragmites australis*. Ecol Appl 10:1110–1118.

Anten NPR, Casado-Garcia R, Nagashima H (2005) Effects of Mechanical Stress and Plant Density on Mechanical Characteristics, Growth, and Lifetime Reproduction of Tobacco Plants. Am Nat 166:650.

Anten NPR, Sterck FJ (2012) Terrestrial vs aquatic plants: How general is the drag tolerance-avoidance trade-off? New Phytol 193:6–8.

Armstrong J, Jones RE, Armstrong W (2006) Rhizome phyllosphere oxygenation in Phragmites and other species in relation to redox potential, convective gas flow, submergence and aeration pathways. New Phytol 172:719–731.

Asaeda T, Manatunge J, Fujino T, Sovira D (2003) Effects of salinity and cutting on the development of *Phragmites australis*. Wetl Ecol Manag 11:127–140.

Auerbach LW, Goodbred SL, Mondal DR, Wilson CA, Ahmed KR, Roy K, Steckler MS, Small C, Gilligan JM, Ackerly BA (2015) Flood risk of natural and embanked landscapes on the Ganges-Brahmaputra tidal delta plain. Nat Clim Chang 5:153–157.

Bang JH, Bae MJ, Lee EJ (2018) Plant distribution along an elevational gradient in a macrotidal salt marsh on the west coast of Korea. Aquat Bot 147:52–60.

Barbier EB, Hacker SD, Kennedy C, Koch EW, Stier AC, Silliman BR (2011) The value of estuarine and coastal ecosystem services. Ecol Monogr 81:169–193.

Battisti D De (2021) The resilience of coastal ecosystems : A functional trait-based perspective. J Ecol:1–14.

Belliard JP, Silinski A, Meire D, Kolokythas G, Levy Y, Van Braeckel A, Bouma TJ, Temmerman S (2019) High-resolution bed level changes in relation to tidal and wave forcing on a narrow fringing macrotidal flat: Bridging intra-tidal, daily and seasonal sediment dynamics. Mar Geol 412:123–138.

Bertness MD (1991) Zonation of *Spartina patens* and *Spartina alterniflora* in a New England Salt Marsh. Ecology 72:138–148.

Borchert SM, Osland MJ, Enwright NM, Griffith KT (2018) Coastal wetland adaptation to sea level rise: Quantifying potential for landward migration and coastal squeeze. J Appl Ecol 55:2876–2887.

Bouma TJ, Friedrichs M, van Wesenbeeck BK, Temmerman S, Graf G, Herman PMJ (2009) Density-dependent linkage of scale-dependent feedbacks: a flume study on the intertidal

macrophyte *Spartina anglica*. Oikos 118:260–268.

Bouma TJ, De Vries MB, Herman PMJ (2010) Comparing ecosystem engineering efficiency of two plant species with contrasting growth strategies. Ecol Soc Am 91:2696–2704.

Bouma TJ, De Vries MB, Low E, Peralta G, Tánczos IC, van de Koppel J, Herman PMJ (2005) Trade-offs related to ecosystem engineering: a case study on stiffness of emerging macrophytes. Ecology 86:2187–2199.

Bradley P, Morris J (1990) Physical characteristics of salt marsh sediments: ecological implications. Mar Ecol Prog Ser 61:245–252.

Brückner MZM, Schwarz C, van Dijk WM, van Oorschot M, Douma H, Kleinhans MG (2019) Salt Marsh Establishment and Eco-Engineering Effects in Dynamic Estuaries Determined by Species Growth and Mortality. J Geophys Res Earth Surf 124:2962–2986.

Bruno JF (2000) Facilitation of cobble beach plant communities through habitat modification by Spartina alterniflora. Ecology 81:1179–1192.

Cao H, Zhu Z, James R, Herman PMJJ, Liquan Z, Yuan L, Bouma TJ, Zhang L, Yuan L, Bouma TJ (2020) Wave effects on seedling establishment of three pioneer marsh species: survival, morphology and biomechanics. Ann Bot 125:345–352.

Carus J, Heuner M, Paul M, Schröder B (2017) Which factors and processes drive the spatio-temporal dynamics of brackish marshes?—Insights from development and parameterisation of a mechanistic vegetation model. Ecol Modell 363:122–136.

Carus J, Paul M, Schröder B (2016) Vegetation as self-adaptive coastal protection: Reduction of current velocity and morphologic plasticity of a brackish marsh pioneer. Ecol Evol 6:1579–1589.

Castillo JM, Fernandez-Baco L, Castellanos EM, Luque CJ, Figueroa ME, Davy AJ (2000) Lower limits of *Spartina densiflora* and *S . maritima* in a Mediterranean salt marsh determined by different ecophysiological tolerances. J Ecol 88:801–812.

Chen Y, Thompson CEL, Collins MB (2012) Saltmarsh creek bank stability: Biostabilisation and consolidation with depth. Cont Shelf Res 35:64–74.

Colmer TD, Flowers TJ (2008) Flooding tolerance in halophytes. New Phytol 179:964–74.

Coops H, van den Brink FWB, Van der Velde G (1996a) Growth and morphological responses of four helophyte species in an experimental water-depth gradient. Aquat Bot 54:11–24.

Coops H, Van der Velde G, Velde G Van Der (1996b) Effects of waves on helophyte stands : mechanical characteristics of stems of *Phragmites australis* and *Scirpus lacustris*. Aquat Bot 53:175–185.

Corenblit D, Baas A, Balke T, Bouma T, Fromard F, Garófano-Gómez V, González E, Gurnell AM, Hortobágyi B, Julien F, Kim D, Lambs L, Stallins JA, Steiger J, Tabacchi E, Walcker R (2015) Engineer pioneer plants respond to and affect geomorphic constraints similarly along water-terrestrial interfaces world-wide. Glob Ecol Biogeogr:n/a-n/a.

Crosby SC, Sax DF, Palmer ME, Booth HS, Deegan LA, Bertness MD, Leslie HM (2016) Salt marsh persistence is threatened by predicted sea-level rise. Estuar Coast Shelf Sci 181:93–99.

Davidson NC (2014) How much wetland has the world lost? Long-term and recent trends in global wetland area. Mar Freshw Res 65:934–941.

Demes KW, Pruitt JN, Harley CDG, Carrington E (2013) Survival of the weakest : increased frond mechanical strength in a wave-swept kelp inhibits self-pruning and increases whole-plant mortality. Funct Ecol 27:439–445.

Duarte CM (2009) Introduction: Global Loss of Coastal Habitats Rates, Causes and Consequences. In: *Global Loss of Coastal Habitats Rates, Causes and Consequences.* p 14–24

Engels JG, Rink F, Jensen K (2011) Stress tolerance and biotic interactions determine plant zonation patterns in estuarine marshes during seedling emergence and early establishment. J Ecol 99:277–287.

Engloner AI (2009) Structure, growth dynamics and biomass of reed (Phragmites australis) - A review. Flora Morphol Distrib Funct Ecol Plants 204:331–346.

Farina JM, Silliman BR, Bertness MD (2009) Can conservation biologists rely on established community structure rules to manage novel systems? ... Not in salt marshes. Ecol Appl 19:413–422.

Garssen AG, Baattrup-Pedersen A, Voesenek LACJ, Verhoeven JTA, Soons MB (2015) Riparian plant community responses to increased flooding a meta-analysis. Glob Chang Biol 21:2881–2890.

Garzon JL, Maza M, Ferreira CM, Lara JL, Losada IJ (2019) Wave Attenuation by Spartina Saltmarshes in the Chesapeake Bay Under Storm Surge Conditions. J Geophys Res Ocean 124:5220–5243.

Gaylord BP, Denny MW, Koehl MAR (2003) Modulation of wave forces on kelp canopies by alongshore currents. Limnol Oceanogr 48:860–871.

Gourgue O, van Belzen J, Schwarz C, Bouma TJ, van de Koppel J, Temmerman S (2021) A Convolution Method to Assess Subgrid-Scale Interactions Between Flow and Patchy Vegetation in Biogeomorphic Models. J Adv Model Earth Syst 13:1–25.

Hallegatte S, Green C, Nicholls RJ, Corfee-Morlot J (2013) Future flood losses in major coastal cities. Nat Clim Chang 3:802–806.

Hellings SE, Gallagher JL, Hellings SE, Gallagher JL (1992) The effects of salinity and flooding on *Phragmites australis*. J Appl Ecol 29:41–49.

Heuner M, Schröder B, Schröder U, Kleinschmit B (2018) Contrasting elevational responses of regularly flooded marsh plants in navigable estuaries. Ecohydrol Hydrobiol 19:38–53.

Heuner M, Silinski A, Schoelynck J, Bouma TJ, Puijalon S, Troch P, Fuchs E, Schröder B, Schröder U, Meire P, Temmerman S (2015) Ecosystem Engineering by Plants on Wave-Exposed Intertidal Flats Is Governed by Relationships between Effect and Response Traits. PLoS One 10:e0138086.

Hu Z, van Belzen J, van der Wal D, Balke T, Wang ZB, Stive M, Bouma TJ (2015) Windows of opportunity for salt marsh vegetation establishment on bare tidal flats: The importance of temporal and spatial variability in hydrodynamic forcing. J Geophys Res Biogeosciences 120.

Jafari NH, Harris BD, Cadigan JA, Day JW, Sasser CE, Kemp GP, Wigand C, Freeman A, Sharp LA, Pahl J, Shaffer GP, Holm GO, Lane RR (2019) Wetland shear strength with emphasis on the impact of nutrients, sediments, and sea level rise. Estuar Coast Shelf Sci 229.

Janousek CN, Mayo C (2013) Plant responses to increased inundation and salt exposure: interactive effects on tidal marsh productivity. Plant Ecol 214:917–928.

Van de Koppel J, Van der Wal D, Bakker JP, Herman PMJ (2005) Self-Organization and Vegetation Collapse in Salt Marsh Ecosystems. Am Nat 165:1–12.

Lemoine DG, Mermillod-blondin F, Barrat-Segretain M-H, Masse C, Malet E (2012) The ability of aquatic macrophytes to increase root porosity and radial oxygen loss determines their resistance to sediment anoxia. Aquat Ecol 46:191–200.

Li X, Ren L, Liu Y, Craft C, Mander Ü, Yang S (2013) The impact of the change in vegetation structure on the ecological functions of salt marshes: the example of the Yangtze estuary. Reg Environ Chang 14:623–632.

Lo VB, Bouma TJ, van Belzen J, Van Colen C, Airoldi L (2017) Interactive effects of vegetation and sediment properties on erosion of salt marshes in the Northern Adriatic Sea. Mar Environ Res 131:32–42.

van Loon-Steensma JM, Hu Z, Slim AP (2016) Modelled Impact of Vegetation Heterogeneity and Salt-Marsh Zonation on Wave Damping. J Coast Res 32:241–252.

van Loon-Steensma JM, Schelfhout HA (2017) Wide Green Dikes: A sustainable adaptation option with benefits for both nature and landscape values? Land use policy 63:528–538.

Maricle BR, Lee RW (2002) Aerenchyma development and oxygen transport in the

estuarine cordgrasses Spartina alterniflora and S. anglica. Aquat Bot 74:109–120.

Marijnissen R, Esselink P, Kok M, Kroeze C, van Loon-Steensma JM (2020) How natural processes contribute to flood protection - A sustainable adaptation scheme for a wide green dike. Sci Total Environ 739:139698.

Mariotti G, Fagherazzi S (2010) A numerical model for the coupled long-term evolution of salt marshes and tidal flats. J Geophys Res 115:F01004.

Möller I, Kudella M, Rupprecht F, Spencer T, Paul M, van Wesenbeeck BK, Wolters G, Jensen K, Bouma TJ, Miranda-Lange M, Schimmels S (2014) Wave attenuation over coastal salt marshes under storm surge conditions. Nat Geosci 7:727–731.

Nafie YA La, Santos CBDL, Brun FG, Katwijk MM Van (2012) Waves and high nutrient loads jointly decrease survival and separately affect morphological and biomechanical properties in the seagrass Zostera noltii. 57:1664–1672.

van der Nat A, Vellinga P, Leemans R, van Slobbe E (2016) Ranking coastal flood protection designs from engineered to nature-based. Ecol Eng 87:80–90.

Nolte S, Koppenaal EC, Esselink P, Dijkema KS, Schuerch M, De Groot A V., Bakker JP, Temmerman S (2013) Measuring sedimentation in tidal marshes: A review on methods and their applicability

in biogeomorphological studies. J Coast Conserv 17:301–325.

Ott JP, Klimešová J, Hartnett DC (2019) The ecology and significance of below-ground bud banks in plants. Ann Bot 123:1099–1118.

Pagès JF, Jenkins SR, Bouma TJ, Sharps E, Skov MW (2019) Opposing Indirect Effects of Domestic Herbivores on Saltmarsh Erosion. Ecosystems 22:1055–1068.

Paul M, Amos CL (2011) Spatial and seasonal variation in wave attenuation over Zostera noltii. J Geophys Res Ocean 116:1–16.

Paul M, Rupprecht F, Möller I, Bouma TJ, Spencer T, Kudella M, Wolters G, van Wesenbeeck BK, Jensen K, Miranda-Lange M, Schimmels S (2016) Plant stiffness and biomass as drivers for drag forces under extreme wave loading: A flume study on mimics. Coast Eng 117:70–78.

Pennings SC, Callaway RM (1992) Salt marsh plant zonation: the relative importance of competition and physical factors. Ecol Soc Am 73:681–690.

Pennings SC, Grant M, Bertness MD (2005) Plant zonation in low-latitude salt marshes : disentangling the roles of flooding , salinity and competition. J Coast Res 93:159–167.

Peralta G, Brun FG, Pérez-Lloréns JL, Bouma TJ (2006) Direct effects of current velocity on the growth, morphometry and architecture of seagrasses: A

case study on *Zostera noltii*. Mar Ecol Prog Ser 327:135–142.

Popoff N, Jaunatre R, Le Bouteiller C, Paillet Y, Favier G, Buisson M, Meyer C, Dedonder E, Evette A (2021) Optimization of restoration techniques: In-situ transplantation experiment of an endangered clonal plant species (Typha minima Hoppe). Ecol Eng 160.

Puijalon S, Bouma TJ, Douady CJ, van Groenendael J, Anten NPR, Martel E, Bornette G (2011) Plant resistance to mechanical stress: evidence of an avoidance-tolerance trade-off. New Phytol 191:1141–9.

Puijalon S, Bouma TJ, Van Groenendael J, Bornette G (2008) Clonal plasticity of aquatic plant species submitted to mechanical stress: Escape versus resistance strategy. Ann Bot 102:989–996.

R Core Team (2020) R: A language and environment for statistical computing.

Rasser MK, Fowler NL, Dunton KH (2013) Elevation and plant community distribution in a microtidal salt marsh of the western Gulf of Mexico. Wetlands 33:575–583.

Renzi JJ, He Q, Silliman BR (2019) Harnessing positive species interactions to enhance coastal wetland restoration. Front Ecol Evol 7:1–14.

Rolletschek H, Rolletschek A, Hartzendorf T, Kohl J (2000) Physiological consequences of mowing and burning of *Phragmites australis* stands for rhizome ventilation and amino acid metabolism. Wetl Ecol Manag 8:425–433.

Rupprecht F, Möller I, Paul M, Kudella M, Spencer T, van Wesenbeeck BK, Wolters G, Jensen K, Bouma TJ, Miranda-Lange M, Schimmels S (2017) Vegetation-wave interactions in salt marshes under storm surge conditions. Ecol Eng 100:301–315.

Schoelynck J, Puijalon S, Meire P, Struyf E (2015) Thigmomorphogenetic responses of an aquatic macrophyte to hydrodynamic stress. Front Plant Sci 6:1–7.

Schoonees T, Gijón Mancheño A, Scheres B, Bouma TJ, Silva R, Schlurmann T, Schüttrumpf H (2019) Hard Structures for Coastal Protection, Towards Greener Designs. Estuaries and Coasts 42:1709–1729.

Schoutens K, Heuner M, Fuchs E, Minden V, Schulte Ostermann T, Belliard JP, Bouma TJ, Temmerman S (2020) Nature-based shoreline protection by tidal marsh plants depends on trade-offs between avoidance and attenuation of hydrodynamic forces. Estuar Coast Shelf Sci 236:11.

Schoutens K, Heuner M, Minden V, Schulte Ostermann T, Silinski A, Belliard J-P, Temmerman S (2019) How effective are tidal marshes as nature-based shoreline protection throughout seasons? Limnol Oceanogr 64:1750–1762.

Schoutens K, Reents S, Nolte S, Evans B, Paul M, Kudella M, Bouma T, Möller I, Temmerman S (2021) Survival of the thickest?

Impacts of extreme wave-forcing on marsh seedlings are mediated by species morphology. Limnol Oceanogr:1–16.

Schulte Ostermann T, Heuner M, Fuchs E, Temmerman S, Schoutens K, Bouma TJ, Minden V (2021a) Unraveling plant strategies in tidal marshes by investigating plant traits and environmental conditions. J Veg Sci:1–17.

Schulte Ostermann T, Kleyer M, Heuner M, Fuchs E, Temmerman S, Schoutens K, Bouma TJ, Minden V (2021b) Hydrodynamics affect plant traits in estuarine ecotones with impact on carbon sequestration potentials. Estuar Coast Shelf Sci 259:107464.

Schulze D, Rupprecht F, Nolte S, Jensen K (2019) Seasonal and spatial within - marsh differences of biophysical plant properties : implications for wave attenuation capacity of salt marshes. Aquat Sci 81:1–11.

Schwarz C, Gourgue O, van Belzen J, Zhu Z, Bouma TJ, van de Koppel J, Ruessink G, Claude N, Temmerman S (2018) Self-organization of a biogeomorphic landscape controlled by plant life-history traits. Nat Geosci 11.

Shah DU, Reynolds TPS, Ramage MH (2017) The strength of plants: Theory and experimental methods to measure the mechanical properties of stems. J Exp Bot 68:4497–4516.

Shen N, Liu C, Yu H, Qu J (2020) Effects of resource heterogeneity and environmental disturbance on the growth performance and interspecific competition of

wetland clonal plants. Glob Ecol Conserv 22:e00914.

Shepard CC, Crain CM, Beck MW (2011) The protective role of coastal marshes: A systematic review and meta-analysis. PLoS One 6.

Silinski A, Fransen E, van Belzen J, Bouma TJTJ, Troch P, Meire P, Temmerman S, Fransen E, Bouma TJTJ, Troch P, Meire P, Temmerman S (2016a) Quantifying critical conditions for seaward expansion of tidal marshes: A transplantation experiment. Estuar Coast Shelf Sci 169:227–237.

Silinski A, Fransen E, Bouma TJ, Meire P, Temmerman S (2016b) Unravelling the controls of lateral expansion and elevation change of pioneer tidal marshes. Geomorphology 274:106–115.

Silinski A, Schoutens K, Puijalon S, Schoelynck J, Luyckx D, Troch P, Meire P, Temmerman S (2018) Coping with waves: Plasticity in tidal marsh plants as self-adapting coastal ecosystem engineers. Limnol Oceanogr 63:799–815.

Silvestri S, Defina A, Marani M (2005) Tidal regime, salinity and salt marsh plant zonation. Estuar Coast Shelf Sci 62:119–130.

Smith CS, Rudd ME, Gittman RK, Melvin EC, Patterson VS, Renzi JJ, Wellman EH, Silliman BR (2020) Coming to terms with living shorelines: A scoping review of novel restoration strategies for shoreline protection. Front Mar Sci 7:1–14.

Smolders S, Plancke Y, Ides S, Meire P, Temmerman S (2015) Role of

intertidal wetlands for tidal and storm tide attenuation along a confined estuary: A model study. Nat Hazards Earth Syst Sci 15:1659–1675.

Spencer T, Schuerch M, Nicholls RJ, Hinkel J, Lincke D, Vafeidis AT, Reef R, McFadden L, Brown S (2016) Global coastal wetland change under sea-level rise and related stresses: The DIVA Wetland Change Model. Glob Planet Change 139:15–30.

Stark J, Plancke Y, Ides S, Meire P, Temmerman S (2016) Coastal flood protection by a combined nature-based and engineering approach: Modeling the effects of marsh geometry and surrounding dikes. Estuar Coast Shelf Sci 175:34–45.

Suzuki T, Zijlema M, Burger B, Meijer MC, Narayan S (2012) Wave dissipation by vegetation with layer schematization in SWAN. Coast Eng 59:64–71.

Taylor BW, Paterson DM, Baxter JM (2019) Sediment dynamics of natural and restored Bolboschoenus maritimus saltmarsh. Front Ecol Evol 7:1–10.

Temmerman S, Meire P, Bouma TJ, Herman PMJ, Ysebaert T, De Vriend HJ (2013) Ecosystem-based coastal defence in the face of global change. Nature 504:79–83.

Temple NA, Sparks EL, Webb BM, Cebrian J, Virden MF, Lucore AE, Moss HB (2021) Responses of two fringing salt marsh plant species along a wave climate gradient. Mar Ecol Prog Ser 675:53–66.

Tessler ZD, Vörösmarty CJ, Grossberg M, Gladkova I, Aizenman H, Syvitski JPM, Foufoula-Georgiou E (2015) Profiling risk and sustainability in coastal deltas of the world. Science (80-) 349:638–643.

Thomsen D, Marsden ID, Sparrow AD (2005) A field experiment to assess the transplant success of salt marsh plants into tidal wetlands. Wetl Ecol Manag 13:489–497.

Torio DD, Chmura GL (2013) Assessing coastal squeeze of tidal wetlands. J Coast Res 29:1049–1061.

Valiela I, Lloret J, Bowyer T, Miner S, Remsen D, Elmstrom E, Cogswell C, Robert Thieler E (2018) Transient coastal landscapes: Rising sea level threatens salt marshes. Sci Total Environ 640–641:1148–1156.

Veldhuis ER, Schrama M, Staal M, Elzenga JTM (2019) Plant stress-tolerance traits predict salt marsh vegetation patterning. Front Mar Sci 5:1–11.

Vuik V, Jonkman SN, Borsje BW, Suzuki T (2016) Nature-based flood protection: The efficiency of vegetated foreshores for reducing wave loads on coastal dikes. Coast Eng 116:42–56.

Wang CH, Lu M, Yang B, Yang Q, Zhang XD, Hara T, Li B (2010) Effects of environmental gradients on the performances of four dominant plants in a Chinese saltmarsh: Implications for plant zonation. Ecol Res 25:347–358.

van Wijnen HJ, Bakker JP (2001) Long-term Surface Elevation Change in Salt Marshes: a Prediction of Marsh Response to Future Sea-Level Rise. Estuar Coast Shelf Sci 52:381–390.

Willemsen PWJM, Borsje BW, Vuik V, Bouma TJ, Suzanne JM, Hulscher H (2020) Field-based decadal wave attenuating capacity of combined tidal flats and salt marshes. Coast Eng 156.

Xue L, Li X, Shi B, Yang B, Lin S, Yuan Y, Ma Y, Peng Z (2021) Pattern-regulated wave attenuation by salt marshes in the Yangtze Estuary, China. Ocean Coast Manag 209:105686.

Zhang X, Nepf H (2021) Wave-induced reconfiguration of and drag on marsh plants. J Fluids Struct 100:103192.

Zhu Z, Vuik V, Visser PJ, Soens T, van Wesenbeeck B, van de Koppel J, Jonkman SN, Temmerman S, Bouma TJ (2020a) Historic storms and the hidden value of coastal wetlands for nature-based flood defence. Nat Sustain.

Zhu Z, Yang Z, Bouma TJ (2020b) Biomechanical properties of marsh vegetation in space and time: effects of salinity, inundation and seasonality. Ann Bot.

6

Stability of a tidal marsh under high flow velocities and implications for nature-based flood defense

Ken Schoutens, Marte Stoorvogel, Mario van den Berg, Kim van den Hoven, Tjeerd J. Bouma, Stefan Aarninkhof, Peter Herman, Jantsje M. van loon-Steensma, Patrick Meire, Jonas Schoelynck, Patrik Peeters, Stijn Temmerman

6.1 Abstract

Nature-based strategies, such as wave attenuation by tidal marshes, are increasingly proposed as a complement to mitigate the risks of failure of engineered flood defense structures such as levees. However, recent analysis of historic coastal storms revealed smaller dike breach dimensions if there were natural, high tidal marshes in front of the dikes. Since tidal marshes naturally only experience weak flow velocities ($\sim$0-0.3 m.s^{-1} during normal spring tides), we lack direct observations on the stability of tidal marsh sediments and vegetation under extreme flow velocities (order of several m.s^{-1}) as may occur when a dike behind a marsh breaches.

As a first approximation, the stability of a tidal marsh sediment bed and winter-state vegetation under high flow velocities were tested in a flume. Marsh monoliths were excavated from *Phragmites australis* marshes in front of a dike along the Scheldt estuary (Dutch-Belgian border area) and installed in a 10 m long flume test section. Both sediment bed and vegetation responses were quantified over 6 experimental runs under high flow velocities up to 1.75 m.s^{-1} and water depth up to 0.35 m for 2 hours. These tests showed that even after a cumulative 12 hours exposure to high flow velocities, erosion was limited to as little as a few millimeters. Manual removal of the aboveground vegetation did not enhance the erosion either. Present findings may be related to the strongly consolidated, clay- and silt-rich sediment and *P. australis* root system in this experiment. During the flow exposure, the *P. australis* stems were strongly bent by the water flow, but the majority of all shoots recovered rapidly when the flow had stopped. Although present results may not be blindly extrapolated to all other marsh types, they do provide a strong first indication that marshes can remain stable under high flow conditions, and confirm the potential of well-developed tidal marshes as a valuable extra natural barrier reducing flood discharges towards the hinterland, following a dike breach. These outcomes promote the consideration to implement tidal marshes as part of the overall flood defense and to rethink dike strengthening in the future.

6.2 Introduction

Low-lying coastal and estuarine areas are increasingly exposed to flood risks as a result of climate change induced sea level rise, increasing storminess, associated storm surges, and land subsidence (Hallegatte et al., 2013; Nicholls et al., 2021; Tessler et al., 2015). Potential impacts in case of floods increase as coastal populations continue to expand (Neumann et al., 2015; Paprotny et al., 2018). This all results in a growing need for climate-resilient flood risk mitigation strategies (Hinkel et al., 2014; McEvoy et al., 2021; Morris et al., 2020). In addition to engineered flood defense structures, such as dikes, the conservation or creation of natural habitats such as tidal marshes and mangroves in front of flood defense structures, can provide additional nature-based flood risk mitigation, by reducing storm impacts on engineered structures (Vuik et al., 2018, 2016; Zhu et al., 2020a), while at the same time providing ecological benefits such as increased biodiversity, water purification and carbon sequestration (Cheong et al., 2013; Schoonees et al., 2019; Smith et al., 2020; Temmerman et al., 2013; Teuchies et al., 2013). However, uncertainty remains about the functionality of natural habitats as buffers against flood risks under extreme storm conditions.

Relying only on earthen dikes or levees as flood defense structures is risky, as past storm events have shown that dikes can fail and may breach, with dramatic consequences for the communities living in the lowlands behind the dikes. For instance, dike breaching caused the death of more than 1800 people during the North Sea storm in 1953 in the Netherlands (Kabat et al., 2009), more than 1500 deaths due to Hurricane Katrina in 2005 in New Orleans, USA (Day et al., 2007), and displaced more than 100 000 people due to cyclone Aila in 2009 in Bangladesh (Auerbach et al., 2015). Dike breaches result from a structural failure of the dike, i.e., when hydrodynamic forces on the dike exceed the structural strength of the dike. During a storm surge, the hydrodynamic stress generated by high water levels, waves and tidal currents might reach this critical threshold, through mechanisms including dike overtopping by waves or flow, seepage (piping) through the dike, and dike erosion as a result (Danka and Zhang, 2015; Vorogushyn et al., 2010). In NW-Europe, dikes are often constructed of an inner core of non-cohesive sandy material, a top layer of cohesive sediment (i.e. clay or silt), and optionally/often a vegetated cover (Morris et al., 2009; van Loon-Steensma and Schelfhout, 2017). Once an initial disturbance of the top layer reaches the inner sandy core, this non-cohesive sediment will erode more easily, potentially leading to a rapidly expanding dike breach (Peeters et al., 2015; Stanczak and Oumeraci, 2012; Visser, 1998). In many embanked regions the land behind the dikes has a lower elevation compared to the sea or estuarine water level during a storm surge. Due to this elevation difference, a dike breach will result in strong flow velocities and deep flooding into the embanked areas.

In addition to improved response strategies like evacuation, the presence of natural tidal marsh habitats in front of dikes can play a role in mitigating the impacts of dike

breaching. Recent analysis of historical dike breach events during the North Sea flood in 1953 in the Netherlands (Zhu et al., 2020a), showed that dike breaches were more narrow and more shallow when tidal marshes were present in front of dikes compared to breaches without tidal marshes in front of them. These findings suggest that tidal marshes serve as an extra natural 'barrier' that restricts the flow discharge towards the dike breach, thereby limiting breach growth and resulting breach width and depth (Fig. 6.1). Calculations indicated that the reduced dike breach dimensions behind marshes decrease the flood discharge, and thereby the speed of flooding, the flood depth and hence the potential damage behind the breached dikes (Zhu et al., 2020a). As a result, evacuation procedures will be facilitated. As such, this study showed a new mechanism of nature-based flood risk mitigation by tidal marshes in front of dikes, in addition to the previously shown function of marshes for attenuation of storm waves, currents, surge levels and erosion (e.g. Möller et al. 2014; Spencer et al. 2015; Stark et al. 2015; Carus et al. 2016; chapter 2: Schoutens et al. 2019). Gaining in depth understanding of this new mechanism is highly valuable, as it may inspire novel nature-based flood designs and new integrated flood risk strategies (Zhu et al., 2020a).
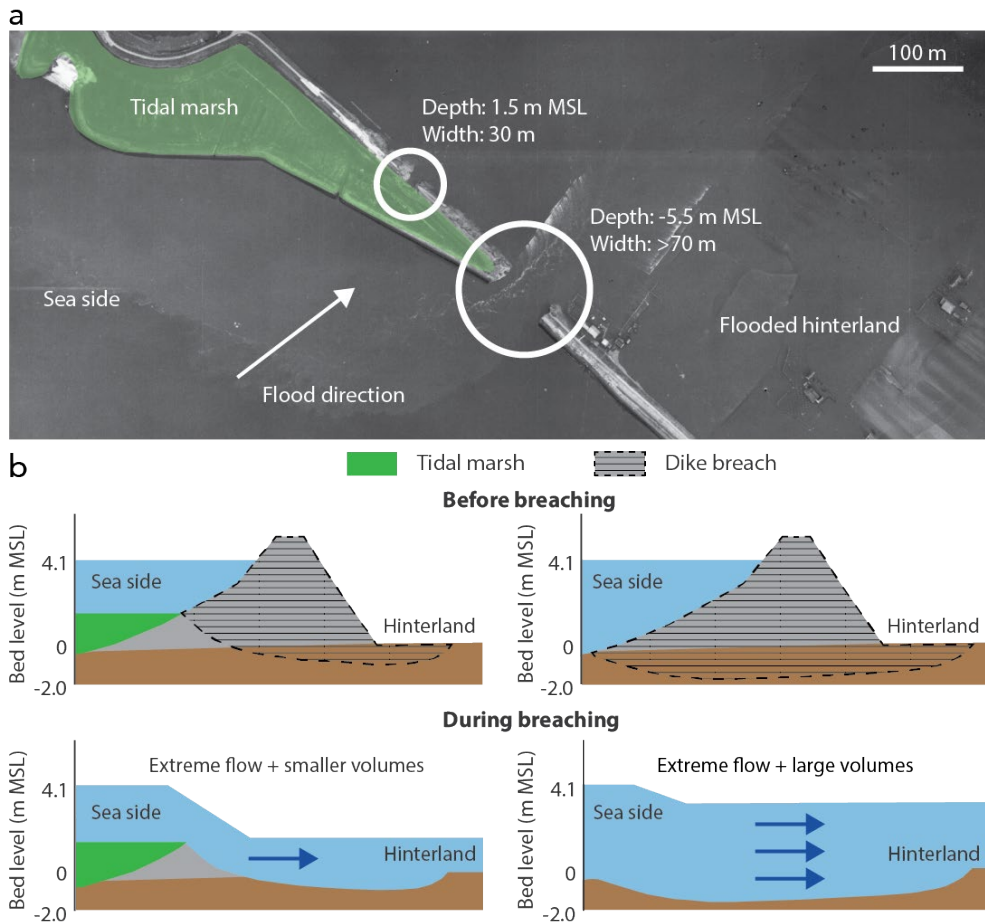
Figure 6.1: Hypothetical explanation of the protective function of tidal marshes in front of a dike breach. An aerial image of two neighboring dike breaches (white circles) at the former Haringvliet estuary (the Netherlands) during the North Sea flood in 1953 (a). Illustration of how flow velocities and water volume differ in case of a dike breach with tidal marsh (left) and without tidal marsh in front of the dike (right) (b). Credit: Figure adapted from Zhu et al. (2020a).

However, key questions remain, as there is a lack of direct observations so far on the stability of tidal marshes under the high flow velocities that may be expected over a marsh towards a dike breach (Fig. 6.1). In the exceptional case of a dike breach during storm surge conditions, flow velocities over a marsh towards a dike breach may reach up to several ms^{-1}. Direct measurements of such situations are lacking, but estimations for the extreme storm surge and dike breach conditions in 1953 in the Netherlands (Fig. 6.1) indicate that the storm surge level was up to 2.6 m above the marsh surface elevation, for which corresponding flow velocities (assuming critical flow conditions) may have reached almost 5 ms^{-1} in dike breaches (based on Zhu *et al.* 2020a). Flow velocities on a marsh right in front of a dike breach are expected to be lower, due to

spreading of the flow over a larger width and due to drag, but may still be in the order of several ms^{-1}. This is much more extreme than the normal tidal conditions under which marsh sediment beds and vegetation naturally develop ~0-0.3 ms^{-1} (Bouma et al., 2005a; chapter 3: Schoutens et al., 2020, 2019; Temmerman et al., 2012). Therefore, a crucial question is how stable a marsh can be under such high flow conditions, and hence whether it may serve as an extra natural barrier restricting the flow discharge towards the inundated land behind the dike breach (Fig. 6.1). Or in other words, can we rely on the additional strength provided by the tidal marsh to the overall flood defense in reducing the flood risk i.e., preventing or limiting the breach to grow in depth and width?

In general, marsh vegetation and the high intertidal elevation of marshes (i.e. reducing water depth) cause drag to the flow and reduce flow velocities (Carus et al., 2016; chapter 2: Schoutens et al., 2019) and wave heights (Möller et al., 2014; chapter 2: Schoutens et al., 2019; Silinski et al., 2016b). As a consequence of attenuating hydrodynamic forces from waves and currents, tidal marshes have the capacity to trap sediments and organic particles and as such build up elevation and strength (Brooks et al., 2021). Tidal marsh sediments typically have a high fraction of silt and clay particles in combination with a variety of small organic compounds, which increases the sediment cohesiveness (Grabowski et al., 2011; Winterwerp et al., 2012). Apart from the small-scale sediment composition, marsh sediments consist of a larger scale network of roots and rhizomes which forms an adhesive between sediments, sediment aggregates and organic compounds (Brooks et al., 2021; Chirol et al., 2021; Gyssels et al., 2005). Belowground plant structures in combination with the cohesive sediments reinforce the structural shear strength of the sediment bed (Bouma et al., 2014; Shepard et al., 2011). Previous flume experiments with simulated storm waves, have confirmed strong resistance of tidal marsh sediments to erosion (Möller et al., 2019, 2014; Spencer et al., 2016). Nevertheless, it is unknown how the tidal marsh vegetation and sediment bed will respond to the high flow conditions during a dike breach event. Moreover, storm surges in NW Europe are typically strongest in the winter season (Hansen et al., 2019; Masselink et al., 2016) when the aboveground plant shoots on tidal marshes die off, and their hydrodynamic attenuation capacity is reduced (chapter 2: Schoutens et al., 2019; Schulze et al., 2019). To understand the effect of high flow velocities on the stability of a tidal marsh with winter-state vegetation, measurements of marsh stability under such conditions are needed.

In this study, we performed flume experiments with tidal marsh monoliths (1.2 m long x 0.8 m wide x 0.4 m high) extracted from the field, exposing them to very high flow velocities in the flume facility to explore the stability of tidal marshes. We studied (1) the resilience of the vegetation in its winter state in combination with (2) the erosion resistance of the sediment. The results of this study will be discussed in light of a new aspect of the nature-based shoreline protection function of tidal marshes, i.e. whether

in case of a dike breach, tidal marshes could persist as an extra natural barrier, restricting the flow discharge towards the low land behind the breached dike, mitigate the impacts of a flood and reduce the flood risk.

6.3 Methods

6.3.1 Experimental setup and monolith extraction:

This flume experiment was conducted in the Mesodrome flume facility at the University of Antwerp (Belgium) (Fig. 6.2a). The flume consists of a 10 m long, 2.0 m wide and up to 1.5 m deep test section and has a maximum pump capacity of 0.6 m^3 s^{-1}. To generate very high flow velocities the width of the test section was reduced to 0.8 m. Within the test section, 8 monoliths were placed to create a marsh of 0.8 m wide and 9.6 m long (Fig. 6.2b).
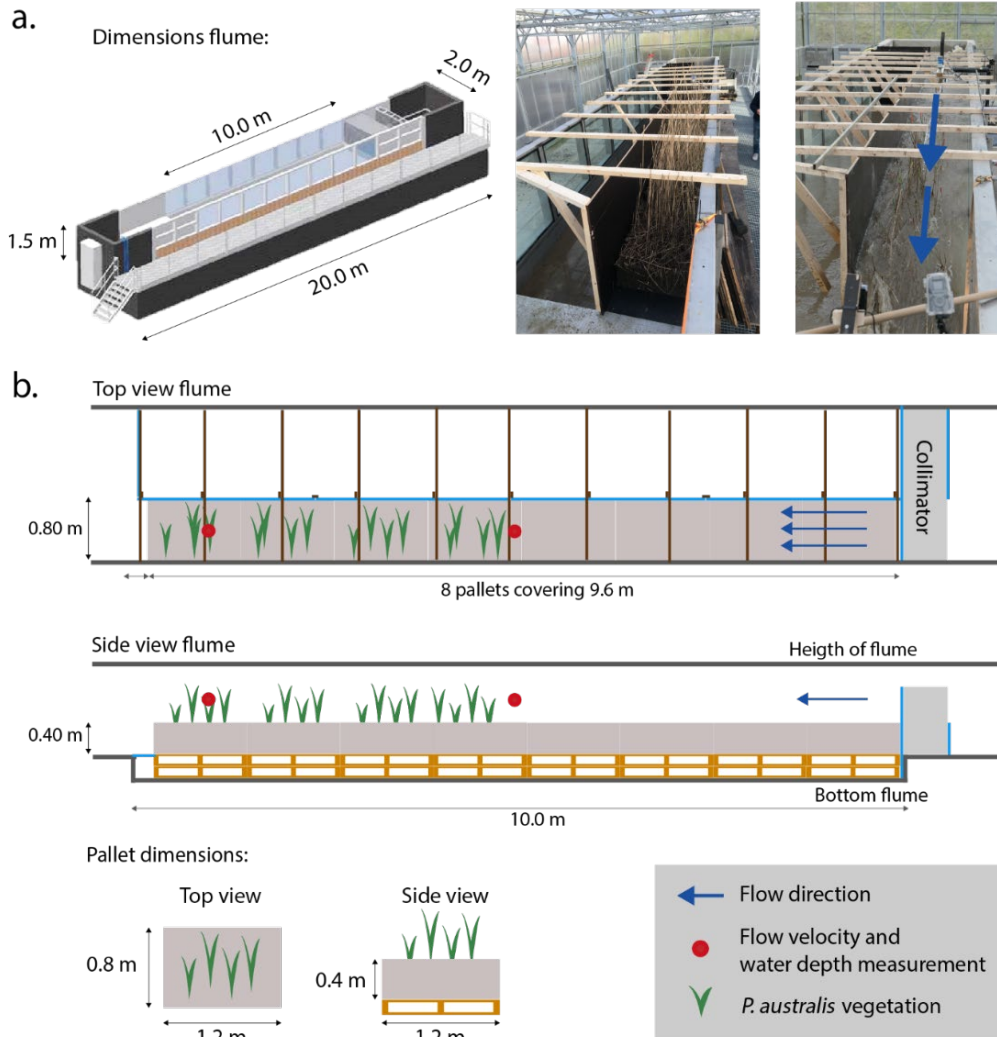
Figure 6.2: Overview of the flume dimensions and experimental setup (a). Schematic top view and side view of the experimental setup in the flume (b). The flow is generated by a pump that forces water through a collimator into the 0.80 m wide test section. Uniform flow was created by removal of the aboveground vegetation in the first meters of the test section.

The monoliths were excavated from tidal marshes in the Scheldt estuary (51.35 N, 4.23 E) as sediment blocks of 0.8 m by 1.2 m in surface area and 0.4 m depth, with vegetation growing on top. The monoliths were excavated on January 20 and 21, 2021, from brackish tidal marshes dominated by a mature *Phragmites australis* (Cav.) Trin. Ex Steud. vegetation which can grow up to 4 meter high (supplementary Fig. 6.1).

Extraction was done by digging a pit, as such creating a vertical cliff in the sediment; then pushing a metal plate horizontally into the cliff at a depth of 0.4 m under the horizontal sediment surface (supplementary Fig. 6.2a); next a rectangular mold of 0.8 by 1.2 m in surface area and 0.4 m high was placed on top of the sediment surface and pushed down gently until it made contact with the metal plate (supplementary Fig, 6.2b). The marsh monolith, contained within a "box" created by the plate and the mold, was lifted and placed on a pallet covered with a thin horizontal, perforated multiplex board (i.e. to support the sediment block, to prevent cracks and to allow a little bit of drainage during the flume experiments). The mold was removed and vertical multiplex boards were attached around the monolith for transport by a truck (supplementary Fig. 6.2c). After placing the monoliths in the flume with a crane, the protective vertical boards were removed from around the monoliths and they were positioned along the 10 m test section (supplementary Fig. 6.2d).

Aboveground biomass of the first 5.6 meters of the monoliths (at the leading edge of the test section) was removed to create a zone without vegetation for the incoming flow before that entered the zone with vegetation remaining along a length of 4 m at the end of the test section (Fig. 6.2b). The remaining shoots were cut at a height just below the wooden beams crossing the flume (Fig. 6.2a) to exclude interference of bending of the shoots with the beams. The beams were needed to keep the setup in place and withstand the hydrodynamic forces. As such the remaining vegetation stems were max. 1 m high. Small gaps in between the different monoliths and at the side edges were filled with sediment to ensure that the sediment bed was continuous across the flume test section. Before the monoliths were exposed to flow velocities, the flume was filled up with water to the sediment surface to let the sediment in the monoliths settle for two days. A first set of 8 monoliths was used as a pilot experiment to find out the desired settings (i.e. combination of water level and flume pump rate) to create maximum possible flow velocities with this flume setup. Next, the second set of 8 monoliths was installed in the flume to have undisturbed monoliths before starting the measurements of tidal marsh stability.

6.3.2 Hydrodynamic flow conditions

The experiments were conducted as six separate runs of 2 hours. Flow velocity and water depths remained constant during each run, but progressively increased from 1.00 to 1.75 ms^{-1} and from 0.15 to 0.35 m with each new run (table 6.1). Flow conditions were defined by the Reynolds number (Re):

$$Re = \frac{(v_{in}.R)}{v}$$

with v_{in} as depth averaged flow velocity (ms^{-1}), R as hydraulic radius which is defined as the cross-sectional area, A (i.e. for rectangular flumes: $A = w.d$ with w being the flume width which was 0.8 m), divided by the wet perimeter of the flow (i.e. for rectangular

flumes: $2d + w$) and v being the kinematic viscosity (10^{-6} m^{2}s^{-1} for water); and the Froude number (Fr):

$$Fr = \frac{v_{in}}{(g.D)^{0.5}}$$

with g as the gravitational acceleration (9.81 ms^{-2}) and D as the hydraulic depth which is defined as A/w, which in a rectangular flume is equal to the water depth, d.

The effect of aboveground vegetation cover on the sediment stability was tested by starting with two runs with the original vegetation cover present over 4 m of length of the test section (run 1 and 2), followed by consecutively manual removal (clipping) of 2 m of vegetation (run 3 and 4) and ending without vegetation cover (run 5 and 6). Flow velocities were measured every run with an electromagnetic flow meter (EMF, Valeport model 801, Totnes, UK) in the middle of the flume width and along a vertical depth gradient with an interval of 5 cm. The flow was measured 4.0 m and 0.8 m before the end of the test section (Fig. 6.2b). Flume-wall effects on the flow were regularly checked by expanding the measurement of flow velocities over a cross-sectional grid. At the same positions, water depth was measured to calculate the slope of the water surface.

6.3.3 Characterization of the monolith sediment composition

Site-specific sediment composition was quantified on six surficial sediment samples after removing the top layer of plant litter. Samples from the sediment bed were taken with a Kopecky ring (5.0 cm in diameter and 5.1 cm high and five replicates) and used to determine dry bulk density (after drying at 70°C for 72 h). Next, six mixed scrape samples of the top 2 cm were used to perform volumetric grain size analyses with a Mastersizer 2000 (Malvern) based on laser diffraction after a combined H_2O_2 and HCl treatment to remove organic compounds and disperse aggregates. Organic matter content was determined with the loss on ignition method, i.e., by ashing the samples for 4 hours at 550 °C in a muffle furnace (Heiri et al., 2001). Shear strength was estimated based on four replicates with a pocket shear vane tester (Eijkelkamp, NL) for the surface sediment and a field inspection shear vane tester (Eijkelkamp, NL) at 10 cm depth. Penetration resistance of the sediment was measured based on four replicates with a penetrologger (Eijkelkamp, NL) with a 1 cm depth interval, and an average of the upper 10 cm was calculated. All samples were taken in close approximation of the monolith extraction site, i.e. within 1-2 meters.

6.3.4 Characterization of the reed vegetation

The marsh was covered with a homogenous *P. australis* vegetation in winter-state, i.e. the aboveground biomass consisted of dead, leafless stems, and leaf litter was lying on the sediment bed in between the standing stems (supplementary Fig. 6.3). The reed vegetation was characterized in the field in the same week as the monolith extraction

(end of January 2021). Shoot densities were counted at three replicate 0.40 x 0.40 m square plots before all aboveground biomass was harvested and dried at 70°C for 72 h to quantify the aboveground biomass. Shoot lengths and basal shoot diameters were measured on 20 shoots, which were harvested to measure biomechanical properties, i.e. the flexural stiffness and Young's modulus. For the latter, the basal 20 cm of the shoots were used to perform three-point bending tests with a universal testing device (Instron 5942, precision ± 0.5%). For more details on the methods to quantify the biomechanical properties we refer to chapter 4: Schoutens et al. (2021). Belowground biomass was quantified from five replicate sediment cores of 0.10 m diameter sampled up to 0.40 m depth (i.e. the same depth as the monoliths), which were sampled at the location of monolith extraction. The cores were frozen and cut into slices (0-2.5 cm; 2.5-5.0 cm; 5.0-10 cm; 10-20 cm; 20-30 cm; 30-40 cm). For each segment, the sediment was washed out and the remaining belowground biomass was dried (at 70°C for 72 h) and weighed.

6.3.5 Vegetation response
Within the vegetated test section, 20 shoots were monitored during the first two runs (i.e. 4 meters of vegetation cover). In the third and fourth experimental run, 12 remaining shoots were monitored. In the fifth and sixth run, all vegetation was removed. The bending of the shoots in response to the high flow velocities was quantified in six categories indicating the shoot bending angle compared to the initial situation before the experimental runs. The categories ranged from shoots that did not suffer any damage or reconfiguration (< 5° bending angle) up to heavily bent shoots (> 35°) and broken shoots (i.e. flushed away or clearly broken shoots). The measurements were done at different moments in time, i.e. during the experimental run, directly after the run when the flow was stopped and after one (or three for run 4) day(s) of recovery.

6.3.6 Sediment bed response
Bed level changes (by erosion or sedimentation) were quantified by measuring the elevation of the sediment bed before and after every experimental run. Pin measurements (following a Sedimentation Erosion Bar, SEB, approach, see Nolte et al. (2013)) were performed along a grid over the 4 m long and 0.8 m wide vegetated part of the test section with a 5 cm interval in the direction parallel to the flume length and a 10 cm interval perpendicular to the flume length, revealing a total of 444 point measurements.

6.4 Results

6.4.1 Properties of the flow, sediment bed and vegetation

Tidal marsh monoliths were exposed to six consecutive runs of two hours each, with water depths ranging from 0.15 to 0.35 m and depth-averaged flow velocities ranging from approximately 1.00 to 1.75 ms^{-1} (table 6.1). Flow velocities increased and the water surface slope decreased from runs 1 and 2 (with vegetation over 4 m of the flume length) to runs 3 and 4 (vegetation partially removed and remaining present over 2 m) and runs 5 and 6 (without vegetation cover) (table 6.1). The combined effect of the flume side walls and the rearrangement of the plant shoots (in response to the flow) towards the center of the flume caused variations of flow velocities over the width of the flume with a standard deviation of 0.1 – 0.2 ms-1. Flow conditions during all runs were estimated to be sub-critical to nearly critical (estimated Froude numbers between 0.81-0.98) and highly turbulent (Reynolds numbers > 10^5) (table 6.1). The sediment was characterized by a high silt fraction (~72%; 2-63 µm) and clay fraction (~17%; < 2 µm), around 20 % of organic matter, and relatively high values of shear strength and penetration resistance (table 6.2a and 6.2b). *P. australis* vegetation in winter has a more modest aboveground biomass compared to the summer situation i.e., smaller, thinner and more flexible shoots (table 6.3). The majority of belowground biomass was found between 10 and 30 cm depth. At a depth below 30 cm, belowground biomass decreased (Fig. 6.3). The sediment bed is covered with a layer of litter (e.g. old leaves) under which a superficial network of fine roots can be found (Fig. 6.7 and supplementary Fig. 6.3).

Table 6.1: Overview of the six experimental runs with varying vegetation cover (m), water depth (*d*, cm), water surface slope (%), flow velocities (*v$_{in}$*, ms^{-1}), Reynolds (*Re*) and Froude (*Fr*) numbers within the vegetation test section.

	Vegetated section (m)	*d (cm)*	*Slope (%)*	*v$_{in}$ (ms^{-1})*	*Re ×10^5 (-)*	*Fr (-)*
run 1	4	15	3.3	1.00 ± 0.03	1.09	0.82
run 2	4	25	4.4	1.38 ± 0.04	2.12	0.88
run 3	2	25	3.1	1.41 ± 0.04	2.17	0.90
run 4	2	35	3.3	1.50 ± 0.03	2.80	0.81
run 5	0	25	2.7	1.54 ± 0.05	2.37	0.98
run 6	0	35	3.1	1.75 ± 0.04	3.27	0.94

Table 6.2: Overview of the sediment characteristics (a) at the extraction site presented as the mean, standard deviation (*SD*) and sample size (*N*). (b) Field studies with recording of shear vane shear strength measurements near the sediment surface in mature tidal marshes.

a.	Unit	Mean ± SD	N
d₅₀	μm	11.76 ± 0.61	6
clay	%	17.19 ± 1.34	6
silt	%	72.21 ± 2.28	6
sand	%	10.60 ± 2.46	6
Organic matter content (LOI)	%	20.03 ± 0.88	6
Dry bulk density	gcm^{-3}	0.64 ± 0.05	5
Shear vane shear strength at surface	kPa	13.01 ± 4.94	4
Shear vane shear strength at 10 cm depth	kPa	31.75 ± 5.94	4
Penetration resistance (top 10 cm)	kPa	190 ± 40	4

b.	Study	*Shear vane shear strength near surface* (kPa)
	Howes et al. 2010	5 – 25
	Gillen et al. 2021	16.6
	Crooks and Pye 2000	10.5 – 17.5
	Wilson et al. 2012	10 ± 7
	Ameen et al. 2017	5 – 20

Table 6.3: Aboveground and belowground properties of reed vegetation, i.e. shoot density, basal shoot diameter, shoot length, shoot mass, aboveground biomass (*AGB*), belowground biomass (*BGB*), flexural stiffness (*EI*) and Young's modulus (*E*) (left) at the monolith extraction sites presented as the mean, standard deviation (*SD*) and sample size (*N*) and (right) compared to peak biomass measurements in literature (*mean ± SD*). (*controlled wave flume experiment).

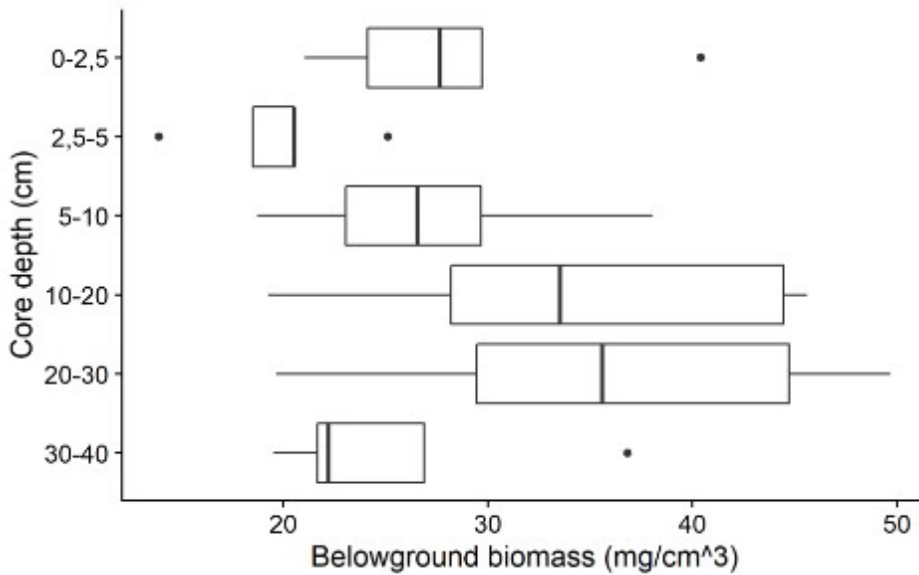|	Unit	Mean ± SD	N	Coops et al. 1996*	Schulte Ostermann et al. 2021	Zhu et al. 2020
Shoot density	Shoots m^{-2}	258 ± 28	3	136 ± 13		309 ± 103
Shoot diameter	mm	4.6 ± 0.8	20	6.8 ± 0.3	5.3 ± 1.2	5.5 ± 0.6
Shoot length	cm	204 ± 52	20	232 ± 17	241 ± 32	236 ± 62
Shoot mass	g shoot^{-1}	4.7 ± 1.3	3	12.2 ± 2.1		
AGB	g m^{-2}	1207 ± 346	3			
BGB	mg cm^{-3}	30 ± 9	5			
EI	Nm^2	0.19 ± 0.15	20	0.55 ± 0.16	0.51 ± 0.41	0.46 ± 0.21
E	10^9 Nm^{-2}	6.7 ± 4.3	20	6.9 ± 1.6		9.4 ± 3.8

Figure 6.3: Belowground biomass up to 40 cm depth represented as boxplots with outliers shown as black dots.

6.4.2 Response of the reed vegetation to high flow velocities

Vegetation of *P. australis* in its winter state was able to cope with short-term very high flow velocities. The response of the reed vegetation and the sediment bed dynamics after an experimental run were the cumulative result of all previous experimental runs. During the two hour runs, the shoots were bent heavily in the direction of the flow, but recovered rapidly after the flow was stopped (Fig. 6.4). Even after four consecutive runs, total damage remained limited as less than 17 % of the sampled shoots were broken and less than 17 % were bent more than 35°.
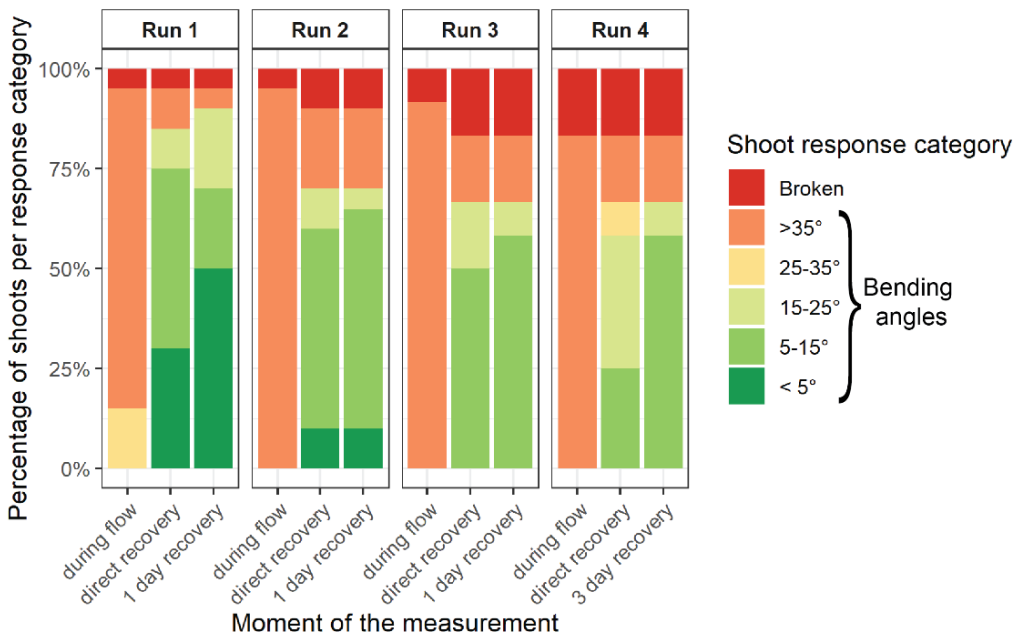

Figure 6.4: Percentage of the reed shoots (n = 20 for run 1 and 2; n = 12 for run 3 and 4) that show a response in terms of breaking and bending angle when exposed to high flow velocities. The response was quantified in six response categories (broken shoots, and 5 shoot bending angles) and was measured at three moments in time (during the flow, directly after the flow stopped, 1 day later after runs 1-3 and 3 days later after final run 4).

6.4.3 Stability of the sediment surface

Over the entire period of the six experimental runs (i.e., 12 hours cumulated exposure time), vertical erosion was limited to a median (± standard deviation) cumulative total erosion of 6.7 ± 2.4 mm only. Over individual runs (2 hours), the median erosion was maximum 2.5 ± 2.5 mm (for run 2) and less than 1.0 mm for all other runs. The first run removed part of the litter and organic debris that was initially covering the sediment surface (Fig. 6.5 and supplementary Fig. 6.3). In the sections where aboveground vegetation was removed, even more litter was removed in the run directly after removal (i.e. in the 4.0 – 2.0 m and 2.0 – 0.0 m distance from the end of the test section

in run 3 and run 5 respectively). The presence or absence of standing *P. australis* shoots had no effect on the bed elevation changes (e.g. ANOVA comparing the vegetated section with the non-vegetated section in run 4: $F_{1,387}$ = 0.171, p = 0.68) and no systematic spatial patterns were found throughout the six runs (Fig. 6.5). Although there is a general trend of slight erosion, at some locations sediment accretion was also observed (Fig. 6.5 and 6.6). Apart from the general trend of limited erosion, outliers of several centimeters of erosion and deposition were observed throughout the entire experiment, as a result of translocated sediment aggregates (Fig. 6.6). After the 5th and 6th run, i.e. respectively after 10 h and 12 h of cumulative high flow velocities, first signs of uprooting appeared and revealed a shallow subsurface mat of fine roots (Fig. 6.7).
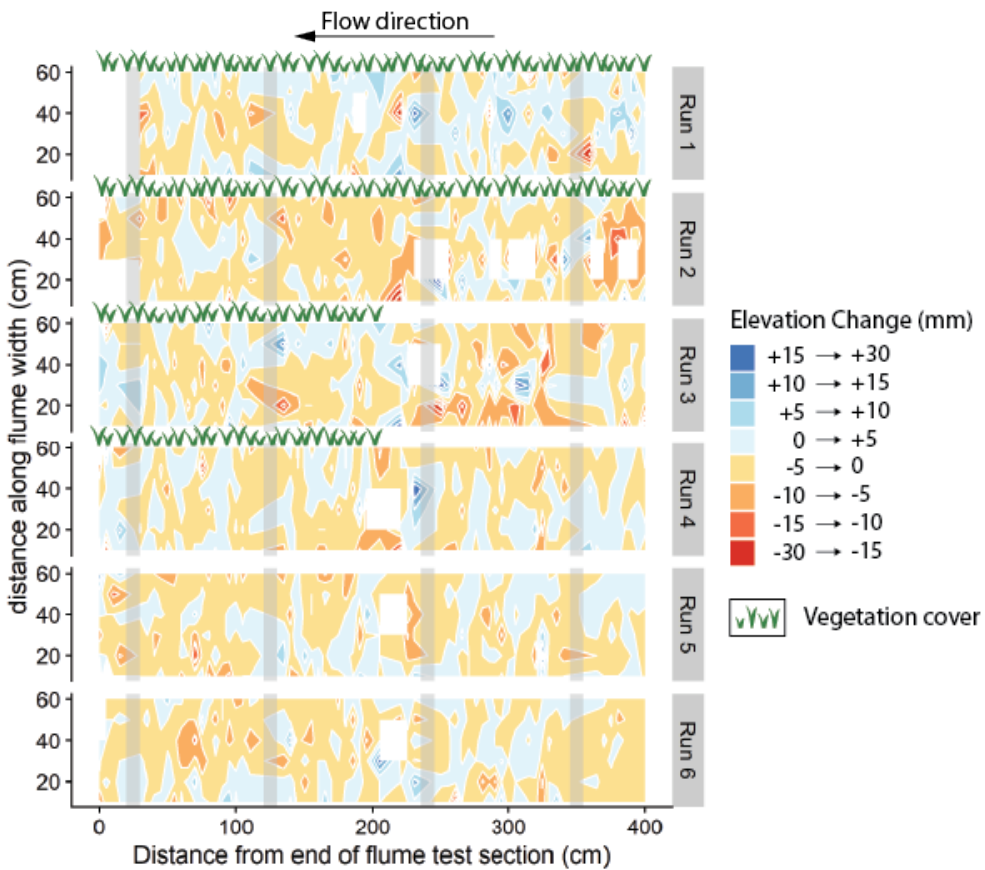

Figure 6.5: Top view of the flume showing the spatial interpolation of the elevation changes measured during the experimental runs (Run 1 - 6). The elevation changes were calculated as the differences in surface elevation before and after each experimental run. The contours are based on a raster of 444 pin measurements (see methods). White spaces represent missing data. Gray bars represent areas where the

space between the pins was 10 cm instead of 5 cm (because of obstruction of the wooden beams supporting the flume construction, see Fig. 6.2).
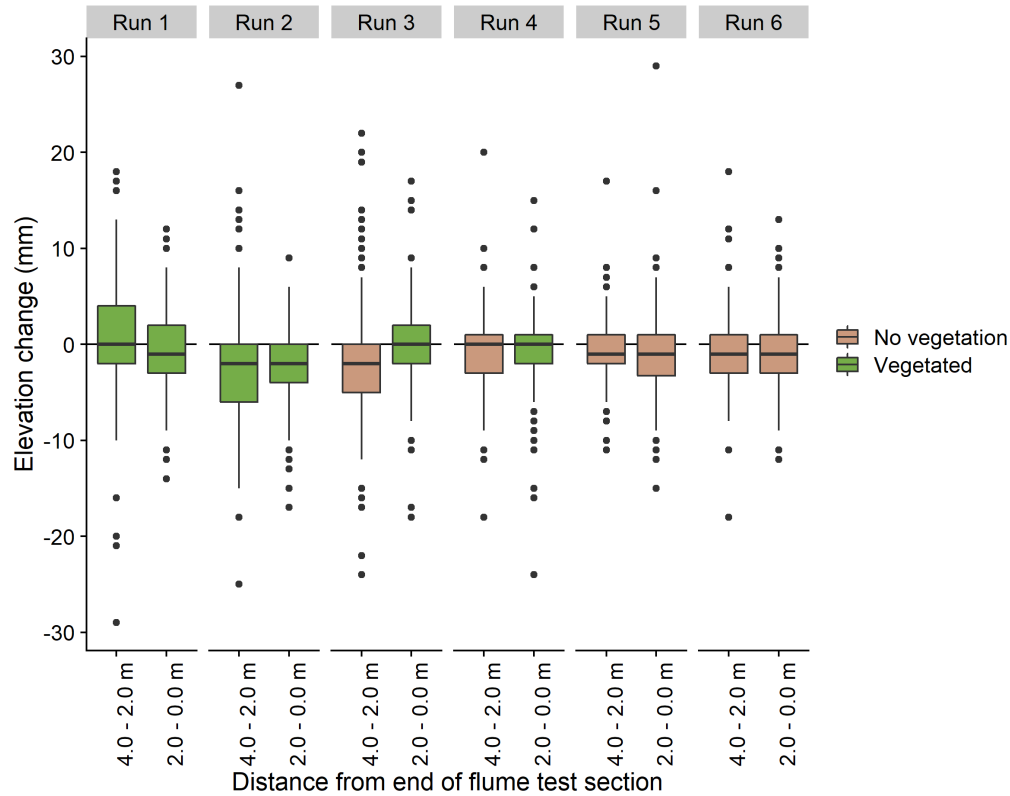
Figure 6.6: Boxplots summarizing the sediment bed elevation changes as a result of the different experimental runs with outliers represented as black dots. The data were split between the first two meters of the test section (having a vegetation cover in runs 1-2, and no vegetation in runs 3-6) and the back-end two meters (with vegetation in runs 1-4, no vegetation in runs 5-6). Presence or absence of vegetation is indicated by green or brown colors, respectively.

Figure 6.7: Sediment surface after the last experimental run with the emerging shallow subsurface mat of fine roots. Note that above-ground shoots have been manually clipped.

6.5 Discussion

In face of global climate change, nature-based shoreline and flood protection strategies are increasingly proposed as an adaptive measure to increase the climate-resilience of traditional, engineered flood protection structures. A recent analysis of historic dike breaches highlighted that tidal marshes, when present in front of dikes, can limit the breach-depth in a dike, and hence serve as an extra natural barrier limiting flooding in case of a dike breach (Zhu et al., 2020a). To gain more insights in the actual robustness of these nature-based solutions, we exposed for the first time extended marsh-lengths to very high flow conditions as are likely to happen when a dike breaches behind the marsh. Our flume tests revealed that both the marsh sediment and marsh vegetation show a high resistance against erosion by extended periods of very high flow velocities.

6.5.1 Stability of tidal marsh vegetation in winter condition

The results in this study suggest that the reduction of aboveground biomass in winter, reduces the experienced drag which then promotes the resistance of the vegetation against high flow velocities. We tested the winter state stability of *P. australis* vegetation, which is a typical dominant species in the high intertidal zone of brackish tidal marshes in NW European estuaries and in many other brackish and freshwater tidal estuaries worldwide (Srivastava et al., 2014). We found a high capacity of *P. australis* to withstand high flow velocities, as most of the aboveground stems (83%) did not break, of which 66.5 % had a less than 25° bending angle at the end of all flume runs

(Fig. 6.4). At first sight, this finding of high resistance of *P. australis* to high flow velocities may be contrasting with previous studies, showing that *P. australis* vegetation has a lower tolerance to strong hydrodynamic forces, in comparison to the pioneer marsh species that grow on lower intertidal elevations in the brackish parts of NW European estuaries (Asaeda et al., 2005; Coops et al., 1994). Yet, this apparent contradiction between our findings and previous studies may be explained by the following hypotheses. *Firstly*, these previous studies focused on the growth of *P. australis* under average hydrodynamic conditions during a whole growing season instead of short-term extremes in winter conditions. The extreme flow conditions generated on the tidal marsh platform close to a dike breach are expected to last for only a limited time period i.e. usually only one or two high tides that coincide with the storm surge event with a marsh inundation depth of several meters and inundation time of two to four hours per high tide (Smolders et al., 2020; Stark et al., 2015; Zhu et al., 2020a). Once the storm surge has passed, normal tidal conditions prevail again, with very shallow water depths (<0.3 m during high spring tides and even no flooding during neap tides) and weak flow velocities (<0.3 m.s^{-1}) typically found for the high intertidal marshes investigated here (Bouma et al., 2005a; Temmerman et al., 2012). Hence, the capacity of *P. australis* shoots to cope with high flow velocities is only required for a limited time period in the order of several hours, while previous studies assessed the growth response of *P. australis* to hydrodynamic conditions over a whole growing season (many months) (Asaeda et al., 2005; Coops et al., 1994). *Secondly*, *P. australis* drops its leaves in winter, which might further contribute to its higher capacity to withstand high flow velocities, as compared to the previous studies on *P. australis* in summer condition. The vulnerability of tidal marsh vegetation to experience stress from hydrodynamic forces is known to be dependent on plant traits that generate high drag forces on the shoots, i.e. plants with high biomass, tall shoots, and stiff stems experience higher drag forces under given hydrodynamic conditions (Bouma et al., 2005b; chapter 3: Schoutens et al., 2020). It should be mentioned that to fit the flume setup of this experiment, *P. australis* shoots were shortened, which could have promoted the resistance during the flow and the recovery process after the flow i.e., shorter shoots experience less drag force during the flow and less downward force during recovery. Nevertheless, compared to values reported in literature for typical *P. australis* summer vegetation, the vegetation from which monoliths were extracted for this experiment had a lower shoot biomass, and stems were thinner and smaller when monolith excavation took place at the start of the winter season in January 2021 (table 6.3). Moreover, compared to the stiff shoots reported for *P. australis* in summer (table 6.3), our results suggest that the remaining winter shoots have a higher flexibility. This might be because the stiffest shoots brake and get washed away and only the slightly more flexible shoots remain in winter, which is in line with studies that monitored shoot stiffness of *P. australis* over an entire season (Zhu et al., 2020b)).

P. australis winter vegetation in front of a dike can handle short-term high flow velocities, i.e. a cumulative 12 hours in this experiment, without losing much of the shoot biomass (<17 % of stems). This finding indicates that after a dike breach has been repaired, the marsh has a high chance to continue providing its shoreline protection function through vegetation-induced attenuation of waves, currents and erosion (Carus et al., 2016; Möller et al., 2014; chapter 2: Schoutens et al., 2019; Sheng et al., 2021; Spencer et al., 2015; Zhang et al., 2022). Furthermore, through survival of the marsh vegetation, the marsh can also sustain its capacity to accumulate suspended sediments that are supplied during regular tidal inundations (Silinski et al., 2016a; Temmerman et al., 2003) and as such, to build up elevation in balance with long-term sea level rise (Temmerman et al., 2004). Studies have demonstrated that tidal marshes in front of dikes, that grow vertically in balance with sea level rise, are very effective in sustaining their nature-based mitigation of waves, and reduction of wave loads on the dikes, under future scenarios of sea level rise (Vuik et al., 2019; Zhu et al., 2020a). Our findings indicate that dike breaching behind marshes, after breaches are repaired, will not compromise this long-term nature-based shoreline protection function of the marshes.

6.5.2 Marsh sediment stability under short-term high flow velocities

The sediment surface in this experiment was highly resistant against erosion by high flow velocities (Fig 6.5 and 6.6). Apart from some outliers, the elevation changes ranged predominantly between – 5 and + 5 mm. Here we note that this range of elevation change is not much more than the measurement accuracy of the SEB method (1.5 mm) (Nolte et al., 2013; van Wijnen and Bakker, 2001). Studies on the sediment stability of tidal marshes against vertical erosion under storm surge conditions confirm the highly stable nature of tidal marsh sediments, both found in flume studies mimicking storm conditions (Möller et al., 2014; Spencer et al., 2016) and field assessments after storms (Pennings et al., 2021). Nevertheless, there are also field studies reporting considerable erosion of marshes after very severe storms, such as in freshwater marshes on the Mississippi deltaic plain after the severe 2005 hurricane season (Howes et al., 2010). Moreover, the generated flow velocities in our study go beyond the flow conditions that may be expected on a marsh during a storm surge (Bennett et al., 2020). Nevertheless, the sediment bed remained stable which indicates that the shear strength of the sediment in our experiment was higher than the exerted shear stress (De Smit et al., 2021). In the subsequent paragraphs, we discuss one by one a total of four possible explanations for the observed extremely high erosion resistance of the sediment bed.

Firstly, sediment composition is known to be a key determinant for the susceptibility to erosion of sediment surfaces (De Battisti et al., 2019; Evans et al., 2021; Lo et al., 2017). Thus our finding of high sediment bed resistance to vertical erosion is likely to also be determined by case-specific sediment properties. The grain size distribution of the mineral sediment fraction plays a major role. Erosion resistance of marsh sediments is known to increase with decreasing grain size and associated increasing

cohesiveness (Christiansen et al., 2000; Feagin et al., 2009; Lo et al., 2017). Tidal marshes that are situated in front of a dike are often situated relatively high in the tidal frame, being sheltered from the incoming hydrodynamics at the shoreward marsh edge and experiencing relatively shallow flooding at high spring tides, allowing fine sediments to settle. This may explain the high proportions of small sediment fractions, i.e. silt and, to a lesser extent, clay, in the tidal marsh monoliths used in our experiment (table 6.2a). The high silt and clay content promotes sediment cohesion and is most likely the first reason why our sediment had such a high resistance against erosion.

Secondly, high elevated, mature marshes in front of a dike, like in our case, are typically characterized by strongly consolidated sediments (Tempest et al., 2015), which increases the erosion resistance of the sediment surface (Watts et al., 2003). This is in line with our penetration resistance measurements that were comparable with values found in NW European salt marshes ranging around 200 kPa in the upper sediment layers (e.g. Are et al. 2002; van de Vijsel et al. 2020). Dry bulk densities in this study indicate a soil texture that is favorable for root growth and water drainage (Bradley and Morris, 1990). Although bulk densities are often higher in deeper soil layers, i.e. more compacted, bulk densities in the top few centimeters in this study where in line with values measured in other, natural marshes along NW European marshes, ranging between 0.50 – 0.65 g.cm^{-3} (Crooks and Pye, 2000; Schulte Ostermann et al., 2021; Tempest et al., 2015; Watts et al., 2003).

Thirdly, organic matter content has a positive impact on the erosion resistance of minerogenic tidal marsh sediments and consists of small organic substances and larger belowground root biomass. Our measurements of Loss on Ignition combine these two components and revealed a relatively high fraction of organic matter in the sediments (20.03 ± 0.88 %), compared to values in literature ranging between 6-20 % for natural mature marshes (Crooks and Pye, 2000; Gillen et al., 2021; Tempest et al., 2015; Watts et al., 2003). In addition to clay particles, small organic substances increase the sediment cohesiveness by forming an adhesive between sediment particles, creating bigger sediment aggregates. Nevertheless, in marshes dominated by organic material (i.e. 80-90 % of the sediment fraction), the sediment properties will be different with a lower bulk density and less consolidation (Brooks et al., 2021) which reduces the sediment stability and increases potential erosion processes (Chambers et al., 2019; Himmelstein et al., 2021).

Fourthly, the presence of vegetation can increase the stability of the sediment by (i) reducing hydrodynamic forces due to friction between the aboveground shoots and the moving water and (ii) by providing structural rigidity for sediments and aggregates through the belowground root system (Cahoon et al., 2020; Vannoppen et al., 2015). The sediment surface stability under the short-term high flow velocities in this study was not affected by the presence or absence of aboveground biomass (Fig. 6.5 and 6.6).

Rapid removal of the dead organic litter and debris covering the sediment surface was observed after the first experimental runs. In natural marsh conditions, however, the larger scales (i.e., less boundary conditions and larger surface areas) might result in a redistribution of this organic matter rather than complete removal as observed in this flume experiment, hence providing a local shielding function for the sediment surface. Although logistical restrictions did not allow to install fresh, undisturbed monoliths for every single run, the elevation changes in run 2-6 might be more similar to the observations after run 1 in which there was a redistribution of organic matter rather than a removal. During the high flow velocities, *P. australis* shoots were completely bended over (Fig. 6.4), hence the friction with the water column was reduced. Although not directly tested, the high fraction of organic matter and the high portion of root biomass at the sediment surface might have had an important contribution to the sediment stability. That is, a high fraction of root biomass near the sediment surface (Fig. 6.3) might cause a decrease in bulk density by creating pores and voids between the sediment particles (Brain et al., 2012; Chen et al., 2012; Jafari et al., 2019). Root networks change the sediment characteristics both through the presence of dead and living roots which then function as a structural framework for the sediment aggregates, promote the formation of pores and enhance drainage capacity, hence increasing the erosion resistance of the sediment surface (Evans et al., 2021; Grabowski et al., 2011; Gyssels et al., 2005). Only in the two highest flow conditions (after 10-12 h of cumulative flow exposure), uprooting of fine roots covering the entire sediment surface was observed (Fig. 6.7). In addition, when roots get exposed at the sediment surface, they will cause local turbulence, which may result in scour features (Bouma et al., 2009; chapter 4: Schoutens et al., 2021). This might suggest that when high flow velocities would continue for a much longer period of time, the top layer of sediment may get damaged or removed, exposing the subsurface sediment layers with lower belowground biomass. When the dike breach is not repaired immediately, the breach dimensions could still enlarge over time (Symonds and Collins, 2004). Moreover, vertical variations in the shape of the roots, e.g. from dense fine roots in the upper sediment layers towards sparser thicker roots in deeper layers (Gillen et al., 2021) or reduced belowground biomass with increasing depth (Howes et al., 2010), can alter the shear strength too. Nevertheless, subsurface shear vane tests indicated highly stable sediments limiting the erosion risk (table 6.2a), even when the top layer of sediment including the dense root network is gone.

6.5.3 Suggestions for further research

Despite the fact that we simulated maximal, near to critical flow conditions in our flume experiment, with depth averaged flow velocities up to 1.75 m.s^{-1} (table 6.1), we recognize that the water depths in our experiment were, for practical reasons, limited to maximum 0.35 m. Under extreme storm surge conditions, when water depths on marshes can be as much as 1.5 to 2.5 m (e.g. Stark et al. 2015; Zhu et al. 2020a), it may

be well possible that maximum flow velocities over a marsh nearby a dike breach reach up to several m.s^{-1}. Therefore, the present flume experiment needs to be regarded as a first test, which reveals promising results on tidal marsh stability and motivates further testing under larger water depths and higher flow velocities.

Current findings are based on one specific tidal marsh characterized by fine, cohesive sediments with a high shear strength and a monospecific *P. australis* vegetation. Although we argue that there are marshes with similar characteristics, we recognize that many other types of vegetated marshes exist e.g., minerogenic and organogenic marshes. Although this study provides insights in the stability of tidal marshes under high flow velocities, further research would be needed to confirm our findings for a wider range of hydrodynamic conditions and variety of marsh types.

Further research should focus on increasing the water depth and the flow velocities to simulate more extreme storm surge conditions. Field experiments with in situ, controlled dike breaches could be an option, however they remain logistically challenging (Peeters et al., 2019, 2015; Wu et al., 2011). Furthermore, such controlled dike breach experiments are usually conducted during calm or moderate weather conditions and during normal tidal conditions, when water depths and flow velocities over marshes are small compared to extreme storm surge conditions. Finding suitable test locations with low elevated marshes in front of a dike is challenging, as the opportunities for in situ dike breach experiments are very limited. Lowering the marsh platform or lowering the dike could be an option to simulate the water depths and flow velocities expected during a dike breach. Experiments in large and deep flume facilities could be an alternative to control the water depth and flow velocity without taking into account the natural tidal cycling.

Apart from experiments with more extreme flow conditions, exploring the sediment stability of different types of vegetated marshes is advised. Several studies point towards the role of plant traits in stabilizing the sediment based on the structure of the root network (Gillen et al., 2021; Howes et al., 2010; Jafari et al., 2019). *In this study, P. australis* formed dense, shallow mats of roots which could benefit the sediment stability compared to species that only develop roots in the deeper sediment layers, suggesting that the type of roots and their structure might play an important role in the sediment stability (De Battisti et al., 2019; Feagin et al., 2009). Other studies emphasize the effect of sediment composition, such as the decreasing sediment stability in function of an increasing fraction of organic substances (Gillen et al., 2021) or an increasing fraction of coarser, sandy sediments (Evans et al., 2021; chapter 2: Schoutens et al., 2019). Moreover, climate induced environmental changes might alter the stability of tidal marshes, i.e. increased stress from inundation by sea level rise and increased hydrodynamic forces from storms could alter the sediment dynamics (Jiang et al., 2020; Schuerch et al., 2018) and the growth of tidal marsh vegetation (Kirwan and

Guntenspergen, 2012). Therefore, testing the sediment stability and stabilizing effect of different vegetation types in different environmental settings (e.g. climate) will contribute to the generality of our findings and could improve our understanding of how the stability of vegetated marshes under extreme flow velocities could change in the future. In the first place, we advise to test vegetated marshes which typically occur in front of dikes, such as salt marsh species (e.g. *Elymus sp.* or *Spartina sp.*), freshwater marsh species and tropical systems such as mangroves.

In the present study, we focus on local surface erosion processes in a mature, high elevated marsh adjacent to the dike. However, the response to extreme flow velocities might change over different spatial scales (Wang et al., 2017). The presence of more complex geomorphological features such as creeks and cliffs, could for instance initiate large scale erosion processes (Symonds and Collins, 2004). Also the age and history of the marsh should be considered, for example young, low-lying developing marshes are expected to have different, less stable sediment characteristics (Evans et al., 2021), which is especially the case when tidal marshes are (re)created, e.g. in managed realignment projects (Tempest et al., 2015; Van Putte et al., 2020). Implementations of nature-based shoreline protection by tidal marshes has increased over the past decades and will further increase in the future. Many projects involve new marsh development on low elevated, initially bare flats in front of the embankment, where sediment accretion might be relatively fast (Oosterlee et al., 2018; Vandenbruwaene et al., 2011), resulting in less consolidated sediments, low bulk densities, poor drainage and hence lower shear strengths (Van Putte et al., 2020; Watts et al., 2003). Experience from existing tidal marsh (re)creation projects suggest that it might take several years before marshes develop with sediments that have enough strength to withstand high shear stresses (Fearnley, 2008; Kadiri et al., 2011; Sha et al., 2018; Tempest et al., 2015) as can be expected on the marsh platform in front of a dike breach. In this respect, further research is needed on the rates of development of marsh sediment strength, as marshes develop from young pioneer marshes to older established marshes.

6.5.4 Implications for flood risk management

Our results indicate that conservation, restoration and creation of tidal marshes in front of engineered flood protection structures such as dikes, provides an extra natural 'barrier' that can remain stable under high flow velocities, and as such may reduce flood depths and damage in case of breaching of the engineered dike. Note that this extra barrier-function requires stable high marshes which need time to develop, but which have the capacity to adapt and develop with changing environmental conditions such as sea level rise. Hence, instead of constructing dikes directly adjacent to the mean low water level, thereby embanking and losing pre-existing tidal marshes and diminishing the chance of new seaward tidal marsh establishment, we stress the benefits of providing enough space for tidal marshes in front of dikes. In areas where coastal development by building of dikes is ongoing, such as in Tianjin (China), Jakarta

(Indonesia), or Port Harcourt (Nigeria) (Martín-Antón et al., 2016; Sengupta et al., 2018; Zhang et al., 2020), land reclamation often leads to degradation of many of the ecosystem functions and can bring extra costs that are often not accounted for in the reclamation project (Tan et al., 2020; Wang et al., 2010). Therefore, preserving part of the tidal marshes in front of newly constructed dikes is strongly advised.

In cases where no tidal marshes are present, the creation of suitable conditions for marsh development is recommended (Van Loon-steensma and Slim, 2013). At locations with enough space shoreward of the dikes (e.g. along shallow bays or lagoons), tidal marsh establishment can be facilitated by creating shallow, sheltered conditions by sediment nourishment and building (temporal) barriers to reduce hydrodynamics and capture sediments (Baptist et al., 2021; Dao et al., 2018; Hofstede, 2003; Hu et al., 2021; Vuik et al., 2019). Furthermore, active planting of marsh plants may eventually further enhance the chances of tidal marsh establishment (Tagliapietra et al., 2018).

At locations where space is limited shoreward of dikes (e.g. embanked estuaries with narrow shipping channels), it is worth to explore areas where there is space for more landward building of a new dike and breaching of the existing dike, so-called managed coastal realignment. Managed realignment creates a sheltered environment, suitable for tidal marsh development between the breached and the new dike. This managed realignment strategy has been implemented in several places over the last decades (Esteves and Williams, 2017; van den Hoven et al., 2022), for instance in Belgium where a total of 2500 ha of tidal marshes will be (re)created by 2030 (Temmerman et al., 2013). In places where managed realignment is not a desirable option, one could think about double-dike systems with transitional polders (i.e., see figure 7 in Zhu *et al.*, 2020). This implies that after a high marsh has established, the land can be converted back to its former (often agricultural) function, while still offering the benefits of an elevated foreshore. However, as stated before, it is important to account for the time needed to develop stable marsh sediments. This means that if we think nature-based solutions are a promising option to cope with sea-level rise, we must plan well in advance in order to initiate the development of new marshes as part of any kind of nature-based flood protection program.

6.6 Acknowledgements

6.7 References

Ameen, A.D., Kolker, A.S., Taylor, C.M., 2017. Vegetation and Shear Strength in a Delta-splay Mouth Bar. Wetlands 37, 1159–1168. https://doi.org/10.1007/s13157-017-0948-7

Are, D., Kemp, G.P., Giustina, F.D., Day, J.W., Scarton, F., 2002. A portable, electrically-driven Dutch cone penetrometer for geotechnical measurements in soft estuarine sediments. J. Coast. Res. 18, 372–378.

Asaeda, T., Fujino, T., Manatunge, J., 2005. Morphological adaptations of emergent plants to water flow: A case study with *Typha angustifolia*, *Zizania latifolia* and *Phragmites australis*. Freshw. Biol. 50, 1991–2001. https://doi.org/10.1111/j.1365-2427.2005.01445.x

Auerbach, L.W., Goodbred, S.L., Mondal, D.R., Wilson, C.A., Ahmed, K.R., Roy, K., Steckler, M.S., Small, C., Gilligan, J.M., Ackerly, B.A., 2015. Flood risk of natural and embanked landscapes on the Ganges-Brahmaputra tidal delta plain. Nat. Clim. Chang. 5, 153–157. https://doi.org/10.1038/nclimate2472

Baptist, M.J., Dankers, P., Cleveringa, J., Sittoni, L., Willemsen, P.W.J.M., Puijenbroek, M.E.B. Van, Vries, B.M.L. De, Leuven, J.R.F.W., Coumou, L., Kramer, H., Elschot, K., 2021. Salt marsh construction as a nature-based solution in an estuarine social-ecological system. Nature-Based Solut. 1, 100005. https://doi.org/10.1016/j.nbsj.2021.100005

Bennett, W.G., van Veelen, T.J., Fairchild, T.P., Griffin, J.N., Karunarathna, H., 2020. Computational modelling of the impacts of saltmarsh management interventions on hydrodynamics of a small macro-tidal estuary. J. Mar. Sci. Eng. 8. https://doi.org/10.3390/JMSE8050373

Bouma, T.J., De Vries, M.B., Low, E., Kusters, L., Herman, P.M.J., Tánczos, I.C., Temmerman, S., Hesselink, A., Meire, P., Regenmortel, S.V., 2005a. Flow hydrodynamics on a mudflat and in salt marsh vegetation: identifying general relationships for habitat characterisations. Hydrobiologia 540, 259–274. https://doi.org/10.1007/s10750-004-7149-0

Bouma, T.J., De Vries, M.B., Low, E., Peralta, G., Tánczos, I.C., van de Koppel, J., Herman, P.M.J., 2005b. Trade-offs related to ecosystem engineering: a case study on stiffness of emerging macrophytes. Ecology 86, 2187–2199. https://doi.org/10.1890/04-1588

Bouma, T.J., Friedrichs, M., Klaassen, P., van Wesenbeeck, B.K., Brun, F.G., Temmerman, S., Van Katwijk, M.M., Graf, G., Herman, P.M.J., 2009. Effects of shoot stiffness, shoot size and current velocity on scouring sediment from around seedlings and propagules. Mar. Ecol. Prog. Ser.

388, 293–297. https://doi.org/10.3354/meps 08130

Bouma, T.J., van Belzen, J., Balke, T., Zhu, Z., Airoldi, L., Blight, A.J., Davies, A.J., Galvan, C., Hawkins, S.J., Hoggart, S.P.G., Lara, J.L., Losada, I.J., Maza, M., Ondiviela, B., Skov, M.W., Strain, E.M., Thompson, R.C., Yang, S., Zanuttigh, B., Zhang, L., Herman, P.M.J., 2014. Identifying knowledge gaps hampering application of intertidal habitats in coastal protection: Opportunities & steps to take. Coast. Eng. 87, 147–157. https://doi.org/10.1016/j.coast aleng.2013.11.014

Bradley, P., Morris, J., 1990. Physical characteristics of salt marsh sediments: ecological implications. Mar. Ecol. Prog. Ser. 61, 245–252. https://doi.org/10.3354/meps 061245

Brain, M.J., Long, A.J., Woodroffe, S.A., Petley, D.N., Milledge, D.G., Parnell, A.C., 2012. Modelling the effects of sediment compaction on salt marsh reconstructions of recent sea-level rise. Earth Planet. Sci. Lett. 345–348, 180–193. https://doi.org/10.1016/j.epsl. 2012.06.045

Brooks, H., Möller, I., Carr, S., Chirol, C., Christie, E., Evans, B., Spencer, K.L., Spencer, T., 2021. Resistance of salt marsh substrates to near-instantaneous hydrodynamic forcing. Earth Surf. Process. Landforms 88, 67–88. https://doi.org/10.1002/esp.4 912

Cahoon, D.R., McKee, K.L., Morris, J.T., 2020. How Plants Influence Resilience of Salt Marsh and Mangrove Wetlands to Sea-Level Rise. Estuaries and Coasts. https://doi.org/10.1007/s1223 7-020-00834-w

Carus, J., Paul, M., Schröder, B., 2016. Vegetation as self-adaptive coastal protection: Reduction of current velocity and morphologic plasticity of a brackish marsh pioneer. Ecol. Evol. 6, 1579–1589. https://doi.org/10.1002/ece3. 1904

Chambers, L.G., Steinmuller, H.E., Breithaupt, J.L., 2019. Toward a mechanistic understanding of "peat collapse" and its potential contribution to coastal wetland loss. Ecology 100, 1–15. https://doi.org/10.1002/ecy.2 720

Chen, Y., Thompson, C.E.L., Collins, M.B., 2012. Saltmarsh creek bank stability: Biostabilisation and consolidation with depth. Cont. Shelf Res. 35, 64–74. https://doi.org/10.1016/j.csr.2 011.12.009

Cheong, S.-M., Silliman, B., Wong, P.P., van Wesenbeeck, B., Kim, C.-K., Guannel, G., 2013. Coastal adaptation with ecological engineering. Nat. Clim. Chang. 3, 787–791. https://doi.org/10.1038/nclim ate1854

Chirol, C., Spencer, K.L., Carr, S.J., Möller, I., Evans, B., Lynch, J., Brooks, H., Royse, K.R., 2021. Effect of vegetation cover and sediment type on 3D subsurface structure and shear strength in saltmarshes. Earth Surf.

Process. Landforms 46, 2279–2297. https://doi.org/10.1002/esp.5174

Christiansen, T., Wiberg, P.L., Milligan, T.G., 2000. Flow and Sediment Transport on a Tidal Salt Marsh. Estuaries and Coasts 50, 315–331. https://doi.org/10.1006/ecss.2000.0548

Coops, H., Geilen, N., Van der Velde, G., 1994. Distribution and growth of the helophyte species *Phragmites australis* and *Scirpus lacustris* in water depth gradients in relation to wave exposure. Aquat. Bot. 48, 273–284.

Crooks, S., Pye, K., 2000. Sedimentological controls on the erosion and morphology of saltmarshes: Implications for flood defense and habitat recreation. Geol. Soc. Spec. Publ. 175, 207–222. https://doi.org/10.1144/GSL.SP.2000.175.01.16

Danka, J., Zhang, L., 2015. Dike Failure Mechanisms and Breaching Parameters. J. Geotech. Geoenvironmental Eng. 141. https://doi.org/10.1061/(ASCE)GT.1943-5606.0001335

Dao, T., Stive, M.J.F., Hofland, B., Mai, T., 2018. Wave Damping due to Wooden Fences along Mangrove Coasts. J. Coast. Res. 34, 1317. https://doi.org/10.2112/jcoastres-d-18-00015.1

Day, J.W., Boesch, D.F., Clairain, E.J., Kemp, G.P., Laska, S.D., Mitsch, W.J., Orth, K., Mashriqui, H., Reed, D.J., Shabman, L., Simenstad, C.A., Streever, B.J., Twilley, R.R., Watson, C.C., Wells, J.T., Whigham, D.F., 2007. Restoration of the Mississippi Delta: Lessons from Hurricanes Katrina and Rita. Science (80-.). 315, 1679–1684. https://doi.org/10.1126/science.1137030

De Battisti, D., Fowler, M.S., Jenkins, S.R., Skov, M.W., Rossi, M., Bouma, T.J., Neyland, P.J., Griffin, J.N., 2019. Intraspecific Root Trait Variability Along Environmental Gradients Affects Salt Marsh Resistance to Lateral Erosion. Front. Ecol. Evol. 7, 1–11. https://doi.org/10.3389/fevo.2019.00150

De Smit, J.C., Kleinhans, M.G., Gerkema, T., Bouma, T.J., 2021. Quantifying natural sediment erodibility using a mobile oscillatory. Estuar. Coast. Shelf Sci. 262, 107574. https://doi.org/10.1016/j.ecss.2021.107574

Esteves, L.S., Williams, J.J., 2017. Managed realignment in Europe: a synthesis of methods, achievements and challenges. Living Shorelines Sci. Manag. Nature-based Coast. Prot. 157–180.

Evans, B.R., Brooks, H., Chirol, C., Kirkham, M.K., Möller, I., Royse, K., Spencer, K., Spencer, T., 2021. Vegetation interactions with geotechnical properties and erodibility of salt marsh sediments. Estuar. Coast. Shelf Sci. 265, 107713. https://doi.org/10.1016/j.ecss.2021.107713

Feagin, R. a, Lozada-Bernard, S.M., Ravens, T.M., Möller, I., Yeager,

K.M., Baird, A.H., 2009. Does vegetation prevent wave erosion of salt marsh edges? Proc. Natl. Acad. Sci. U. S. A. 106, 10109–13. https://doi.org/10.1073/pnas.0901297106

Fearnley, S., 2008. The soil physical and chemical properties of restored and natural back-barrier salt marsh on Isles Dernieres, Louisiana. J. Coast. Res. 24, 84–94. https://doi.org/10.2112/05-0620.1

Gillen, M.N., Messerschmidt, T.C., Kirwan, M.L., 2021. Biophysical controls of marsh soil shear strength along an estuarine salinity gradient. Earth Surf. Dyn. 9, 413–421. https://doi.org/10.5194/esurf-9-413-2021

Grabowski, R.C., Droppo, I.G., Wharton, G., 2011. Erodibility of cohesive sediment: The importance of sediment properties. Earth-Science Rev. 105, 101–120. https://doi.org/10.1016/j.earscirev.2011.01.008

Gyssels, G., Poesen, J., Bochet, E., Li, Y., 2005. Impact of plant roots on the resistance of soils to erosion by water: a review. Prog. Phys. Geogr. 29, 189–217. https://doi.org/10.1191/0309133305pp443ra

Hallegatte, S., Green, C., Nicholls, R.J., Corfee-Morlot, J., 2013. Future flood losses in major coastal cities. Nat. Clim. Chang. 3, 802–806. https://doi.org/10.1038/nclimate1979

Hansen, F., Kruschke, T., Greatbatch, R.J., Weisheimer, A., 2019. Factors Influencing the Seasonal Predictability of Northern Hemisphere Severe Winter Storms. Geophys. Res. Lett. 46, 365–373. https://doi.org/10.1029/2018GL079415

Heiri, O., Lotter, A.F., Lemcke, G., 2001. Loss on ignition as a method for estimating organic and carbonate content in sediments: reproducibility and comparability of results. J. Paleolimnol. 25, 101–110. https://doi.org/10.1016/0009-2541(93)90140-E

Himmelstein, J., Vinent, O.D., Temmerman, S., Kirwan, M.L., 2021. Mechanisms of Pond Expansion in a Rapidly Submerging Marsh. Front. Mar. Sci. 8, 1–15. https://doi.org/10.3389/fmars.2021.704768

Hinkel, J., Lincke, D., Vafeidis, A.T., Perrette, M., Nicholls, R.J., Tol, R.S.J.J., Marzeion, B., Fettweis, X., Ionescu, C., Levermann, A., James, R., Tol, R.S.J.J., Marzeion, B., Fettweis, X., Ionescu, C., Levermann, A., 2014. Coastal flood damage and adaptation costs under 21st century sea-level rise. Proc. Natl. Acad. Sci. U. S. A. 111, 3292–3297. https://doi.org/10.1073/pnas.1222469111

Hofstede, J.L.A., 2003. Integrated management of artificially created salt marshes in the Wadden Sea of Schleswig-Holstein, Germany. Wetl. Ecol. Manag. 11, 183–194. https://doi.org/10.1023/A:1024248127037

Howes, N.C., FitzGerald, D.M., Hughes, Z.J., Georgiou, I.Y., Kulp, M.A., Miner, M.D., Smith, J.M., Barras, J.A., 2010. Hurricane-induced failure of low salinity wetlands. Proc. Natl. Acad. Sci. U. S. A. 107, 14014–14019. https://doi.org/10.1073/pnas.0914582107

Hu, Z., Borsje, B.W., Belzen, J. Van, Willemsen, P.W.J.M., 2021. Mechanistic Modeling of Marsh Seedling Establishment Provides a Positive Outlook for Coastal Wetland Restoration Under Global Climate Change Geophysical Research Letters. Geophys. Res. Lett. 48, 1–12. https://doi.org/10.1029/2021GL095596

Jafari, N.H., Harris, B.D., Cadigan, J.A., Day, J.W., Sasser, C.E., Kemp, G.P., Wigand, C., Freeman, A., Sharp, L.A., Pahl, J., Shaffer, G.P., Holm, G.O., Lane, R.R., 2019. Wetland shear strength with emphasis on the impact of nutrients, sediments, and sea level rise. Estuar. Coast. Shelf Sci. 229. https://doi.org/10.1016/j.ecss.2019.106394

Jiang, L., Gerkema, T., Idier, D., Slangen, A.B.A., Soetaert, K., 2020. Effects of sea-level rise on tides and sediment dynamics in a Dutch tidal bay. Ocean Sci. 16, 307–321. https://doi.org/10.5194/os-16-307-2020

Kabat, P., Fresco, L.O., Stive, M.J.F., Veerman, C.P., Van Alphen, J.S.L.J., Parmet, B.W.A.H., Hazeleger, W., Katsman, C.A., 2009. Dutch coasts in transition. Nat. Geosci. 2, 450–452.

https://doi.org/10.1038/ngeo572

Kadiri, M., Spencer, K.L., Heppell, C.M., Fletcher, P., 2011. Sediment characteristics of a restored saltmarsh and mudflat in a managed realignment scheme in Southeast England. Hydrobiologia 672, 79–89. https://doi.org/10.1007/s10750-011-0755-8

Kirwan, M.L., Guntenspergen, G.R., 2012. Feedbacks between inundation , root production , and shoot growth in a rapidly submerging brackish marsh. J. Ecol. 100, 764–770. https://doi.org/10.1111/j.1365-2745.2012.01957.x

Lo, V.B., Bouma, T.J., van Belzen, J., Van Colen, C., Airoldi, L., 2017. Interactive effects of vegetation and sediment properties on erosion of salt marshes in the Northern Adriatic Sea. Mar. Environ. Res. 131, 32–42. https://doi.org/10.1016/j.marenvres.2017.09.006

Martín-Antón, M., Negro, V., Del Campo, J.M., López-Gutiérrez, J.S., Esteban, M.D., 2016. Review of coastal land reclamation situation in the world. J. Coast. Res. 1, 667–671. https://doi.org/10.2112/SI75-133.1

Masselink, G., Scott, T., Poate, T., Russell, P., Davidson, M., Conley, D., 2016. The extreme 2013/2014 winter storms: Hydrodynamic forcing and coastal response along the southwest coast of England. Earth Surf. Process. Landforms 41, 378–391.

https://doi.org/10.1002/esp.3836

McEvoy, S., Haasnoot, M., Biesbroek, R., 2021. How are European countries planning for sea level rise? Ocean Coast. Manag. 203, 105512. https://doi.org/10.1016/j.ocecoaman.2020.105512

Möller, I., Bouma, T.J., Brendel, M., Brooks, H., Cao, H., Carr, S., Chirol, C., Christie, E., Dennis, R., Eggermond, A., Evans, B., Lustig, J., Miranda-Lange, M., Nolte, S., Paul, M., Reents, S., Rolfe, C., Royse, K., Schoutens, K., Spencer, K., Temmerman, S., Kudella, M., 2019. Response of ecologically-mediated shallow intertidal shore transitions to extreme hydrodynamic forcing (RESIST), in: Presentation at Hydralab Symposium, Bucharest. pp. 1–9.

Möller, I., Kudella, M., Rupprecht, F., Spencer, T., Paul, M., van Wesenbeeck, B.K., Wolters, G., Jensen, K., Bouma, T.J., Miranda-Lange, M., Schimmels, S., 2014. Wave attenuation over coastal salt marshes under storm surge conditions. Nat. Geosci. 7, 727–731. https://doi.org/10.1038/ngeo2251

Morris, M., Hassan, M., Kortenhaus, A., Visser, P., 2009. Breaching Processes: A state of the art review. FLOODsite Publ. 70.

Morris, R.L., Boxshall, A., Swearer, S.E., 2020. Climate-resilient coasts require diverse defence solutions. Nat. Clim. Chang. 10, 485–487. https://doi.org/10.1038/s41558-020-0798-9

Neumann, B., Vafeidis, A.T., Zimmermann, J., Nicholls, R.J., 2015. Future coastal population growth and exposure to sea-level rise and coastal flooding - A global assessment. PLoS One 10. https://doi.org/10.1371/journal.pone.0118571

Nicholls, R.J., Lincke, D., Hinkel, J., Brown, S., Vafeidis, A.T., Meyssignac, B., Hanson, S.E., Merkens, J.L., Fang, J., 2021. A global analysis of subsidence, relative sea-level change and coastal flood exposure, Nature Climate Change. https://doi.org/10.1038/s41558-021-00993-z

Nolte, S., Koppenaal, E.C., Esselink, P., Dijkema, K.S., Schuerch, M., De Groot, A. V., Bakker, J.P., Temmerman, S., 2013. Measuring sedimentation in tidal marshes: A review on methods and their applicability in biogeomorphological studies. J. Coast. Conserv. 17, 301–325. https://doi.org/10.1007/s11852-013-0238-3

Oosterlee, L., Cox, T.J.S., Vandenbruwaene, W., Maris, T., Temmerman, S., Meire, P., 2018. Tidal Marsh Restoration Design Affects Feedbacks Between Inundation and Elevation Change. Estuaries and Coasts 41, 613–625. https://doi.org/10.1007/s12237-017-0314-2

Paprotny, D., Sebastian, A., Morales-Nápoles, O., Jonkman, S.N., 2018. Trends in flood losses in Europe over the past 150 years. Nat. Commun. 9. https://doi.org/10.1038/s41467-018-04253-1

Peeters, P., Visser, K.P., Mostaert, F., 2019. Large-scale Dike Breach Experiments in Belgium: Data Report Wijmeers & Outlook future experiments. Version 3.0. FHR Reports, 00_089_3. Antwerp, Belgium.

Peeters, P., Zhao, G., De Vos, L., Visser, P.J., 2015. Large-scale dike breaching experiments at Lillo in Belgium. Scour Eros. - Proc. 7th Int. Conf. Scour Erosion, ICSE 2014 289–297. https://doi.org/10.1201/b177 03-36

Pennings, S.C., Glazner, R.M., Hughes, Z.J., Kominoski, J.S., Armitage, A.R., 2021. Effects of mangrove cover on coastal erosion during a hurricane in Texas, USA. Ecology 102, 1–8. https://doi.org/10.1002/ecy.3 309

Schoonees, T., Gijón Mancheño, A., Scheres, B., Bouma, T.J., Silva, R., Schlurmann, T., Schüttrumpf, H., 2019. Hard Structures for Coastal Protection, Towards Greener Designs. Estuaries and Coasts 42, 1709–1729. https://doi.org/10.1007/s1223 7-019-00551-z

Schoutens, K., Heuner, M., Fuchs, E., Minden, V., Schulte-Ostermann, T., Belliard, J.P., Bouma, T.J., Temmerman, S., 2020. Nature-based shoreline protection by tidal marsh plants depends on trade-offs between avoidance and attenuation of hydrodynamic forces. Estuar. Coast. Shelf Sci. 236, 11. https://doi.org/10.1016/j.ecss. 2020.106645

Schoutens, K., Heuner, M., Minden, V., Schulte Ostermann, T., Silinski, A., Belliard, J.-P., Temmerman, S., 2019. How effective are tidal marshes as nature-based shoreline protection throughout seasons? Limnol. Oceanogr. 64, 1750–1762. https://doi.org/10.1002/lno.11 149

Schoutens, K., Reents, S., Nolte, S., Evans, B., Paul, M., Kudella, M., Bouma, T., Möller, I., Temmerman, S., 2021. Survival of the thickest? Impacts of extreme wave-forcing on marsh seedlings are mediated by species morphology. Limnol. Oceanogr. 1–16. https://doi.org/https://doi.org /10.1002/lno.11850

Schuerch, M., Dolch, T., Bisgwa, J., Vafeidis, A.T., 2018. Changing sediment dynamics of a mature backbarrier salt marsh in response to sea-level rise and storm events. Front. Mar. Sci. 5, 1–14. https://doi.org/10.3389/fmars. 2018.00155

Schulte Ostermann, T., Kleyer, M., Heuner, M., Fuchs, E., Temmerman, S., Schoutens, K., Bouma, T.J., Minden, V., 2021. Hydrodynamics affect plant traits in estuarine ecotones with impact on carbon sequestration potentials. Estuar. Coast. Shelf Sci. 259, 107464. https://doi.org/10.1016/j.ecss. 2021.107464

Schulze, D., Rupprecht, F., Nolte, S., Jensen, K., 2019. Seasonal and spatial within - marsh differences of biophysical plant properties : implications for wave attenuation capacity of salt marshes. Aquat. Sci. 81, 1–11.

https://doi.org/10.1007/s0002
7-019-0660-1

Sengupta, D., Chen, R., Meadows, M.E., 2018. Building beyond land: An overview of coastal land reclamation in 16 global megacities. Appl. Geogr. 90, 229–238. https://doi.org/10.1016/j.apge og.2017.12.015

Sha, X., Xu, K., Bentley, S.J., Robichaux, P.A., 2018. Characterization and modeling of sediment settling, consolidation, and suspension to optimize coastal Louisiana restoration. Estuar. Coast. Shelf Sci. 203, 137–147. https://doi.org/10.1016/j.ecss. 2018.02.008

Sheng, Y.P., Rivera-Nieves, A.A., Zou, R., Paramygin, V.A., Angelini, C., Sharp, S.J., 2021. Invasive *Phragmites* provides superior wave and surge damage protection relative to native plants during storms. Environ. Res. Lett. 16. https://doi.org/10.1088/1748-9326/abf288

Shepard, C.C., Crain, C.M., Beck, M.W., 2011. The protective role of coastal marshes: A systematic review and meta-analysis. PLoS One 6. https://doi.org/10.1371/journ al.pone.0027374

Silinski, A., Fransen, E., Bouma, T.J., Meire, P., Temmerman, S., 2016a. Unravelling the controls of lateral expansion and elevation change of pioneer tidal marshes. Geomorphology 274, 106–115. https://doi.org/10.1016/j.geo morph.2016.09.006

Silinski, A., Heuner, M., Troch, P., Puijalon, S., Bouma, T.J., Schoelynck, J., Schröder, U., Fuchs, E., Meire, P., Temmerman, S., 2016b. Effects of contrasting wave conditions on scour and drag on pioneer tidal marsh plants. Geomorphology 255, 49–62. https://doi.org/10.1016/j.geo morph.2015.11.021

Smith, C.S., Rudd, M.E., Gittman, R.K., Melvin, E.C., Patterson, V.S., Renzi, J.J., Wellman, E.H., Silliman, B.R., 2020. Coming to terms with living shorelines: A scoping review of novel restoration strategies for shoreline protection. Front. Mar. Sci. 7, 1–14. https://doi.org/10.3389/fmars. 2020.00434

Smolders, S., Teles, M.J., Leroy, A., Maximova, T., Meire, P., Temmerman, S., 2020. Modeling storm surge attenuation by an integrated nature-based and engineered flood defense system in the Scheldt estuary (Belgium). J. Mar. Sci. Eng. 8. https://doi.org/10.3390/JMSE 8010027

Spencer, T., Brooks, S.M., Evans, B.R., Tempest, J.A., Möller, I., 2015. Southern North Sea storm surge event of 5 December 2013 : Water levels , waves and coastal impacts. Earth Sci. Rev. 146, 120–145. https://doi.org/10.1016/j.ears cirev.2015.04.002

Spencer, T., Möller, I., Rupprecht, F., Bouma, T.J., van Wesenbeeck, B.K., Kudella, M., Paul, M., Jensen, K., Wolters, G., Miranda-Lange, M., Schimmels, S., 2016. Salt marsh surface survives

true-to-scale simulated storm surges. Earth Surf. Process. Landforms 41, 543–552. https://doi.org/10.1002/esp.3 867

Srivastava, J., Kalra, S.J.S., Naraian, R., 2014. Environmental perspectives of *Phragmites australis* (Cav.) Trin. Ex. Steudel. Appl. Water Sci. 4, 193–202. https://doi.org/10.1007/s1320 1-013-0142-x

Stanczak, G., Oumeraci, H., 2012. Modeling sea dike breaching induced by breaking wave impact-laboratory experiments and computational model. Coast. Eng. 59, 28–37. https://doi.org/10.1016/j.coast aleng.2011.07.001

Stark, J., Van Oyen, T., Meire, P., Temmerman, S., 2015. Observations of tidal and storm surge attenuation in a large tidal marsh. Limnol. Oceanogr. 60, 1371–1381. https://doi.org/10.1002/lno.10 104

Symonds, A.M., Collins, M.B., 2004. Sediment dynamics associated with managed realignment; Freiston Shore. The Wash, UK. Coast. Eng. https://doi.org/10.1142/9789 812701916

Tagliapietra, D., Baldan, D., Barausse, A., Buosi, A., Curiel, D., Guarneri, I., Pessa, G., Rismondo, A., Sfriso, A., Smania, D., Ghirardini, A.V., 2018. Protecting and restoring the salt marshes and seagrasses in the lagoon of Venice, Management and restoration of Mediterranean coastal lagoons in Europe.

Tan, L., Ge, Z., Zhou, X., Li, S., Li, X., Tang, J., 2020. Conversion of coastal wetlands, riparian wetlands, and peatlands increases greenhouse gas emissions: A global meta-analysis. Glob. Chang. Biol. 26, 1638–1653. https://doi.org/10.1111/gcb.1 4933

Temmerman, S., Govers, G., Wartel, S., Meire, P., 2004. Modelling estuarine variations in tidal marsh sedimentation: Response to changing sea level and suspended sediment concentrations. Mar. Geol. 212, 1–19. https://doi.org/10.1016/j.marg eo.2004.10.021

Temmerman, S., Govers, G., Wartel, S., Meire, P., 2003. Spatial and temporal factors controlling short-term sedimentation in a salt and freshwater tidal marsh, Scheldt estuary, Belgium, SW Netherlands. Earth Surf. Process. Landforms 28, 739–755. https://doi.org/10.1002/esp.4 95

Temmerman, S., Meire, P., Bouma, T.J., Herman, P.M.J., Ysebaert, T., De Vriend, H.J., 2013. Ecosystem-based coastal defence in the face of global change. Nature 504, 79–83. https://doi.org/10.1038/natur e12859

Temmerman, S., Moonen, P., Schoelynck, J., Govers, G., Bouma, T.J., 2012. Impact of vegetation die-off on spatial flow patterns over a tidal marsh. Geophys. Res. Lett. 39, n/a-n/a. https://doi.org/10.1029/2011 GL050502

Tempest, J.A., Harvey, G.L., Spencer, K.L., 2015. Modified sediments and subsurface hydrology in natural and recreated salt marshes and implications for delivery of ecosystem services. Hydrol. Process. 29, 2346–2357. https://doi.org/10.1002/hyp.10368

Tessler, Z.D., Vörösmarty, C.J., Grossberg, M., Gladkova, I., Aizenman, H., Syvitski, J.P.M., Foufoula-Georgiou, E., 2015. Profiling risk and sustainability in coastal deltas of the world. Science (80-.). 349, 638–643. https://doi.org/10.1126/science.aab3574

Teuchies, J., Vandenbruwaene, W., Carpentier, R., Bervoets, L., Temmerman, S., Wang, C., Maris, T., Cox, T.J.S., Van Braeckel, A., Meire, P., 2013. Estuaries as Filters: The Role of Tidal Marshes in Trace Metal Removal. PLoS One 8, 1–11. https://doi.org/10.1371/journal.pone.0070381

van de Vijsel, R.C., van Belzen, J., Bouma, T.J., van der Wal, D., Cusseddu, V., Purkis, S.J., Rietkerk, M., van de Koppel, J., 2020. Estuarine biofilm patterns: Modern analogues for Precambrian self-organization. Earth Surf. Process. Landforms 45, 1141–1154. https://doi.org/10.1002/esp.4783

van den Hoven, K., Kroeze, C., van Loon-Steensma, J.M., 2022. Characteristics of realigned dikes in coastal Europe: Overview and opportunities for nature-based flood protection. Ocean Coast. Manag. 222, 106116. https://doi.org/10.1016/j.ocecoaman.2022.106116

van Loon-Steensma, J.M., Schelfhout, H.A., 2017. Wide Green Dikes: A sustainable adaptation option with benefits for both nature and landscape values? Land use policy 63, 528–538. https://doi.org/10.1016/j.landusepol.2017.02.002

Van Loon-steensma, J.M., Slim, P.A., 2013. The Impact of Erosion Protection by Stone Dams on Salt- Marsh Vegetation on Two Wadden Sea Barrier Islands. J. Coast. Res. 29, 783–796. https://doi.org/10.2112/JCOASTRES-D-12-00123.1

Van Putte, N., Temmerman, S., Verreydt, G., Seuntjens, P., Maris, T., Heyndrickx, M., Boone, M., Joris, I., Meire, P., 2020. Groundwater dynamics in a restored tidal marsh are limited by historical soil compaction. Estuar. Coast. Shelf Sci. 244, 106101. https://doi.org/10.1016/j.ecss.2019.02.006

van Wijnen, H.J., Bakker, J.P., 2001. Long-term Surface Elevation Change in Salt Marshes: a Prediction of Marsh Response to Future Sea-Level Rise. Estuar. Coast. Shelf Sci. 52, 381–390. https://doi.org/10.1006/ecss.2000.0744

Vandenbruwaene, W., Maris, T., Cox, T.J.S., Cahoon, D.R., Meire, P., Temmerman, S., 2011. Sedimentation and response to sea-level rise of a restored marsh with reduced tidal exchange: Comparison with a natural tidal marsh. Geomorphology 130, 115–126.

https://doi.org/10.1016/j.geo
morph.2011.03.004

Vannoppen, W., Vanmaercke, M., De
Baets, S., Poesen, J., 2015. A
review of the mechanical effects
of plant roots on concentrated
flow erosion rates. Earth-
Science Rev. 150, 666–678.
https://doi.org/10.1016/j.ears
cirev.2015.08.011

Visser, P.J., 1998. Breach growth in
sand-dikes. TU delft PhD Diss.

Vorogushyn, S., Merz, B.,
Lindenschmidt, K.E., Apel, H.,
2010. A new methodology for
flood hazard assessment
considering dike breaches.
Water Resour. Res. 46.
https://doi.org/10.1029/2009
WR008475

Vuik, V., Borsje, B.W., Willemsen,
P.W.J.M., Jonkman, S.N., 2019.
Salt marshes for flood risk
reduction: Quantifying long-
term effectiveness and life-cycle
costs. Ocean Coast. Manag. 171,
96–110.
https://doi.org/10.1016/j.ocec
oaman.2019.01.010

Vuik, V., Jonkman, S.N., Borsje, B.W.,
Suzuki, T., 2016. Nature-based
flood protection: The efficiency
of vegetated foreshores for
reducing wave loads on coastal
dikes. Coast. Eng. 116, 42–56.
https://doi.org/10.1016/j.coast
aleng.2016.06.001

Vuik, V., van Vuren, S., Borsje, B.W., van
Wesenbeeck, B.K., Jonkman,
S.N., 2018. Assessing safety of
nature-based flood defenses:
Dealing with extremes and
uncertainties. Coast. Eng. 139,
47–64.

https://doi.org/10.1016/j.coast
aleng.2018.05.002

Wang, H., van der Wal, D., Li, X., van
Belzen, J., Herman, P.M.J., Hu, Z.,
Ge, Z., Zhang, L., Bouma, T.J.,
2017. Zooming in and out: Scale
dependence of extrinsic and
intrinsic factors affecting salt
marsh erosion. J. Geophys. Res.
Earth Surf. 122, 1455–1470.
https://doi.org/10.1002/2016J
F004193

Wang, X., Chen, W., Zhang, L., Jin, D., Lu,
C., 2010. Estimating the
ecosystem service losses from
proposed land reclamation
projects: A case study in Xiamen.
Ecol. Econ. 69, 2549–2556.
https://doi.org/10.1016/j.ecole
con.2010.07.031

Watts, C.W., Tolhurst, T.J., Black, K.S.,
Whitmore, A.P., 2003. In situ
measurements of erosion shear
stress and geotechnical shear
strength of the intertidal
sediments of the experimental
managed realignment scheme at
Tollesbury, Essex, UK. Estuar.
Coast. Shelf Sci. 58, 611–620.
https://doi.org/10.1016/S0272
-7714(03)00139-2

Wilson, C.A., Hughes, Z.J., FitzGerald,
D.M., 2012. The effects of crab
bioturbation on Mid-Atlantic
saltmarsh tidal creek extension:
Geotechnical and geochemical
changes. Estuar. Coast. Shelf Sci.
106, 33–44.
https://doi.org/10.1016/j.ecss.
2012.04.019

Winterwerp, J.C., van Kesteren, W.G.M.,
van Prooijen, B., Jacobs, W.,
2012. A conceptual framework
for shear flow–induced erosion
of soft cohesive sediment beds. J.
Geophys. Res. Ocean. 117, 1–17.

https://doi.org/10.1029/2012J
C008072

Wu, W., Altinakar, M., Al-Riffai, M., Bergman, N., Bradford, S., Cao, Z., Chen, Q., Constantinescu, S., Duan, J., Gee, D., Greimann, B., Hanson, G., He, Z., Hegedus, P., Hoestenberghe, T., Huddleston, D., Hughes, S., Imran, J., Jia, Y., Zhang, L., 2011. Earthen Embankment Breaching. J. Hydraul. Eng. 137, 1549–1564. https://doi.org/10.1061/(asce) hy.1943-7900.0000498

Zhang, W., Ge, Z., Li, S., Tan, L., Zhou, K., Li, Y., Xie, L., 2022. The role of seasonal vegetation properties in determining the wave attenuation capacity of coastal marshes : Implications for building natural defenses. Ecol. Eng. 175, 106494. https://doi.org/10.1016/j.ecole ng.2021.106494

Zhang, Y., Chen, R., Wang, Y., 2020. Tendency of land reclamation in coastal areas of Shanghai from 1998 to 2015. Land use policy 91, 104370. https://doi.org/10.1016/j.land usepol.2019.104370

Zhu, Z., Vuik, V., Visser, P.J., Soens, T., van Wesenbeeck, B., van de Koppel, J., Jonkman, S.N., Temmerman, S., Bouma, T.J., 2020a. Historic storms and the hidden value of coastal wetlands for nature-based flood defence. Nat. Sustain. https://doi.org/10.1038/s4189 3-020-0556-z

Zhu, Z., Yang, Z., Bouma, T.J., 2020b. Biomechanical properties of marsh vegetation in space and time: effects of salinity, inundation and seasonality.

Ann. Bot. https://doi.org/10.1046/j.1365 -2087.1998.00089.x

7

Discussion

7.1 Objectives and context

The aim of this thesis was to explore the role of species-specific plant traits in the mutual interactions between plants, hydrodynamic forces and sediments and its consequences for the spatial-temporal effectiveness of tidal marshes as nature-based shoreline protection. In this context, new insights and a better understanding of the driving processes were derived from both field monitoring and field experiments as well as flume experiments. The results and conclusions from the different chapters are combined in a conceptual figure below (Fig. 7.1).

Climate change induced sea level rise and increasing storminess alongside the growing pressure by human interference in strongly urbanized coastal areas increase the risk of coastal flood hazards (Feser et al. 2015; Neumann et al. 2015; Taherkhani et al. 2020; MacManus et al. 2021). To mitigate this risk, adaptations to the existing engineered shoreline protection infrastructure are needed (Vitousek et al. 2017). Nature-based solutions by conservation and creation of ecosystems such as tidal marshes, are increasingly proposed as cost-effective, ecological complement to the traditional shoreline protection (Borsje et al. 2011; Duarte et al. 2013; Temmerman et al. 2013; Vuik et al. 2016; Marijnissen et al. 2020). Implementation of tidal marshes in front of engineered shoreline protection infrastructures such as dikes, will reduce the impact of hydrodynamic forces from waves and currents on these protective structures (Vuik et al. 2016). Nevertheless, implementations of tidal marshes as additional shoreline protection measure are hampered due to the uncertainties about their effectiveness (Möller 2019), especially under conditions for which protection is most desired, e.g. shorelines exposed to strong hydrodynamic forces and storm surges. For successful implementation of tidal marshes as complementing shoreline protection, the need for enough space and the right hydrodynamic conditions is discussed.

7.2 Plant trait dependent shoreline protection

The field measurements in this study emphasize the role of tidal marsh vegetation in shoreline protection, and more specifically, I highlight the role of species-specific plant traits and how they determine the wave and current attenuation capacity of tidal marsh vegetation (chapter 3: Schoutens et al. (2020)). I showed that *B. maritimus* had a higher attenuation rate as a result of stiffer, longer shoots and higher aboveground biomass compared to *S. tabernaemontani* which had more flexible, short shoots and a lower biomass. Similar trends of plant trait dependent attenuation of hydrodynamic forces have been evaluated earlier (Bouma et al. 2010; Ysebaert et al. 2011; Yang et al. 2012; Tempest et al. 2015). Studies on the hydrodynamic attenuation capacity of tidal marsh plants all confirm this positive correlation between attenuation capacity and plant traits that increase the experienced friction (Fig. 7.1), i.e. drag forces on the shoots (Paul et al. 2016; Rupprecht et al. 2017; Silinski et al. 2018; Vuik et al. 2018). Nevertheless, there is a limit to this relationship too. Once the plants are fully

submerged, the ratio between canopy height and water depth will decrease which will reduce the friction between the wave orbital velocities and the vegetation canopy (chapter 2: Schoutens et al. (2019) and Chapter 3: Schoutens et al. (2020)). Depending on the characteristics of the incoming wave, the wave attenuation capacity might be totally different, e.g. short-period wind waves vs long-period ship waves (Anderson et al. 2011). The relation between plant traits and wave attenuation capacity becomes even more complex when considering both the hydrodynamic characteristics (water depth, wave height and wave period) and the reconfiguration capacity of plants, e.g. through shoot bending (Paul and Amos 2011; Rupprecht et al. 2017).

The measurements in chapter 3: Schoutens et al. (2020) took place in summer when aboveground vegetation is at peak biomass, nevertheless, most extreme waves and currents in NW Europe are observed during the winter season. This seasonal variation in exposure and storminess was accounted for in a field monitoring campaign where plant morphology and wave and current attenuation rates were monitored throughout a complete growing season, including the winter months (chapter 2: Schoutens et al. (2019)). I found that in autumn the most shoreward, pioneer marsh plants deteriorated, broke off and were washed away with the tides, hence aboveground biomass was almost completely gone. Consequently, the attenuation of waves and currents diminished and the hydrodynamic forces were able to penetrate further into the marsh, towards the dike. In the higher marshes along the dike, conditions are more sheltered from hydrodynamic exposure which limits the removal of dead standing biomass that could, at least for a short time period, reduce hydrodynamic forces such as waves and currents in case of a storm surge. Although in the pioneer marshes aboveground biomass is washed away, the belowground biomass persisted as a network of roots which reduced the risk of sediment erosion (Fig. 7.1). Hence, a stable sediment bed in pioneer marshes could facilitate the persistence, and reduce the risk of erosion in more landward, higher marshes. By limiting the erosions risk, the sediment bed maintains its elevation relative to mean high water, which ensures the contribution of bottom friction to attenuation of hydrodynamic forces from waves and currents (Fagherazzi et al. 2007; Mariotti and Fagherazzi 2013; Pascolo et al. 2018).

The hypothesis that the presence of shoreward pioneer tidal marshes can protect higher elevated marshes close to dikes is in line with, a new, additional shoreline protection function of tidal marshes that was proposed recently (Zhu et al. 2020). Their analysis of historical dike breaches, suggest that higher tidal marshes adjacent to embankments serve as a stable barrier in front of the breach, thereby reducing the flood discharge through the breach, which restricts the erosion of the breach, hence narrowing the dimensions of the dike breach, and reducing the flooding depth and potential damage in the lowlands behind the dike breach. With a flume experiment (chapter 6), I show the first experimental results of the stability of such a well-developed high marsh in its winter-state during high flow velocities as can be

generated on the marsh platform in front of a dike breach. These findings provide an argument for nature managers and policymakers to allow enough space for tidal marsh development. Although past research shows that waves and currents are attenuated over a short distance of several tens of meters (Möller and Spencer 2002; Ysebaert et al. 2011; Carus et al. 2016; Silinski et al. 2018), my results give some first indications and evidence of the added protection values gained when providing enough space for tidal marshes to develop a gradient of shoreward pioneer zones and landward high marshes (Fig. 7.1).

7.3 Plant trait dependent growth and survival

The capacity to attenuate hydrodynamic forces from waves and currents is especially relevant in areas where shorelines are exposed to, and under stress of such hydrodynamic forces. Implementing tidal marshes as a successful complementary shoreline protection requires that plant establishment and spatial expansion into established tidal marshes is possible under the given hydrodynamic forces (Zhao et al. 2020). This process of marsh establishment can be initiated by three processes: (i) clonal expansion of the existing adjacent marsh, (ii) settling of adult propagules or (iii) seedling establishment (Hu et al. 2015). Crucial in those three processes is the ability of the species to cope with the local environmental conditions (Cao et al. 2020), such as waves, currents and stress from tidal inundation, which in this thesis is shown to be dependent on species-specific plant traits (Fig. 7.1).

My results (chapter 2: Schoutens et al. (2019) and chapter 5) show that the species growing in the shoreward, wave-exposed marsh zone have plant traits favoring avoidance of mechanical stress from waves, that means: smaller, more flexible shoots (Fig. 7.1), which are plant traits known to reduce (avoid) drag forces felt by the plants from hydrodynamics (Puijalon et al. 2005; Shepard et al. 2011; Paul et al. 2016). Although this growth capacity comes with a trade-off of having a relatively low wave and current attenuation capacity (Bouma et al. 2010, Ysebaert et al. 2011, Rupprecht et al. 2017, incl. chapter 3: Schoutens et al. (2020)), the ability of this species to grow in the most seaward marsh zone might generate enough wave and current attenuation to create a niche in the adjacent more landward located marsh zone that facilitates the growth of a second species with plant traits that are slightly less capable to avoid mechanical stress (i.e., taller, stiffer shoots) (Fig. 7.1). Interestingly, the plant traits of the second species zone have a higher wave attenuation capacity. The plant trait dependent trade-off between growth capacity under hydrodynamic forces and attenuation capacity of hydrodynamic forces is suggested to result in a niche differentiation, i.e. a spatial distribution of plant species and, consequently, a spatial distribution of the plant trait dependent attenuation of hydrodynamic forces (Fig. 7.1). As such, this trade-off forms a spatial self-organization of species and their plant trait dependent attenuation capacity.

This thesis shows the first field and flume measurements on plant trait dependent growth in response to hydrodynamic forces from waves and currents which might be an additional driver of spatial species distribution (in addition to sediment salinity and tidal inundation period (Bertness 1991; Pennings and Callaway 1992)). Knowledge of plant trait dependent growth has important implications for successful restoration or establishment of tidal marshes (Wolters et al. 2008). Seedlings and propagules might settle in spring and summer (Schwarz et al. 2011), nevertheless a successful marsh establishment requires that the newly established plants have the ability to handle the prevailing hydrodynamic forces in combination with tidal inundation stress to eventually expand, e.g. clonally, to form a mature marsh ecosystem. Field transplantation experiments (chapter 5) learn us that not only interspecific variation in plant traits determines plant growth, but also intraspecific variation in growth responses is reflected by the same plant traits. In other words, plant individuals (both inter- and intraspecific) that grew small, thin and flexible shoots and a low aboveground biomass survived better under the combined stress from hydrodynamics and tidal inundation. Hence, variation in plant traits has consequences for spatial selection and resulting spatial distribution of both inter- and intraspecific variation in plant traits and shoreline protection capacity.
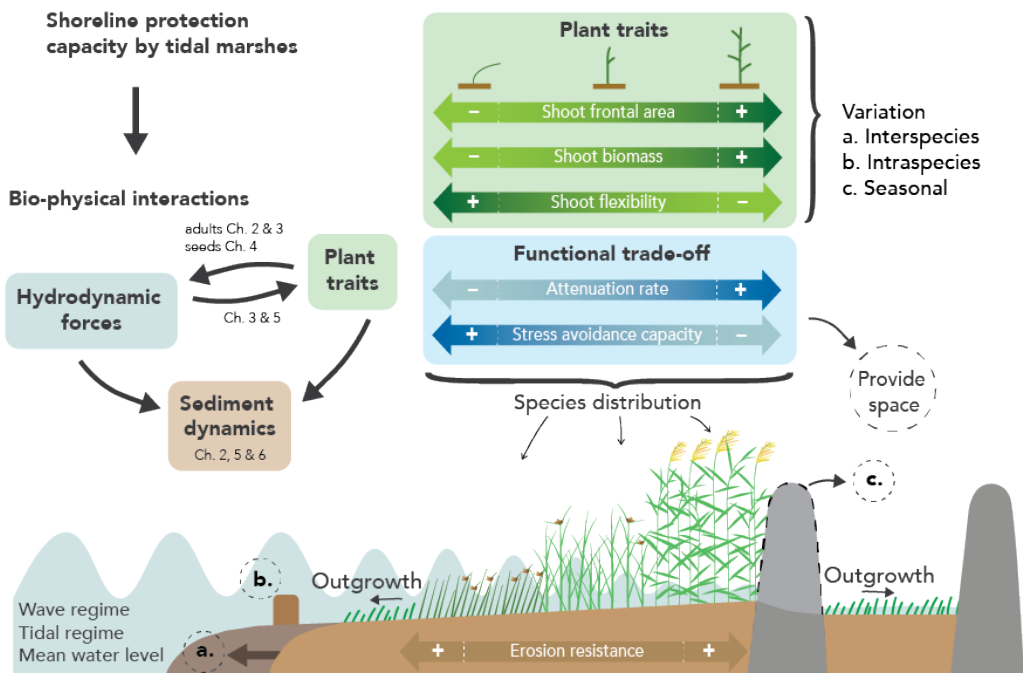

Figure 7.1: Nature-based shoreline protection capacity by tidal marshes depends on bio-physical interactions between plant traits, hydrodynamic forces and sediment dynamics. Along a cross-shore sea-to-land gradient, the exposure to hydrodynamic forces and inundation stress reduces in the landward direction. Inter- and intraspecific

variation as well as seasonal changes in plant traits (green box: plant traits) also follow a cross-shore gradient which creates functional trade-offs between the capacity to cope with and the capacity to attenuate hydrodynamic forces (blue box: functional trade-off). We suggest this trade-off plays a role in the formation of a self-organized spatial distribution of species and accordingly, the spatial distribution of wave attenuation rates. Species distribution and diversity along a cross-shore transect was observed to be an important part of the overall efficiency of the tidal marsh shoreline protection capacity, as illustrated by the stabilizing effect of belowground biomass that ensures the erosion resistance both in the shoreward pioneer zones and in the landward higher marshes. To take full advantage of the nature-based shoreline protection capacity of tidal marshes, management recommendations are made which increase the resilience and reliability of the shoreline protection functions by allowing space for cross-shore tidal marsh development (dashed circles): shoreward expansion by sediment nourishment (a) or creating (temporal) sheltered conditions by barriers in front of the marsh (b) and in case shoreward expansion is limited by available space, managed realignment (c) by building a new dike more landward and breaching the existing dike is proposed.

7.4 Implications for nature-based management of shoreline erosion risk

Species-specific plant traits play an important role in the mutual interactions between the vegetation itself, the hydrodynamic forces and the sediment stability. My results illustrate that this interaction is a key component in the tidal marsh shoreline protection capacity. Here I elucidate my findings in **two key messages** for shoreline managers and policy makers; (i) for tidal marsh creation and plant establishment, environmental conditions should allow species to settle and develop into mature marsh plants and (ii) once a marsh has established there should be space to allow the development of a mature marsh ecosystem including the cross-shore gradient from the low elevated shoreward pioneer marsh towards the higher elevated landward marshes adjacent to the embankment (Fig. 7.1). Below I elaborate to explain these two key messages.

Concerning the **first key message**, this research shows that growth and survival following the initial phase of marsh plant establishment depend on the capacity of the species to cope with the prevailing conditions throughout the seasons (chapter 5) including occasionally extreme hydrodynamic forces (chapter 4: Schoutens et al. (2021)). To initiate marsh establishment, creation of suitable conditions are needed, i.e. suitable elevation within the tidal frame, hydrodynamic forces, salinity, sediment properties, etc. Furthermore, concerning the **second key message**, the presented pioneer field observations and experiments (chapter 2: Schoutens et al. (2019) and chapter 3: Schoutens et al. (2020)) show that apart from the conditions that allow tidal marsh plants to grow and survive, their resilience and effectiveness for wave and

current attenuation might be promoted by allowing the development of a species distribution in function of plant traits and environmental conditions. Variation in species-specific plant traits results in variation in functionality, e.g. both the capacity to cope with hydrodynamic forces and the capacity to attenuate them, hence increasing the reliability of tidal marshes as a complementary shoreline protection under a range of environmental circumstances (Renzi et al. 2019; Battisti 2021). Species diversity should thus be promoted by allowing enough space for marsh development and expansion.

To meet these goals, several suggestions are given; mitigating the risk of disturbances by e.g. storm waves during the establishment of propagules and seedlings can be accomplished by installing temporary artificial fences or barriers that create conditions sheltered from hydrodynamic forces (Fig. 7.1) (Hofstede 2003; Dao et al. 2018). When these structures are made from organic materials (e.g. wooden branches or so-called brushwood), they will eventually deteriorate naturally (Vuik et al. 2019). Before this time, the marsh should have enough time to develop into a mature marsh, with a high enough resistance to higher levels of hydrodynamic forces once the barrier has disappeared. This method can be used to create more space for marsh development too, i.e. the fences or barriers could be used to enclose an area which could be filled with sediment, e.g. dredged materials, which, after some consolidation, can form the base for tidal marshes to expand or for new tidal marshes to develop (Tagliapietra et al. 2018). Unfortunately, in heavily embanked estuarine regions, the width of the river channel is often too narrow to allow shoreward tidal marsh creation. In some cases however, there is the option to replace the existing dike with a new, more landward situated dike, which is commonly known as "managed realignment" (French 2006b; Turner et al. 2007; Luisetti et al. 2011). When the old dike is breached, a marsh can form within the zone between the breached old dike and the more landward new dike – which is then called the managed realignment site (Fig. 7.1). This management strategy has multiple examples over the past decades (Maris et al. 2007; Esteves and Williams 2017), but sometimes there are uncertainties about the future success of the project (Brady and Boda 2017). These uncertainties include abiotic factors such as providing suitable flooding conditions and suitable hydrodynamic forces (French 2006b), or accounting for changes in the environment such as climate change induced sea level rise or a deficit of sediment supply which might hamper the development of vegetation (Esteves 2013). Moreover, biotic variation and interactions with the abiotic environment might create even more uncertainty (Brückner et al. 2019).

The uncertainties of managed realignment often causes suspicion from different stakeholders, the public opinion and policymakers (Myatt et al. 2003). Moreover, managed realignment is often perceived as giving up valuable land for less valuable wetlands and hence remains a delicate topic (De La Vega-Leinert et al. 2018), especially since some people will lose their land property which has not only economic value but

typically, and often even more important, also historical or personal value. This means that a broad political and public support is needed for whom predictability and reliability along with communication and participation is crucial. In this context, the presented data provides insights on suitable conditions for plant establishment and growth and more specifically how this varies between species depending on their plant traits. Hence, this thesis adds to an improved planning and a better predictability of tidal marsh restoration or creation projects, e.g. by implementing the conceptual processes in models that describe tidal marsh development (Borsje et al. 2011).

7.5 Limitations and future research

Over the past decades, research on nature-based shoreline protection by tidal marshes has shown the potential protection function, the cost-effectiveness and the ecological benefits of tidal marshes (Turner et al. 2007; Temmerman et al. 2013; Sutton-Grier et al. 2015; Tiggeloven et al. 2022). The results in this thesis emphasize the protection capacity of tidal marshes but also bring some important nuances and restrictions regarding their resilience and reliability. This illustrates the necessity of a good understanding of the driving processes within the ecosystem.

I provided new insights in the spatial-temporal variability in tidal marsh shoreline protection capacity as a result of contrasting species-specific plant traits. The species-specific plant trait dependent trade-off between being able to grow under hydrodynamic forces and the capacity to attenuate them, was suggested to result in a spatial self-organization along a cross-shore exposure gradient. Nevertheless, the field and flume studies in this thesis look at responses over short term to seasonal time scales. Additionally, this thesis focused on plant-scale interactions along cross-shore transects. To fully understand the role of the plant-scale interactions within the shoreline protection capacity of tidal marshes, processes on different scales need to be considered too (Leonardi and Fagherazzi 2015; Bendoni et al. 2016).

In the first place, geomorphological landscape features such as creek networks, mass-erosion by cliff collapse and the shape of the tidal flat-marsh edge transition (convex/concave) are important drivers of sediment dynamics and hydrodynamics (Wang et al. 2017; Reed et al. 2018; Willemsen et al. 2022). For example, ridges and runnels can act as a sediment source for the inner marsh (Schuerch et al. 2019) and creeks have a crucial role in sediment transport towards the higher elevated marsh zones as well as drainage of the marsh platform creating multiple gradients (elevation, sediment type, salinity, etc.) throughout the marsh (Reed et al. 1999; Kearney and Fagherazzi 2016). Small-scale topographical variance can initiate plant settlement which can evolve in a vegetation patch (Xie et al. 2019; Cao et al. 2021a). Through density-dependent feedbacks, scale-dependent feedbacks will get stronger (Bouma et al. 2009). As a result of these feedbacks, sediment accretion within a patch and erosion

between patches will result in a channel network (Temmerman et al. 2007). Concerning the wave propagation towards and through the vegetation, both the wave characteristics and the shape of the cross-shore bathymetry are determinant for the bottom friction (Möller and Spencer 2002) which in case of a rough surface or a steep slope can initiate waves to break through which much of the wave energy is lost (Tonelli et al. 2010). Therefore, when considering tidal marsh conservation or restoration, the dynamic surface topography and how it interacts with both biotics and abiotic variables, is of key importance for understanding the shoreline protection efficiency of the marsh.

In this thesis, the stabilizing role of belowground biomass was emphasized, however uncertainties remain as some studies suggest that the presence of belowground biomass from e.g. roots is difficult to directly link with sediment stability (Feagin et al. 2009). Moreover, only recently more attention goes to the role of root characteristics and how this varies between species (Chirol et al. 2021; Evans et al. 2021; Marin-Diaz et al. 2021).

Secondly, tidal marsh development takes place over longer time periods (i.e. several years to decades) in which short-term extreme events (e.g. storm surges creating cliffs) can have long-term impacts (Van de Koppel et al. 2005) and in which small and slow changes in the environmental settings play a crucial role (Schuerch et al. 2016). For instance, the slow process of sea level rise is increasing the water depth on top of marsh platforms, which could drown the marshes (Schepers et al. 2017; Himmelstein et al. 2021). However, when the environmental conditions allow (e.g. sediment supply (Ma et al. 2014)), tidal marshes can grow vertically and maintain their positions within the tidal frame by trapping sediments (Morris et al. 2002; French 2006a). Additionally, human-induced interference by for example dike reinforcements or dredging of the shipping channel will change the environmental settings locally, e.g. slope of the intertidal section in front of the embankment (Dam et al. 2013; Zhu et al. 2019), and on large scales which can alter the tidal marsh development through changes in tidal range (Balke et al. 2016).

To account for the environmental variation on multiple spatial and temporal scales, a modeling approach is preferred (Fagherazzi et al. 2012; Schwarz et al. 2015, 2018; van Belzen et al. 2017; Gourgue et al. 2021). In that respect, this thesis provides valuable data for the calibration of vegetation parameters in models. Present wave propagation models do not include the spatial variation in plant traits, i.e. as a result of species distribution, however, in this thesis it was shown that this might be a crucial process in the climate persistence of the tidal marsh shoreline protecting function. One of the main challenges is the incorporation of the vegetation characteristics, i.e., the vegetation structure is complex and vegetation properties can change in relation to hydrodynamic forces (Möller 2006; Hu et al. 2014). Nevertheless, this can also raise the question

whether the classical quantification of plant traits is representative for the wave- and current attenuation capacity (Zhang and Nepf 2021). For example, the quantification of frontal area or aboveground biomass might overestimate the experienced drag forces as a result of reconfiguration of the plants under hydrodynamic forcing (Paul et al. 2016). Moreover, the effect of a vegetation canopy is different from the effect of a single plants (Paul et al. 2012; Schwarz et al. 2015). When considering a vegetation canopy, shielding of the outer individuals will protect the inner individuals from strong hydrodynamic forces (Sand-Jensen 2003; Peralta et al. 2008; Rupprecht et al. 2017). However, this means that the attenuation effect of the canopy is lower compared to that of the sum of individual plants (i.e. the inner individuals experience less friction and drag). The difference in functional traits between a vegetation canopy and a single plant has implications for both the attenuation capacity of hydrodynamic forces as well as the growth and survival chance of individual shoots. Such a density-dependence is important to consider in data interpretation as it can have contrasting implications at different scales (Temmerman et al. 2007; Bouma et al. 2009). Depending on the research question, it might be worth to think of alternative proxies that are more representative for the induced friction and the experienced drag.

In a next step, the model simulations allow to test the resilience and reliability of the tidal marsh shoreline protection function in changing climate conditions, e.g. how will the shoreline protection function of tidal marshes persist under future climate scenarios in which the impact of waves will increase and sea level will rise? Accompanied with long-term field monitoring of the evolution of existing tidal marshes and (re)created tidal marshes, we then have the opportunity to train and modify the models if needed and to advice shoreline protection managers and policy makers with more detail to implement adaptations to the management whenever required and to give more case-specific advice on future projects. In this context, the dynamic nature of tidal marshes should be taken into account when taking management decisions (Allen 2000). Both marsh expansion and marsh retreat are part of the natural dynamics which are affected by coupled local disturbances such as cliff erosion and changes on larger, estuarine scale such as sediment supply (Schuerch et al. 2019; Finotello et al. 2020; Wang et al. 2020; Willemsen et al. 2022).

The research in this thesis has a few limitations which need some nuance for the interpretation of the results, but it is argued that the principles described are applicable and similar to other situations. For example, the main focus in this study was on NW European, brackish marsh plant species with a perennial life cycle strategy. Although this is a specific situation, similar situations and especially, similar species-specific plant traits can be observed in other tidal marshes in mid-latitude, temperate climate zones (e.g. marshes in China and the USA e.g. Yang et al. 2012 and Garzon et al. 2019). Nevertheless, multiple tidal marsh species have a different life strategy and totally different plant traits (e.g. *Salicornia sp.*). This is especially important when considering

marsh expansion and the formation of geomorphological features in the landscape such as creeks and cliffs (Schwarz et al. 2018; Evans et al. 2019). As seen in chapter 4: Schoutens et al. (2021), the clonal expansion through tiller growth differed strongly between species, i.e. the two species that were most vulnerable for shoot damage did produce many new tillers in contrast to no observed outgrowth of the two species that did not suffer damage. Here I suggested that breakage and regrowth or rapid expansion might be a survival strategy. Apart from the plant-scale survival, the step-length of vertical outgrowth is known to shape the landscape by inducing cliff formation as a result of the stabilizing effect of dense root networks and the hydrodynamic attenuation effect of high shoot densities (Cao et al. 2021b). To explore the generality of the processes described in this thesis, research involving more species, e.g. salt marsh species and freshwater marsh species, and a bigger range of environmental settings, e.g. tidal marshes including cliffs, could add to the understanding of the mutual feedbacks and plant trait dependent trade-offs. Moreover, when considering the observed processes, my findings might even be applicable to other ecosystems with a nature-based shoreline protection capacity such as mangroves or seagrass meadows (Twomey et al. 2020; Hespen et al. 2021).

I focused on the stress responses of hydrodynamic forces from waves and currents, however tidal marshes are exposed to many other stressors. My findings show a combined stress response from hydrodynamics and tidal inundation. Although disentangling these stressors could be interesting, this would not represent natural meaningful conditions. Moreover, the combination of multiple stressors might affect the overall stress on the plants (Crotty et al. 2017) which is a topic that future research could elaborate on, i.e. how is plant trait dependent growth affected by combinations of environmental stress conditions such as tidal inundation, hydrodynamics, salinity, sediment characteristics, pollution, interactions with other organisms such as other plant species, benthos, birds, ...

The extensive field monitoring in this thesis delivered a large and detailed dataset on hydrodynamics (waves, currents, water levels), sediment dynamics (elevation change, sediment composition) and plant properties (morphology, biomechanics, survival) which could provide valuable input for future research (e.g. modeling of tidal marsh development) and is available on the server of BfG (Germany).

7.6 References

Allen, J. 2000. Morphodynamics of Holocene salt marshes: a review sketch from the Atlantic and Southern North Sea coasts of Europe. Quat. Sci. Rev. **19**: 1155–1231. doi:10.1016/S0277-3791(99)00034-7

Anderson, M. M. E., J. M. J. Smith, and S. K. S. McKay. 2011. Wave dissipation by vegetation. Coastal and Hydraulics Engineering Technical Note ERDC/CHL CHETN-I-82.

Balke, T., M. Stock, K. Jensen, T. J. Bouma, and M. Kleyer. 2016. A global analysis of the seaward salt marsh extent: The importance of tidal range. Water Resour. Res. **52**: 3775–3786. doi:10.1002/2015WR018318

Battisti, D. De. 2021. The resilience of coastal ecosystems : A functional trait-based perspective. J. Ecol. 1–14. doi:10.1111/1365-2745.13641

van Belzen, J., J. van de Koppel, M. L. Kirwan, and others. 2017. Vegetation recovery in tidal marshes reveals critical slowing down under increased inundation. Nat. Commun. **8**: 15811. doi:10.1038/ncomms15811

Bendoni, M., R. Mel, L. Solari, S. Lanzoni, S. Francalanci, and H. Oumeraci. 2016. Insights into lateralmarsh retreatmechanism through localized field measurements. Water Resour. Res. **52**: 1446–1464. doi:10.1002/2014WR015716

Bertness, M. D. 1991. Zonation of *Spartina patens* and *Spartina*
alterniflora in a New England Salt Marsh. Ecology **72**: 138–148.

Borsje, B. W., B. K. van Wesenbeeck, F. Dekker, P. Paalvast, T. J. Bouma, M. M. van Katwijk, and M. B. de Vries. 2011. How ecological engineering can serve in coastal protection. Ecol. Eng. **37**: 113–122. doi:10.1016/j.ecoleng.2010.11.027

Bouma, T. J., M. Friedrichs, B. K. van Wesenbeeck, S. Temmerman, G. Graf, and P. M. J. Herman. 2009. Density-dependent linkage of scale-dependent feedbacks: a flume study on the intertidal macrophyte *Spartina anglica*. Oikos **118**: 260–268. doi:10.1111/j.1600-0706.2008.16892.x

Bouma, T. J., M. B. De Vries, and P. M. J. Herman. 2010. Comparing ecosystem engineering efficiency of two plant species with contrasting growth strategies. Ecol. Soc. Am. **91**: 2696–2704. doi:10.1890/09-0690.1

Brady, A. F., and C. S. Boda. 2017. How do we know if managed realignment for coastal habitat compensation is successful? Insights from the implementation of the EU Birds and Habitats Directive in England. Ocean Coast. Manag. **143**: 164–174. doi:10.1016/j.ocecoaman.2016.11.013

Brückner, M. Z. M., C. Schwarz, W. M. van Dijk, M. van Oorschot, H. Douma, and M. G. Kleinhans.

2019. Salt Marsh Establishment and Eco-Engineering Effects in Dynamic Estuaries Determined by Species Growth and Mortality. J. Geophys. Res. Earth Surf. **124**: 2962–2986. doi:10.1029/2019JF005092

Cao, H., Z. Zhu, J. Belzen, and others. 2021a. Salt marsh establishment in poorly consolidated muddy systems: effects of surface drainage, elevation, and plant age. Ecosphere **12**. doi:10.1002/ecs2.3755

Cao, H., Z. Zhu, P. M. J. Herman, S. Temmerman, J. de Smit, L. Zhang, L. Yuan, and T. J. Bouma. 2021b. Plant traits determining biogeomorphic landscape dynamics: a study on clonal expansion strategies driving cliff formation at marsh edges. Limnol. Oceanogr. 6–82. doi:10.1002/lno.11915

Cao, H., Z. Zhu, R. James, and others. 2020. Wave effects on seedling establishment of three pioneer marsh species: survival, morphology and biomechanics. Ann. Bot. **125**: 345–352. doi:10.1093/aob/mcz136

Carus, J., M. Paul, and B. Schröder. 2016. Vegetation as self-adaptive coastal protection: Reduction of current velocity and morphologic plasticity of a brackish marsh pioneer. Ecol. Evol. **6**: 1579–1589. doi:10.1002/ece3.1904

Chirol, C., K. L. Spencer, S. J. Carr, I. Möller, B. Evans, J. Lynch, H. Brooks, and K. R. Royse. 2021. Effect of vegetation cover and sediment type on 3D subsurface structure and shear strength in saltmarshes. Earth Surf. Process. Landforms **46**: 2279–2297. doi:10.1002/esp.5174

Crotty, S. M., C. Angelini, and M. D. Bertness. 2017. Multiple stressors and the potential for synergistic loss of New England salt marshes. PLoS One **12**: 1–13. doi:10.1371/journal.pone.0183058

Dam, G., S. E. Poortman, A. J. Bliek, and Y. Plancke. 2013. Long-term modeling of the impact of dredging strategies on morpho- and hydrodynamic developments in the Western Scheldt. *WODCON XX: The Art of Dredging*. 1–14.

Dao, T., M. J. F. Stive, B. Hofland, and T. Mai. 2018. Wave Damping due to Wooden Fences along Mangrove Coasts. J. Coast. Res. **34**: 1317. doi:10.2112/jcoastres-d-18-00015.1

Duarte, C. M., I. J. Losada, I. E. Hendriks, I. Mazarrasa, and N. Marbà. 2013. The role of coastal plant communities for climate change mitigation and adaptation. Nat. Clim. Chang. **3**: 961–968. doi:10.1038/nclimate1970

Esteves, L. S. 2013. Is managed realignment a sustainable long-term coastal management approach? J. Coast. Res. **65**: 933–938. doi:10.2112/si65-158.1

Esteves, L. S., and J. J. Williams. 2017. Managed realignment in Europe: a synthesis of methods, achievements and challenges. Living Shorelines Sci. Manag. Nature-based Coast. Prot. 157–180.

Evans, B. R., H. Brooks, C. Chirol, M. K. Kirkham, I. Möller, K. Royse, K. Spencer, and T. Spencer. 2021. Vegetation interactions with geotechnical properties and erodibility of salt marsh sediments. Estuar. Coast. Shelf Sci. **265**: 107713. doi:10.1016/j.ecss.2021.107713

Evans, R. Ben, I. Möller, T. Spencer, and G. Smith. 2019. Dynamics of salt marsh margins are related to their three-dimensional. Earth Surf. Process. Landforms **44**: 1816–1827. doi:DOI: 10.1002/esp.4614

Fagherazzi, S., M. L. Kirwan, S. M. Mudd, G. R. Guntenspergen, S. Temmerman, A. D. Alpaos, J. Van De Koppel, and J. M. Rybczyk. 2012. Numerical Models of Salt Marsh Evolution: Ecological, Geomorphic, and Climat Factors. Rev. Geophys. **50**. doi:10.1029/2011RG000359.1. INTRODUCTION

Fagherazzi, S., C. Palermo, M. C. Rulli, L. Carniello, and A. Defina. 2007. Wind waves in shallow microtidal basins and the dynamic equilibrium of tidal flats. J. Geophys. Res. **112**: F02024. doi:10.1029/2006JF000572

Feagin, R. a, S. M. Lozada-Bernard, T. M. Ravens, I. Möller, K. M. Yeager, and A. H. Baird. 2009. Does vegetation prevent wave erosion of salt marsh edges? Proc. Natl. Acad. Sci. U. S. A. **106**: 10109–13. doi:10.1073/pnas.0901297106

Feser, F., M. Barcikowska, O. Krueger, F. Schenk, R. Weisse, and L. Xia. 2015. Storminess over the North Atlantic and northwestern Europe-A review. Q. J. R. Meteorol. Soc. **141**: 350–382. doi:10.1002/qj.2364

Finotello, A., M. Marani, L. Carniello, M. Pivato, M. Roner, L. Tommasini, and A. D'alpaos. 2020. Control of wind-wave power on morphological shape of salt marsh margins. Water Sci. Eng. **13**: 45–56. doi:10.1016/j.wse.2020.03.006

French, J. 2006a. Tidal marsh sedimentation and resilience to environmental change: Exploratory modelling of tidal, sea-level and sediment supply forcing in predominantly allochthonous systems. Mar. Geol. **235**: 119–136. doi:10.1016/j.margeo.2006.10.009

French, P. W. 2006b. Managed realignment - The developing story of a comparatively new approach to soft engineering. Estuar. Coast. Shelf Sci. **67**: 409–423. doi:10.1016/j.ecss.2005.11.035

Garzon, J. L., M. Maza, C. M. Ferreira, J. L. Lara, and I. J. Losada. 2019. Wave Attenuation by Spartina Saltmarshes in the Chesapeake Bay Under Storm Surge Conditions. J. Geophys. Res. Ocean. **124**: 5220–5243. doi:10.1029/2018JC014865

Gourgue, O., J. van Belzen, C. Schwarz, T. J. Bouma, J. van de Koppel, and S. Temmerman. 2021. A Convolution Method to Assess Subgrid-Scale Interactions Between Flow and Patchy Vegetation in Biogeomorphic Models. J. Adv. Model. Earth

Syst. **13**: 1–25. doi:10.1029/2020MS002116

Hespen, R. Van, Z. Hu, Y. Peng, B. W. Borsje, M. Kleinhans, T. Ysebaert, and T. J. Bouma. 2021. Analysis of coastal storm damage resistance in successional mangrove species. Limnol. Oceanogr. 1–16. doi:10.1002/lno.11875

Himmelstein, J., O. D. Vinent, S. Temmerman, and M. L. Kirwan. 2021. Mechanisms of Pond Expansion in a Rapidly Submerging Marsh. Front. Mar. Sci. **8**: 1–15. doi:10.3389/fmars.2021.70476 8

Hofstede, J. L. A. 2003. Integrated management of artificially created salt marshes in the Wadden Sea of Schleswig-Holstein, Germany. Wetl. Ecol. Manag. **11**: 183–194. doi:10.1023/A:102424812703 7

Hu, Z., J. van Belzen, D. van der Wal, T. Balke, Z. B. Wang, M. Stive, and T. J. Bouma. 2015. Windows of opportunity for salt marsh vegetation establishment on bare tidal flats: The importance of temporal and spatial variability in hydrodynamic forcing. J. Geophys. Res. Biogeosciences **120**. doi:10.1002/2014JG002870.Re ceived

Hu, Z., T. Suzuki, T. Zitman, W. Uittewaal, and M. Stive. 2014. Laboratory study on wave dissipation by vegetation in combined current-wave flow. Coast. Eng. **88**: 131–142. doi:10.1016/j.coastaleng.2014. 02.009

Kearney, W. S., and S. Fagherazzi. 2016. Salt marsh vegetation promotes efficient tidal channel networks. Nat. Commun. **7**. doi:10.1038/ncomms12287

Van de Koppel, J., D. Van der Wal, J. P. Bakker, and P. M. J. Herman. 2005. Self-Organization and Vegetation Collapse in Salt Marsh Ecosystems. Am. Nat. **165**: 1–12.

De La Vega-Leinert, A. C., S. Stoll-Kleemann, and E. Wegener. 2018. Managed Realignment (MR) along the Eastern German Baltic Sea: A Catalyst for Conflict or for a Coastal Zone Management Consensus. J. Coast. Res. **34**: 586–601. doi:10.2112/JCOASTRES-D-15-00217.1

Leonardi, N., and S. Fagherazzi. 2015. Effect of local variability in erosional resistance on large-scale morphodynamic response of salt marshes to wind waves and extreme events. Geophys. Res. Lett. **42**: 5872–5879. doi:10.1002/2015GL064730.Re ceived

Luisetti, T., R. K. Turner, I. J. Bateman, S. Morse-Jones, C. Adams, and L. Fonseca. 2011. Coastal and marine ecosystem services valuation for policy and management: Managed realignment case studies in England. Ocean Coast. Manag. **54**: 212–224. doi:10.1016/j.ocecoaman.2010. 11.003

Ma, Z., T. Ysebaert, D. van der Wal, D. J. de Jong, X. Li, and P. M. J. Herman. 2014. Long-term salt marsh vertical accretion in a tidal bay with reduced sediment

supply. Estuar. Coast. Shelf Sci. **146**: 14–23. doi:10.1016/j.ecss.2014.05.001

MacManus, K., D. Balk, H. Engin, G. McGranahan, and R. Inman. 2021. Estimating Population and Urban Areas at Risk of Coastal Hazards, 1990–2015: How data choices matter,.

Marijnissen, R., P. Esselink, M. Kok, C. Kroeze, and J. M. van Loon-Steensma. 2020. How natural processes contribute to flood protection - A sustainable adaptation scheme for a wide green dike. Sci. Total Environ. **739**: 139698. doi:10.1016/j.scitotenv.2020.139698

Marin-Diaz, B., L. L. Govers, D. van der Wal, H. Olff, and T. J. Bouma. 2021. How grazing management can maximize erosion resistance of salt marshes. J. Appl. Ecol. **58**: 1533–1544. doi:10.1111/1365-2664.13888

Mariotti, G., and S. Fagherazzi. 2013. Wind waves on a mudflat : The influence of fetch and depth on bed shear stresses. Cont. Shelf Res. **60**: S99–S110. doi:10.1016/j.csr.2012.03.001

Maris, T., T. Cox, S. Temmerman, P. De Vleeschauwer, S. Van Damme, T. De Mulder, E. Van Den Bergh, and P. Meire. 2007. Tuning the tide: Creating ecological conditions for tidal marsh development in a flood control area. Hydrobiologia **588**: 31–43. doi:10.1007/s10750-007-0650-5

Möller, I. 2006. Quantifying saltmarsh vegetation and its effect on wave height dissipation: Results from a UK East coast saltmarsh. Estuar. Coast. Shelf Sci. **69**: 337–351. doi:10.1016/j.ecss.2006.05.003

Möller, I. 2019. Applying uncertain science to nature-based coastal protection: Lessons from shallow wetland-dominated shores. Front. Environ. Sci. **7**. doi:10.3389/fenvs.2019.00049

Möller, I., and T. Spencer. 2002. Wave dissipation over macro-tidal saltmarshes: Effects of marsh edge typology and vegetation change. J. Coast. Res. **36**: 506–521. doi:10.2112/1551-5036-36.sp1.506

Morris, J. T., P. V Sundareshwar, C. T. Nietch, B. Kjerfve, and D. R. Cahoon. 2002. Responses of coastal wetlands to rising sea level. Ecology **83**: 2869–2877. doi:10.1890/0012-9658(2002)083[2869:ROCWTR]2.0.CO;2

Myatt, L. B., M. D. Scrimshaw, and J. N. Lester. 2003. Public perceptions and attitudes towards a forthcoming managed realignment scheme: Freiston Shore, Lincolnshire, UK. Ocean Coast. Manag. **46**: 565–582. doi:10.1016/S0964-5691(03)00035-8

Neumann, B., A. T. Vafeidis, J. Zimmermann, and R. J. Nicholls. 2015. Future coastal population growth and exposure to sea-level rise and coastal flooding - A global assessment. PLoS One **10**. doi:10.1371/journal.pone.0118571

Pascolo, S., M. Petti, and S. Bosa. 2018. On the wave bottom shear stress

in shallow depths: The role of wave period and bed roughness. Water (Switzerland) **10**: 1348–1367. doi:10.3390/w10101348

Paul, M., and C. L. Amos. 2011. Spatial and seasonal variation in wave attenuation over Zostera noltii. J. Geophys. Res. Ocean. **116**: 1–16. doi:10.1029/2010JC006797

Paul, M., T. J. Bouma, and C. L. Amos. 2012. Wave attenuation by submerged vegetation: Combining the effect of organism traits and tidal current. Mar. Ecol. Prog. Ser. **444**: 31–41. doi:10.3354/meps09489

Paul, M., F. Rupprecht, I. Möller, and others. 2016. Plant stiffness and biomass as drivers for drag forces under extreme wave loading: A flume study on mimics. Coast. Eng. **117**: 70–78. doi:10.1016/j.coastaleng.2016.07.004

Pennings, S. C., and R. M. Callaway. 1992. Salt marsh plant zonation: the relative importance of competition and physical factors. Ecol. Soc. Am. **73**: 681–690.

Peralta, G., L. van Duren, E. Morris, and T. Bouma. 2008. Consequences of shoot density and stiffness for ecosystem engineering by benthic macrophytes in flow dominated areas: a hydrodynamic flume study. Mar. Ecol. Prog. Ser. **368**: 103–115. doi:10.3354/meps07574

Puijalon, S., G. Bornette, and P. Sagnes. 2005. Adaptations to increasing hydraulic stress: morphology, hydrodynamics and fitness of two higher aquatic plant species. J. Exp. Bot. **56**: 777–86. doi:10.1093/jxb/eri063

Reed, D. J., T. Spencer, A. L. Murray, J. R. French, and L. Leonard. 1999. Marsh surface sediment deposition and the role of tidal creeks: Implications for created and managed coastal marshes. J. Coast. Conserv. **5**: 81–90. doi:10.1007/BF02802742

Reed, D., B. Van Wesenbeeck, P. M. J. Herman, and E. Meselhe. 2018. Tidal flat-wetland systems as flood defenses : Understanding biogeomorphic controls. Estuar. , Coast. Shelf Sci. **213**: 269–282. doi:10.1016/j.ecss.2018.08.017

Renzi, J. J., Q. He, and B. R. Silliman. 2019. Harnessing positive species interactions to enhance coastal wetland restoration. Front. Ecol. Evol. **7**: 1–14. doi:10.3389/fevo.2019.00131

Rupprecht, F., I. Möller, M. Paul, and others. 2017. Vegetation-wave interactions in salt marshes under storm surge conditions. Ecol. Eng. **100**: 301–315. doi:10.1016/j.ecoleng.2016.12.030

Sand-Jensen, K. 2003. Drag and reconfiguration of freshwater macrophytes. Freshw. Biol. **48**: 271–283. doi:10.1046/j.1365-2427.2003.00998.x

Schepers, L., M. Kirwan, G. Guntenspergen, and S. Temmerman. 2017. Spatio-temporal development of vegetation die-off in a submerging coastal marsh. Limnol. Oceanogr. **62**: 137–150. doi:10.1002/lno.10381

Schuerch, M., J. Scholten, S. Carretero, F. García-Rodríguez, K. Kumbier, M. Baechtiger, and V. Liebetrau. 2016. The effect of long-term and decadal climate and hydrology variations on estuarine marsh dynamics: An identifying case study from the Río de la Plata. Geomorphology **269**: 122–132. doi:10.1016/j.geomorph.2016.06.029

Schuerch, M., T. Spencer, and B. Evans. 2019. Coupling between tidal mudflats and salt marshes affects marsh morphology. Mar. Geol. **412**. doi:10.1016/j.margeo.2019.03.008

Schwarz, C., T. J. Bouma, L. Q. Zhang, S. Temmerman, T. Ysebaert, and P. M. J. Herman. 2015. Interactions between plant traits and sediment characteristics influencing species establishment and scale-dependent feedbacks in salt marsh ecosystems. Geomorphology **250**: 298–307. doi:10.1016/j.geomorph.2015.09.013

Schwarz, C., O. Gourgue, J. van Belzen, and others. 2018. Self-organization of a biogeomorphic landscape controlled by plant life-history traits. Nat. Geosci. **11**: 672–677. doi:10.1038/s41561-018-0180-y

Schwarz, C., T. Ysebaert, Z. Zhu, L. Zhang, T. J. Bouma, and P. M. J. Herman. 2011. Abiotic factors governing the establishment and expansion of two salt marsh plants in the Yangtze Estuary, China. Eco-Healthy Wetl. **31**: 1011–1021.

doi:10.1007/s13157-011-0212-5

Shepard, C. C., C. M. Crain, and M. W. Beck. 2011. The protective role of coastal marshes: A systematic review and meta-analysis. PLoS One **6**. doi:10.1371/journal.pone.0027374

Silinski, A., K. Schoutens, S. Puijalon, J. Schoelynck, D. Luyckx, P. Troch, P. Meire, and S. Temmerman. 2018. Coping with waves: Plasticity in tidal marsh plants as self-adapting coastal ecosystem engineers. Limnol. Oceanogr. **63**: 799–815. doi:10.1002/lno.10671

Sutton-Grier, A. E., K. Wowk, and H. Bamford. 2015. Future of our coasts: The potential for natural and hybrid infrastructure to enhance the resilience of our coastal communities, economies and ecosystems. Environ. Sci. Policy **51**: 137–148. doi:10.1016/j.envsci.2015.04.006

Tagliapietra, D., D. Baldan, A. Barausse, and others. 2018. Protecting and restoring the salt marshes and seagrasses in the lagoon of Venice.

Taherkhani, M., S. Vito, P. L. Barnar, N. Frazer, T. R. Anderson, and C. H. Fletcher. 2020. Sea-level rise exponentially increases coastal flood frequency. Sci. Rep. **10:6466**: 1–17. doi:10.1038/s41598-020-62188-4

Temmerman, S., T. J. Bouma, J. Van de Koppel, D. Van der Wal, M. B. De Vries, and P. M. J. Herman. 2007. Vegetation causes channel

erosion in a tidal landscape. Geology **35**: 631. doi:10.1130/G23502A.1

Temmerman, S., P. Meire, T. J. Bouma, P. M. J. Herman, T. Ysebaert, and H. J. De Vriend. 2013. Ecosystem-based coastal defence in the face of global change. Nature **504**: 79–83. doi:10.1038/nature12859

Tempest, J. A., I. Möller, and T. Spencer. 2015. A review of plant-flow interactions on salt marshes: the importance of vegetation structure and plant mechanical characteristics. Wiley Interdiscip. Rev. Water **2**: 669–681. doi:10.1002/wat2.1103

Tiggeloven, T., H. Moel, V. T. M. Zelst, B. K. Wesenbeeck, H. C. Winsemius, D. Eilander, and P. J. Ward. 2022. The benefits of coastal adaptation through conservation of foreshore vegetation. J. Flood Risk Manag. 1–15. doi:10.1111/jfr3.12790

Tonelli, M., S. Fagherazzi, and M. Petti. 2010. Modeling wave impact on salt marsh boundaries. J. Geophys. Res. **115**: C09028. doi:10.1029/2009JC006026

Turner, R. K., D. Burgess, D. Hadley, E. Coombes, and N. Jackson. 2007. A cost-benefit appraisal of coastal managed realignment policy. Glob. Environ. Chang. **17**: 397–407. doi:10.1016/j.gloenvcha.2007.05.006

Twomey, A. J., K. R. O. Brien, D. P. Callaghan, and M. I. Saunders. 2020. Synthesising wave attenuation for seagrass : Drag coefficient as a unifying indicator. Mar. Pollut. Bull. **160**. doi:10.1016/j.marpolbul.2020.111661

Vitousek, S., P. L. Barnard, C. H. Fletcher, N. Frazer, L. Erikson, and C. D. Storlazzi. 2017. Doubling of coastal flooding frequency within decades due to sea-level rise. Sci. Rep. **7**: 1–9. doi:10.1038/s41598-017-01362-7

Vuik, V., B. W. Borsje, P. W. J. M. Willemsen, and S. N. Jonkman. 2019. Salt marshes for flood risk reduction: Quantifying long-term effectiveness and life-cycle costs. Ocean Coast. Manag. **171**: 96–110. doi:10.1016/j.ocecoaman.2019.01.010

Vuik, V., S. N. Jonkman, B. W. Borsje, and T. Suzuki. 2016. Nature-based flood protection: The efficiency of vegetated foreshores for reducing wave loads on coastal dikes. Coast. Eng. **116**: 42–56. doi:10.1016/j.coastaleng.2016.06.001

Vuik, V., H. Y. Suh Heo, Z. Zhu, B. W. Borsje, and S. N. Jonkman. 2018. Stem breakage of salt marsh vegetation under wave forcing: A field and model study. Estuar. Coast. Shelf Sci. **200**: 41–58. doi:10.1016/j.ecss.2017.09.028

Wang, C., S. Smolders, D. P. Callaghan, J. van Belzen, T. J. Bouma, Z. Hu, Q. Wen, and S. Temmerman. 2020. Identifying hydro-geomorphological conditions for state shifts from bare tidal flats to vegetated tidal marshes. Remote Sens. **12**. doi:10.3390/rs12142316

Wang, H., D. van der Wal, X. Li, and others. 2017. Zooming in and

out: Scale dependence of extrinsic and intrinsic factors affecting salt marsh erosion. J. Geophys. Res. Earth Surf. **122**: 1455–1470. doi:10.1002/2016JF004193

Willemsen, P. W. J. M., B. P. Smits, B. W. Borsje, P. M. J. Herman, J. T. Dijkstra, T. J. Bouma, and S. J. M. H. Hulscher. 2022. Modeling Decadal Salt Marsh Development : Variability of the Salt Marsh Edge Under Influence of Waves and Sediment Availability. Water Resour. Res. **58**: 1–23. doi:10.1029/2020WR028962

Wolters, M., A. Garbutt, R. M. Bekker, J. P. Bakker, and P. D. Carey. 2008. Restoration of salt-marsh vegetation in relation to site suitability, species pool and dispersal traits. J. Appl. Ecol. **45**: 904–912. doi:10.1111/j.1365-2664.2008.01453.x

Xie, T., B. Cui, S. Li, and J. Bai. 2019. Topography regulates edaphic suitability for seedling establishment associated with tidal elevation in coastal salt marshes. Geoderma **337**: 1258–1266. doi:10.1016/j.geoderma.2018.07.053

Yang, S. L., B. W. Shi, T. J. Bouma, T. Ysebaert, and X. X. Luo. 2012. Wave attenuation at a salt marsh margin : A case study of an exposed coast on the Yangtze Estuary. Estuaries and Coasts **35**: 169–182. doi:10.1007/s12237-011-9424-4

Ysebaert, T., S. Yang, L. Zhang, Q. He, T. J. Bouma, and P. M. J. Herman. 2011. Wave attenuation by two contrasting ecosystem engineering salt marsh macrophytes in the intertidal pioneer zone. Wetlands **31**: 1043–1054. doi:10.1007/s13157-011-0240-1

Zhang, X., and H. Nepf. 2021. Wave-induced reconfiguration of and drag on marsh plants. J. Fluids Struct. **100**: 103192. doi:10.1016/j.jfluidstructs.2020.103192

Zhao, Z., L. Yuan, W. Li, B. Tian, and L. Zhang. 2020. Re-invasion of Spartina alterniflora in restored saltmarshes: Seed arrival, retention, germination, and establishment. J. Environ. Manage. **266**: 110631. doi:10.1016/j.jenvman.2020.110631

Zhu, C., L. Guo, D. S. van Maren, B. Tian, X. Wang, Q. He, and Z. B. Wang. 2019. Decadal morphological evolution of the mouth zone of the Yangtze Estuary in response to human interventions. Earth Surf. Process. Landforms **44**: 2319–2332. doi:10.1002/esp.4647

Zhu, Z., V. Vuik, P. J. Visser, and others. 2020. Historic storms and the hidden value of coastal wetlands for nature-based flood defence. Nat. Sustain. doi:10.1038/s41893-020-0556-z

8

Supplementary information

8.1 Supplementary information: Chapter 2

Figure S2.1: Pictures taken at Krautsand in winter (left, January 2016) and summer (right, September 2016) with, respectively, low and high aboveground biomass of B. maritimus.
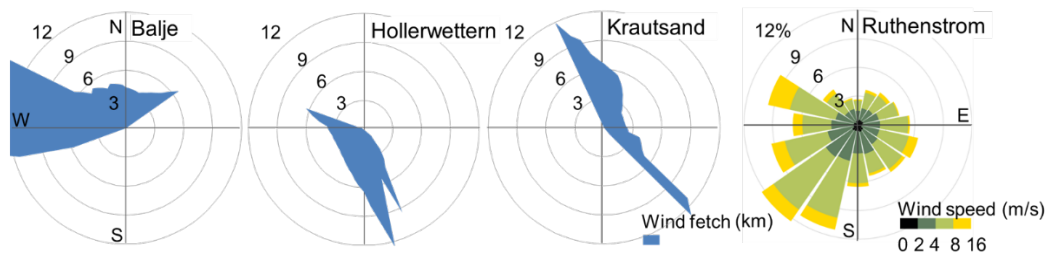

Figure S2.2: Wind fetch for each wind direction per study site and wind rose diagram from the Ruthenstrom weather station showing the wind conditions during the study period from December 2015 until May 2017.
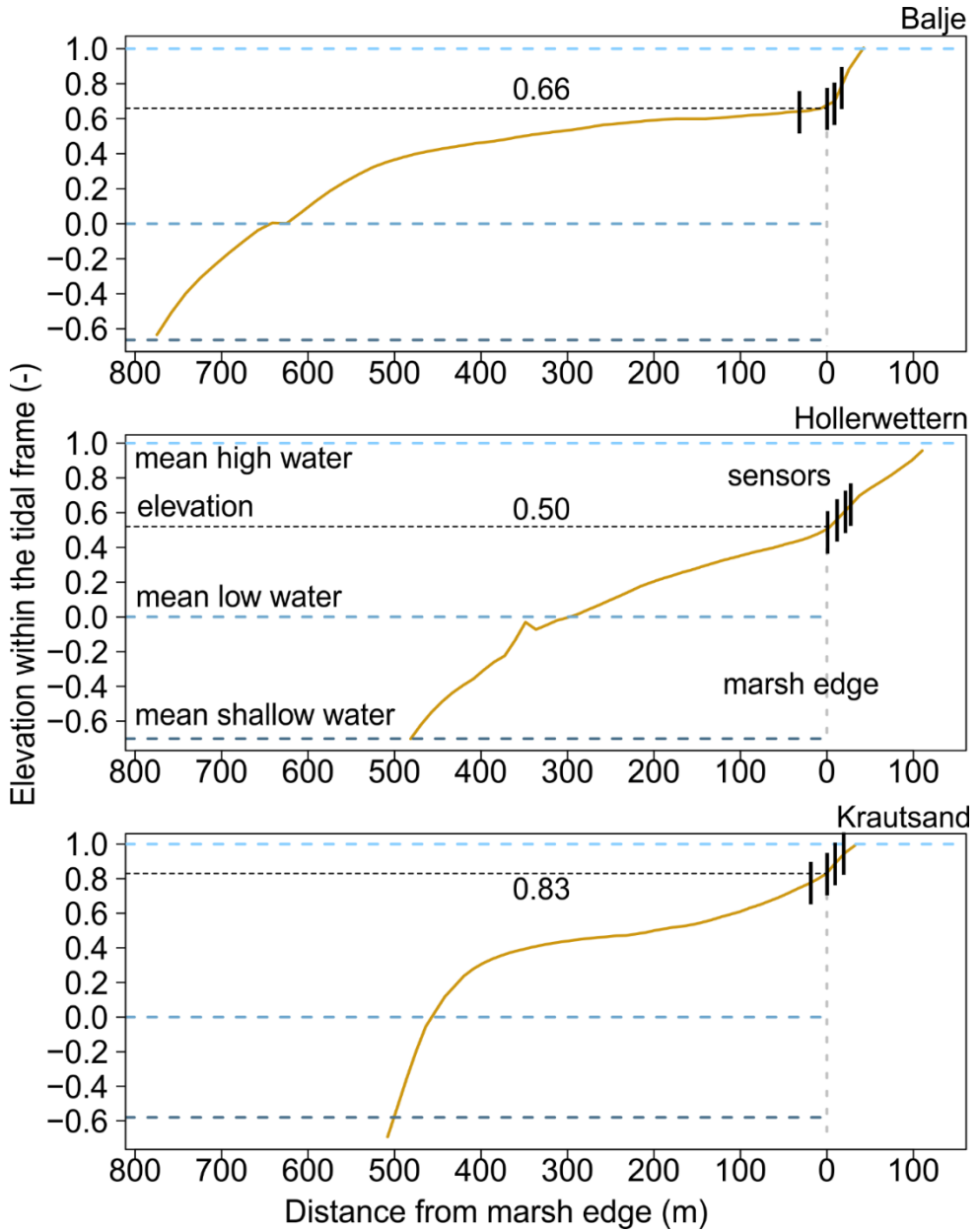
Figure S2.3: Cross section of the topography of the study areas from the shipping channel to the marsh edge. The tidal area in Krautsand form a concave topography in front of the marsh edge while Balje and Hollerwettern have a more convex topography.

8.2 Supplementary information: Chapter 3
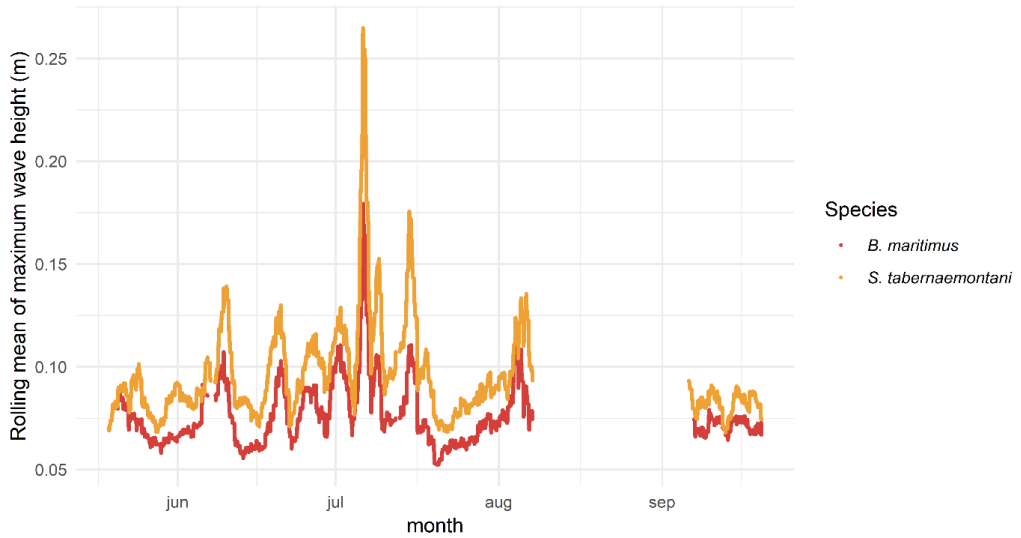
Figure S3.1: The time series of the incoming maximum wave heights (H_{max}; m) per species based on a moving average per tide during the growing season from May to October 2016. Wave heights are consequently higher in *S. tabernaemontani* compared to *B. maritimus*. No data recordings were taken over a 30-day period around August-September.
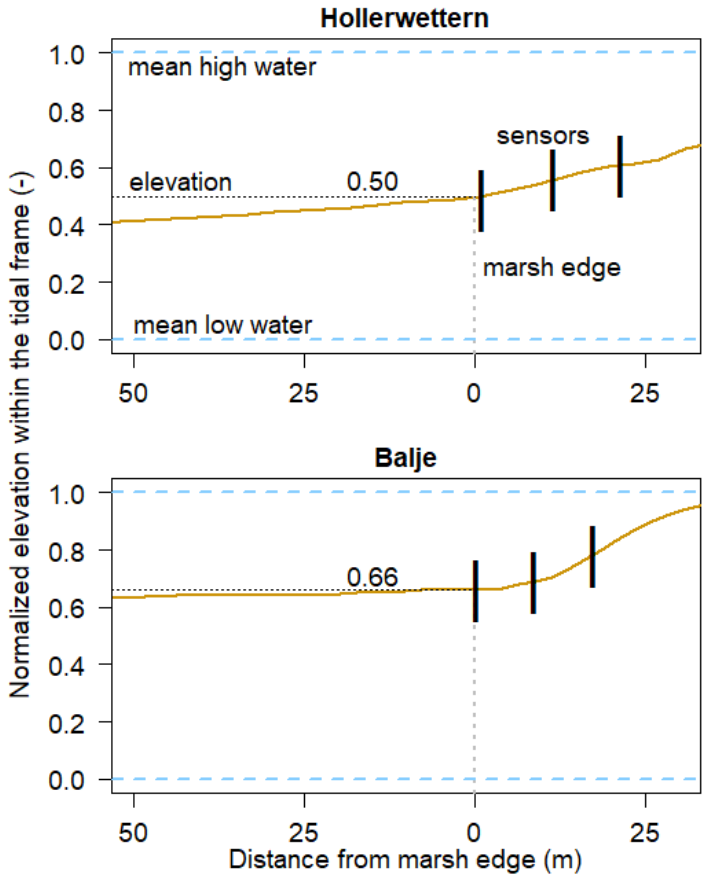
Figure S3.2: Cross section of the topography of Hollerwettern and Balje from the shipping channel to the marsh edge. The elevations are normalized by tidal range as (Elevation – Mean low water)/(Mean high water – Mean low water).

8.3 Supplementary information: Chapter 4

8.3.1 Outgrowth and uprooting

Figure S4.1: Pictures of the *B. maritimus* seedlings illustrate the partial uprooting of shoots and the point of breakage at the connection between the roots and the stem. Rhizomes ensure the anchoring of the uprooted seedling. In between the seedlings under investigation, other seedlings were growing as a result of clonal outgrowth. These were clipped each day to exclude them from the experiments.

8.3.2 Representative current load on plants

Following Madsen (1994), who defined "a representative periodic wave by its near-bottom orbital velocity amplitude u_{br} ..." for irregular waves in spectral domain, a similar approach is used here, however, in time domain. Furthermore, the kinetic energy is used to obtain a measure for the cumulative load due to orbital velocity at the investigation zones.

The velocity was measured by ADV-sensors, installed 30 cm in front of the seaward edge of each pallet row, the measurement volume of the sensors was 5 cm above the concrete bottom.

The time series of the horizontal component of orbital velocity were analyzed with zero-down-crossing, thus providing minimum and maximum values for all individual velocity oscillations of the generated irregular waves. Very small oscillations around zero were ignored by applying a threshold band with the size of 0.7 % of ($u_{max} - u_{min}$) of the complete time series. In case a pronounced spike was detected in the recorded signal due to a disturbance in the measurement, this event was manually removed from the list of velocity oscillations. From the corrected list the average of positive (u_c, crest) and negative (u_t, trough) maximum velocities were calculated and an average velocity amplitude u_{br} was derived:

$$u_{br} = \frac{1}{2}\left(\frac{1}{n}\sum u_c + \frac{1}{n}\left|\sum u_t\right|\right)$$

With n Number of detected waves

         u_c Maximal positive velocity of an individual wave [m/s]

         u_t Maximal negative velocity of an individual wave [m/s]

This value is very close to the value calculated in frequency domain by Madsen (1994), here reduced to uni-directional flow:

$$u_{br} = \sqrt{2\int S_{ub}(\omega)d\omega}$$

With ω radian frequency = $2\pi f$, f is the frequency

         S_{ub} velocity spectrum [(m/s)^{2}s]

In order to find a representative time T_r for the period of the orbital velocity, the following approach is used. A sinusoidal wave with the amplitude u_{br} and the period T_m is considered. T_m is the average period of all velocity oscillations in the selected time interval. As positive and negative velocities both have to be considered as loading cases

for the plants and because the sine function is point symmetric, 2 times the integral from 0 to $t=T_m/2$ is considered as velocity load for the representative velocity oscillation:

$$2\int_0^t u_{br}\sin\left(\frac{2\pi}{T}t\right)dt = -2u_{br}\frac{T_m}{2\pi}\cos\frac{2\pi}{T}t = 2u_{br}\frac{T_m}{\pi}\left(\text{for } t = \frac{T_m}{2}\right)$$

The representative period T_r is considered as the duration of a rectangular load with the same area as the integral given above:

$$u_{br}T_r = 2u_{br}\frac{T_m}{\pi}$$

$$T_r = \frac{2T_m}{\pi} = 0.637 \cdot T_m$$
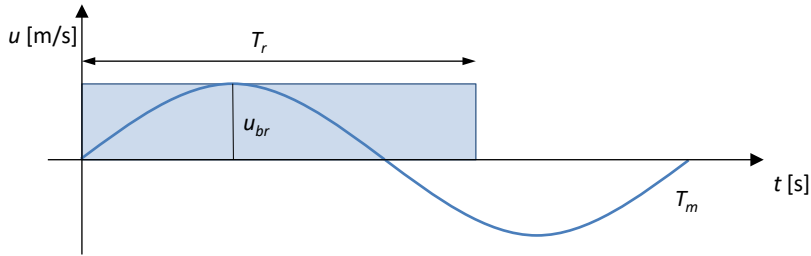
In order to derive a meaningful parameter which includes the duration of velocity load, the kinetic energy $E_{kin,r}$ of the representative orbital velocity is considered:

$$E_{kin,r} = \frac{m \cdot u_{br}^2}{2}$$

With m unit mass of 1 kg

In physics energy times the duration is known as action S with the unit Joule-second [Js]. As duration t, where the velocity is affecting the plants, the number of detected oscillations n multiplied with the representative period T_r is determined. For a wave sequence with n velocity oscillations the action S can then be calculated as

$$S = E_{kin,r} \cdot t = \frac{1 \cdot u_{br}^2}{2} \cdot nT_r$$

It should be noted that the action S alone is not sufficient as measure for the wave load, because the same S can be obtained by a long duration with small energy and a short

duration with high energy, while the latter will have more impact on plant behavior than the first. In the context of this study, S can be used for comparison, as all wave runs were composed of 1000 waves.
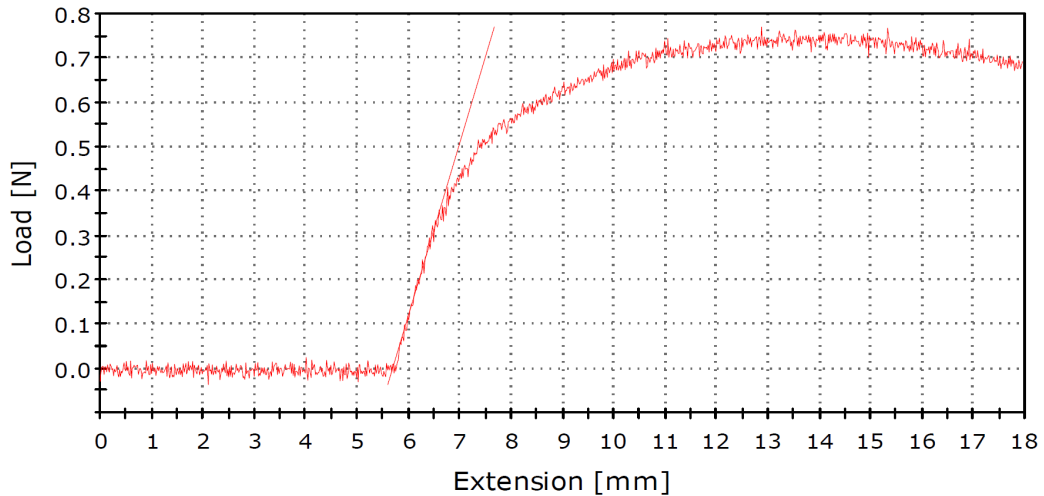
8.3.3 Stress-strain curve

Figure S4.2: Stress-strain curve (red curve) generated by the Instron Bleuhill 3.0 software from a three-point bending test on the basal stem part of a *S. tabernaemontani* seedling. The curve describes the relation between vertical deflection of the stem (Extension; on the X-axis) and the bending force of the stem (Load; on the Y-axis) which enables the calculation of the slope from the elastic deformation zone on the curve (F/D). This calculation was done automatically by the soft

8.3.4 References

Madsen, O.S. (1994) Spectral Wave-Current Bottom Boundary Layer Flows, 24th International Conference on Coastal Engineering, Kobe, Japan

8.4 Supplementary information: Chapter 5

Figure S5.1: The three dominant species of the brackish marshes along the Elbe estuary, Germany. The figures illustrate their distinct shape and morphology. *Schoenoplectus tabernaemontani* (C.C.Gmel.) Palla growing as the first pioneer at the marsh edge, *Bolboschoenus maritimus* (L.) Palla growing more landwards and *Phragmites australis* (Cav.) Trin. ex Steud growing even more landwards, towards the dike.
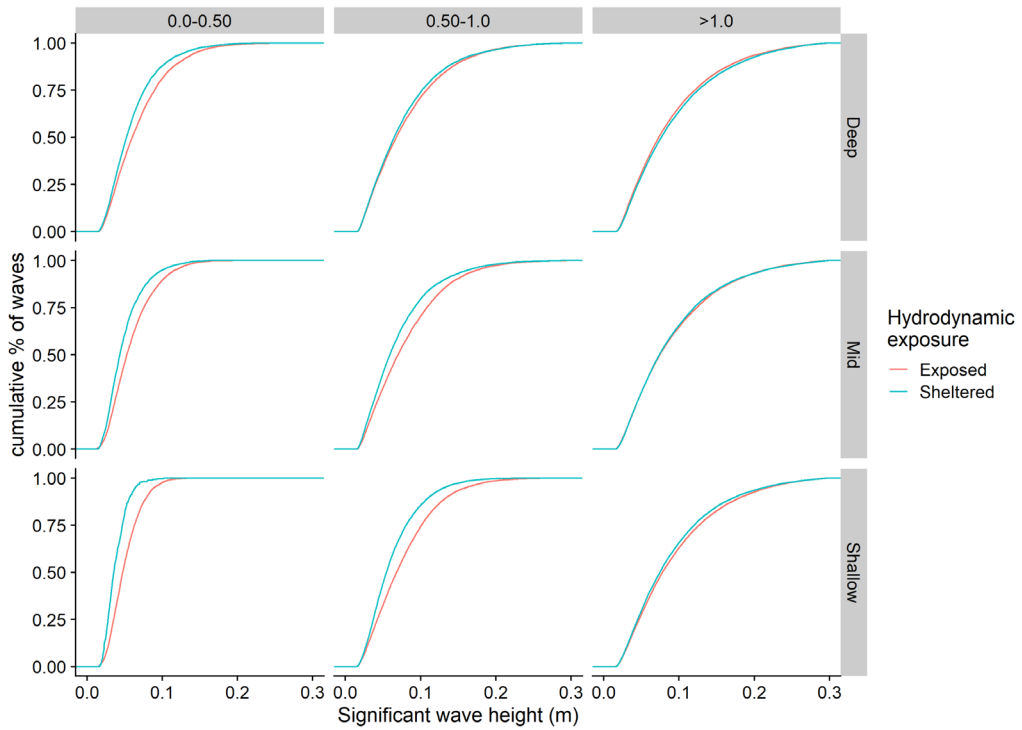
Figure S5.1: Cumulative frequency of significant wave heights for the two hydrodynamic exposure treatments and the three inundation treatments. The wave heights were split in three inundation depth categories (0.0 – 0.5 m; 0.5 – 1.0 m and >1.0 m) to show the effect of the wave barrier which was 70 cm tall at installation. During the winter season (December 2018 – March 2019), the wave barriers broke and therefore, the data from this period were excluded from the graph.
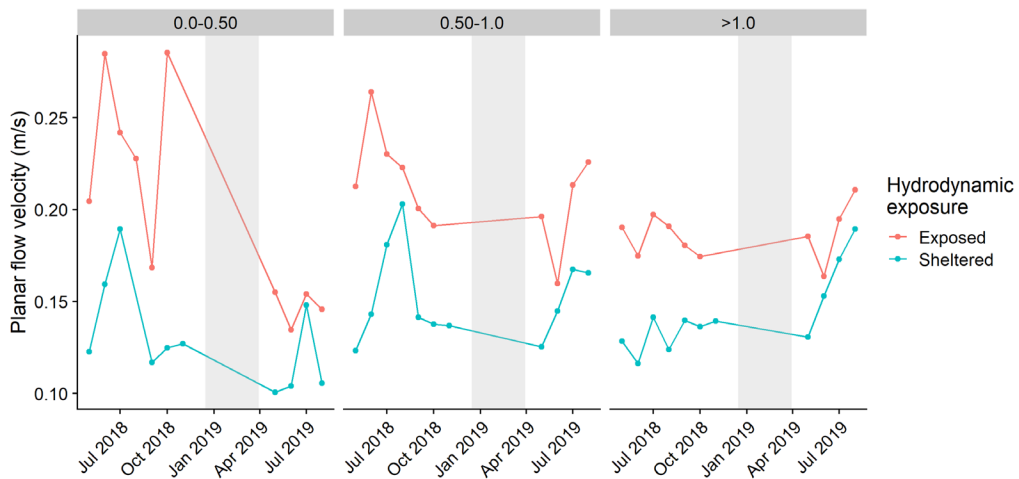
Figure S5.2: Planar flow velocity shown as a monthly average for the two hydrodynamic exposure treatments at the deep inundation sites. Planar flow velocities were categorized over three inundation depths (0.0 – 0.5 m; 0.5 – 1.0 m and >1.0 m) to show the effect of the wave barrier which was 70 cm tall at installation. During the winter season indicated with a gray background (December 2018 – March 2019), the ADVs were removed from the field to prevent damage during storm events.
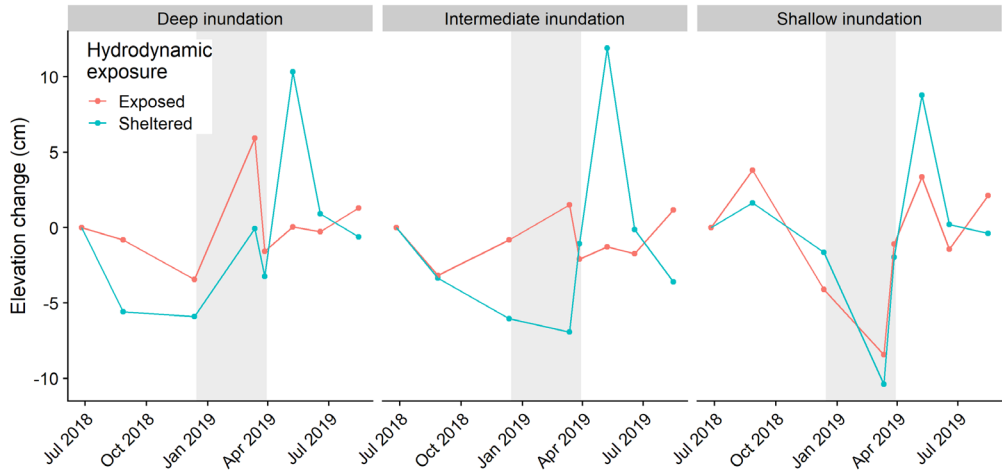

Figure S5.3: Absolute elevation (m NHN) of all sites, i.e. three inundation treatments and two hydrodynamic exposure treatments over the entire experimental period (May 2018 – August 2019). During the winter season indicated with a gray background (December 2018 – March 2019), the wave barriers broke and erosion events took place in the more sheltered and shallow sites.

Table S5.1: Overview of the flexural stiffness EI (Nm^2), Young's modulus E (N/m^2) and the second moment of area I (m^4) for the three species measured in August 2019. Per species, the mean and standard error are given for every treatment in which at least 5 shoots survived.

Inundation	Wave	*S. tabernaemontani*	*B. maritimus*	*P. australis*
		EI (Nm^2)		
Shallow	Exposed	0.17 ± 0.03	0.06 ± 0.01	0.02 ± 0.003
	Sheltered	0.28 ± 0.02	0.06 ± 0.01	0.02 ± 0.004
Intermediat	Exposed	0.13 ± 0.01	0.04 ± 0.01	
	Sheltered	0.12 ± 0.02	0.05 ± 0.01	
Deep	Exposed			
	Sheltered	0.09 ± 0.02		
		E (N/m^2)		
Shallow	Exposed	3.0 e8 ± 1.7 e7	8.9 e8 ± 9.1 e7	2.0 e9 ± 2.4 e8
	Sheltered	3.6 e8 ± 4.1 e7	9.0 e8 ± 1.1 e8	2.7 e9 ± 3.7 e8
Intermediat	Exposed	3.9 e8 ± 2.6 e7	8.6 e8 ± 8.9 e7	
	Sheltered	3.3 e8 ± 2.1 e7	7.1 e8 ± 6.1 e7	
Deep	Exposed			
	Sheltered	3.4 e8 ± 2.9 e7		
		I (m^4)		
Shallow	Exposed	7.3 e-10 ± 1.7 e-10	1.2 e-10 ± 2.6 e-11	8.9 e-12 ± 1.8 e-12
	Sheltered	1.1 e-9 ± 1.5 e-10	9.1 e-11 ± 1.5 e-11	6.7 e-12 ± 1.4 e-12
Intermediat	Exposed	4.3 e-10 ± 6.3 e-11	4.7 e-11 ± 1.0 e-11	
	Sheltered	5.2 e-10 ± 1.0 e-10	9.2 e-11 ± 1.9 e-11	
Deep	Exposed			
	Sheltered	2.6 e-10 ± 5.1 e-11		

Table S5.2: Grainsize distribution (%) of the six sites sampled in August 2019.

Inundation	Wave	Clay	Silt	Sand
Shallow	Exposed	12.0	66.6	21.4
	Sheltered	9.9	51.8	38.3
Intermediat	Exposed	6.8	40.8	52.4
	Sheltered	4.4	31.5	64.1
Deep	Exposed	3.1	20.6	76.3
	Sheltered	3.7	34.4	61.9

8.5 Supplementary information: Chapter 6

Figure S6.1: Dominant *P. australis* vegetation at the monolith extraction site in front of a dike along the Scheldt estuary, January 2021.
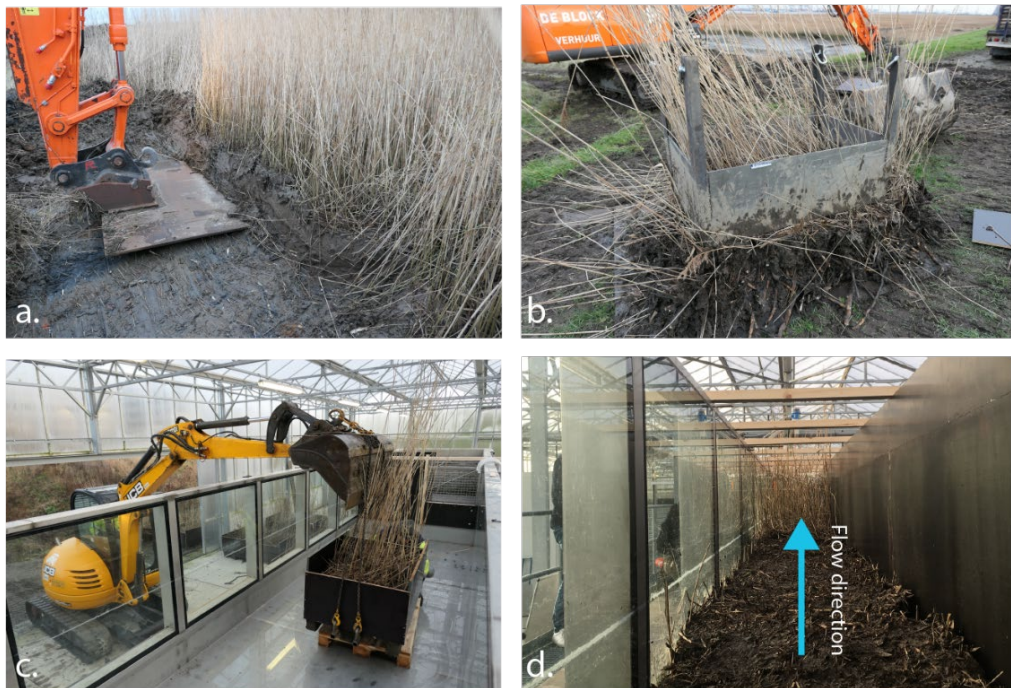

Figure S6.2: Monolith extraction in the field and installation in the flume. First, big clumps of marsh sediment were excavated with a big metal plate attached to a crane.

The metal plate cut the clump at 40 cm depth (a). Next, placed on top of the sediment surface and pushed down gently until it made contact with the metal plate (b). The monoliths were placed on pallets and protected for transport and installation in the flume (c). When all monoliths were in place and protection plates were removed, the walls narrowing the flume were installed and aboveground biomass of the first monoliths was removed before starting the experimental runs (d).

Figure S6.3: Illustration of sediment surface cover before the experimental runs and after the second experimental run. Before the monoliths were exposed to high flow velocities, the sediment surface was covered with debris of old leaves and broken shoots. After the first experimental run, most of this organic layer was washed away. Paint-colored dots were added to the organic material covering the sediment bed to visualize the difference in surface cover between the runs.